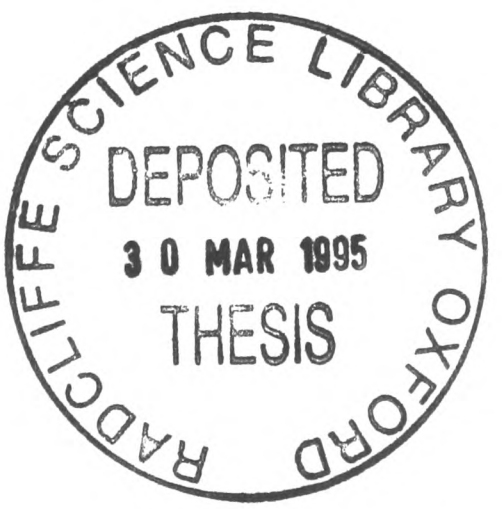
The Effect of Ammonia on Development in Dictyostelium discoideum

The Effect of Ammonia on Development in *Dictyostelium discoideum*

A thesis submitted to the Board of the Faculty of Biological Sciences, University of Oxford, in partial fulfilment of the requirements for the degree of Doctor of Philosophy

Lynne Davies

December, 1994



Abstract

Abstract

The effect of ammonia upon development in *Dictyostelium discoideum*

Upon starvation, individual amoebae of *D.discoideum* cooperate to produce a cell aggregate. The aggregate then elongates into a slug which moves chemotactically towards food sources. Culmination of the developmental cycle results in the formation of a fruiting body containing differentiated stalk and spore cells. Ammonia is produced naturally in the aggregates during starvation and is implicated in the regulation of the developmental cycle. Addition of excess ammonia leads to inhibition of aggregation, increased slug migration, delay of culmination and the promotion of spore formation.

This thesis examines the possible intracellular mechanism(s) through which ammonia might affect developmental processes. It has been postulated that ammonia might act by directly inhibiting a particular enzymatic activity, alternatively it could act as a weak base to raise the pH of the cytosol or an intracellular compartment. To investigate these possibilities, the effects of a variety of weak bases were tested on aggregation and culmination.

All of the weak bases tested inhibited development in a dose-dependent way, which argues against the notion that ammonia acts by direct enzyme inhibition since the bases are structurally distinct. In addition, the inhibition potencies of the bases varied according to their protonophoric activity: the most effective protonophores were also the most effective developmental inhibitors. This suggested that the bases were likely to be acting to neutralize an intracellular compartment in these experiments,a result which implicates acidic compartments in the control of development.

That weak bases can indeed dissipate the pH of intracellular vesicles was confirmed *in vitro* by monitoring acidification of isolated vesicles in the presence of the bases. *In vivo* experiments using ^{31}P-NMR probes of the vesicular system confirmed this and showed that cytosolic pH was stable in the presence of bases.

Genetic evidence for the role of acidic compartments in development was also gathered. Both the acidification-defective (Hgr) mutants and a mutant created by antisense expression of a fraction of the B subunit cDNA of the vacuolar H^+-ATPase were defective in development, displaying developmental behaviour reminiscent of weak base-treated wild-type strains. This shows that defective vacuolar acidification can mimic the effect of addition of ammonia and indicates that an acidic vesicle is the target of ammonia *in vivo*.

Submitted for the degree of Doctor of Philosophy
Michaelmas term, 1994
Lynne Davies, Wadham College

Acknowledgements

Acknowledgements

My thanks must go first to my supervisor, Dr Julian Gross for his invaluable encouragement, support and advice throughout the course of this project. I am very grateful to Dr Peter Newell for his assistance and laboratory space. My gratitude is also extended to Drs Michel Satre and Jean-Baptiste Martin for welcoming me to their laboratories in Grenoble. This work would have been impossible without the gift of B subunit cDNA from Dr R.Dottin and B subunit antibody from Prof. T. Steck. I would also like to thank Professor George K. Radda for granting me the opportunity to work in the Department of Biochemistry and the Medical Research Council for funding.

Many thanks are due to my colleagues in the slime mould group - Calvin, Carmela, Claire, Eamonn, Fabiana, Frances, Gang, Katalin, Kathryn, Kunde, Nick, Nigel and Phil, without whom none of this would have been enjoyable. In particular, I am indebted to Frances for the introduction to slime moulds, to Nigel for an introduction to molecular biology and to Mr Ken Johnson for processing numerous photographs.

This thesis would have been impossible without the support of friends at Wadham - Alan, Sharon, Andy and Christine - in particular to Kim, Dave and the two Steves - it would have been impossible without you!

My love and gratitude to Michael for his support and advice (on style if not content!). Finally, my deepest thanks go to my parents: Gethin and Joan Davies and to my brother Iwan for their support and encouragement through the (seemingly endless?) years of study - diolch o galon am bopeth!

Abbreviations

Abbreviations

AC	ammonium chloride
2-AEP	2-aminoethylphosphonate
ALC	anterior-like cells
AO	acridine orange
8Br-cAMP	8-bromo cyclic adenosine monophosphate
Cl_2MDP	dichloromethylene diphosphonate
cAMP	cyclic adenosine monophosphate
cGMP	cyclic guanosine monophosphate
CQ	chloroquine
ecmA	extracellular matrix protein A
ecmB	extracellular protein B
IA	imidazole
h	hours
LPS	lower pad solution
MA	methylamine
MDR	multidrug resistance
MCS	multiple cloning site
ml	millilitres
µl	microlitres
mM	millimolar
µM	micromolar
nM	nanomolar
NMR	nuclear magnetic resonance
OA	octylamine
PA	propylamine
ΔpH	pH gradient
$\Delta\Psi$	membrane potential
pH_i	cytosolic pH
pH_v	vesicular pH
PKA	protein kinase A

ppm	parts per million
pstA	prestalk A
pstB	prestalk B
psp	prespore
X-gal	galactose attached to a chromophore (X) which is activated by cleavage from the sugar by ß-galactosidase

Contents

Contents

Abstract i

Acknowledgements ii

Abbreviations iii

Contents v

Chapter 1 - Introduction 1

1.1 Why study *Dictyostelium discoideum*? 1

1.2 The life cycle of *D.discoideum* 2

1.2.1 Overview 2

1.2.2 Amoebal characteristics and growth 2

1.2.3 Aggregation 3

1.2.4 Mound and first finger formation 3

1.2.5 Slugging 4

1.2.6 Culmination 5

1.3 Regulation of the life cycle 6

1.3.1 Choices in the developmental pathway 6

1.3.2 Cyclic AMP 6

1.3.3 DIFs 11

1.3.4 Weak acids 13

1.3.5 Ammonia 14

1.4 Theories of weak base action 17

1.4.1 Possible primary intracellular target of ammonia 17

1.4.2 Predictions on the action of ammonia *in vivo* 18

1.4.3 Differences in the ability of bases to raise cytosolic pH 19

1.4.4 Variation in the ability of bases to raise vesicular pH 21

1.4.5 Implications for the action of weak bases 24

1.5 The Endocytic System in *D.discoideum* 25

1.5.1 Structure of the endocytic system 25

1.5.2 pH of compartments in the system 26
1.5.3 Measurement of intracellular pH 26
1.5.4 Role of ATPases in acidification 28
1.5.5 The vacuolar H^+-ATPase 29
1.5.6 Mutations of the vacuolar H^+-ATPase 30
1.5.7 Acidification-defective mutants 31
1.6 Aims of the thesis 34

Chapter 2 - Materials and Methods 35
2.1 Cell stocks, growth and maintenance 35
2.11 NC4 (wild-type) 35
2.12 Ax2 (axenic strain) 35
2.13 Hgr mutants 36
2.14 Vacuolar acidification-defective mutants 36
2.15 Solutions 37
2.2 Development *in vivo* 37
2.21 Preparation of cells 37
2.22 Aggregation 38
2.23 Culmination 38
2.24 Chemotaxis 39
2.25 Weak base solutions 39
2.26 Statistical analyses 40
2.27 Photographs 40
2.3 Vesicle acidification *in vitro* 40
2.31 Isolation of vesicles 40
2.32 Buffers and solutions 41
2.33 Determination of vesicle acidity by fluorescence 41
2.34 Protein assays 42
2.35 Statistical analyses 42
2.4 ^{31}P-NMR conditions 42
2.41 Buffers and solutions 42
2.42 ^{31}P-NMR parameters 43

2.43 Experimental conditions 43
2.44 Treatment of results 44
2.5 Preparation and cloning of plasmids 44
2.51 Sequencing of the B subunit cDNA fragment 44
2.52 Southern blotting 45
2.53 Cloning cDNA fragment through vectors 45
2.54 Solutions 47
2.6 Generation of a vacuolar H^+-ATPase-defective strain 48
2.61 Buffers and solutions 48
2.62 Transformation of Ax2 51
2.63 Detection of plasmid expression 52
2.64 Antisense expression of cDNA 52
2.65 Developmental studies with an acidification-defective transformant 53
Chapter 3 - Effects of Weak Bases on Aggregation, Culmination and Chemotaxis 54
3.1 Introduction 54
3.2 Results 55
3.2.1 Effects of weak bases on aggregation 55
3.2.2 Effects of the weak bases on culminants 59
3.2.3 Effects of weak bases on chemotaxis 61
3.3 Discussion 63
3.3.1 Effects on aggregation 63
3.3.2 Inhibition of culmination 63
3.3.3 Effects on chemotaxis 64
3.3.4 Implications for the mechanism of action of ammonia 65
3.3.5 Possible regulation of aggregation and culmination through an acidic vesicle 68
3.4 Conclusions 69

Chapter 4 - The Effects of Weak Bases on Vesicle Acidification *in vitro* 70

4.0 Introduction 70

4.0.1 Aims of the experiments 70

4.0.2 Acidic vesicles in *Dictyostelium* 71

4.1 Results 71

4.1.1 Assay of vesicular acidification by fluorescence spectroscopy 71

4.1.2 The effects of weak bases on vesicular acidification in NC4 73

4.1.3 Similar results for inhibition of acidification in Ax2 74

4.2 Discussion 76

4.2.1 Effect of the bases on vesicular acidification 76

4.2.2 Correlation with the effects on aggregation and culmination 78

4.2.3 Differences between the *in vivo* and *in vitro* systems 78

4.2.4 Possible reasons for the relative inefficiency of imidazole 80

4.3 Conclusions 80

Chapter 5 - The Effects of Weak Bases on Intracellular pH *in vivo* 82

5.1 Introduction 82

5.1.1 Use of NMR to measure pH *in vivo* 82

5.1.2 Use of probes to label the endocytic system 84

5.2 Results 85

5.2.1 Appearance of NMR spectra in the absence of probes 85

5.2.2 Resonances arising from 2-AEP 87

5.2.3 Effect of weak bases on 2-AEP resonances 88

5.2.4 Resonances arising from Cl_2MDP 91

5.2.5 Effect of weak bases on Cl_2MDP resonances 93

5.2.6 Effects of weak bases on cytoplasmic pH 94

95

5.3 Discussion 95

5.3.1 Effect of the bases on endosomal pH 95

5.3.2 Cytoplasmic pH remains stable in the presence of bases 98

5.3.3 Comparison with aggregation, culmination and *in vitro* acidification 100

5.3.4 Conclusion and summary 102

Chapter 6 - Acidification-defective (Hgr) Mutants and Their Response to Weak Bases 103

6.1 Introduction 103

6.2 Results 104

6.2.1 Growth characteristics of the Hgr strains 104

6.2.2 Developmental characteristics 106

6.2.3 Effect of pH on the developmental morphologies 107

6.2.4 Effects of weak bases on the development of selected Hgr strains 110

6.3 Discussion 111

6.3.1 Similarity of acidification-defective strains to weak base-treated wild-type 111

6.3.2 Correlation between growth rates and hypersensitivity to inhibition of aggregation 112

6.3.3 Other defects induced by defective endosomal acidification 114

6.4 Conclusion 115

Chapter 7 - Generation of an Acidification-defective Strain by Antisense 116

7.1 Introduction 116

7.2 Results 117

7.2.0 Cloning the antisense fragment into the pVeII plasmid 117

7.2.1 Developmental phenotype of the antisense strains 118

7.2.2 Growth characteristics of the strains 120

7.2.3 Western analysis of vacuolar H^+-ATPase expression 121
7.2.4 Development at various pH values 122
7.2.5 Sensitivity of aggregation to weak bases 122
7.2.6 Slugging in the antisense strains 122
7.2.7 Measurement of intracellular pH by NMR 123
7.3 Discussion 124
7.4 Conclusions 126

Chapter 8 - Conclusions 128
8.1 Summary 128
8.1.1 Effects of weak bases on aggregation and culmination 128
8.1.2 Intracellular pH in response to weak base challenge 129
8.1.3 Genetic confirmation of the role of vesicles in development 129
8.2 Implications for the signal transduction pathway of ammonia *in vivo* 130
8.2.1 Properties of acidic vesicles 130
8.2.2 Possible effects of ammonia and changes in pH_v on components of the cAMP signal transduction pathway 132
8.2.3 Implications for the control of differentiation 135
8.3 Conclusions and future directions 136

Appendices 137

References 145

Publications 162

Chapter 1

Chapter 1 *Introduction*

1.1 Why study *Dictyostelium discoideum*?

Development in *D.discoideum* proceeds through a series of well-defined morphological stages which are distinguishable by eye. Cell differentiation occurs in parallel and particular cell types become localised in specific areas of the multicellular aggregate. A number of substances have been implicated in the regulation of development and cell-type specification in *D.discoideum*. This study focusses on the role of one of these putative regulators - ammonia - in the control of development. Inferences are made for its function in cell-type specification and regulation.

D.discoideum is a particularly amenable organism for the study of development. Its life cycle consists of separate growth and development phases; the developmental cycle has a number of morphological stages with associated levels of cell differentiation; it can be cultured axenically for the production of large quantities of material and lastly, it is haploid, so genetic studies can be conducted without the complication of heterozygosity.

In *Drosophila*, asymmetry of the egg is induced by the presence of a gradient of maternal RNA in the egg. This results in a ready-made gradient of *bicoid* from a maximum at the anterior pole to a minimum at the posterior pole such that the egg is asymmetric. The *bicoid* signal acts in concert with other maternal mRNA gradients with the result that cell division generates non-identical daughter cells (Frigerio *et al.*, 1986; Driever & Nüsslein-Volhard, 1988; St Johnston *et al.*, 1989). Asymmetry of cell populations is thus established. The mechanism by which biological pattern formation occurs in D.discoideum is of particular interest since the multicellular state is generated not by cell division but by aggregation of individual amoebae. Asymmetry of the multicellular state is thus generated in the absence of maternal cues. The

specification of cell type and the spatial organization of the cells must therefore be induced by environmental cues, or could arise from inhomogeneity in the cell types making up the aggregate.

1.2 The life cycle of *D.discoideum*

1.2.1 Overview

In the presence of a plentiful food source, *D.discoideum* amoebae exist as haploid individual cells and divide asexually. However, when nutrients become scarce, starved amoebae cooperate to form a multicellular aggregate. Development of the aggregate and differentiation of the cellular mass then occur in parallel to form an aggregate containing spatially organized stalk and spore cells (**figure 1.1**). A sexual cycle is also possible as a result of fusion of two sexually compatible strains or a single competent strain. One amoeba ingests the other by phagocytosis and a cell wall is built up around the resultant diploid to form a resistant macrocyst.

1.2.2 Amoebal characteristics and growth

Amoebae of *D.discoideum* are commonplace in forest soils, where they feed on the bacteria present in the leaf litter (Bonner, 1982). In the laboratory, wild-type strains can be cultivated in association with bacteria on supplemented agar plates. Strains have also been isolated (Loomis, 1971; Sussman, 1987) that are capable of growing axenically in liquid media. Typically, cells double in about 8h in axenic medium and grow to a concentration of 1-2 x 10^7 cells/ml. The cell cycle of *D.discoideum* differs from that of mammalian cells in that the G_1 period is absent. Mitosis is followed by an S phase lasting less than 30 minutes and the majority of the cell cycle is composed of the G_2 phase, lasting roughly 6.5h (Weijer *et al.*, 1984a).

1.2.3 Aggregation

The developmental cycle in *D.discoideum* is triggered by the depletion of the food source (Raper, 1940). As amoebae starve, they draw together in streams towards a central mound comprising 10^5 cells or less, forming a recognisable mound within eight to ten hours under normal conditions.

Aggregation is dependent upon cyclic AMP (cAMP) production. Upon starvation, certain cells generate cAMP signals autonomously. Cyclic AMP is then secreted in a pulsatile fashion and adjacent cells respond to the cAMP emitted by their neighbours with a burst of cAMP synthesis internally (Ross *et al.*, 1975). This is subsequently effluxed to complete a signal-relay process (Devreotes, 1982; Firtel, 1991) producing waves of the chemoattractant throughout the aggregation field. Perception of the cAMP signal by neighbouring cells elicits a chemotactic response towards the maximal concentration of the wave, ceasing as soon as the maximal concentration has passed (Tomchik & Devreotes, 1981). This cell migration towards an aggregation centre eventually becomes visible as streams leading to a central mound.

1.2.4 Mound and first finger formation

After 8-10h, the cells cohere into a tight mound due to expression of cell surface contact site proteins (Siu, 1990) and an enclosing slime sheath forms, delineating the aggregate (Loomis, 1972). It is at this point that heterogeneity is detected in the cell types present in the mound. Cells expressing the prestalk A (pst A) and prestalk B (pst B) gene products are peppered throughout (Tasaka & Takeuchi, 1981; Williams *et al.*, 1989), as are cells that stain with antibodies to prespore gene products (Early *et al.*, 1988). Aggregative genes are now suppressed (Schaap, 1986), probably as a result of increased cAMP concentration, since high (mM) levels of cAMP suppress aggregative gene expression in vitro (Oyama & Blumberg, 1986).

A tip then appears at the apical surface of the mound. By this stage, the distribution of cell types within the aggregate is asymmetric. Most of the prestalk population sorts to the tip and the base of the aggregate (at the contact site with the supporting surface) while cells expressing prespore markers remain in the body of the mound. A number of prestalk-like cells (anterior-like cells or "ALC") remain scattered in the prespore zone. Physiological differences in the cell types become evident at the tipped mound stage also. Yamamoto & Takeuchi (1983) and Gee et al.(1994) showed that the tipped mound stains differentially with neutral red, a weakly basic dye that accumulates in acidic compartments. The tips and bases of aggregates stain deeply whereas the bulk of the mound remains unstained (**figure 1.2**). The location of these deeply staining cells correlates with the prestalk zone, indicating that the acidic vesicles of prestalk cells are more acidic than those of prespore cells.

Over the next few hours, the tip of the aggregate extends and the whole structure elongates to produce a standing slug or "first finger". Prestalk gene expression is restricted to the anterior 25% of the finger and to cells at the very base where the finger is anchored to the substratum. The remainder constitutes prespore gene expression, excepting the ALC.

1.2.5 Slugging

Under certain environmental conditions, the first finger falls over onto the substratum and migrates as a pseudoplasmodium (or "slug") for periods ranging from hours to a few days. Alternatively, the first finger collapses into itself and commences culmination immediately if the environmental conditions are suitable. Culmination usually requires low humidity, low ammonia levels, low pH and overhead light (Newell *et al.*, 1969; Schindler & Sussman, 1977). The control of slugging will be discussed in more detail later.

The neutral-red staining pattern seen in the tipped mound is maintained in the slug (Yamamoto & Takeuchi, 1983; Gee et al., 1994) and reflects the basic division between the prestalk and prespore zones. Recent work has further refined understanding of the extent of differentiation at this stage, uncovering heterogeneity in the prestalk and the prespore zone. At the extreme anterior of the slug, all cells express the *ecmA* gene, which encodes an extracellular matrix protein specific to these prestalk A (pst A) cells (Williams *et al.*, 1987). A central cone of cells in the prestalk zone (prestalk B or "pst B" cells) express another extracellular matrix protein gene: *ecmB*, in addition to *ecmA* (Williams *et al.*, 1989). Between this pst A/B zone and the prespore zone a further pstO cell subtype is located: expressing the *ecmA* gene, but at significantly lower levels than those cells at the extreme anterior (Early *et al.*, 1993). A number of cells that express the pst genes are scattered throughout the prespore region - the anterior-like cells (ALC) - which consist of a mixture of cells with weak expression of the *ecmA* or *ecmB* genes or both (Devine & Loomis, 1985; Gaskell *et al.*, 1992). These cells lack the sorting behaviour that confines pst A,B and O cells to the anterior of the slug. Removal of the anterior section relieves this inhibition and the ALC then sort to the anterior of the cut fragment to replace the excised prestalk zone. The ALC population is replaced in the prespore zone over the period of a few hours, probably by conversion of prespore cells to ALC (Sternfeld & David, 1982). The prespore region is in itself heterogeneous: deletions of successive portions of the prespore-specific SP60 promoter restricts expression of the gene progressively to more anterior sections of the prespore zone (Haberstroh & Firtel, 1990)

1.2.6 Culmination

At culmination, fruiting body formation is initiated in favourable environmental conditions (*ie.* low humidity, low pH, low NH_3 concentrations, high CO_2 concentrations and overhead light). If a period of slugging has been undertaken, then upon culmination the tip of the slug stops moving whilst its rear proceeds until it sits under the tip to form a "mexican hat" structure. If

culmination follows on directly from first finger formation, then the finger simply spreads laterally until the mexican hat is formed (**figure 1.1**).

Culmination is characterized by the maturation of spore and stalk cells in parallel with morphological changes designed to raise the spore mass to the apex of the stalk. Maturation of the prestalk cells to stalk is effected in a central cone region of the tip and a stalk tube grows downwards towards the substratum. The prespore mass moves up the stalk to its final position at the tip of the stalk and the subsequent maturation of the prespore mass into heat- and detergent-resistant spores is seen as the sorus becomes yellowed and opaque. In the wild, the formation of this fine-stalked fruiting body raises the spore mass above ground level, so that efficient spore dispersal can occur. If spores fall into humid conditions, then they rupture, releasing four amoebae. Factors regulating culmination are discussed in more detail below.

1.3 Regulation of the life cycle

1.3.1 Choices in the developmental pathway

Choices are made at various stages in the life cycle. A decision must be made between growth and development and later in the aggregate, between slugging and culmination. At the level of the individual cell, the choice between prestalk or prespore pathways and their various subdivisions is presented. Many substances that are produced endogenously by *D.discoideum* have been implicated in the regulation of development and differentiation. Their possible roles in the control of the life cycle are discussed below.

1.3.2 Cyclic AMP (cAMP)

cAMP is an indicator of cell starvation and is produced endogenously from ATP breakdown. It was initially identified as the chemoattractant in aggregation by Konijn *et al.* (1967) and is secreted at a rate of about 3 pmoles/10^8 cells/h

(Schaap *et al.*, 1984) in a pulsatile fashion. Secretion may be effected either by a membrane carrier (not yet identified) or possibly by vesicle-mediated exocytosis (Maeda & Gerisch, 1977). During aggregation, external cAMP is detected by surface cAMP receptors and studies with cAMP analogues indicate that the same surface receptor mediates chemotaxis, activation of adenylyl cyclase, guanylyl cyclase and the induction of differentiation (Van Haastert & Kein, 1983; Schaap & Van Driel, 1985), implicating cAMP in the control of numerous aspects of morphogenesis and cell differentiation.

Role of cAMP in the control of development

The importance of cAMP in development has been made evident by the study of overproduction mutants. The *rdeA* mutants produce $cAMP_i$ (internal cAMP) precociously and excessively and the time taken to complete the developmental cycle is reduced (Abe & Yanagisawa, 1983).

cAMP pulses at aggregation promote the expression of cAMP receptors (cARs, which are linked via G proteins to adenylate cyclase and to the components of the chemotactic signal transduction pathway), cAMP phosphodiesterase and the contact sites for aggregation (Gerisch, 1987). When receptors then are stimulated with external cAMP ($cAMP_e$), this induces the synthesis of cAMP internally ($cAMP_i$) by the activation of adenylate cyclase; $cAMP_i$ is then extruded, completing a signal-relay response. Adaptation occurs as cAR phosphorylation is induced by cAMP, while the extruded cAMP is rapidly broken down by cAMP phosphodiesterase, allowing the cARs to be dephosphorylated and to become responsive again to cAMP. Such adaptation and deadaptation cycles underlie the cAMP oscillations in aggregation (Vaughan & Devreotes, 1988).

For aggregation to occur, cells must respond to the cAMP signal relay in order to induce expression of the aggregative genes and chemotax towards aggregation centres. Cells which cannot respond (*car1*$^-$) do not aggregate (Sun

& Devreotes, 1991). Stimulation of a cAR activates a chemotactic signal transduction pathway, on a more rapid time-scale than is observed for the signal-relay response (Kimmel & Firtel, 1991), giving local phosphorylation of the myosin II heavy chain so that it associates with the cytoskeleton. Formation of pseudopodia is consequent and occurs within 5 seconds of cAMP binding (Newell & Liu, 1992). Cells exposed to this concentration wave of cAMP move up the gradient and stop once the peak of the wave has passed with the result that cells move towards the aggregation centre in pulses (Tomchik & Devreotes, 1981; Van Haastert, 1991).

Knowledge of the intracellular signalling cascade that links external cAMP stimulation to an actin/myosin response is as yet incomplete. Stimulation of cells by cAMP *in vitro* elicits a transient rise in intracellular cyclic GMP ($cGMP_i$), peaking within ten seconds (Van Haastert, 1987) and a rise in intracellular IP_3 displaying similar kinetics upon phospholipase C activation (Europe-Finner & Newell, 1987). As IP_3 is known to mobilise Ca^{2+} from intracellular stores (Europe-Finner & Newell, 1991; Flaadt *et al.*, 1993), this implicates Ca^{2+} in the control of chemotaxis. Activation of the cAMP receptor triggers a transient influx of Ca^{2+} within 5-10s by a $G_\alpha 2$-independent mechanism (Milne & Devreotes, 1993). The role of this calcium influx has not yet been determined.

In the mound, the tip region is thought to be a source of cAMP pulses (Traynor *et al.*, 1992) since cells move around and towards the tip region in waves, probably in response to cAMP pulses (Siegert & Weijer, 1992). It has been suggested that differential chemotaxis to cAMP is at the root of a sorting out mechanism whereby the prestalk cells scattered throughout the mound sort to the tip region. Tip cells have a shorter refractory period to cAMP than the posterior cells and cAMP phosphodiesterase levels are higher in the anterior region than in the posterior (Wang *et al.*, 1988). The anterior-like cells (ALCs) that remain scattered throughout the prespore zone may remain there due to

their unresponsiveness to cAMP in comparison with pst cells (Sternfeld & David, 1981; Mee *et al.*, 1986; Traynor *et al.*, 1992).

Cyclic AMP plays a central role in aggregation and culmination, eliciting diverse responses. This diversity may be due in part to the variety of cAMP receptors that are expressed at the different stages of development. cAR1 was isolated by Klein *et al.*(1988) and is expressed in early development. Its disruption prevents cells from entering the developmental programme, although some adenylate cyclase activation by external cAMP remains (Sun & Devreotes, 1991), indicating that another receptor sub-type may exist at this stage.

Receptor sub-type cAR2 is expressed predominantly in the prestalk cells of the slug (Saxe *et al.*, 1992). A third subtype (cAR3) is expressed at lower levels than the cAR1 receptor and has its maximal expression at the mound stage in the prespore zone (Saxe *et al.*, 1994). Disruption of the *car3* gene gives no obvious phenotype (Johnson *et al.*, 1993), suggesting that another receptor is able to substitute for its activity. A further receptor (cAR4) has also been identified (Saxe *et al.*, 1991) which is initially expressed at tip elongation, with its maximal expression at the anterior of the pseudoplasmodium (Ginsburg *et al.*, 1994). cAR1 at least is linked to a heteromeric G protein system (Firtel *et al.*, 1989) and since eight G_α subunits are expressed at different times in development (Cubitt *et al.*, 1992), the availability of a range of cAMP receptors and associated G_α subunits provides an array of different possible combinations that could lead to variable responses to cAMP at different times of development and in different cell types.

The G protein system links cAMP receptors to adenylate cyclase activity and there is evidence of heterogeneity in this population also. Two adenylate cyclases have been cloned (Pitt et al., 1992). One is expressed at aggregation (ACA) and the other (ACG) is expressed only at spore germination. Pupillo *et*

al.(1992) showed that multiple cAMP receptors are linked to adenylate cyclase in *D.discoideum* and that *car1*⁻ mutants and *gα2*⁻ mutants showed full activity with respect to adenylate cyclase activation, indicating that other cAMP receptors or G proteins must be present. Evidence that cAMP-stimulated adenylate cyclase activity is necessary for development to proceed comes from study of the *synag* mutants (Theibert & Devreotes, 1986), which show no cAMP-stimulated adenylate cyclase activity and are aggregation defective. A schematic representation of cAMP signalling pathways is given in **figure 1.3**.

Culmination, like aggregation, is highly dependent on the ability of the cells to produce and respond to cAMP. There is some evidence that culmination is initiated by a burst of internal cAMP production (Abe & Yanagisawa, 1983; Merkle *et al.*, 1984) resulting from adenylate cyclase activation. The intracellular culmination signalling pathways downstream of cAMP have not yet been fully elucidated, but activation of cAMP-dependent protein kinase A (PKA) is an important step in the cascade. De Gunzberg & Veron (1982) demonstrated that elevation of intracellular cAMP increased the activity of cAMP-dependent PKA by dissociating its regulatory subunit from the catalytic subunit. Mutants which overexpress the regulatory subunit under the prestalk-specific *ecm A* promoter or contain PKA that is unable to bind cAMP with the result that the PKA C subunit is permanently inactivated, are blocked in culmination (Mann & Firtel, 1991; Harwood *et al.*, 1992).

The role of cAMP in differentiation

In early development, nanomolar cAMP oscillations are produced with a periodicity of 6-10mins (Kimmel & Firtel, 1991). Later in development, cAMP levels augment and micromolar cAMP pulses are produced. Such differences in the periodicity of the pulses may enable the vegetative and early developmental genes (such as *discoidin I* and *II*) to be suppressed in aggregation and the later aggregation genes to be activated (Gerisch, 1987; Firtel *et al.*, 1989).

cAMP is essential also for the induction of both prespore and prestalk genes. Pulses of exogenous cAMP induce a number of developmental genes *in vitro* (Town & Gross, 1978; Kay, 1979) whilst inhibiting differentiation if added in excess. Yamada & Okamoto (1992) report that prespore and prestalk genes show differential responsiveness to excess external cAMP. In early development addition of exogenous cAMP inhibits prespore (SP96, D19) differentiation, whereas prestalk (ecmA/B) differentiation is only inhibited if cAMP is added at 0-2h. If added after this, prestalk-specific genes are always detected at about 10h. It has been noted that cAMP activates the expression of only some prestalk genes. The expression of both *Dd-ras* and *ecmA* is stimulated by extracellular cAMP whereas the expression of *ecmB* and of *pDd26* is inhibited by $cAMP_e$ (Berks & Kay, 1990; Esch & Firtel, 1991). Hence, the effects of cAMP on gene expression are varied and complex.

It is unclear at present whether external cAMP affects gene expression by eliciting a rise in intracellular cAMP or whether the internal signal transduction pathway is non-cAMP-dependent as suggested by experiments where adenylate cyclase inactivation has no effect on cAMP-dependent post-aggregative gene expression (Pitt *et al.*, 1993).

Later in development, it is thought that an increase in intracellular cAMP triggers spore maturation (Kay, 1989). The *rde A* mutant has elevated $cAMP_i$ and forms spores in monolayers whereas wild type cells do not (Abe & Yanagisawa, 1983). Also, treatment of wild type cells in monolayers with 8-Br-cAMP (a cell permeable analogue of cAMP) induces spore formation whereas cAMP itself does not (Kay, 1989).

1.3.3 DIFs

The existence of differentiation-inducing factor ("DIF") was proposed by Town *et al.* (1976), who noted the density dependence of stalk cell formation *in vitro* in monolayers and postulated that a hydrophobic, diffusible substance was necessary for stalk cell formation. Five active DIF species have since been

identified (Kay *et al.*, 1988; Masento *et al.*, 1988; Morris *et al.*, 1988) and 95% of the total activity is due to DIF-1, a chlorinated alkyl phenone.

DIF-1 is first detected at the tip stage and is produced maximally during slugging (Brookman *et al.*,1982). It induces prestalk gene expression *in vitro* at nanomolar concentrations (Williams *et al.*,1987) and represses prespore gene expression (Early & Williams, 1988), thus acting antagonistically to ammonia. The work of Early & Williams (1988) indicated that repression of the D19 prespore gene was occurring at the transcriptional level, implying that DIF might be acting like a steroid hormone. In addition, weak acids such as DES (diethylstilboestrol) and butyrate, which promote stalk cell formation, also elevate DIF levels (Kwong & Weeks, 1989). A further indication that DIF is required for both differentiation and development was obtained from the study of DIF-less mutant (HM44), which is arrested at the mound stage and fails to generate prestalk cells (Kopachik *et al.*,1983).

DIF is distributed unequally through the multicellular aggregate and Brookman *et al.* (1987) show that its concentration is highest at the posterior end of the slug and declines towards the anterior, which is unexpected since DIF would be anticipated to be highest in the anterior zone as it promotes prestalk differentiation. Kwong *et al.*(1990) have discovered that the greatest rate of DIF synthesis is in the *ecmA/B*-expressing cell population at the slug anterior, whilst Naylor *et al.*(1992) report that the DIF-inactivating enzyme - DIF-1 dechlorinase - is located solely in the anterior zone. It has been suggested either that the high concentration of DIF assigned to the posterior zone might be due in the greater part to DIF present in the slime sheath rather than in the prespore cell mass, or that prespore cells are somehow "protected" from the high DIF concentration in their environment, perhaps by the prespore promotion property of ammonia in the posterior region. It has been proposed therefore that ammonia and DIF might constitute a pair of morphogens acting antagonistically (Gross *et al.*, 1981; Kay & Jermyn, 1983).

There is no evidence at present to indicate that DIF acts on elements of the cAMP signal transduction pathway as has been proposed for ammonia and recent work suggests that the antagonistic action of DIF is not mediated through an acidic vesicle, since DIF has no effect on *in vitro* vesicle acidification (Giglione & Gross, unpublished).

1.3.4 Weak acids

Weak acids have been implicated in the control of development in *D.discoideum* and have also been proposed as antagonists to ammonia in the prestalk zone (Inouye, 1990). Prestalk cells are more highly catabolic during development than prespore cells (Yamamoto & Takeuchi, 1983) and therefore would be expected to produce more ammonia than prespore cells. However, Inouye (1990) reports that stalk cells also produce a weak acid and proposes that a weak acid, with a small diffusion range could counteract the effects of ammonia in the prestalk zone. Propionate, acetate and succinate are all released as by-products of protein breakdown (Williams *et al.*, 1984; McConaghy *et al.*, 1984) and propionate has been demonstrated to promote stalk cell differentiation whilst inhibiting spore cell differentiation (Gross *et al.*, 1983; Town *et al.*, 1987). Further support for the theory of Inouye (1990) comes from the observation that prestalk cells are more susceptible to acidification by weak acids than prespore cells, probably because their plasma membrane proton pump activity is lower (Inouye, 1989).

Culmination is promoted by both weak acids and low pH (Inouye, 1988). Williams *et al.* (1984) reported that weak acids inhibit the secretion of cAMP, with a consequent increase in $cAMP_i$. However, a later study by Schaap *et al.* (1994) has shown that weak acids (propionate and dimethyloxazolidinedione) inhibit adenylate cyclase. Since weak acids lower the cytoplasmic pH (Van Duijn & Inouye, 1991; Brénot *et al.*, 1992), it is likely that the decrease in the cytosolic pH induced by weak acids inhibits adenylate cyclase activity directly, as the pH optimum of the enzyme is around 7.8 (Schaap *et al.*, 1994). As it has

been reported that a rise in cAMP precedes culmination (Abe & Yanagisawa, 1983; Merkle *et al.*, 1984) and that the pH of the anterior section of the slug drops by about 0.5 units at culmination (Rand, 1985), it is unlikely that promotion of culmination by weak acids is mediated via cAMP, unless another adenylate cyclase with a lower pH optimum is dominant at culmination.

1.3.5 Ammonia

Ammonia is produced endogenously by amoebae in millimolar quantities (Schindler & Sussman, 1977) as a by-product of protein catabolism and is a candidate for a diffusible morphogen in *D.discoideum*. It exerts its effect at many levels: promoting slugging over culmination, acting as an inhibitor of aggregation, and its presence favours the prespore pathway in the prestalk/prespore choice.

Control of aggregation

In excess, ammonia prevents or delays aggregation (Lonski, 1976; Williams *et al.*, 1984; Riley & Barclay, 1990). It has also been found that some slugger mutants (*ie.* those that have a prolonged migratory phase) are hypersensitive to the inhibition of aggregation by ammonia (Schindler & Sussman, 1979; Gee *et al.*, 1994). It has also been reported that ammonia speeds up cell movement (Bonner *et al.*, 1989; .; Van Duijn & Inouye, 1991); but there may be differential effects depending on the cell type since Feit *et al.* (1990) report that in the aggregate, ammonia prevents the movement of ALC to the tip of the aggregate. It could be that the ALC are cells whose chemotaxis to the cAMP pulses of the tip has been inhibited by the build up of ammonia in the posterior region of the aggregate. Alternatively the tip region itself may inhibit the sorting of ALC to the anterior as its removal relieves this inhibition.

Control of slugging

Migration of the slug is directed by the anterior section. Kosugi & Inouye (1989) have shown that the slug orients itself, tip first, away from high concentrations of ammonia. In the wild this is a survival mechanism, enabling the slugs to move away from indicators of starvation (*eg.* high ammonia concentration) to an environment where conditions are favourable for spore dispersal. Many further lines of evidence indicate that the decision to slug is controlled by ammonia. Schindler & Sussman (1977) showed that exposure of slugs to an ammonia-removing enzyme cocktail induced culmination. Bonner *et al.* (1985) demonstrated that low pH favours slugging, as does development on a substratum with low buffering capacity (Newell *et al.*, 1969). Both of these conditions would increase the NH_3:NH_4^+ ratio (Inouye, 1988) and high humidity may promote slugging by slowing the evaporation of ammonia.

A number of mutants have been isolated which have a prolonged slugging phase or are completely unable to culminate (Newell & Ross, 1982). Some of each group have been found to be hypersensitive to the inhibition of culmination or aggregation by ammonia (Schindler & Sussman, 1979; Gee *et al.*, 1994), further supporting the notion that the decision between slugging and culmination is controlled by ammonia.

Control of culmination

Several lines of evidence have implicated ammonia in the control of culmination. Enzymatic removal of ammonia results in premature culmination (Schindler & Sussman, 1977) and a number of the slugger mutants are hypersensitive to ammonia (Schindler & Sussman, 1979; Newell & Ross, 1982; Gee *et al.*, 1994). A further indication that ammonia affects culmination has been obtained by Hopper *et al.* (1993). Their work suggests that cAMP-dependent protein kinase A is inhibited by ammonia.

Control of the prespore/prestalk choice

There is much evidence that ammonia regulates cell differentiation. Premature stalk maturation is induced by the removal of ammonia in the presence of DIF (Wang & Schaap, 1989) and in monolayer cultures (where differentiation is separated from morphogenesis), stalk differentiation is inhibited by the addition of ammonia whereas the expression of prespore markers is enhanced (Bradbury & Gross, 1989; Kwong & Weeks, 1990; Riley & Barclay, 1990). At least one of the slugger mutants displays an abnormally small prestalk zone (McWilliams, 1982) and Feit *et al.* (1990) show that ammonia treatment reduces the volume of the prestalk zone in wild type slugs.

Possible signal transduction pathways for ammonia

Initially, a hypothesis in which NH_3 exerts its many developmental effects by interfering with cAMP production was proposed by Schindler & Sussman (1978) and gained weight as a result of the work of Williams *et al.* (1984) who showed that NH_3 inhibited $cAMP_i$ accumulation. Since the cAMP relay system is essential for aggregation and a burst of $cAMP_i$ synthesis essential for culmination, it has been proposed that ammonia might affect aggregation and culmination by interfering directly or indirectly with the production of cAMP by adenylate cyclase. Further circumstantial evidence for this theory comes from the work of Hopper *et al.* (1993) who show that protein kinase A, a downstream target of cAMP in development (cAMP-dependent PKA), is regulated by ammonia. The possible roles of cAMP and PKA in transducing the ammonia signal will be explored further in chapter 8.

It has repeatedly been shown that processes that are inhibited by ammonia are also dependent upon the correct functioning of PKA. For example, aggregation is inhibited by ammonia (Williams *et al.*, 1984; Feit, 1988; Siegert & Weijer, 1989) and cells that are deficient in PKA activity do not aggregate (Simon *et al.*, 1989; Firtel & Chapman, 1990). Bonner & Williams (1994) have demonstrated that inhibition of PKA under the prestalk promoter *ecmA*

generates slugs that are defective in phototaxis - an effect which is mimicked by treating slugs with ammonia (Darcy & Fisher, 1990). Finally, culmination is inhibited by ammonia (Schindler & Sussman, 1977) or by expression of a dominant inhibitor of PKA under the *ecmA* promoter (Harwood *et al.*, 1992; Hopper *et al.*, 1993). However, recent experiments by Schaap *et al.* (1994) cast doubt on the notion that ammonia influences PKA via an effect on cAMP production (see chapter 8).

1.4 Theories of weak base action

1.4.1 Possible primary intracellular target of ammonia

It has been demonstrated that it is the unprotonated moiety (NH_3) of ammonia that is the active species in inhibition of aggregation and culmination, since lowering the pH of externally added ammonium salts (hence decreasing the NH_3:NH_4^+), reduces the efficiency of inhibition by the base (Schindler & Sussman, 1977; Sternfeld & David, 1979; Gross *et al.*, 1983; Neave *et al.*, 1983; Riley & Barclay, 1990). Since the unprotonated form of the weak base is the active agent, ammonia must either exert its effect intracellularly or some extracellular receptor or enzyme must be specifically inhibited by the unprotonated form. No evidence has been presented to show that the unprotonated form is a direct inhibitor of any intracellular or extracellular enzyme, so the remaining option is that ammonia might act as a weak base to raise intracellular pH, either the cytoplasmic pH or the pH of acidic compartments.

If acting intracellularly, then ammonia could act as:

(a) a general metabolic inhibitor, reducing cell viability

(b) a specific inhibitor of some intracellular enzyme *eg.* adenylate cyclase

(c) a weak base raising cytosolic pH

(d) a weak base raising acidic vesicle pH

It has previously been shown that some of the effects of ammonia are reversible (Schindler & Sussman, 1977) demonstrating that ammonia does not reduce cell viability. There is no clear record of ammonia as a specific inhibitor of aggregative or of culminant enzymes. It has been proposed that ammonia might raise cytosolic pH (Gross *et al.*, 1983) or that it might act by raising the pH of an intracellular compartment (Gross *et al.*, 1988).

1.4.2 Predictions concerning the action of ammonia in vivo

Specific predictions can be made and investigated in relation to the behaviour of ammonia. To permit distinction between a model for weak base action *in vivo* in which ammonia specifically inhibits particular enzymes, a model where cytosolic pH is raised and one in which effects are elicited by raising the pH of some vesicular acidic space, the effects of an array of weak bases are studied. In the first part of this thesis, a comparative study will be made of various weak bases in an attempt to discover the intracellular target of ammonia.

If ammonia were acting as a specific inhibitor, then other, chemically distinct weak bases ought not to produce similar effects. If acting as a weak base, then other weak bases ought to mimic the effects of ammonia. In brief, the basis for distinction between the cytosolic pH model and the vesicular model is as follows: all weak bases of similar pK_as ought to raise cytosolic pH to similar extents. On the other hand, if ammonia acted by dissipating a pH gradient between the acidic vesicle and the cytosol, then the efficiency of dissipation of the gradient by the bases ought to be a function of their ability to act as protonophores, a property which is dependent on their hydrophobicity. The following sections set out a theoretical framework for the action of weak bases *in vivo* and make specific predictions for each of the possible models for weak base action. A variety of weak bases are considered (imidazole, ammonia, methylamine, propylamine, octylamine and chloroquine), which vary in hydrophobicity, structure and pK_a (see **Appendix I**).

1.4.3 Differences in the ability of bases to raise cytosolic pH

If bases were acting to raise cytosolic pH, then any differences in their efficiency of action would be due either to differences in their ability to enter the cytosol, or to variations in their proton-trapping capacities.

Passage of an unprotonated base across a lipid bilayer

The rate of transmembrane passage of an unprotonated base is dependent upon its lipid solubility (hydrophobicity) and its conformation. Trans-membrane diffusion is often described in terms of the Solubility-Diffusion model (Diamond *et al.*, 1974), which considers that resistance to the entry of a molecule into (and exit from) a membrane is negligible, therefore one can assume that transfer across a membrane is dominated by partition into the bilayer. Using this assumption, the following equation can be derived

$$P = \frac{K_p . D_m}{d} \qquad 1$$

where P = permeability coefficient, K_p = partition coefficient, D_m = diffusion coefficient within membrane and d = width of membrane. According to Overton's rule (Overton, 1899), permeability coefficients correlate with oil-water partition coefficients (a measure of hydrophobicity), a prediction that is borne out experimentally (Bar-On & Degani, 1985; Walter & Gutknecht, 1986) for all but the smallest molecules. Some smaller molecules traverse the membrane faster than is predicted by Overton's rule, because the membrane acts like a polymeric sieve (Lieb & Stein, 1969). Molecules that are smaller than the sieve pore size are able to traverse easily and those that are larger than the pore size cross according to their ability to partition into the membrane. An alternative explanation is that transient aqueous pores exist in the membrane (Weaver *et al.*, 1984). Either way, the analogy of a membrane with an oil-water partition system holds only for molecules that are larger than the pore size. In practice, the analogy breaks down for molecules with a molecular weight less than about 50 (Walter & Gutknecht, 1986). Therefore,

one would expect all unprotonated amines (with M_w > 50) to cross the membrane in line with their partitioning coefficients into octanol. Ammonia (M_w = 18) and methylamine (M_w = 32) are the only exceptions to the rule as they have molecular weight less than 50. Therefore, both would be more likely to cross the membrane than predicted by their hydrophobicity. A general conclusion is that highly hydrophobic bases (those with positive log $P_{octanol}$ values) will able to cross biological membranes more easily than hydrophilic ones. The passage of bases across membranes may also be influenced by their structure. Large molecules with a number of ring structures require higher activation energy for insertion into the membrane than weak bases composed simply of aliphatic chains.

In practice, the differences in the rate of passage of the bases are small, for example, literature values for permeability of methylamine and propylamine across bilayers are 1.0 x 10^{-6} and 4.3 x 10^{-6} cm/sec respectively (Bar-On & Degani, 1985), which translate into small differences (less than 1 second) in the rate at which equilibrium base concentration is set up across the membrane. Therefore, if the inhibitory efficiency of the bases was solely dependent upon the rate of passage of the unprotonated form across the membrane, then various weak bases would be expected only to display small differences (of the order of seconds) in their rate of inhibition. Consequently, since long-term exposure to ammonia is required to elicit developmental effects, weak bases are not expected to be acting *in vivo* by affecting cytosolic pH.

Accumulation and protonation of the base in the cytosol

Weak bases would be expected to accumulate in the cytosol as the external and cytosolic base concentrations equilibrate. External unprotonated base will enter the cytosol and equilibrate with the external unprotonated base concentration. However, a proportion of the internal unprotonated base will be protonated as the equilibrium is re-established. This proportion is dependent upon the pK_a of the base and on the pH of the cytosol. Therefore, if bases are added which have equivalent pK_a values, then they will give rise

to the same cytosolic concentration of unprotonated base, and hence will raise cytosolic pH_i to the same extent.

1.4.4 Variation in the abilities of bases to raise vesicular pH

The ability of weak bases to raise the pH of acidic vesicles will be dependent on three properties

(a) their ability to traverse biological membranes

(b) their proton-trapping capacity in the cytosol

(c) their ability to generate a proton leak across the vesicular membrane

Passage of the base across lipid bilayers

The passage of the bases across the lipid bilayer into the cytosol and then across the vesicular compartment into the acidic vesicle is governed by the same factors as those mentioned in section 1.4.2.

Accumulation and protonation of the base in vesicular compartments

Accumulation of weak bases in intracellular acidic vesicles is well documented. Ammonia concentrates in the acidic space of chloroplast thylakoids (Good, 1960; Crofts, 1967; Rottenberg *et al.*, 1972). Chloroquine concentrates in the lysosomes (Ohkuma & Poole, 1981; Hollemans *et al.*, 1981) and in the food vacuoles of malarial parasites (Krogstad *et al.*, 1985; Krogstad & Schlesinger, 1987).

The rate of accumulation of the bases in such compartments is dependent both on the acidity of the vesicle and on the pK_a of the base. When a proton gradient is generated across a vesicular membrane, the concentration of total base (protonated and unprotonated) within the acidic compartment will increase since the equilibrium within the vesicle shifts as the base is protonated. The level of accumulation of bases within the acidic compartment can be described by the following relationship

$$\frac{[B + BH^+]_{in}}{[B + BH^+]_{out}} = \frac{K_a + [H^+]_{in}}{K_a + [H^+]_{out}} \qquad \mathbf{2}$$

where $[B + BH^+]$ represents the total base concentration (adapted from Schuldiner *et al.*, 1972). If the pK_a of the base is much higher than either the internal or external pH, then K_a is much lower than either $[H^+]_{in}$ or $[H^+]_{out}$, so equation **2** above can be approximated to

$$\frac{[B + BH^+]_{in}}{[B + BH^+]_{out}} = \frac{[H^+]_{in}}{[H^+]_{out}} \qquad \mathbf{3}$$

hence, accumulation of the base within the compartment will be strongly dependent on the pH gradient. However, if the pK_a of the base is significantly lower than the pH of either compartment, then K_a will be much higher than $[H^+]_{in}$ or $[H^+]_{out}$. Under these conditions, equation **2** simplifies to

$$\frac{[B + BH^+]_{in}}{[B + BH^+]_{out}} = 1 \qquad \mathbf{4}$$

The overall result, for a base with a high pK_a value, is that the level of accumulation in the vesicle will be dependent upon the proton gradient, but the lower the pK_a of the base, the greater the tendency to distribute equally across the membrane independently of the ΔpH. None of the bases used in this study has a pK_a lower than both the external pH (7.3) and the vesicular pH (a minimum of 4.3), but imidazole (pK_a = 7.1) would be expected to accumulate in the vesicle to a lesser extent than ammonia (pK_a = 9.3). By the same token, methylamine, propylamine and octylamine would accumulate to a fractionally greater extent than ammonia, since they all have a pK_a of 10.2. Methylamine, propylamine and octylamine should be equally efficient in proton-trapping since they have identical pK_a values. Diamines, such as chloroquine (pK_{a1} = 8.1, pK_{a2} = 10.2) will accumulate in the vesicle with the following relationship to

monobasic amines

$$(f_{base})^2 = f_{CQ} \qquad \mathbf{5}$$

where f is the accumulation factor of the weak base (Reijngoud & Tager, 1976). It is expected then that chloroquine would produce a greater decrease in the H^+ concentration than the other bases, as it would be able to dissipate more of the pH gradient than other bases before osmotic pressure prevented further accumulation.

The conclusion is that bases with identical pK_a values would be expected to accumulate within acidic vesicles to the same extent. A base with a lower pK_a value would have a greater tendency to distribute equally across the membrane, independently of the pH gradient.

Generation of a proton-leak across the membrane

It is often assumed that protonated bases are incapable of crossing lipid bilayers (de Duve *et al.*, 1974; Hollemans *et al.*, 1981). However, a wealth of references refer to bases as protonophores. For example, methylamine and ammonia are well-known uncouplers of electron flow from phosphorylation across the thylakoid membranes of chloroplasts (Crofts, 1967; Mitchell, 1966; Rottenberg *et al.*, 1972). Recent ^{1}H-NMR studies by Nissani & Ginsburg (1989) indicate that some protonated bases are indeed capable of diffusing across bilayers without significantly perturbing the bilayer structure. This confirms that some bases are able to act as proton-shuttlers rather than relying solely on proton-trapping within the vesicular compartment for dissipation of pH (see **figure 1.4**). It follows that bases which are good proton-shuttlers will be able to dissipate a pH gradient at lower concentrations than bases whose protonated species are less capable of traversing membranes.

Nissani & Ginsburg (1989) used *E.coli* vesicles which were acidified by an

ATPase and shown to generate a ΔpH and ΔΨ (membrane potential), reasoning that if a protonated species were able to back-flux across the vesicular membrane, ΔΨ should decrease as well as ΔpH. They found that the amines tested differed greatly in their ability to dissipate the transmembrane pH gradient; of the three bases chloroquine, octylamine and propylamine, chloroquine was by far the most effective (requiring 0.125μM to produce a change in ΔpH of -0.5) and propylamine the least effective (needing 900μM to produce the same relative ΔpH change). They postulated that the variation in efficiency correlated with the ability of the protonated and unprotonated bases to traverse the membrane. Variation could not be ascribed to differences in proton titration by the bases since their pK_as are fairly similar. They concluded that despite the fact that intercalation of an ion into a bilayer is energetically unfavourable, some of the protonated base trapped in the vesicle leaks back into the cytosol and estimated that for example, only 0.05% of the total octylamine flux would need to be in the protonated form to account for its effect on pH dissipation. These findings strongly suggest that the differences in the efficiencies of the bases in dissipating pH gradient across the membrane can be ascribed to differences in the ability of the protonated species to back-flux across a membrane as a result of their varying hydrophobicities. Therefore, if acting to dissipate a transmembrane pH gradient, weak bases would be expected to vary in their efficiency of inhibition according to their hydrophobicity and hence their ability to act as proton shuttles. As octylamine is far more hydrophobic than ammonia, for example, it would be expected to be the more effective protonophore.

1.4.5 Implications for the action of weak bases

The theory discussed above suggests a way to probe the target of ammonia inhibition of aggregation and culmination *in vivo* by using an array of weak bases with different hydrophobicities, chemical structures and pK_as. If all mimic ammonia, then it would imply that ammonia is not acting as a specific enzyme inhibitor, rather that it is the weak base activity of ammonia that is

responsible for its inhibitory activity. If acting to raise cytosolic pH, then each base with identical pK_as should act similarly. However, if a dependence of inhibitory efficiency on the hydrophobicity of the base was found then it would implicate an acidic vesicle as the intracellular target of ammonia.

1.5 - The Endocytic System in *D.discoideum*

In view of the possibility that the inhibitory effects of ammonia on aggregation and culmination may be exerted via neutralization of an acidic compartment, a brief overview is given below of the nature of the extensive endocytic system in *D.discoideum* and of the components that are involved in its acidification.

1.5.1 Structure of the endocytic system

D.discoideum amoebae possess an active endocytic system, shown schematically in **figure 1.5**. During phagocytosis, membrane is internalized at the rate of three cell surface equivalents per hour according to measurements of the rate of intake of labelled plasma membrane that is associated with phagocytosed beads (De Chastellier *et al.*, 1983). Fluid-phase pinocytosis also proceeds at a rate that matches or is higher than that in macrophages with reported values ranging from 0.0045 - 0.014pl fluid internalized/min/cell in the axenic strains when measured with the fluorescent marker FITC-dextran (Bof *et al.*, 1992; Kayman & Clarke, 1983; Thilo & Vogel, 1980). Wild-type cells lacking the axenic mutation rely on bacterial food supplies and generally have lower pinocytic rates; for example, in strain DdB the pinocytosis rate reaches a maximum of 0.0001pl fluid internalized/min/cell (Kayman & Clarke, 1983).

From these data, it is evident that *D.discoideum* possess extensive internal membrane compartments. It is not known whether endocytic organelles are transient structures. If so, their activities would change according to their age and place in the endocytic "traffic". A corollary is that the components of

vesicular membranes (and consequently their contents) would be constantly changing upon fusion with new compartments (Dunn & Maxfield, 1992). An alternative view is that vesicles are stable structures which interact with each other via vesicular shuttles (Griffiths & Gruenberg, 1991).

1.5.2 pH of compartments in the endocytic system

Many of the components of the endocytic system have low internal pH, which is a prerequisite for the dissociation of ligands imported from membrane receptors and enables degradation of imported macromolecules and bacteria. The pH gradient between the cytosol and the intravesicular space provides a driving force for the transport of ions (such as Ca^{2+} and phosphate), amino acids, carbohydrates and lytic enzymes (Yamashiro & Maxfield, 1988; Stevens, 1992) as is well documented for plant vacuoles (Matile, 1978). The endocytic system is also essential for targetting proteins that are synthesized in the endoplasmic reticulum to their correct intracellular sites. As proteins are processed, they acquire surface oligosaccharides, the nature of which depends partly on the protein structure and partly on the intracellular compartment in which they are located. Each compartment contains specific receptors for these complex sugar chains and specific modification enzymes, which determine the subsequent trafficking of the proteins. In *D.discoideum*, such post-translational modification of proteins results in differential N-glycosylation of polypeptides which are then passed at varying rates to the Golgi apparatus for further processing or are constitutively secreted. Those that are processed in a regulated manner are targetted to the highly acidic lysosomal compartments for export (Cardelli *et al.*, 1986) and there is evidence that increasing the pH of such compartments perturbs protein sorting and targetting (Cardelli *et al.*, 1989).

1.5.3 Measurement of intracellular pH in D.discoideum

In this thesis, two techniques are employed in studying the pH of intracellular compartments in response to weak base treatment:

Vesicular acidification in vitro

An endomembrane or "acidosome" fraction can be isolated from whole cells which is rich in vacuolar H^+-ATPase and is capable of acidifying *in vitro* (Padh *et al.*, 1989a; Rooney & Gross, 1992). This is used to test directly whether or not weak bases are capable of dissipating a pH gradient across vesicular membranes and to determine their inhibitory efficiencies of the bases. Effectively, the isolated vesicle is used as a model system to study the passage of weak bases in their charged and uncharged forms across biological membranes in the presence of a pH gradient.

Intracellular pH measurement by NMR

^{31}P nuclear magnetic resonance (^{31}P-NMR) is a powerful tool for measuring intracellular pH and is used in this thesis to probe the effects of weak bases on endosomal and cytosolic pH, simultaneously and *in vivo*. This allows a direct determination of the primary intracellular target of weak bases.

Living cells contain a plethora of intracellular phosphate-containing compounds and the ^{31}P-NMR resonances of a number of these are pH-sensitive, so they act as natural intracellular pH probes. Some compartments at different pH values can be distinguished, for example external and cytosolic pH can be observed. More importantly, the endosomal system can be labelled with various plasma membrane-impermeable ^{31}P-containing probes whose resonances are easily distinguished from those of naturally-occurring phosphate compounds (Satre *et al.*, 1989; Pelorgeas *et al.*, 1992; Brénot *et al.*, 1992). In their 1992 study, Brénot *et al.* demonstrated that the endocytic system contains a variety of compartments at different pH values. Using various phosphonate compounds as pH-sensitive ^{31}P-NMR probes of the endocytic system, they showed that the compounds first entered a highly acidic "early endosomal" compartment (pH 4.3) with a t½ of 18mins. The probe then appeared in a "late endosomal" compartment (pH 5.8-6.0) before passing being translocated to the cytosol (pH 7.2-7.4). Fluorescence marker studies indicate that the terminal organelle in

the vesicular traffic is not the lysosome but a post-lysosomal recycling compartment (at pH 6.2), as yet undocumented in higher eukaryotes (Aubry, 1994). In other systems (Mellman *et al.*, 1986; Yamashiro & Maxfield, 1988), it is well documented that acidification of the endocytic system is effected by proton-pumping ATPases. Brénot *et al.*'s (1992) results suggest that this is also the case in *D.discoideum* as induction of an aerobic-anaerobic transition to disable ATPases gave a dramatic increase in the early endosomal pH.

1.5.4 Role of ATPases in compartment acidification

More direct evidence for the existence of specific proton pumps comes from the work of Padh *et al.* (1989a; 1989b), who observed that the cytosol of amoebae is studded with vacuoles up to about 2μM diameter which are shown to be acidic by virtue of their ability to concentrate the weak base acridine orange. Uptake of this base is inhibited by NBD-Cl (7-chloro-4-nitrobenzo-2-oxa-1,3-diazole) a specific inhibitor of the vacuolar-type ATPases (V-type ATPases) and the ability of vesicles to concentrate acridine orange co-distributes with an NBD-Cl-sensitive ATPase activity on sucrose density gradients. Such NBD-Cl-sensitive ATPase activity had previously been found to be associated with other acidifying organelles such as the lysosomes (Al-Awqati, 1986; Mellman *et al.*, 1986) and is characteristic of the V-H^+-ATPases in general. Uncoupling with nigericin (at micromolar concentration) or weak bases stimulated the ATPase activity twenty-fold, suggesting that the pump generates a membrane potential (Padh *et al.*, 1989a).

V-H^+-ATPases have been isolated from a profusion of endomembrane fractions and there is debate as to their distribution *in vivo*. Heuser *et al.*'s (1993) electron micrographic study showed that the contractile vacuole system of *D.discoideum* is populated with V-ATPases and it is likely that the vesicles of Padh *et al.* (1989a) are fragments of this contractile vacuole. Fok *et al.* (1993) observed V-ATPases as immunofluorescence resulting from treatment with the antibody to the 57kDa (B) subunit of the mammalian chromaffin granule V-

ATPase and generated specific antibodies to the 100 and 68 kDa subunits of this V-ATPase, which co-localised with the anti-B subunit antibody. Moreover it has been discovered that the distribution of these antibodies closely resembles that of calmodulin, suggesting that the V-ATPase pool in *D.discoideum* is associated with Ca^{2+}-storage vesicles (Zhu *et al.*, 1993). A study by Nolta *et al.* (1993), indicated that other organelles in addition to the contractile vacuole system were stained by a polyclonal antiserum raised against the lysosomal and acidosomal cell fractions. Immunoreactive sections of the cell included cytoplasmic clusters of vacuoles and tubules of diameter 0.1-1μm. This polyclonal antiserum labelled fewer cytoplasmic compartments than were able to concentrate acridine orange, suggesting that there is a heterogeneity in the cellular population of V-ATPases, a notion which is backed up by the fact that the chromaffin B-subunit antibodies of Fok *et al.* (1993) recognised only the contractile vacuole system.

1.5.5 The vacuolar H^+-ATPase

Vacuolar ATPase contributes roughly one third to the total ATPase activity of lysates of axenically-grown cells (Padh *et al.*, 1989b) and is sensitive to inhibition by Bafilomycin A_1 (Bowman *et al.*, 1988) as well as NBD-Cl (Padh *et al.*, 1989a). Vanadate, which inhibits the P-type ATPases of the plasma membrane (Nelson, 1992), has no effect on the V-type ATPase at μM concentrations. In *D.discoideum*, the enzyme has an optimum pH of 8.0 and depends on Mg^{2+}-ATP for its function (Padh, 1989). In vacuolar systems their function is to create a proton-motive force across the membrane using ATP and since they are not usually directly coupled to ion transport they also generate a membrane potential, which can be dissipated by the entry of chloride or other ions (Nelson, 1992; Stevens, 1992; Padh, 1989). Since they operate below thermodynamic equilibrium, they are unable to make ATP at the expense of the generated proton-motive force (Harvey, 1992), probably because one of the membrane proteolipids is double the size of that in the F-ATPase, thus generating a proton slip (Moriyama & Nelson, 1988). In their primary

sequence and quaternary protein structure, the V-ATPases are shown to be distant homologues of the F-ATPases (Bowman *et al.*, 1992; Nelson & Taiz, 1989), but they bear a closer resemblance to the ATPases of archaebacteria, suggesting that the eukaryotic V-ATPases may result from a primaeval parasitic relationship between archaebacteria and eukaryotic species (Gogarten *et al.*, 1989).

The V-ATPase bears many structural similarities to the F- and P-type ATPases. Eight subunits have so far been identified by gel electrophoresis (Nolta *et al.*, 1991) and the structure of the ATPase is shown in **figure 1.6**. The 90 and 17kDa subunits are integral to the membrane, whereas the 68 and 53 kDa (57 kDa by some reports, see Fok *et al.*, 1993) subunits make up the hexameric head structure. Normally the A subunit (68 kDa) is the catalytic subunit and the B (53/57 kDa) subunit has a regulatory high-affinity nucleotide-binding function (Gluck, 1993). The remainder of the subunits make up the stalk region.

1.5.6 Mutations of the vacuolar ATPase

Mutations in the vacuolar ATPases are known to have wide-ranging effects. One of the best-studied systems in this respect is yeast, where a range of mutations affecting the V-ATPase and the acidification system have been discovered. Where acidification of the vesicles is inhibited, amino acid and Ca^{2+} transporters no longer function (Ohsumi & Anraku, 1981; Ohsumi & Anraku, 1983). Vacuolar membrane ATPase (*vma*) mutants have been isolated (Hirata *et al.*, 1990; Ohya *et al.*, 1991; Umemoto *et al.*, 1990), whose growth is inhibited in high pH media and show significant perturbation of cytosolic Ca^{2+} levels. Ohya *et al.* (1991) show that the cytosolic Ca^{2+} concentration in one such mutant is 900nM in comparison to 150-180nM in the wild-type.

1.5.7 Acidification-defective mutants in D.discoideum

It is a prediction of a vesicular model for weak base action (Gross et al., 1988) that cell strains harbouring defects in the acidification of endosomal compartments should be arrested in development as are aggregates treated with high ammonia concentrations (Schindler & Sussman, 1977). It is likely also that they could resemble the slugger mutants, some of which have been demonstrated to be hypersensitive to ammonia (Gee et al., 1994). To test this prediction, the developmental characteristics of a number of acidification-defective mutants are examined in this study.

The Hgr mutants

A number of endocytosis-deficient mutants have been generated in *D.discoideum* by chemical mutagenesis of an axenic parent strain (Bof *et al.*, 1992). Some of these isolates have been found to be defective in vesicular acidification. For example, the average endosomal pH of the isolates Hgr5 and Hgr8 is roughly 0.5 pH units higher than in the parent strain (Bof *et al.*, 1992; Klein *et al.*, 1988). The difference between the pH of the early endosomal compartments in the mutants and in Ax2 is even more marked: Ax2 rapidly acidifies its early endosomes to a minimum pH of 4.6, whereas Hgr 8 only achieves a pH_{min} of 6.0 (Aubry *et al.*, 1993). Hence, the very acidic early endosomal compartment that is normally observed is absent in this mutant. NMR profiles using an endocytic probe show that the very acidic pH 4.3 compartment of Ax2 is absent in both Hgr5 and Hgr8 and that both of these strains have markedly decreased ATPase activity (Bof *et al.*, 1992). However, the precise genetic lesions responsible for their phenotype are unknown and could arise in any of the following areas: ATPase activity, membrane proton permeability, endosomal ion channels essential for generation and maintenance of a pH gradient or the association of endocytic vesicles with acidosomes (Padh *et al.*, 1991). In chapter 6, the developmental morphologies of four Hgr mutants are examined. In addition, they are tested for hypersensitivity to weak bases and for pH-dependence of growth and development.

Inhibition of vacuolar acidification by antisense

Antisense inhibition is a powerful mechanism used by both prokaryotes and eukaryotes to regulate gene expression. For example, in prokaryotes, maintenance of specific bacterial plasmids at cell division is assured by antisense regulation. Plasmids R1 and F encode an mRNA - *sok* - that is complementary to an endogenously-coded mRNA - *mok* - whose protein product induces the expression of a cytotoxic factor encoded by *hok*. If a cell segregates without a plasmid, then the *hok* gene is translated and the cell dies (Gerdes *et al.*, 1992). Similar systems operate in eukaryotes, where RNA:RNA interactions are mediated by initiation factors such as eIF4a and RNP1A (reviewed in Nellen & Liechtenstein, 1993). Although the exact nature of the mechanism of antisense inhibition of gene expression has not been elucidated, it is generally accepted that antisense mRNA binds to a strand of complementary mRNA and prevents its translation. Antisense:sense hybrids are rarely found in cells, so they are probably rapidly recognized and degraded by dsRNases. Antisense inhibition occurs by preventing translation of the endogenous mRNA by proteins, by sequestering it in an inappropriate compartment or by increasing its rate of degradation (reviewed in Green *et al.*, 1986; Nellen & Lichtenstein, 1993). It is thought that specific secondary structures are required for antisense-mediated inhibition to occur. In bacteria, stem-loop secondary structure formation is required in both the *copT* fragment of the *repA* mRNA and antisense *copA* strand for the formation of a hybridized "kissing complex" (Blomberg *et al.*, 1990) which prevents translation of the *repA* mRNA. In *D.discoideum*, Scherczinger *et al.* (1992) find that the length of the antisense mRNA is important in determining its biological activity: partial mRNAs are generally more effective than full length mRNA, suggesting that the full-length mRNA cannot form the secondary structure required for inhibition, or perhaps forms an incompatible secondary structure. It has also been suggested that specific helper proteins are required for sense:antisense interactions (Nellen & Lichtenstein, 1993). The absence of appropriate secondary structure or helper proteins may explain why some antisense

transformation experiments fail. It is intriguing that some sense strand transformations have been reported to give inhibition similar to that observed with antisense strands. This phenomenon could be attributed to the fact that the plasmids used to transform a sense fragment contain additional promoters that could operate bidirectionally, thus producing antisense mRNA. Alternatively, the sense fragment could be titrating out factors required for translation of the endogenous sense mRNA (Scherczinger *et al.*, 1992).

Antisense inhibition has been used with varying degrees of success in *D.discoideum*. Crowley *et al.* (1985) report that *discoidin I* expression is reduced twentyfold in cells transformed with antisense cDNA of a portion of the gene under a constitutively active promoter. No discoidin I mRNA was detected in transformed cells, implying that the sense-antisense hybrids were unstable. Scherczinger *et al.* (1992) placed antisense fragments of the MHCII (myosin heavy chain II) gene under a constitutively active promoter to reduce expression and found that 3' fragments roughly a quarter to a half of the length of the genomic cDNA were more effective than full length cDNA or 5' fragments in inhibiting MHCII expression. In contrast, disruption of V4 gene expression (involved in the transition from the growth to the developmental phase) can be effected by antisense expression of the full length cDNA (McPherson & Singleton, 1992). It has been reported that antisense expression has no effect on the level of endogenous mRNA or on protein expression (Green *et al.*, 1986). The occurrence of endogenous antisense regulation may explain why some antisense experiments work whilst others do not. Some proteins may be naturally regulated by antisense, so that cells contain the required accessory proteins for mediating RNA interactions. Antisense inhibition might only work when endogenous antisense mechanisms exist.

As the precise genetic lesion in the Hgr mutants is not known, a mutant created by antisense expression of a partial cDNA to the B subunit of the vacuolar H^+-ATPase (kindly provided by Dr R. Dottin) is examined in chapter

7. The B subunit is considered to be a good target for antisense inhibition as it has been shown that inhibiting its expression in yeast prevents the functioning of the ATPase (Ohya *et al.*, 1991; Yamashiro *et al.*, 1990).

Antisense mutants are expected to display similar characteristics to the Hgr mutants in their developmental morphology and response to weak bases. Since these mutants are created specifically by interfering with vacuolar ATPase expression, their phenotype can be ascribed specifically to this defect and not to any secondary mutation.

1.6 Aims of the thesis

In summary, the aim of this thesis is to attempt to elucidate the intracellular target of ammonia through which its developmental effects are mediated. In chapter 3, the effects of a variety of weak bases on the developmental processes of aggregation, chemotaxis and culmination are presented. In the light of these results, the effects of these same bases on cytoplasmic and vesicular acidification are probed: *in vivo* by ^{31}P-NMR and *in vitro* by studying vesicular acidification directly (chapters 4 and 5). Chapters 6 and 7 describe the effect of mutations in the vacuolar acidification systems on development, and the response of such mutants to weak bases. Finally, conclusions for the mode of action of ammonia are drawn in chapter 8.

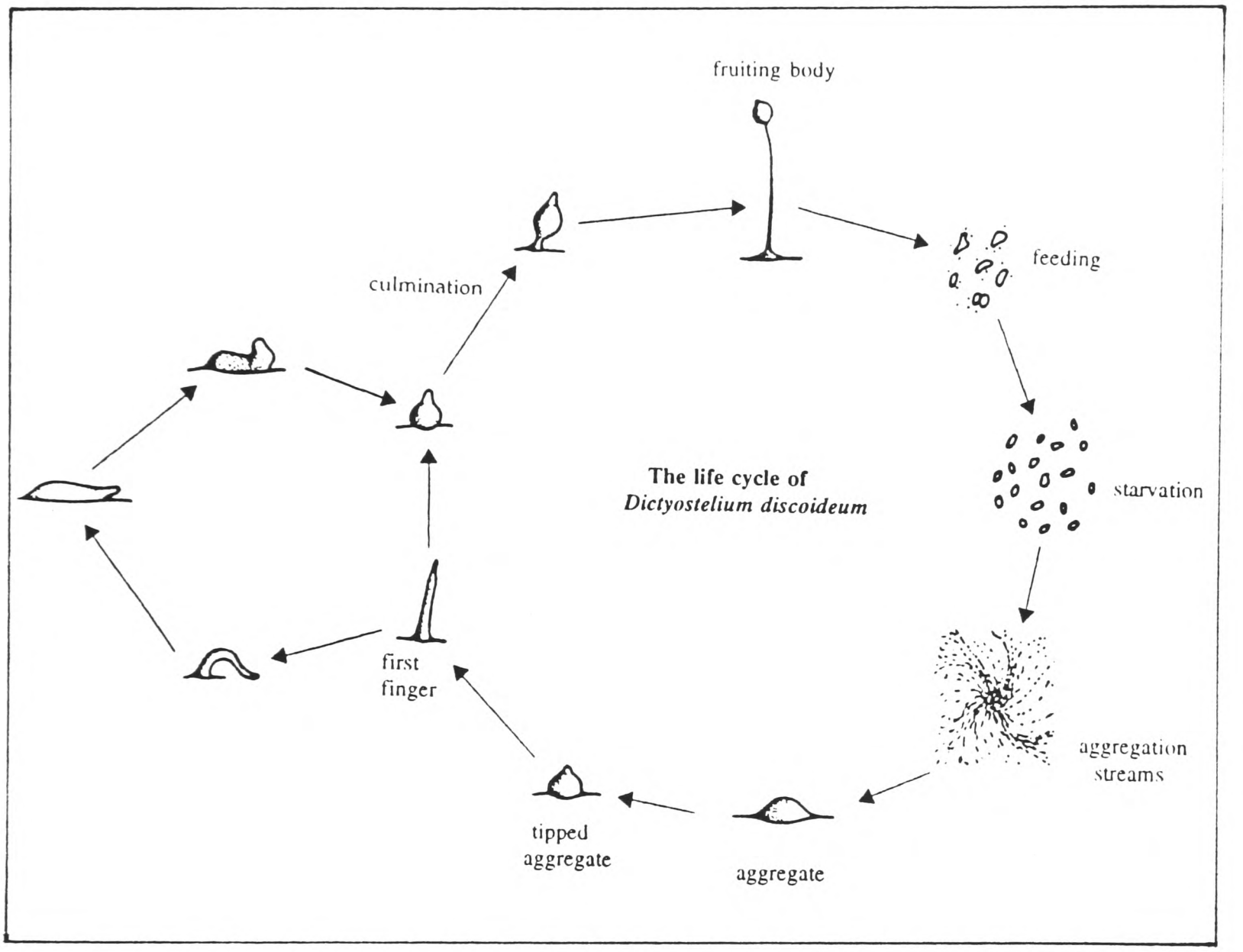


Figure 1.1: The life cycle of *Dictyostelium discoideum*

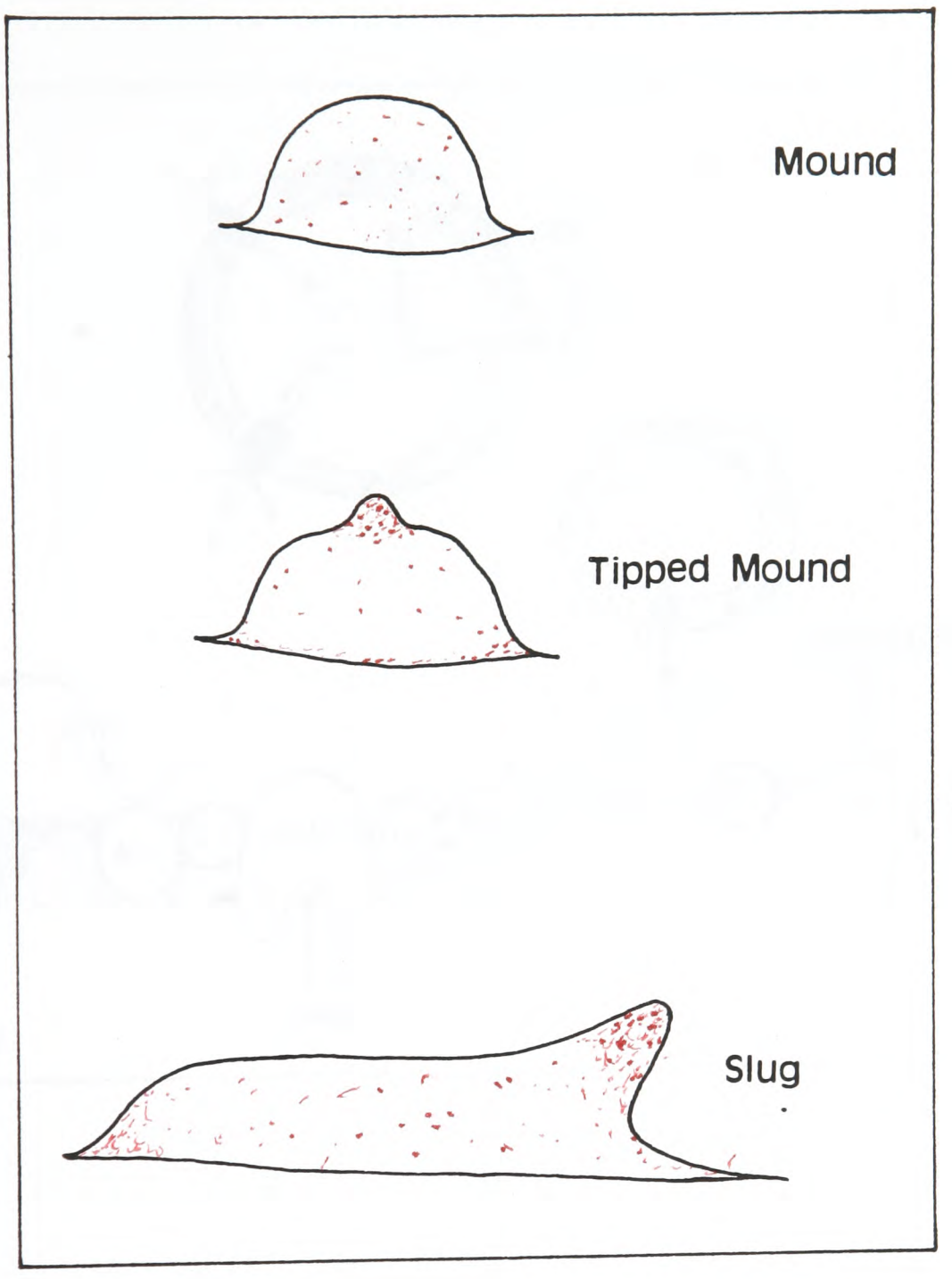


Figure 1.2: Neutral-red staining of *D.discoideum* through the life cycle (after Yamamoto & Takeuchi, 1983)

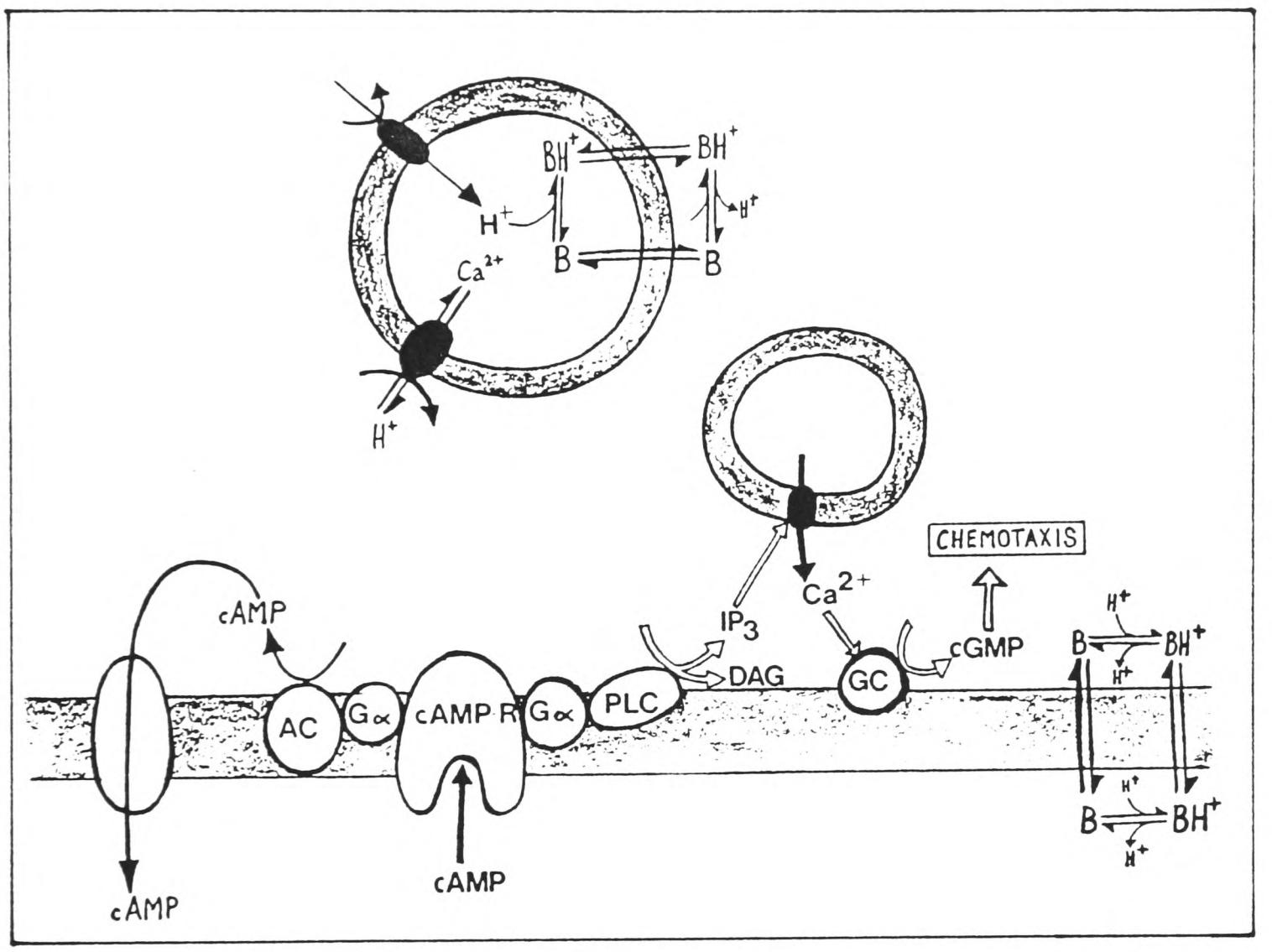


Figure 1.3: Signal transduction pathways implicated in the control of development in *D.discoideum*. PLC = phospholipase C, GC = guanylate cyclase, DAG = diacylglycerol, cAMP-R = cAMP receptor, AC = adenylate cyclase, PDE = cAMP phosphodiesterase.

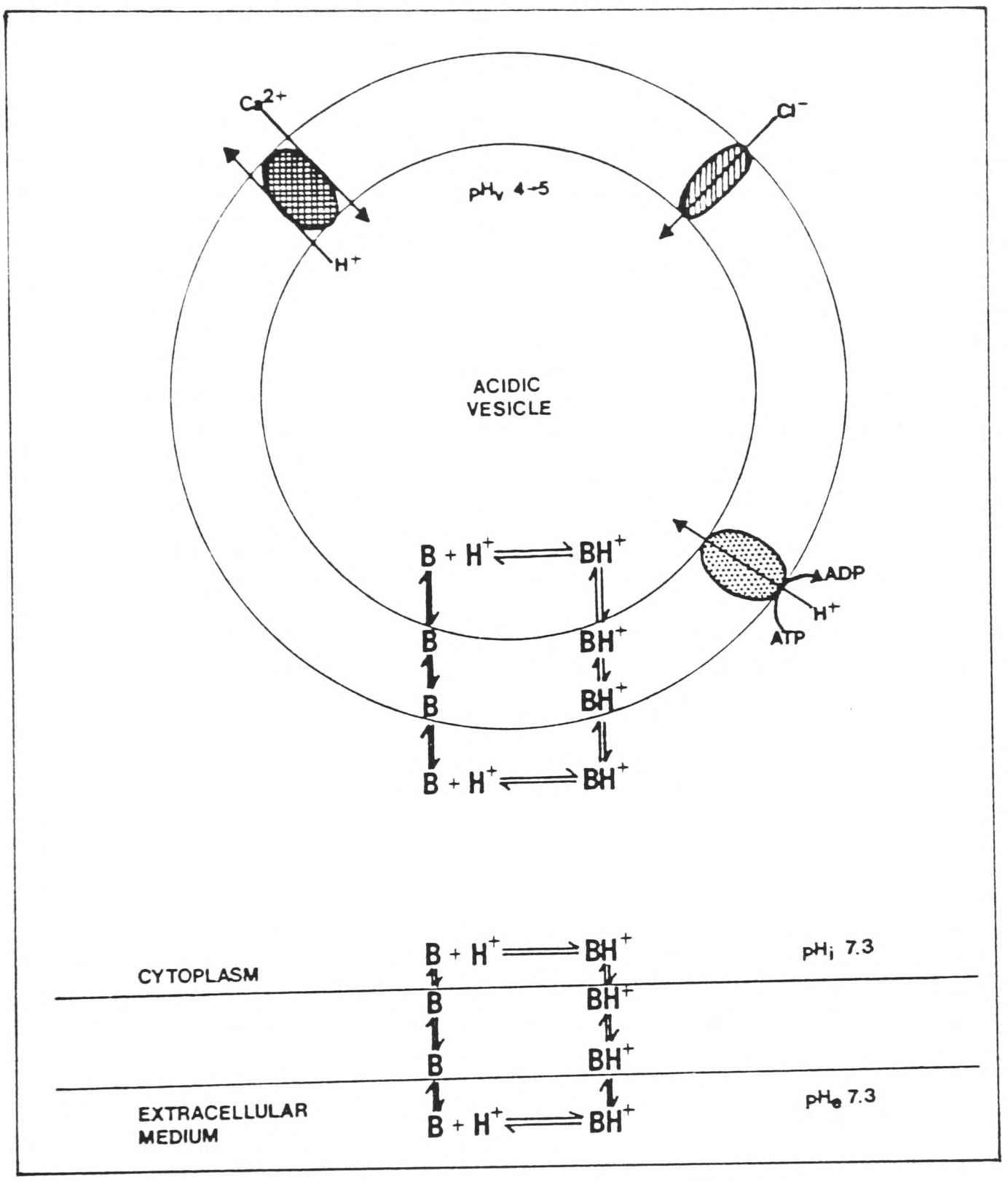


Figure 1.4: The acidic vesicle. Model for the effect of weak bases on intracellular pH.

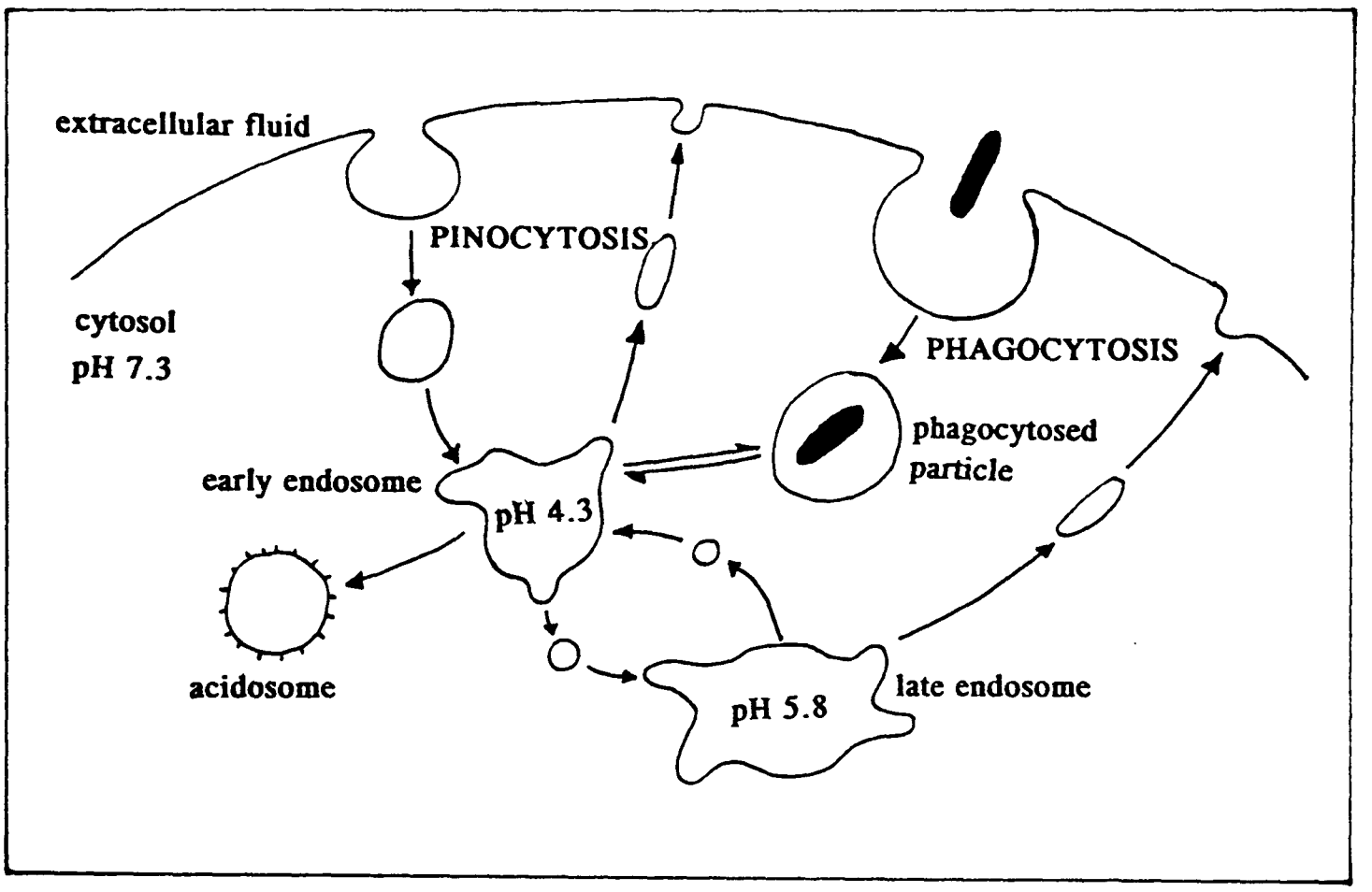


Figure 1.5: Model of the endocytic system of *D.discoideum*

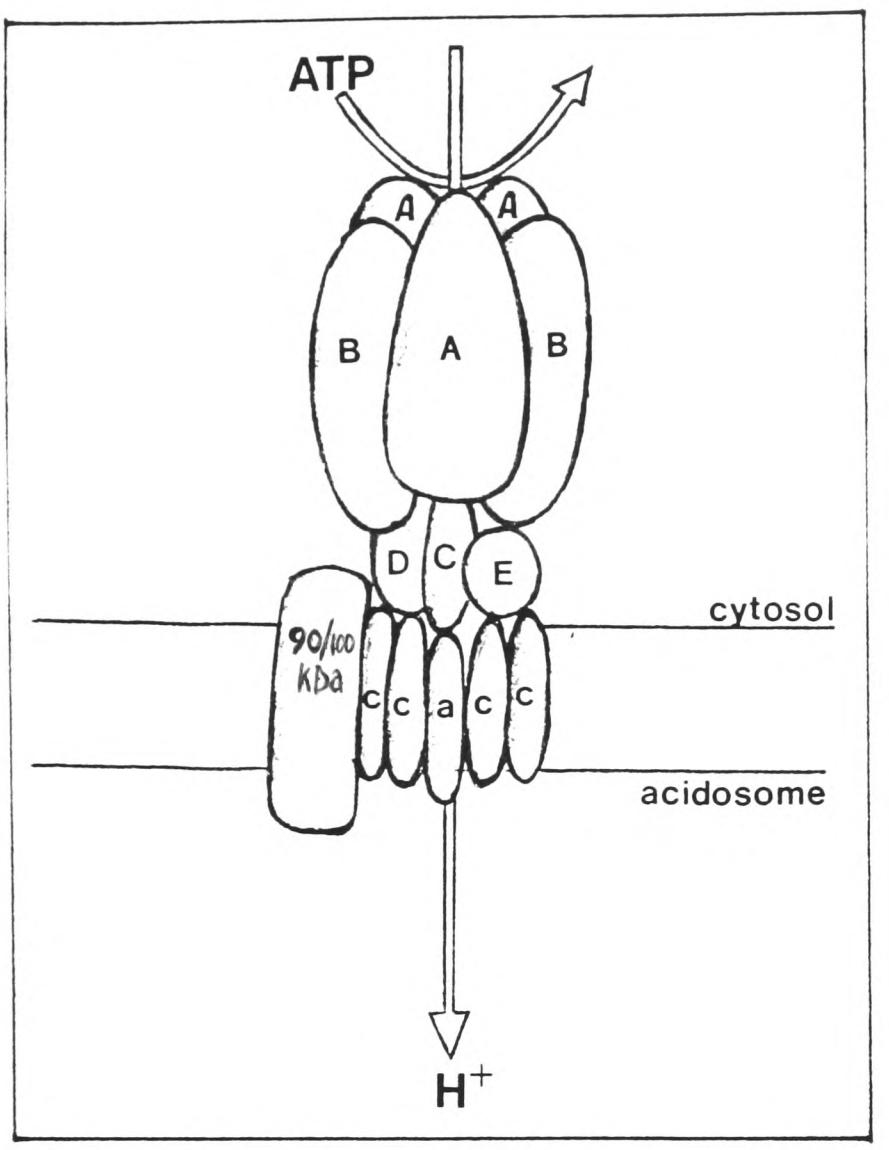


Figure 1.6: The vacuolar H^+-ATPase of eukaryotes (after Nelson, 1992)

Subunits	**M_R (kDa)**	**Location**
	90*/100$	membrane
A	68*	head (ATPase)
B	53*/57$	head (NTP-binding)
C	42*	link
D	37*	link
E	25*	link
a	17*	membrane
c	15*	membrane

* Determined by Nolta *et al.* (1993)

$ Determined by Fok *et al.* (1993)

Chapter 2

Chapter 2 *Materials and Methods*

2.1 - Cell stocks, growth and maintenance

2.11 NC4 (wild-type strain)

Lawns of *Klebsiella aerogenes* on SM (standard medium) -agar plates (Sussman, 1966) were inoculated with spores of the wild-type strain NC4 to produce individual colonies and were maintained at 22°C in the dark. Spores were obtained from silica gel stocks kept at 4°C. Large quantities of cells were obtained by harvesting cells from the growing edges of colonies into SS (salt solution) and mixing these with an equal volume of *K.aerogenes* before being spread onto SM-agar plates (mass plates). If kept at 22°C in the dark, amoebae exhaust the bacterial food supply by about 24h. A typical yield is about 10^8 cells per plate.

2.12 Ax2 (axenic strain)

Amoebae obtained from liquid nitrogen stocks or spores stored on silica gel were inoculated into Ashax medium (pH 6.5 or pH 6.0) and left stationary for 1 week at 22°C before being put into a shaker (180rpm). Such stocks grew with a doubling time of roughly 8h and were subcultured during the log phase of growth. Subcultures were set up at not less than 5 x 10^4 cells/ml and reached a plateau level of about 2 x 10^7 cells/ml by 72h. After 3 months of subculturing, the doubling time increased and fresh cultures were obtained from stocks.

For long-term storage, spores were harvested from bacterial plates in salt solution, mixed with silica gel and stored at 4°C. Alternatively, amoebae were spun down and mixed with horse serum (containing 5% DMSO (Sigma)) before being aliquotted to straws for storage in liquid nitrogen.

2.13 Hgr mutants (derivatives of Ax2)

Amoebae of the Hgr mutants (kindly provided by Dr M.Satre, Centre d'Etudes Nucléaires, Grenoble) were stored in liquid nitrogen or as Silica gel stocks as described for Ax2. Liquid nitrogen storage from growing, shaking cultures was the preferred method of storage of some strains as spore formation is impaired in some strains.

Growing cultures were obtained by aliquotting liquid nitrogen stocks into Ashax at pH 6.0 containing 5mM MDP (methylene diphosphonate, pH 6.0, Sigma). The presence of MDP (a cytotoxic drug that kills wild-type cells when taken up by endocytosis, to which the endocytosis-deficient Hgr mutants are resistant) ensured that selection pressure was maintained. Cells were maintained in stationary culture under Ashax (containing 5mM MDP) until needed for experiments. Then they were subcultured into MDP-free Ashax (pH 6.0) at 10^5 cells/ml and shaken at 22°C in a rotary shaker at 180 rpm. The mutants displayed doubling times varying between 13h (Hgr1) and 25h (Hgr5) and under these conditions a growth plateau was reached between 3 x 10^6 cells/ml (Hgr5) and 1.5 x 10^7 cells/ml. Cells were grown in MDP-free medium for 12h before use in developmental assays.

2.14 Vacuolar acidification-defective mutants (Ax2 derivatives)

These cells were maintained as liquid nitrogen stocks as described for the Hgr mutants (above). For growth, cells were placed in Ashax (pH 6.0, containing 20µg/ml G418 (Sigma) to maintain selection pressure for the plasmid) in stationary culture in the dark at 22°C until a continuous lawn of cells was produced. Cell aliquots were then placed in Ashax (pH 6.0, containing at least 20µg/ml G418) at 10^5 cells/ml and shaken at 180 rpm in the dark at 22°C. All cultures were grown for 12h in the absence of G418 before use.

2.15 Solutions

SM-Agar (Sussman,1987) per litre:

10g Bactopeptone (DIFCO)

10g Glucose (Merck)

1g $MgSO_4$ (Merck)

2.2g KH_2PO_4 (Merck)

1g K_2HPO_4 (Merck)

1g Yeast extract (Oxoid)

12g Agar N°3 (Oxoid)

Autoclaved at 15psi, 20mins

Ashax per litre:

14.3g Peptone (Oxoid)

7.2g Yeast extract (Oxoid)

0.48g KH_2PO_4 (Merck)

0.64g Na_2HPO_4 (Merck)

18g D-Maltose (Aldrich)

0.25g Dihydrostreptomycin (Sigma)

pH to 6.0/6.5 with NaOH and autoclaved at 15psi, 20mins

SS (salt solution) (Bonner, 1947), per litre:

0.6g NaCl (Rose Chemicals)

0.75g KCl (Merck)

0.3g $CaCl_2.2H_2O$ (Merck)

Autoclaved at 15psi, 20mins

2.2 - Development *in vivo*

2.21 Preparation of cells

(i) Bacterially-grown cultures: Cells from the growing edges of colonies were then plated in association with *K.aerogenes* on mass plates and incubated overnight at 22°C. Once the bacterial food supply was exhausted, the plates

became translucent (about 24h) and cells were harvested from the plates into LPS (Lower pad solution) at pH 7.3. Cells were then washed repeatedly by centrifugation at 190 x g for 2min in LPS. Cell pellets thus obtained were resuspended finally in an appropriate volume of LPS (or LPS + weak base solution).

(ii) Axenically-grown cells: Cells in the log phase of growth (5 x 10^5 to 5 x 10^6 cells/ml) were pelleted by centrifugation at 190 x g for 4mins. The cell pellets were washed and resuspended as described above for the bacterially-grown cells.

2.22 Aggregation

For easy visualization of aggregate types, amoebae were placed on quartered black Whatman filters (n°. 29, boiled three times in distilled water before use) at a final density of 5 x 10^6 cells/cm^2. The filters were supported on white Whatman filter circles (grade 17, 5.5cm) in Petri dishes. These filters were presoaked in 2.25ml of LPS or weak base solution. In experiments where only wild-type cells were being used, the number of mounds present on each filter was scored using a Nikon SMZ-2T light microscope after 15h in a dark, humid box at 22°C. When mutant (slow-aggregating) cells were being compared with wild-type cells, aggregate numbers were scored after 15 and 40h. Results are expressed as percentage aggregation relative to the control.

2.23 Culmination

Cells were plated on black Whatman filters at a final density of 5 x 10^6 cells/cm^2, as for aggregation. These filters were supported on white Whatman filter circles pre-soaked in LPS. Aggregates were allowed to develop to the first finger stage (approximately 15-18h) before being transferred to fresh white support filters pre-soaked in LPS or weak base solutions. At 40h after transfer, the proportion of aggregates that had culminated on each plate was scored. The height of the culminants was also noted. Results are expressed as percentage culmination relative to the control.

2.24 Chemotaxis

The chemotactic assay was the "spreading" method of Bonner et al. (1966). Before the final centrifugation, the cell suspension was split into equal volumes and then pelleted. Pellets were then resuspended in LPS or LPS-weak base solutions before being re-pelleted by centrifugation. Each pellet contained roughly 10^9cells/ml. Aliquots (0.1 ml containing 10^8 cells) were spotted onto the surface of LPS-agar or LPS-agar containing weak bases at various concentrations (all at pH 7.3). These plates were prepared by boiling DIFCO bacto-agar with LPS (1% agar) and then adding an appropriate volume of concentrated (1M) base solution once the agar had cooled below 50°C (to avoid evaporation of volatile bases).

Once cells were added, the plates were placed in a humid chamber in the dark at 22°C. The cell spots were scored for chemotactic competence (defined by the presence of an annulus) at both 6 and 24 hours. Photographs were taken as described below (section **2.27**).

2.25 Weak base solutions

Developmental assays were carried out using Lower Pad Solution (LPS) as a buffer

<u>LPS, per litre</u>

1.5g KCl (20mM)

0.5g dihydrostreptomycin sulphate (1mM)

5.45g KH_2PO_4 (40mM)

The pH was adjusted to 7.3 using KOH and the solution sterilized by filtration through a Millipore Sterivex-GS 0.22µm filter unit.

KCl and KH_2PO_4 were obtained from Merck and dihydrostreptomycin from Sigma.

Weak Bases

Ammonium chloride (Fisons), methylamine hydrochloride, propylamine hydrochloride, imidazole, octylamine (Sigma) and chloroquine diphosphate (Fluka) were made up as concentrated (0.5M) solutions in magnesium-free LPS. Magnesium was omitted as $Mg_3(PO_4).4H_2O$ is insoluble in NH_4^+-containing solutions, producing monoclinic crystals which interfere with cell counting. No difference was seen between control developmental assays using LPS containing Mg^{2+} and those using Mg^{2+}-free LPS.

2.26 Statistical analyses

The quantitative results given are the result of at least three independent experiments. Results are presented as the average of all values and the error bars reflect the standard deviation from the mean.

2.27 Photographs

Photographs of aggregate and culminant morphologies and of the chemotactic response were taken with a Ricoh KR-10M camera attached to a Nikon SMZ-2T light microscope using Ilford Pan F (iso 50°) black and white film. Magnifications are noted in the legend of each figure.

2.3 Vesicle acidification *in vitro*

2.31 Isolation of vesicles

Vesicles were isolated from axenically growing or bacterially-grown cells and assayed for acidification by the method of Rooney & Gross (1992). Exponentially growing cells (Ax2) were harvested from the log phase of growth between $5x10^5$ and $1x10^6$ cells/ml from a total volume of 600ml, or from mass plates (NC4) into SS, yielding between 3 and $6x10^8$ cells in total. Cells were centrifuged at 190 x g for 2mins, washed three times in sucrose buffer and counted before final resuspension in 40ml sucrose buffer. This suspension was then lysed by passage through a 2.5µm pore Nucleopore filter (25mm diameter), collecting the lysate on ice. From this point onwards, the

preparation was kept at 0-4°C. The lysate was spun once again at 190 x g to ensure that cells were completely lysed. Sucrose was then added to the supernatant to increase the concentration to 38% (w/w) and the pH readjusted to 8.5 before centrifuging at 27,000g for 1h in a Beckman JA-20 rotor to pellet nuclei and mitochondria. The sucrose density of the supernatants was then reduced to 10% (w/w) before centrifuging at 39,000g to pellet the light membrane fraction. Pellets were washed once before resuspension in 1ml assay buffer and kept on ice for no more than 12h before use.

2.32 Buffers and solutions

Sucrose Buffer per litre:

34.24g sucrose (100mM)
0.38 glycine (5mM)
0.154g dithiothreitol (1mM)
0.0017g PMSF (10μM)

pH adjusted to 8.5 with NaOH (PMSF and dithiothreitol were made up in 0.5ml EtOH and added just before use). Glycine was obtained from Merck and the remainder from Sigma.

Assay buffer per litre:

34.24g sucrose (100mM)
7.46g KCl (100mM)
1.19g Hepes (5mM)
1.02g $MgCl_2$ (5mM)
pH to 7.3 with NaOH

Chemicals were obtained from Sigma (sucrose, Hepes) or Merck (KCl, $MgCl_2$).

2.33 Determination of vesicle acidity by fluorescence

Immediately before use, 25μl of vesicle suspension was added to a cuvette containing 1.925ml of assay buffer at 25°C and 2μM acridine orange (Aldrich). A magnetic stirrer was used to aerate the solution and to ensure rapid mixing

of added solutions. Baseline fluorescence was then determined in the Shimadzu RF-5001PC spectrofluorophotometer at an excitation wavelength of 480nm and an emission wavelength of 530nm. Weak bases were added as concentrated solutions in assay buffer.

2.34 Protein assay

Protein assays were conducted according to a modified Lowry assay (Peterson, 1977) using Bovine Serum Albumin (Sigma) as a standard. Determinations were conducted in triplicate.

2.35 Statistical analyses

Data points on graphs are the result of at least three independent experiments and error bars represent the standard deviation from the mean.

2.4 ^{31}P NMR conditions

2.41 Buffers and solutions

Mes buffer:

40mM Mes (2-[N-morpholino] ethane sulphonate, Merck) in ddH_2O

pH adjusted to 6.5 with NaOH

Resuspension solution:

1.2ml D_2O

2µl Antifoam A agent 289 (Sigma)

Mes-Na buffer (40mM) added to a total volume of 20ml (inclusive of resuspended pellet)

Endocytic probes:

Probes were added as concentrated solutions in Mes-Na (40mM) and the pH of the solutions adjusted to 6.5 with NaOH. AEP (2-aminoethylphosphonate, Sigma) was made as a 0.2M stock solution and used at a final concentration of 7.5mM. Cl_2MDP (dichloromethylene diphosphonate, provided by Dr Helmut

Blum of Henkel, Düsseldorf) was again made as a 0.2M stock solution, but added at a concentration of 5mM (Ax2 cells) or 2.5mM (pVeII and pdv-gal cells).

Weak base solutions:

1M ammonium chloride (Fisons), propylamine, imidazole, octylamine (Sigma) and chloroquine (Fluka) were made up in 40mM Mes-Na and the pH of the solutions adjusted to 6.5 with NaOH.

2.42 ^{31}P NMR parameters

In vivo NMR spectra of Dictyostelium amoebae were obtained as described previously (Satre and Martin, 1985) at 22°C on a Bruker AMX400 spectrometer operating at a phosphorus frequency of 162 MHz with 60° pulse width, 0.48s acquisition time, 1.2s repetition delay and gated Waltz proton decoupling. Data were stored every 750 scans. Application of a Gaussian line broadening (GB = 0.04, LB = -6) preceded Fourier transformation. Chemical shifts are given with respect to orthophosphoric acid at 0ppm.

2.43 Experimental conditions

Dictyostelium Ax2 amoebae (3.6×10^8 ml^{-1}) were suspended in 40mM Mes-Na, 6% D_2O (v/v) and 5 µl Antifoam agent 289 at pH 6.5 in a final volume of 20ml and bubbled with O_2. After temperature equilibration at 22°C in the NMR spectrometer for 15min, AEP at 7.5mM or Cl_2MDP at 5/2.5mM was added to the suspension. After 45 min, weak base solution was added and data collected for 15min before any further addition of base. Alternatively, cells were removed for washing in ice-cold 40mM Mes-Na, pH 6.5 after the first addition of base. After three washes, the cells were resuspended as above and data collected for a further 15 min before re-addition of base. Previously described *in vivo* ^{31}P NMR calibration curves were used (Brénot *et al.*, 1992; Pelorgeas *et al.*, 1992).

2.44 Treatment of results

Chemical shift data were converted into pH values by the method of Martin *et al.* (1987) using *in vivo* calibration curves for the endocytic probes obtained by Brénot *et al.* (1992) and Pelorgeas *et al.* (1992). Conversion tables are contained in **Appendix IV**. Unless stated otherwise, conclusions are based on the results of at least three independent determinations. Calculations of the amount of probe in the various compartments were obtained by weighing peaks cut from photocopies of spectra.

2.5 Preparation and cloning of plasmids

2.51 Sequencing of the vacuolar ATPase B subunit cDNA fragment

The B subunit cDNA fragment was isolated and partially sequenced by Dr Robert Dottin (Hunter College, City University of New York) and consists of 830bp at the 3' end of the gene. This was obtained as an insert in plasmid PTZ 18U. Full sequencing of the cDNA was carried out using the T^7 sequencing kit (Pharmacia). T7 (Pharmacia) and -40 (USB Ltd.) primers were used for initial sequencing. Further primers (20mers) were designed on the basis of sequencing (synthesized by V.Cooper, Department of Organic Chemistry, University of Oxford) and used to probe the remainder of the sequence.

Sequencing reactions were conducted using 10µg of PTZ 18U-dvac (**figure 7.2**) as a template. This was denatured in 0.2M NaOH (Merck) for 5min at 22°C, neutralized with NH_4OAc (5M, pH 5.2) and the denatured DNA precipitated by centrifugation at 12000g for 10min in ethanol. The resulting pellet was dried and resuspended in annealing buffer containing 20ng of the appropriate primer, according to the instructions of the kit. After incubation at 37°C (20min) and 22°C (10min), solutions were centrifuged briefly and added to the extension solution (7µl of enzyme premix: Label Mix A, $\alpha^{35}S$ dATP (20µCi) and 1 unit of T7 polymerase) for 5min at 37°C. Termination was conducted over 10min by adding 2.5µl of either ddG, ddA, ddT or ddC, pre-heated to 37°C to 4.5µl aliquots of the extension solution. Stop-mix was added to terminate the

reactions. The samples were then heated to 80°C and centrifuged briefly before loading onto an acrylamide gel: 15ml 20% acrylamide/46% urea concentrate (Biorad), 2.5ml 10x TBE, 32.5ml diluent (Biorad), 400µl 10% ammonium persulphate, 20µl TEMED (Sigma). The gel was run in 0.5x TBE at 50-55°C for 2h before fixing in a 10% methanol/ 10% acetic acid mixture for 1h. After transferring the gel to Whatman no.1 filter paper and drying, the gel was then exposed overnight to X-ray film (Kodak) at -70°C before developing.

2.52 Southern blotting

Genomic DNA of the strain Ax2 was prepared from 10^{10} cells, pelleted, washed in 0.2% NaCl and then lysed in ice-cold nuclear lysis buffer. Nuclei were pelleted by centrifugation (8000g/10min) and resuspended in HMK containing 0.2% SDS and 100mM NaCl. Proteins were then extracted by sequential treatment with equilibrated phenol, phenol: chloroform: isoamylalcohol (68:14:8) and chloroform. NaOAc (Merck) was then added to a final concentration of 300mM and 2 volumes of ethanol added. DNA was extracted from the ethanol:water interface, washed in ethanol and dried before resuspending in water.

DNA (10µg total) for Southern blotting was cut with EcoRI/XbaI, EcoRI/HindIII, PstI, PstI/EcoRI, PstI/XbaI and PstI/BglII (Promega) cut in the recommended restriction buffers. Aliquots were then run out on a 0.8% agarose/TBE gel and photographed under UV (Sigma polaroid 667 b/w film). Southern blotting was then conducted according to the method of Southern (1975).

2.53 Cloning cDNA fragment through vectors

All plasmid maps are shown in figure 7.2. The cDNA fragment (dvac) was sequenced as described above to determine its orientation in the plasmid PTZ 18U and then cloned through the plasmid Bluescript (Stratagene) for insertion in the antisense direction into the discoidin promoter-containing vector pVeII

(Morandini, 1993). In the first instance, the cDNA was excised from PTZ 18U by cutting with PstI (1 unit per µg of plasmid for 3h at 37°C in the buffer recommended by the manufacturer, Promega), separated from the vector by electrophoresis on a TAE gel (0.5x) and then excised under long-wave UV light before being purified by the Geneclean procedure (Stratech Scientific).

The dvac cDNA was then ligated into pBluescript SK- (pre-cut with PstI, treated with alkaline phosphatase (Boehringer) and phenol extracted), using T4 DNA ligase (Pharmacia) at 15°C overnight. Aliquots of the ligation mixture were then transformed into *E.Coli* DH5α cells by electroporation (Dower *et al.*, 1988; Taketo, 1988), plated onto L-Broth/ampicillin plates spread with X-galactose (Calbiochem) and left overnight at 37°C. The following day, white colonies (those that had incorporated the dvac fragment and so interrupted the *lacZ* gene whose protein product - ß-galactosidase - is responsible for generating a blue colour by splitting the chromophore from X-galactose) were picked and grown in 3ml L-broth (+ 50µg/ml ampicillin) overnight at 37°C. Plasmid DNA was then extracted from each of the solutions using the Promega Wizard Miniprep system and samples of the resultant plasmids tested for insertion of the dvac fragment by cutting with PstI or with KpnI/BglII (according to manufacturer's instructions). Fragments were separated on an agarose gel to verify that they were of the expected length. A suitable colony was selected for large-scale plasmid preparation and grown overnight in 1l of L-Broth + 50µg/ml ampicillin. Cells were lysed the following day by alkaline lysis and plasmid DNA isolated by density gradient centrifugation in CsCl (Ish-Horowicz & Burke, 1981). A sample of the plasmid was then re-cut with PstI to ensure that the integrity of the construct was maintained.

The dvac cDNA fragment was then excised from the multiple cloning site of pBluescript-dvac using KpnI/BamHI and genecleaned (method as above). Similarly, the pVeII plasmid (constructed by P.Morandini) was cut with KpnI/BamHI and the plasmid extracted, genecleaned and phosphatased. The

dvac fragment was then ligated into the pVeII plasmid. Antisense orientation was assured by the choice of restriction cutting sites. Ligation products were miniprepped as before and the resultant plasmids products (pdv) cut with KpnI/BamHI or KpnI/BglII to ensure that insertion into pVeII had occurred correctly and that the dvac fragment was in the antisense direction. A suitable pdv miniprep product was then chosen for amplification (as before) and an aliquot of the resulting plasmid re-cut with the appropriate restriction enzymes.

A further plasmid (pdv-gal) was created by insertion of a 5kb fragment of plasmid pAct15-gal containing the LacZ gene (encoding ß-galactosidase) by blunt end ligation into the PvuII site of pdv. Plasmid pdv was cut with PvuII whilst the LacZ fragment of pAct15-gal was excised with XbaI/ScaI and isolated by the geneclean procedure. Both the lacZ 5kb fragment and the linearized pdv were end-filled to ensure that no sticky or ragged ends remained and the pdv plasmid phosphatased as before. Blunt end ligation was then conducted with j:i ratios optimized for ligation (Sambrook *et al.*, 1989). Ligations were then miniprepped and an appropriate plasmid chosen for electroporation into DH5α cells by cutting aliquots of each miniprep with ClaI.

2.54 Solutions

TBE per litre:

10.9g Tris base (Sigma)

5.56g Boric acid (Sigma)

20ml 0.5M Na_2EDTA (Sigma) pH 8.0

Nuclear lysis buffer per litre:

Magnesium acetate. $4H_2O$	(Merck)	2.14g
NaCl	(Merck)	0.58g
Hepes (30)	(Sigma)	7.15g
Sucrose	(Sigma)	100g

2% Non-idet P40 (Sigma) 20ml

Volume adjusted to 1l with ddH_2O and the pH adjusted to 7.5 with NaOH.

TAE per litre:

0.04M Tris (Sigma)

10mM EDTA (Sigma)

In 1l distilled water

L-Broth per litre:

10g Bactotryptone (GIBCO)

5g yeast extract (Oxoid)

5g NaCl (Analar)

pH adjusted to 7.2 with NaOH before autoclaving (15psi/15min)

L-Broth agar per litre

15g Oxoid agar no.3

Made up to 1l with L-Broth and microwaved before pouring into 90mm petri dishes. Sterilized under UV overnight.

Ampicillin:

Ampicillin (Sigma) was made up in water at 10mg/ml and filter sterilized (Nalgene, 0.2µm pore size) before freezing in aliquots at -20°C. Ampicillin was added to L-Broth at 50µg/ml for the maintenance of plasmid selection.

2.6 Generation of a vacuolar ATPase-defective strain

2.61 Buffers and solutions

MES/HL5 per litre:

10g Oxoid peptone

14g glucose (Sigma)

5g yeast extract (Oxoid)

1g MES (Merck)

250µg dihydrostreptomycin (Sigma)
Made up to one litre with distilled water and adjusted pH to 7.0.

HBS per litre:
2g NaCl
0.09g KCl
0.03g Na_2HPO_4
1.3g Hepes
0.25g Glucose
pH adjusted to 7.05 with NaOH, then filter sterilized. Glucose and Hepes were obtained from Sigma and the remainder from Merck.

$CaCl_2$
10.8g $CaCl_2.2H_2O$ in 20ml distilled water
or 5.9g $CaCl_2.2H_2O$ (Merck) in 20ml distilled water
Sterilized by filtration

Z-buffer per litre:
240ml NaH_2PO_4 (40mM)
40ml Na_2HPO_4 (60mM)
100ml KCl (10mM)
10ml $MgSO_4$ (1mM)
Made up to 1l with distilled H_2O. All chemicals were purchased from Merck.

Staining solution
5mM $K_3[Fe(CN)_6]$ (Sigma)
5mM $K_4[Fe(CN)_6]$ (Sigma)
1mM X-galactose
(20µl/ml of a 2% solution in dimethylformamide)
1mM EGTA (Merck)
(made up in Z buffer)

2x Loading buffer:

1.0ml 1M Tris (pH 6.8)

2.0ml 1M DTT

2.0ml 20% SDS

2.0ml 100% glycerol

2.0 ml ddH_2O

0.2ml Bromophenol blue (1%)

All chemicals were obtained from Sigma.

SDS-PAGE gels:

Resolving gel

4.6ml ddH_2O

2.7ml 30% Acrylamide mix (Biorad)

(29.2% acrylamide and 0.8% N,N'-methylene-bis-acrylamide)

2.5ml 1.5M Tris (pH 8.8 with HCl)

0.1ml 10% SDS

0.1ml 10% APS (ammonium persulphate)

0.006ml TEMED

Stacking gel

3.4ml ddH_2O

0.83ml 30% Acrylamide mix (Biorad)

0.63ml 1.0M Tris (pH to 6.8 with HCl)

0.05ml 10% SDS

0.05ml 10% APS

0.005ml TEMED

Electrode buffer (5x stock solution):

15.1g Tris base

94g Glycine

300ml ddH_2O

50ml 10% SDS

pH adjusted to 8.3 with HCl

Volume made up to 1000ml with ddH_2O, diluted 1 in 5 for a working solution in distilled water.

Ponceau S:

2g Ponceau S (Sigma)

30g TCA

30g Sulphosalicylic acid

ddH_2O to 100ml

Diluted 1 in 10 for a working solution

(Solutions other than acrylamide were from Sigma).

PBS (phosphate buffered saline):

8g NaCl

0.2g KCl

1.44g Na_2HPO_4

0.24g KH_2PO_4

0.02% sodium azide (Sigma)

Added ddH_2O to 800ml and adjusted the pH to 7.4 with HCl before making up to one litre. All chemicals were from Merck.

2.62 Transformation of Ax2 by calcium phosphate precipitation

Aliquots (10ml) of axenically-growing Ax2 cells (1-2 x 10^6 cells/ml) were placed in sterile Petri dishes and the cells allowed to settle for 10min. The solution was then aspirated and replaced with 7ml MES/HL5 (pH 7.0) for 30min. Plasmid DNA (12µg of plasmid pVeII, pdv or pdv-gal) in 0.562ml HBS was placed in a sterile 15 ml centrifuge tube and 38µl 2M $CaCl_2$ added whilst vortexing. After 25min, the DNA/$Ca_3(PO_4)_2$ suspension was added evenly to the cells and left for 4h to allow adsorption of DNA by the cells. This was quickly replaced with 2ml of 10% glycerol in HBS for 3min. The glycerol/HBS is then

aspirated and quickly replaced with Ashax (pH 6.0) and left overnight at 22°C for the cells to recover. After 12-16h, the medium was replaced with Ashax containing 10µg/ml of the selection agent G418 (Sigma). Thereafter the medium was changed every other day for 1 week. Roughly two weeks after transformation, cell colonies appeared and were plated onto agar in association with *K.aerogenes*. The resultant colonies were screened for mutants (in the case of the pdv and pdv-gal strains). Developmentally abnormal colonies were then returned to axenic medium and the G418 concentration steadily increased. The developmental morphology was checked with each G418 increment. In all experiments, pVeII-transformed cells were used as controls.

2.63 Detection of plasmid expression with β-galactosidase staining

An alternative strategy was also employed for isolation of pdv-gal-transformed cells, relying on the presence of a *lacZ* reporter gene in plasmid pdv-gal. Cells were transformed as above and upon appearance of colonies on agar plates, an impression was made of the colony pattern with a nitrocellulose filter (Schleider & Schuell BA-S85, 0.45µm). Attached cells were fixed in 1% glutaraldehyde (Sigma) in Z buffer, washed in Z buffer, permeabilized with 0.1% NP-40 in Z buffer (20mins), then washed and stained with Staining Solution (containing the chromophore X-galactose) at 37°C for 1-2h.

2.64 Antisense expression of cDNA in Ax2

The level of expression of the B subunit of the vacuolar H^+-ATPase in pVeII, pdv and pdv-gal (late log phase cells at various levels of G418 selection from 20µg/ml to 200µg/ml) was determined by Western blotting using a polyclonal antiserum to the B subunit (kindly provided by Prof.T.Steck, University of Chicago, USA).

Protein samples were prepared from 10^7 cells by washing the cells in PBS and then resuspending the cell pellet in 200µl PBS and 20µl 20% SDS for disruption by sonication (16 microns for 30sec). Sonicated samples were then

centrifuged briefly (1000g/2min) and the supernatants retained. An aliquot (30µl) was used immediately for protein determination (Biorad protein assay) whilst 150µl 2x Loading Buffer was added to the remainder for electrophoresis. Samples containing equivalent protein concentrations from pVeII, pdv and pdv-gal were then heated briefly (1min) at 80°C before loading onto an acrylamide gel (resolving gel: 8% acrylamide). Rainbow molecular weight markers (Amersham) were used alongside the samples. The gel was run in electrode buffer using Biorad minigel apparatus for 1.5-2h at 120V and the resolved proteins then transferred to nitrocellulose membrane (Biorad) in ice-cold transfer buffer (4 parts electrode buffer: 1 part methanol) at 250mA for 2h. Filters were then stained with Ponceau S to ensure that efficient transfer had occurred before being washed repeatedly in PBS and blocked in a 5% skimmed milk solution in PBS for 3h. After a further wash, polyclonal antibody was added at a concentration of 1:1000 in PBS (0.1ml/cm^2 of filter) and left to bind overnight. The filter was washed thoroughly in PBS and secondary antibody (anti-rabbit) added according to the ECL protocol (Amersham). Relative estimations of the densities of the protein bands were made using a Biorad GS-670 Imaging Densitometer. Estimations are made by two methods - (i) density profiling through a protein band and (ii) relative intensity of whole bands (assuming 100% intensity for pVeII in both cases). Values presented are the results of three independent determinations.

2.65 Developmental studies with an acidification - defective transformant

The developmental morphologies of the transformed strains were studied as for Ax2 except that LPS at a range of pH values (5.0 - 8.0) was used. Aggregation experiments were conducted as for the Ax2 and Hgr strains.

Chapter 3

Chapter 3 *The Effects of Weak Bases on Aggregation, Culmination and Chemotaxis*

3.1 Introduction

Ammonia has long been implicated in the control of development in *Dictyostelium* and is produced endogenously as a by-product of protein breakdown (Gregg *et al.*, 1954). Externally-added ammonia inhibits both aggregation (Siegert & Weijer, 1989; Williams *et al.*, 1984) and culmination whilst promoting slug formation (Bonner *et al.*, 1985; Schindler & Sussman, 1977). The ability of ammonia to influence more than one stage of the developmental cycle presents the possibility that its effects might be mediated at each stage by a common mechanism. There are three possible levels at which ammonia might act. First, ammonia could inhibit specific enzymes; second, it could be acting as a weak base to raise cytosolic pH (pH_i) or finally, it could be raising the pH of intracellular acidic compartments (pH_v).

Bonner et al. (1985) showed that culmination is favoured by low pH and suggested that this was due to the lowering of the active concentration of the NH_3 species in low pH solutions. Numerous experiments have confirmed that the effect of ammonia on developmental processes is dependent upon the pH of the solution (Schindler & Sussman, 1977; Williams *et al.*, 1984), indicating that the active species is the unprotonated base NH_3. Consequently, this implies that ammonia might act as a weak base to alter intracellular pH (Gross *et al.*, 1983). In other systems, weak bases have been shown to be targetted towards acidic vesicles (De Duve *et al.*, 1974; Poole & Ohkuma, 1981; Krogstad *et al.*, 1985; Nissani & Ginsburg, 1989) which are present in cells at all stages of growth and development. Since ammonia is a weak base and thus concentrates in acidic compartments, a model has been proposed in which the effects of ammonia at aggregation and culmination are mediated by changes in the pH of internal acidic compartments (Gross *et al.*, 1988).

The experiments described below are designed to probe the mechanism of action of ammonia on the processes of aggregation and culmination, by comparison with a variety of other weak bases (imidazole, methylamine, propylamine, octylamine and chloroquine), since all weak bases ought to inhibit aggregation and culmination if the inhibitory action of ammonia *in vivo* is mediated by a weak base effect. Furthermore, if all these chemically distinct bases have similar effects, this would exclude the possibility that ammonia was acting as a specific inhibitor of some enzyme involved in both culmination and aggregation. In addition, as mentioned in section **1.4** the use of bases with a range of hydrophobicities and pK_a values permits a distinction to be made between the vesicular and cytosolic models for weak base action. Differences in the inhibitory efficiencies should be dependent only on pK_a if acting to raise cytosolic pH, but should be a function of the protonophoric capacity of the bases if acting on intracellular acidic compartments.

3.2 Results

3.2.1 - Effects of weak bases on aggregation in vivo

Wild-type NC4 cells in the log phase of growth were harvested and placed at a concentration of 5×10^6 cells/cm^2 on filters, supported by pads soaked in Lower Pad solution (LPS) alone or in LPS containing various concentrations of weak base solutions. All the experiments were conducted at pH 7.3 so that the external pH corresponded with the pH of the cytoplasm (pH 7.2-7.4). When the internal and external pH values are similar, bases with similar pK_as should distribute equally across the cytoplasmic membrane. Use of this pH also facilitated comparison with other research into culmination (Schindler & Sussman, 1977).

Base concentrations are expressed in terms of the unprotonated species as it has been found that this is the active, freely cell-permeable species. Raising

the pH of the medium decreases the concentration of ammonia required for biological effects (Williams *et al.* 1984; Schindler & Sussman, 1977) indicating that the active species in inhibition is the unprotonated base. Unprotonated base concentrations are calculated using the Henderson-Hasselbalch equation (**Appendix II**).

Incubating cells in the absence of ammonia resulted in the production of aggregates at about 12h, and culmination by 24h. Increasing the ammonia concentration had three effects. First, the number of aggregates on each filter was reduced without a concomitant increase in aggregate size; second, aggregation was delayed; third, increasing the ammonia concentration affected the morphologies of those aggregates that did appear on the filters. Therefore, scoring for quantitative results was carried out both at 15h and 48h to ensure that the aggregate number remained stable. In addition, photographs were taken at 15h to record any delay in aggregation induced by the bases.

Reduction of aggregate number

Figure 3.1 shows the effect of the bases ammonia (**i**), methylamine (**ii**), propylamine (**iii**) and chloroquine (**iv**) on the number of aggregates. Similar effects were observed with imidazole and octylamine (not shown). With each of the bases, dose-dependent inhibition of aggregate number was seen without an accompanying increase in aggregate size. For ammonia (**i**), a noticeable effect was seen at 220μM (**B**) (20mM total base) with total inhibition of aggregation (**D**) at 990μM ammonia (90mM total base). **Figure 3.2** depicts the effect of imidazole, ammonia and octylamine on aggregate number quantitatively. The inhibitory effect cannot be attributed to changes in the osmolarity of the solutions surrounding the cells since treatment with solutions containing up to 150mM NaCl had no effect on cell aggregation (not shown). No initial stimulation of the number of aggregates by low base concentrations was observed, which is in contrast to the effect of low ammonia concentrations on *D.mucoroides* (Feit, 1988).

From **figures 3.1** and **3.2** it is evident that there is a great difference in the inhibitory efficiencies of the bases. **Figure 3.3** provides a comparison of the efficiency of inhibition for all of the bases used. Imidazole is required at the highest concentration for inhibition (IC_{50} 3.3mM), whereas octylamine and chloroquine are needed only in very low concentrations (IC_{50} of 0.04μM and 0.3μM respectively, see below).

Base	Inhibition of Aggregation IC_{50} (unprotonated base) μM
imidazole	3300
ammonia	130
methylamine	14
propylamine	3
chloroquine	0.3
octylamine	0.04

Table 3a: Weak base concentrations that induce 50% inhibition of aggregation at pH 7.3

Delay of aggregation

Figure 3.1 shows that the extreme effect of adding high weak base concentrations was to inhibit aggregation completely (**D**). At intermediate concentrations, addition of bases reduced the aggregate number and delayed the onset of aggregation significantly. For example, in **figure 3.1 (i)** in the control situation (**A**) aggregates have reached the "mexican hat" stage and are beginning to culminate, whereas cells developed in the presence of 220μM ammonia (**B**) are only at the first finger stage at 15h, at 330μM NH_3 (**C**) streams have not yet disappeared whilst at 990μM (**D**) aggregation is

completely inhibited. This translates into a delay in development of roughly 8h at 330μM ammonia.

Morphologies of the culminants

As well as inhibiting aggregation at high base concentration, it was observed that the bases affected the morphologies of those aggregates that did form, in a dose-dependent manner. Thus, the aggregates that formed on the control plates culminated fully to produce normal fruits and at higher (non-inhibitory) concentrations of base, species arrested in the various stages of development were seen. Initially it was thought that this effect was due to a delay in aggregation caused by the bases. However, arrested species such as mounds, fingers and slugs, if present after 48h, failed to develop further, even after four days. Indeed, at the higher concentrations of base, any mounds formed after 24h usually disaggregated back into a lawn of cells, indicating that further development was inhibited and that aggregation (or possibly cell adhesion) is a fluid and reversible process in *Dictyostelium*. A further indication that the process of development is fluid is that aggregation of weak base-inhibited cells can be induced by replacing the base solution with base-free buffer (not shown). Where culminants were formed, their morphologies were often unusual. In general, the spore head appeared larger in relation to the stalk than in untreated controls and the stalk significantly thickened.

Aggregate size

Weak bases reduced aggregate density, resulting in complete inhibition of aggregation at the higher base concentrations. In agreement with Lonski (1976) it was found that the size of aggregation territories did not increase as aggregate numbers decreased, as it does in other slime mould species such as *D.mucoroides* (Lonski, 1976; Feit, 1988).

3.2.2 - The effects of weak bases on culmination

Amoebae were developed on filters in the absence of base to the first finger stage and then transferred to fresh buffer or to ammonia-containing buffer solutions. After 48h, the number of fruiting bodies was scored to give a measure of culmination and the morphologies of all the aggregates on the filters noted. In addition to being affected by ammonia, slug formation is known to be dependent on humidity levels and the roughness of the filter surface. Even when the humidity is maintained at a high level and identical filters used, formation of slugs could not be guaranteed. The reduction in the number of fruiting bodies formed after 48h was therefore taken as a convenient measure of the extent of culmination.

Control filters that had been maintained on ammonia-free solutions after the first finger stage typically formed culminants within 8-10 hours. These culminants were typically 6-8mm in height and consisted of a long fine stalk supporting a well-defined spore head (**figure 3.4 A**). **Figure 3.4** shows the effect of exposing first fingers to ammonia. At low concentrations (330 - 770μM), production of fruiting bodies was not prevented, but the fruiting body height diminished and the thickness of the stalk increased (**figure 3.4, B** and **C**). In general, the spore heads of such culminants were proportionally larger than those of the controls. At the highest concentrations used (above 990μM), the base prevented fruiting altogether and resulted in the arrest of species earlier in the developmental cycle (for example, the occasional migrating slug could be seen even at 48h) or gave irregularly shaped mounds (**figure 3.4 D**).

Figure 3.5 demonstrates that other bases inhibit culmination similarly. Total inhibition of normal culmination occurs at 39μM propylamine. A few species display large, bulbous spore heads and very short, thick stalks and a number are arrested as first fingers/slugs (**C**). Even at a lower concentration the effect is severe, at 27μM (**B**) the stalks are significantly thicker than in the control situation (**A**). The right hand sequence shows similar inhibition by imidazole.

At 31mM (**C**), normal culmination is absent; a few club-shaped species are present and some have arrested as slugs/first fingers, but the majority have reverted to the mound stage. Methylamine, chloroquine and octylamine also inhibited culmination in a dose-dependent fashion, although their inhibitory efficiencies differed greatly. Graphs quantifying their effect on culmination are shown in **figure 3.6** and IC_{50} values derived from this figure for the inhibition of culmination by each base are given below:

Base	Culmination IC_{50} (μM)
imidazole	10,300
ammonia	680
methylamine	35
propylamine	27
chloroquine	0.6
octylamine	0.5

Table 3b: IC_{50} values for inhibition of culmination by weak bases at pH 7.3.

The ammonia concentration required to give half-maximal inhibition of culmination (0.66 ± 0.25 mM) was found to be higher than that of 0.17mM quoted by Schindler & Sussman (1979). This disparity is ascribed to the fact that their aggregates were in contact with a larger volume of ammonium chloride whereas the filters used in this experiment contained only 2.25ml of base solution. Experiments were conducted in which identical aggregates were placed on filters exposed to 2.25mls or 30mls of weak base solution. The lower volumes were contained in support filter pads and the larger volume was obtained by placing a millipore filter and support pad on glass beads in a

reservoir of 30mls of solution. Control cells aggregated and culminated to similar extents on each of the three control filters. However, the inhibitory capacity of the weak base increased with the wetness of the filter. **Figure 3.7** shows the extent of culmination in the two situations. The left hand sequence shows an inhibition experiment conducted with 2.25mls of base in a support pad. In the reservoir situation (right hand sequence), half-maximal inhibition of ammonia was obtained with 0.17 ± 0.19mM, in close agreement with the data of Schindler & Sussman (1979), indicating that the disparity in our results is due simply to a difference in the experimental set up. Presumably, the increased fluid volume allows more base to remain in contact with the aggregates, prevents evaporation of the added weak base and prevents evaporation of the ammonia produced endogenously by the aggregates.

The inhibitory effect on culmination was reversible. When 48h filters were transferred to LPS-containing support pads, arrested mounds developed through to form normal fruiting bodies. This indicated that the action of the bases was not due to a cytotoxic effect, a conclusion that is confirmed by nuclear magnetic resonance data (**chapter 5**), where it is noted that high base concentrations that elicit a biological effect do not significantly hasten cell death in the NMR situation.

3.2.3 Effects of weak bases on chemotaxis

It was considered possible that the inhibitory effects of the bases on aggregation and culmination might have been due to an inhibition of the chemotactic response in the cells. Rather than affecting the cAMP relay response the weak bases could inhibit chemotactic signal transduction and prevent the cell movements necessary for culmination and aggregation, rather than affecting the cAMP-dependent signalling processes necessary for aggregation and culmination. The efficiency of chemotaxis in the presence of three of the bases (imidazole, ammonia and propylamine) was therefore tested.

The chemotactic competence of NC4 cells was measured by a spreading assay (Bonner *et al.*, 1966; Bonner *et al.*, 1970). The basis of this assay is that cells in a high density patch (approximately 10^9 cells/ml) produce cAMP phosphodiesterase which degrades the cAMP in the surrounding agar, creating a concentration gradient of cAMP. Chemotactically-competent cells then move outwards from the centre of the patch in an annulus, moving up the cAMP concentration gradient. Annuli are clearly visible under the light microscope after a few hours.

In **figure 3.9**, the normal course of chemotaxis is shown on agar containing cAMP (1mM) and buffered with phosphate at pH 7.3 (left hand sequence) and on pH 7.3 agar without cAMP (right hand sequence). Chemotaxis to cAMP does not occur under these conditions unless cAMP is present in the agar. At 6h, the annulus is visible on the cAMP-containing plate and at 24h is still clearly seen (dark circles around the cell patch are bubbles in the agar surface). This assay is particularly useful as aggregation capacity and chemotactic competence can be measured simultaneously.

In the absence of cAMP, chemotaxis does not occur at any of the base concentrations tested. The effects of the three bases were then probed. **Figure 3.10** shows chemotaxis at 24h in the presence of ammonium chloride at 11 (**A**), 110 (**B**), 220 (**C**) and 550µM (**D**). At higher base concentrations, aggregation is inhibited, but chemotaxis occurs even at the highest concentration (24h results were chosen to show the effects on aggregation simultaneously).

At the higher base concentrations, a pool of liquid develops around the cells which tends to obscure annulus formation, since the cells no longer migrate only in one plane along the agar surface but tend to migrate also to the surface of the liquid. However, it is still clear that chemotaxis has occurred. The formation of this ring of liquid is a property of the cells. Dots of cell-free base

solution placed on the surface of the agar are quickly absorbed: only in the presence of the cells is this pool of liquid seen. This suggests that water is being extruded by the cells osmotically to dilute the surrounding base solution. **Figure 3.11** shows that similar results are obtained in the presence of imidazole (**i**) and propylamine (**ii**). At the higher concentrations, the line of the annulus is blurred as cells float off in the large pool of liquid surrounding them, particularly in the case of propylamine.

3.3 Discussion

3.3.1 Effects of the weak bases on aggregation

The experiments show that treatment of aggregation-competent amoebae with base has three effects. First, the aggregate number is reduced in a dose-dependent manner without increasing aggregate size and a complete knock-out of aggregation can be achieved at high base concentrations; second, the onset of aggregation is delayed in a dose-dependent manner and third, the bases affect the morphologies of those aggregates that are formed on the filters. The fact that the aggregate number is reduced without a concomitant increase in the size of aggregation territories suggests that the weak bases reduced both the efficiency with which signals were propagated from cell to cell and the efficiency of signal initiation by individual "pacemaker" cells.

3.3.2 Inhibition of culmination

Each of the bases inhibited culmination in a dose-dependent way, but their inhibitory efficiencies varied by orders of magnitude (**figure 3.8**). The absolute concentration of weak base required to inhibit culmination was some four-fold greater than that required to give inhibition of aggregation in most cases but this may be due simply to the fact that the bases are able to diffuse freely into each cell in the aggregation experiments whereas the aggregate presents a barrier to base diffusion at culmination. High weak base concentrations gave

complete inhibition of culmination, resulting in aggregates that were arrested in development between the first finger and the fruiting body. Presumably, these arrested species are unable to produce the rise in cAMP that enables culmination to occur. Where culmination did occur, then the species formed had disproportionately large spore masses and short stalks (see **figure 3.4 D**). This may reflect a perturbation of stalk cell maturation by ammonia and promotion of the prespore pathway. The observed effect of the weak bases is in agreement with the data of Gross *et al.* (1983) from monolayer situations, in which ammonia suppresses stalk cell differentiation, and with the observations of Ferrari & Gross (unpublished) that methylamine and ammonia promote spore cell formation in the monolayer situation. If weak bases are acting by inhibiting cAMP accumulation, then the tentative conclusion might be drawn that extreme inhibition of accumulation inhibits culmination, whilst lower base concentrations promote spore cell formation in the aggregate at the expense of stalk cell formation.

3.3.3 Effects on chemotaxis

The data indicate that the inhibitory effect of the bases on aggregation are not due to inhibition of chemotaxis, since chemotaxis occurs under conditions where aggregation is inhibited (**figures 3.10** and **3.11**). This is in agreement with the work of Van Duijn & Inouye (1991) which showed that the efficiency of chemotaxis is not affected by ammonia or methylamine.

If weak bases are acting on an acidic vesicle, then they might prevent sequestration of cytosolic Ca^{2+} (as the vesicle is a calcium storage site with a membrane Ca^{2+}/H^{+}-ATPase that can act as an antiport (Rooney & Gross, 1992)). If this is the case then lowering cytosolic Ca^{2+} should not be a prerequisite for chemotaxis. The process of chemotaxis is dependent upon the cytosolic Ca^{2+} concentration as an IP_3 rise should induce the release of Ca^{2+} from internal stores, leading to the activation of guanylate cyclase (Small *et al.*, 1986) with consequent stimulation of chemotaxis. Weak base treatment would be expected

to reduce vesicular sequestration of Ca^{2+} (thus mimicking or augmenting external cAMP-mediated stimulation of chemotaxis by raising cytosolic Ca^{2+} concentrations) or to have no effect on the level of cytosolic Ca^{2+}. Either way by this reasoning, weak bases should not antagonise induction of chemotaxis.

3.3.4 Implications for the mechanism of action of ammonia

Since all the bases used (imidazole, methylamine, propylamine, octylamine and chloroquine) are chemically distinct from ammonia (**Appendix I**), the observation that they can elicit the same effect (**figures 3.1, 3.2** and **3.3**) suggests that ammonia is not acting as a specific enzyme inhibitor or being metabolized to an inhibitor but rather that it acts as a weak base. The next question is whether the observed effect is due to increases in cytosolic pH or due to neutralization of an intracellular acidic compartment.

The bases were shown to affect aggregation in the following decreasing order of potency: octylamine > chloroquine > propylamine > methylamine > ammonia > imidazole. Only 0.04μM unprotonated octylamine, was required for 50% inhibition of aggregation compared with 3500μM imidazole. With the exception of imidazole and chloroquine, increasing hydrophobicity leads to increased efficiency in inhibition of aggregation. Along with the fact that weak bases are known to be targetted towards acidic compartments (Roos & Boron, 1981), this strongly suggests that they are acting to neutralise an intracellular acidic compartment (**table 3c** below).

It has previously been argued (Gross *et al.*, 1983) that ammonia might raise cytosolic pH. However, equal concentrations of the unprotonated form of the weak base (with identical pK_a values) should raise cytosolic pH by the same extent, since the concentrations of the unprotonated species should equilibrate across the membrane with an accompanying rise in cytosolic pH (see **section 1.4**). Although the unprotonated bases would have differing rates of partition into and diffusion across the membrane, the differences in the rate of

establishing equilibrium would be expected to be of the order of seconds or minutes. A highly hydrophobic, long-chain alkylamine such as octylamine would reach the point of equilibration sooner than say, propylamine, but the difference in effect is likely to be in the order of minutes if not less (Roos & Boron, 1981). In order to account for the long term differences in the efficiencies of the bases observed in aggregation, it would have to be postulated that the differences in the rate of attainment of the equilibrium were of the order of hours. Moreover, the long term effect of the bases cannot be mimicked by a short pulse of base at the start of development, since the effect of the base is reversible even after a few hours exposure, suggesting that the continued presence of base is necessary to elicit the inhibitory effect. The conclusion is that the bases should be equally effective in inhibiting aggregation if they were to act by raising the pH of a cytoplasmic compartment.

Base	Hydrophobicity log $P_{octanol}$	Aggregation IC_{50} (μM)	Culmination IC_{50} (μM)
imidazole	0.13	3300	10,300
ammonia	-1.37[*1]	130	680
methylamine	-0.57	14	35
propylamine	0.31	3	27
octylamine	2.90	0.04	0.5
chloroquine	4.29 ± 0.12[*2]	0.3	0.6

Table 3c: Correlation between the hydrophobicity of the bases and their efficiencies in inhibiting aggregation and culmination. The hydrophobicity of the bases expressed in terms of their partitioning in octanol (log $P_{octanol}$), positive values are indicative of relative hydrophobicity and negative values, relative hydrophicility. All values are taken from the data of Leo, Hansch &

Elkins (1971) and represent true log $P_{octanol}$ values with the exception of *1 which is an extrapolation from log P_{CHCl3} and *2 which derives from my own calculation based on the method of Leo, Hansch & Elkins (1971) for calculating the log $P_{octanol}$ values of unknown compounds (see **Appendix III** for calculation).

The differential potencies of the bases in correlation with their hydrophobicities as listed above (excepting imidazole and chloroquine) suggests that they are acting to neutralize an intracellular acidic compartment. Where there is a large pH difference between two compartments, bases with different hydrophobicities would be expected to display differences in their ability to dissipate the pH gradient. Again, the bases should show little difference in their ability to equilibrate across the vesicular membrane, but the more hydrophobic bases would be more capable of setting up a proton-leakage cycle by virtue of their ability to back-flux across the membrane easily as the protonated species. In the case of the more hydrophobic bases (propylamine, octylamine and chloroquine), the presence of long hydrophobic chains would "shield" the charge from the membrane by a combination of an electron-inductive effect and steric shielding; thus allowing the base to act as a highly efficient proton-shuttle across the membrane (**figure 1.4**). This would explain why octylamine is required in such low concentrations to inhibit aggregation; as an effective proton shuttle it would be constantly recycled around the vesicular membrane, counteracting the acidification of the vesicle by its vacuolar H^+-ATPase. The lesser potency of ammonia is consistent with it being a less effective proton shuttle. NH_4^+ can cross a lipid bilayer (Thomas, 1974) as can protonated methylamine, being small enough to pass through bilayer pores created by lipid chain motions (**section 1.4**). The charge density, size and cyclic structure of protonated imidazole precludes its passage through a lipid bilayer. Although chloroquine also has a cyclic ring system, it should be able to traverse membranes, having a long hydrophobic arm that intercalates into lipid bilayers, facilitating trans-membrane passage (**Appendix III**). From

the hydrophobicity data, chloroquine would be expected to be the most effective base at inhibiting aggregation and culmination. However, the data show that octylamine is the more effective. Possible explanations include steric hindrance to the passage of chloroquine across the bilayer (relative to octylamine); the existence of some cytoplasmic or membrane sink for chloroquine or that chloroquine is actively effluxed from the cytoplasm. Results with isolated vesicles indicate that the latter possibility is the most likely (see chapter 4).

These data provide strong, if circumstantial, evidence that the effect of ammonia upon aggregation is mediated via an acidic vesicle. It is also worth noting that the IC_{50} value for the inhibition of aggregation by ammonia (130μM) is very similar to the IC_{50} value for inhibition of cAMP relay derived from the data of Williams et al. (1984), which indicates that the effect seen here on aggregation might be attributable to an (indirect) inhibition by ammonia of cAMP production by adenylate cyclase.

3.3.5 Possible regulation of aggregation through the acidic vesicle

It has been suggested that neutralization of the acidic vesicle by ammonia could influence its cytosolic Ca^{2+} sequestration capacity, as the vesicular membrane contains a H^+/Ca^{2+} antiporter (Rooney & Gross, 1992). It could be postulated that NH_3 raises the cytosolic $[Ca^{2+}]$ with consequent inhibition of adenylate cyclase, which is known to be inhibited by high Ca^{2+} concentrations in mammals (De Bernardi *et al.*, 1991; Boyajian *et al.*, 1991), resulting in a lowering of $[cAMP_i]$ and concurrent inhibition of aggregation or culmination. Since it has been proposed that both processes are dependent upon cAMP (Abe & Yanagisawa, 1983; Merkle *et al.*, 1984; Williams *et al.*, 1984), ammonia might affect adenylate cyclase activity. Certainly, adenylate cyclase activity is therefore important in the developmental process and has been shown to be developmentally regulated. Activity is undetectable in exponentially growing vegetative cultures, but increases during aggregation to an activity of 20pmoles cAMP/10^7 cells at 3h of starvation and doubling by 4h (Klein, 1976), with a

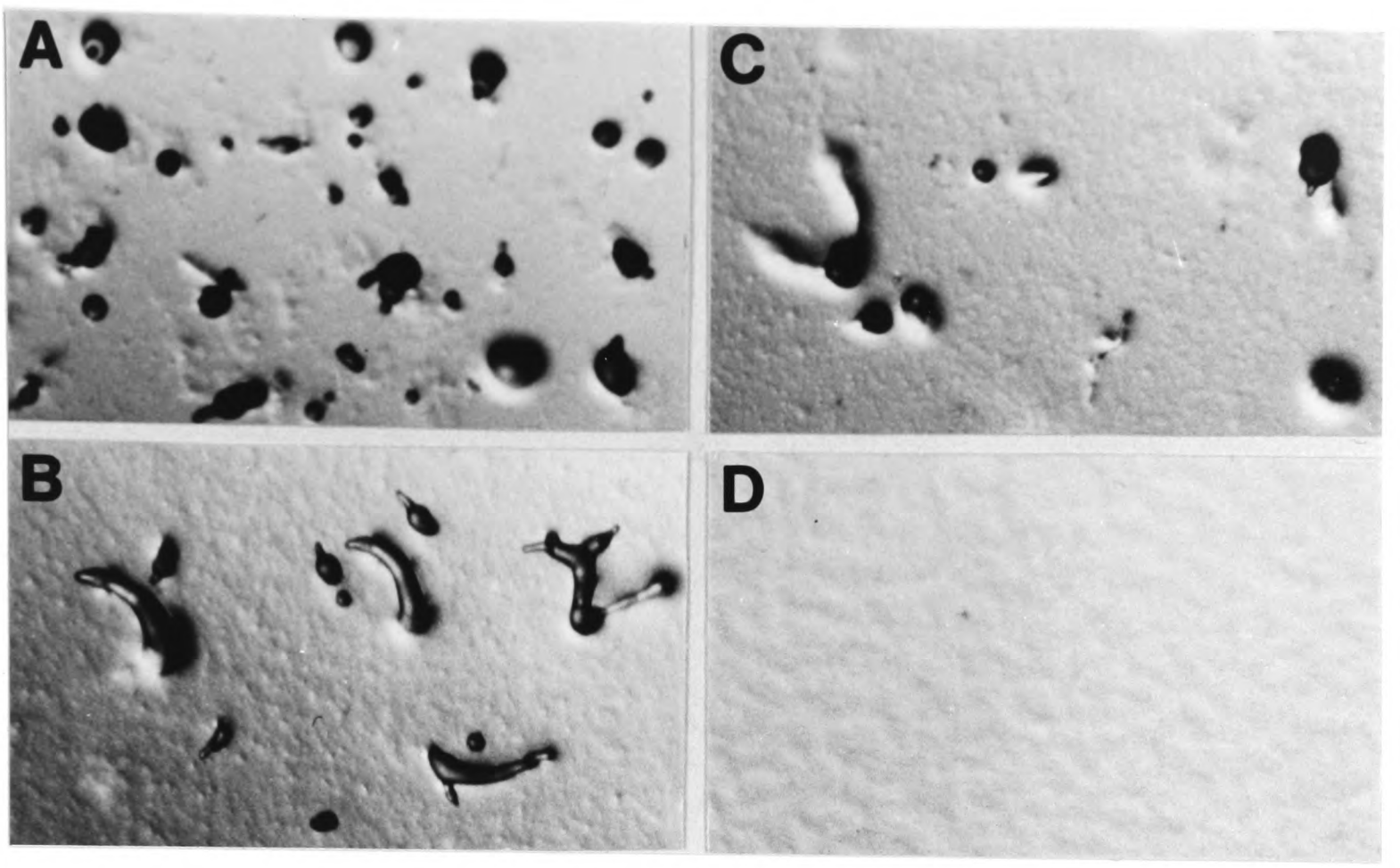
further peak observed at culmination (Abe & Yanagisawa, 1983). However, cells in which the aggregation adenylate cyclase is knocked out (*aca*$^-$) are capable of culminating (Pitt *et al.*, 1993). It is possible that ammonia could affect components of the cAMP signalling pathway downstream of adenylate cyclase, or might act upon another signalling pathway converging with that of cAMP upon such enzymes as cAMP-dependent PKA.

3.4 Conclusions

These experiments demonstrate that all weak bases can inhibit development both at aggregation and at culmination and that the order of potency of inhibition of the bases for culmination correlates well with the order obtained for inhibition of aggregation (**figure 3.12**). It is therefore possible that they act via the same mechanism at both stages.

Since the inhibitory activity of ammonia can be mimicked by wide variety of chemically distinct weak bases, the implication is that ammonia is not inhibiting specific enzymes but rather that it acts as a weak base. Postulating an acidic vesicle as the target of the bases in inhibition of aggregation and culmination provides an explanation for their differences in potency. Therefore, chapter 4 examines the efficiency of the bases in inhibiting vesicle acidification directly.

(i)



(ii)

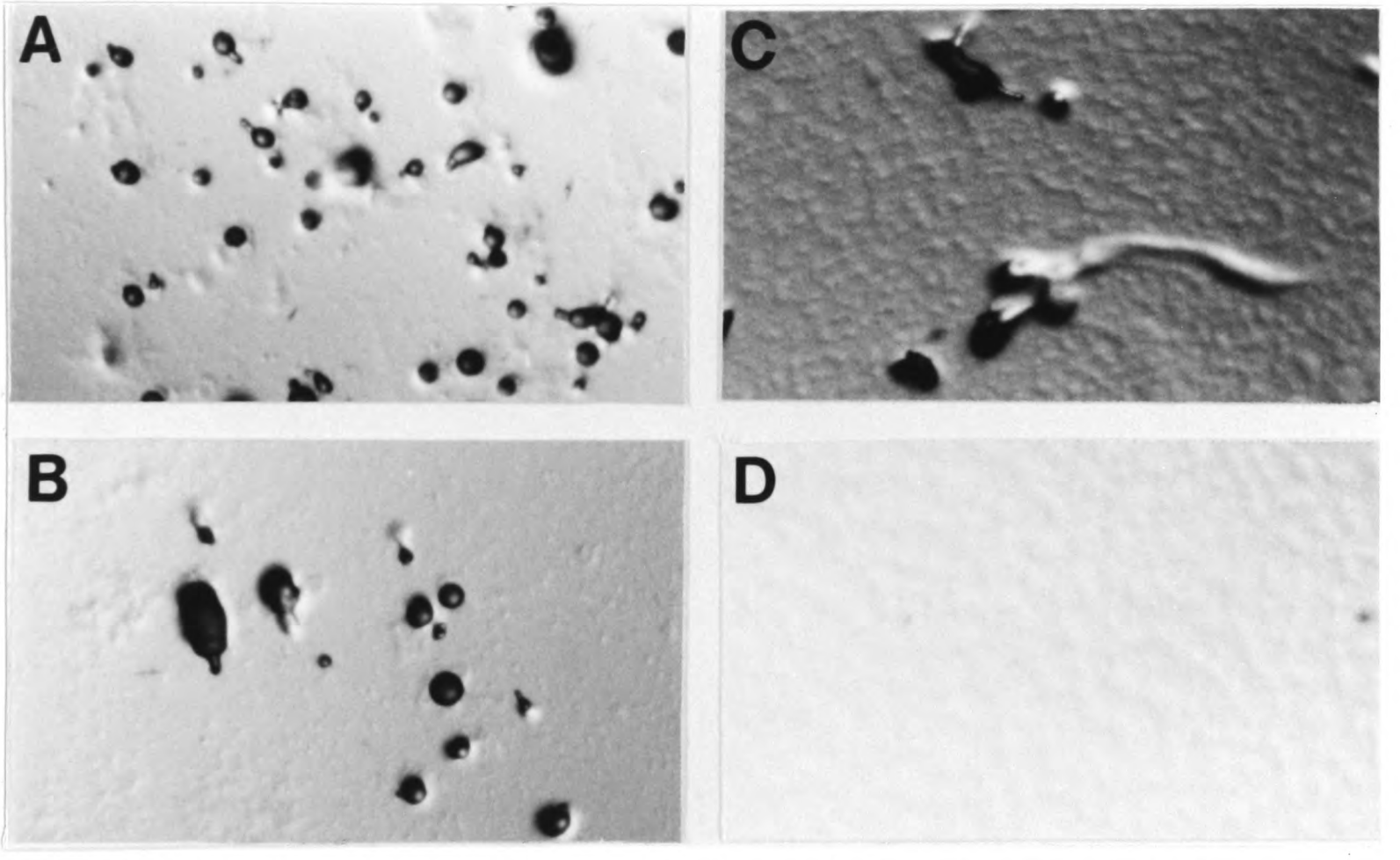
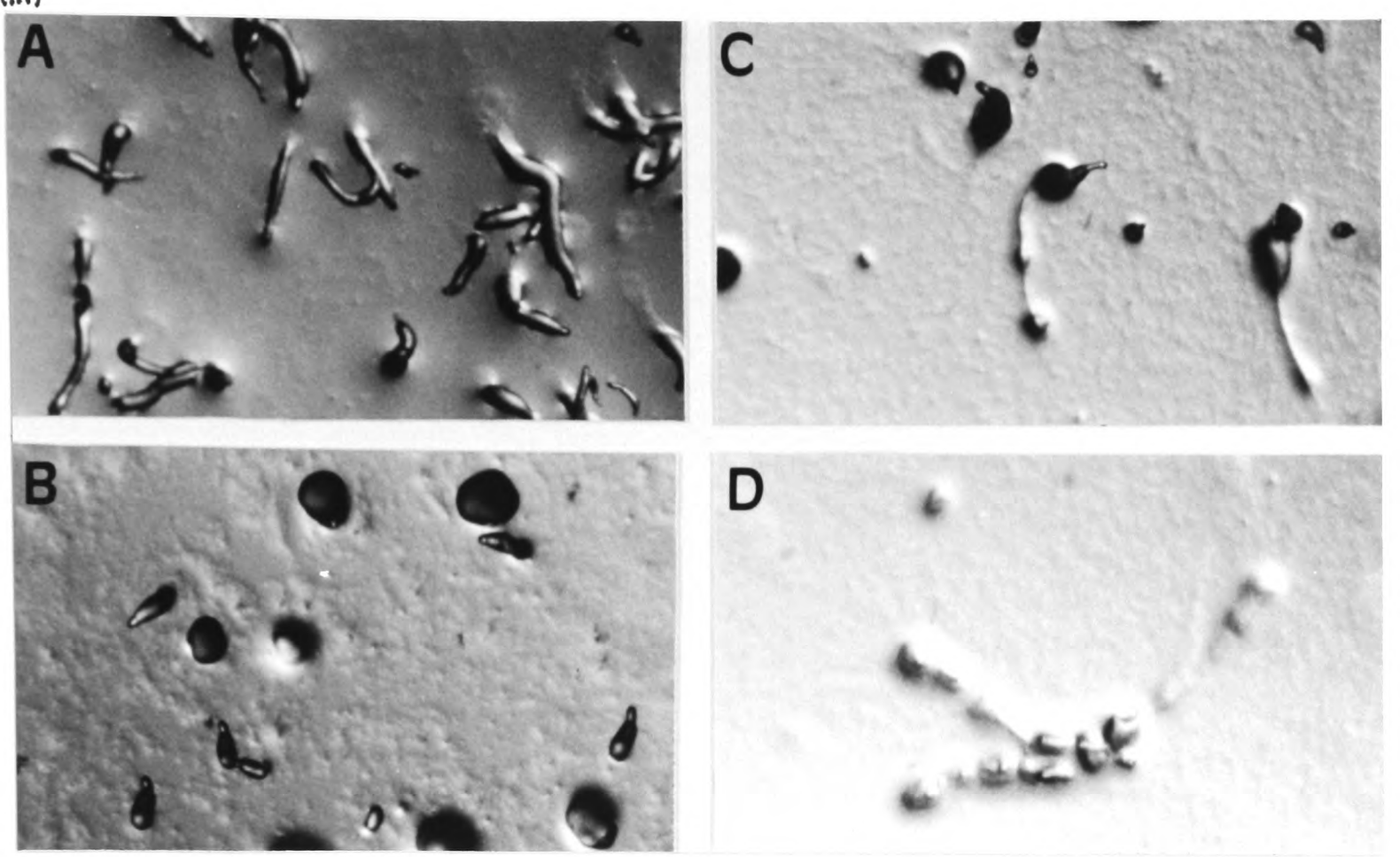


Figure 3.1: Reduction of aggregate number by weak base treatment (pH 7.3, base concentrations are given as the unprotonated form).

(i) Effect of ammonia - (A) LPS control, (B) 220µM, (C) 330µM, (D) 990µM.

(ii) Effect of methylamine - (A) LPS control, (B) 5µM, (C) 22µM, (D) 35µM.

(iii)



(iv)

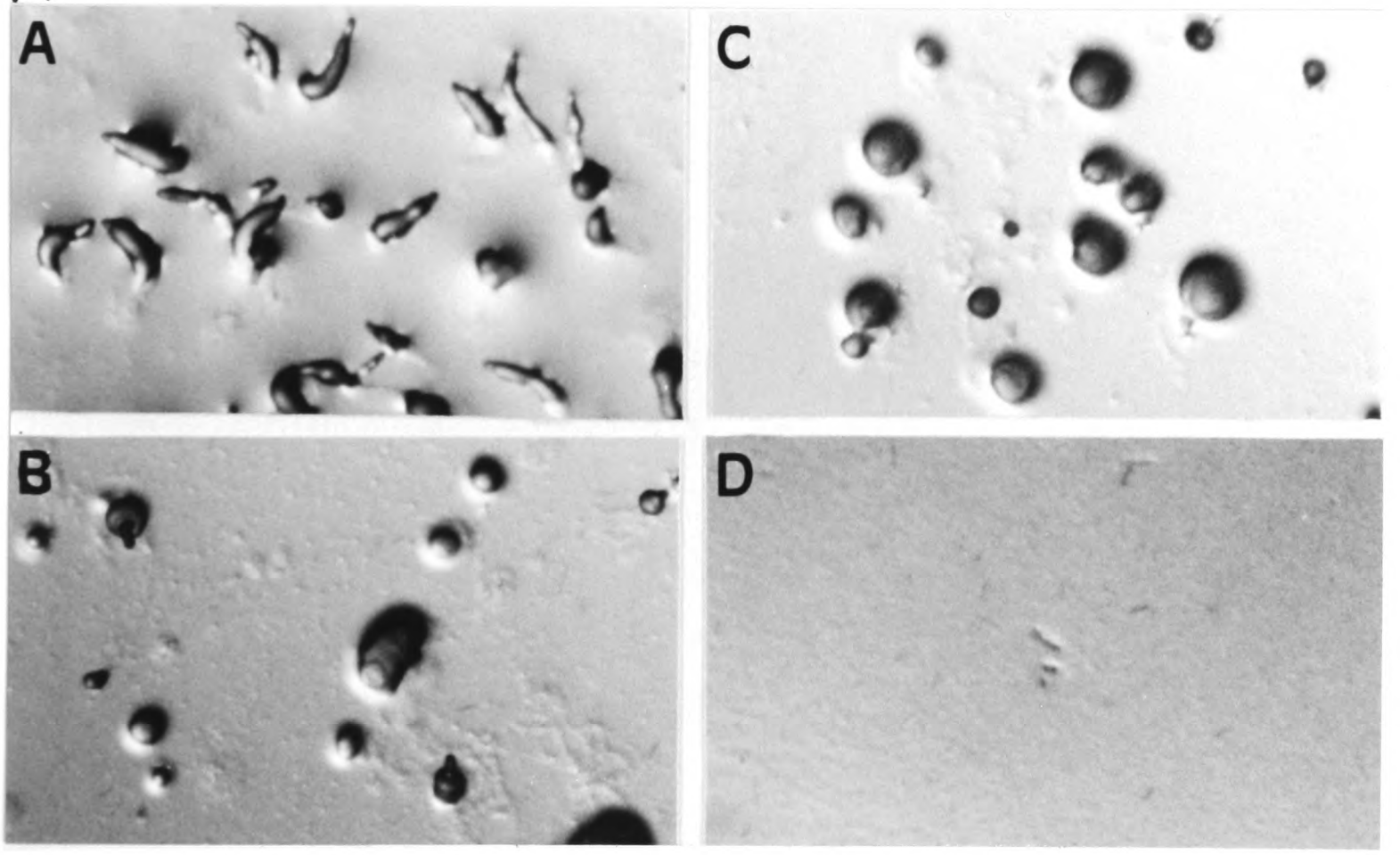
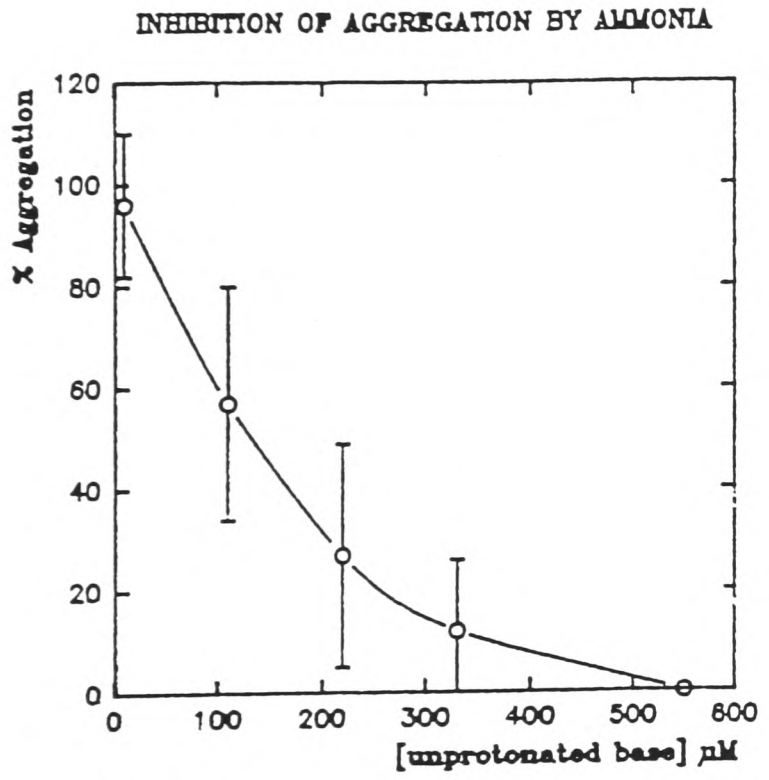
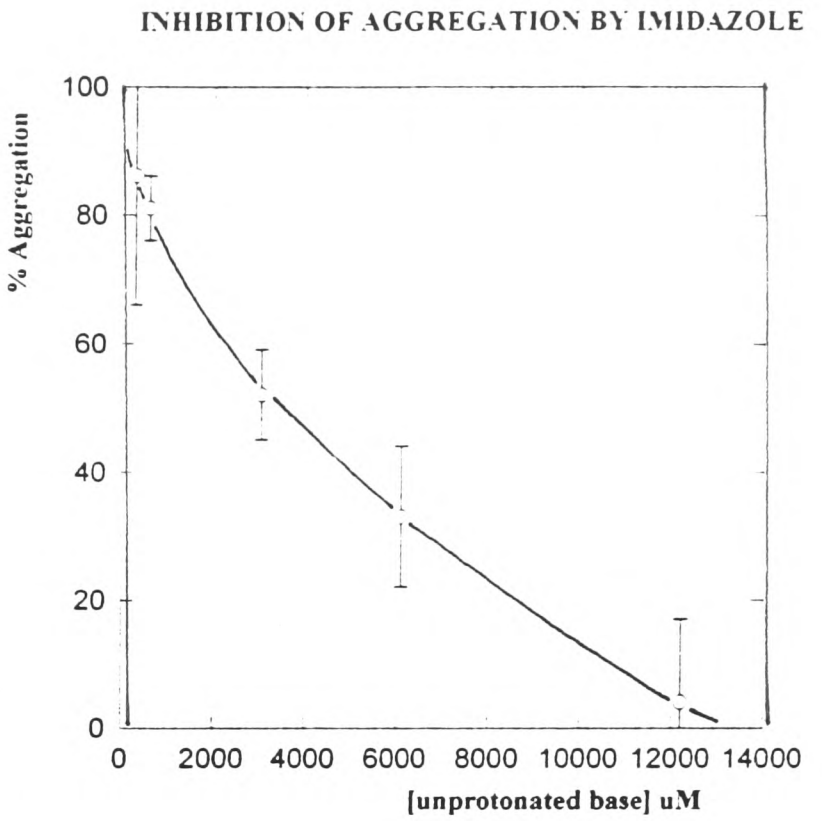


Figure 3.1 (continued):

(iii) Effect of propylamine - (A) LPS control, (B) 4μM, (C) 8μM, (D) 12μM.

(iv) Effect of chloroquine - (A) LPS control, (B) 0.1μM, (C) 0.17μM, (D) 1.7μM.





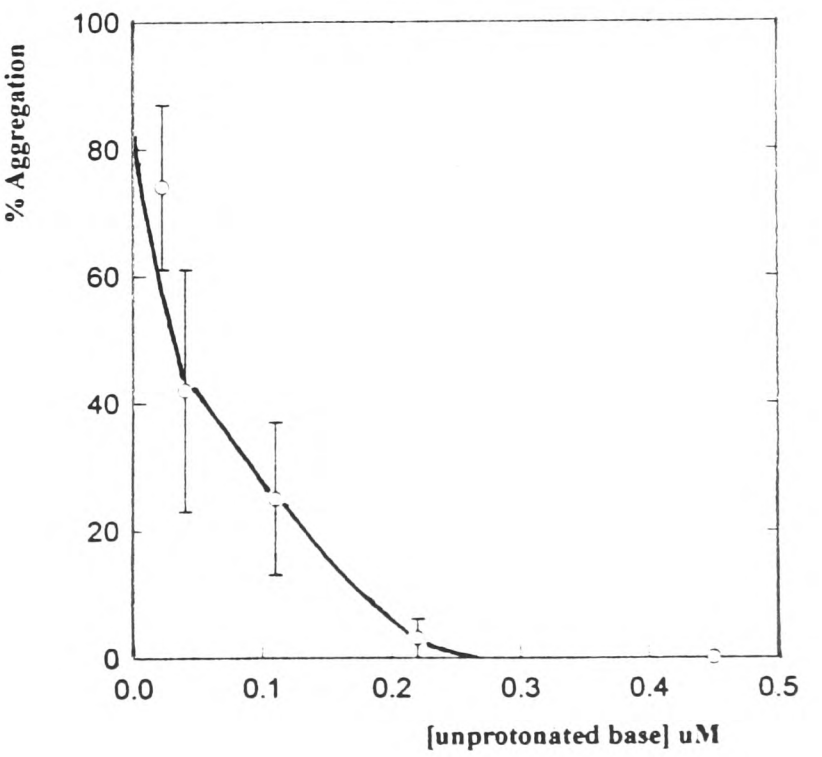


Figure 3.2: Inhibition of aggregation on filters (pH 7.3) by imidazole, ammonia and octylamine (unprotonated base concentrations given).

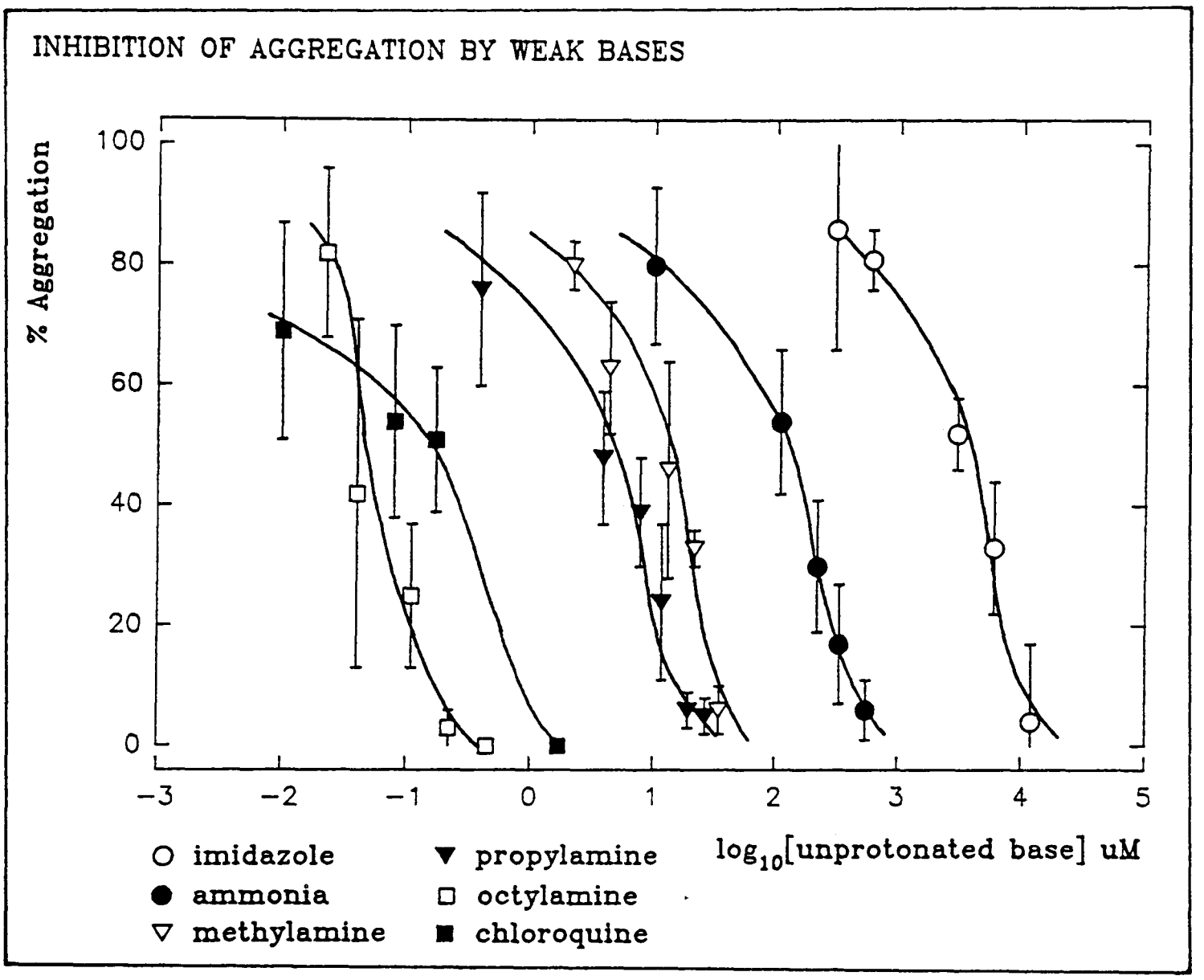


Figure 3.3: Log_{10}dose vs. response graph for the inhibition of aggregation by the various weak bases.

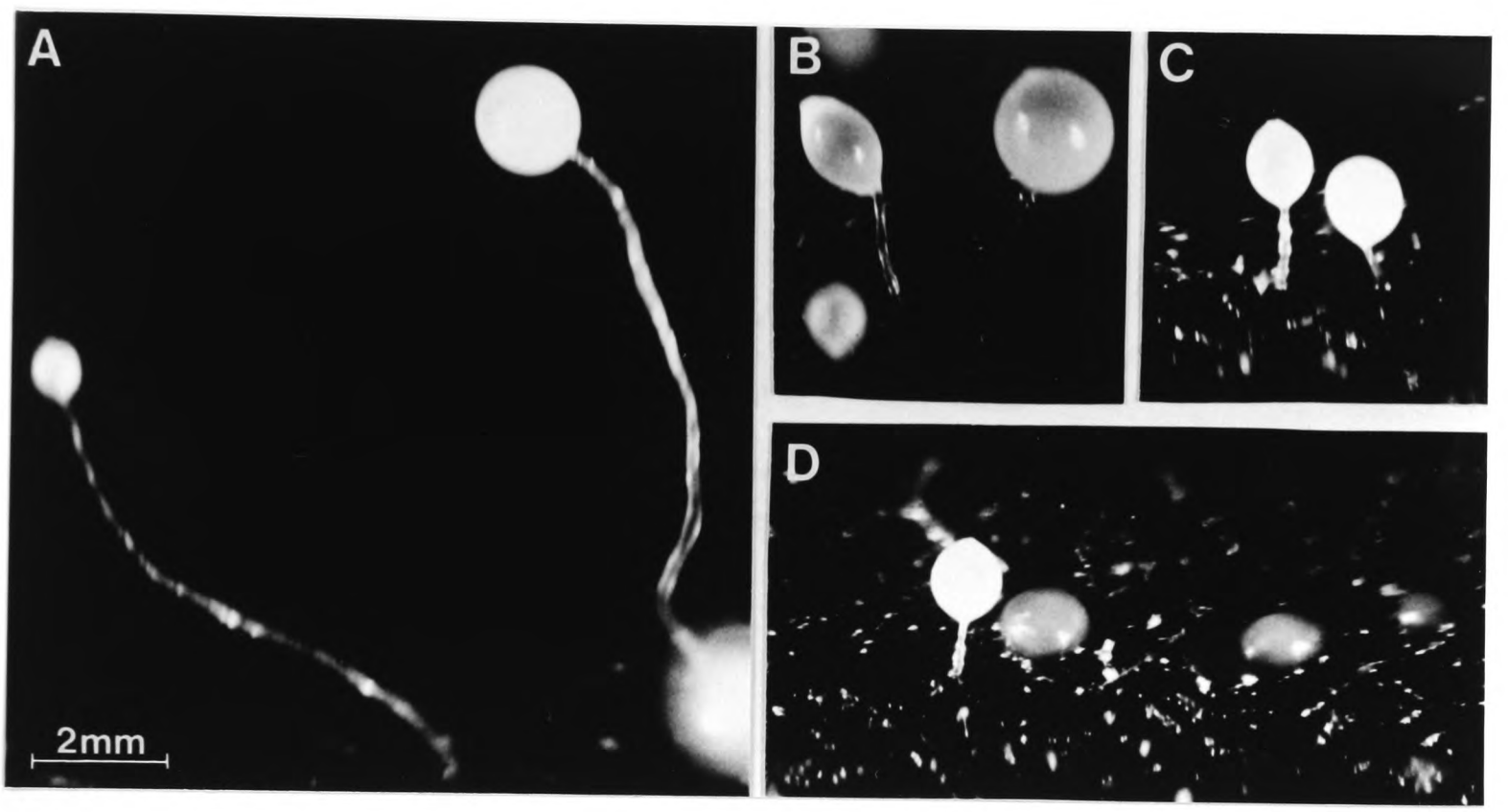


Figure 3.4: Inhibition of NC4 culmination on filters by ammonia. (A) LPS control, (B) 330μM, (C) 770μM (D) 990μM.

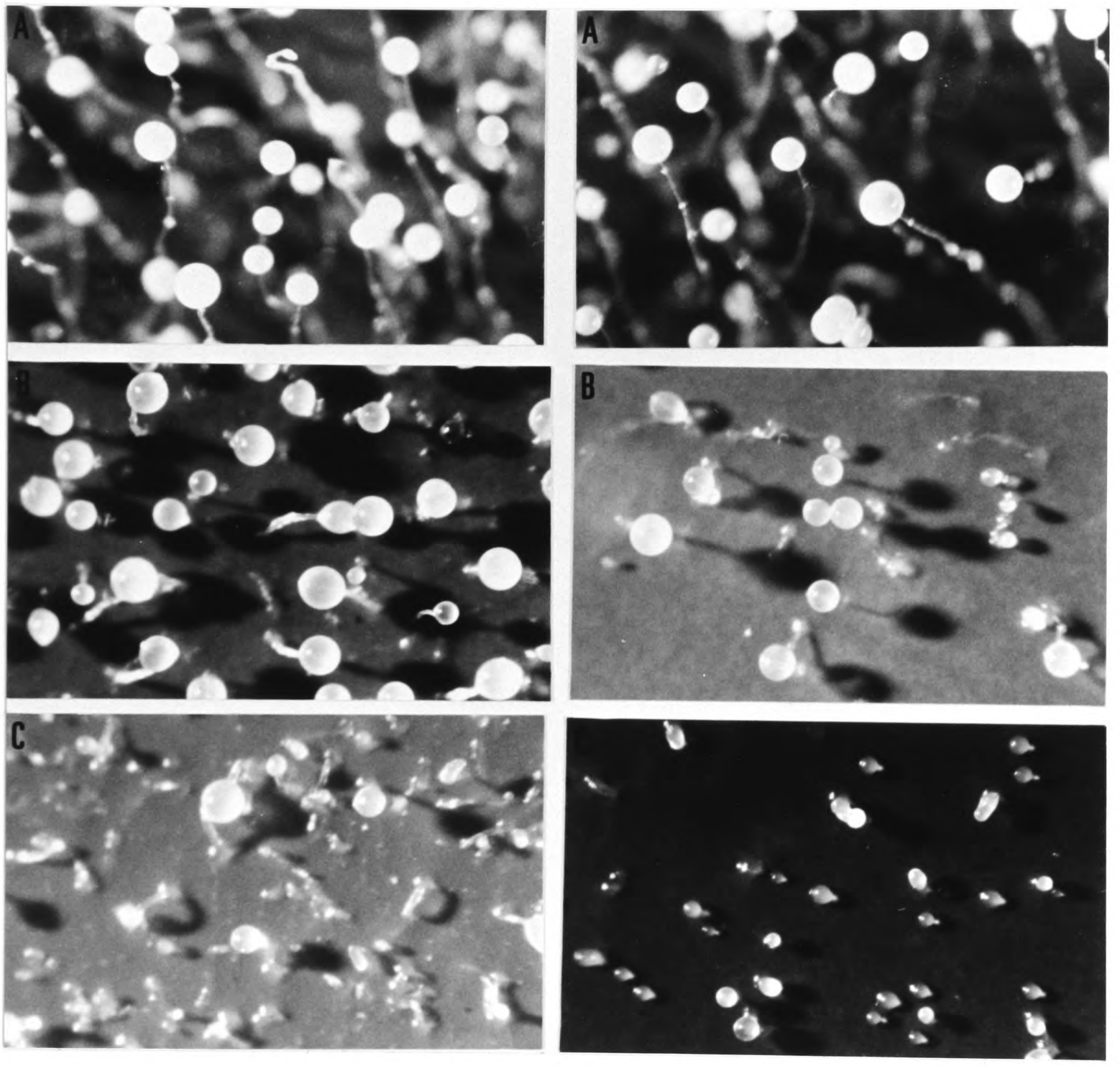
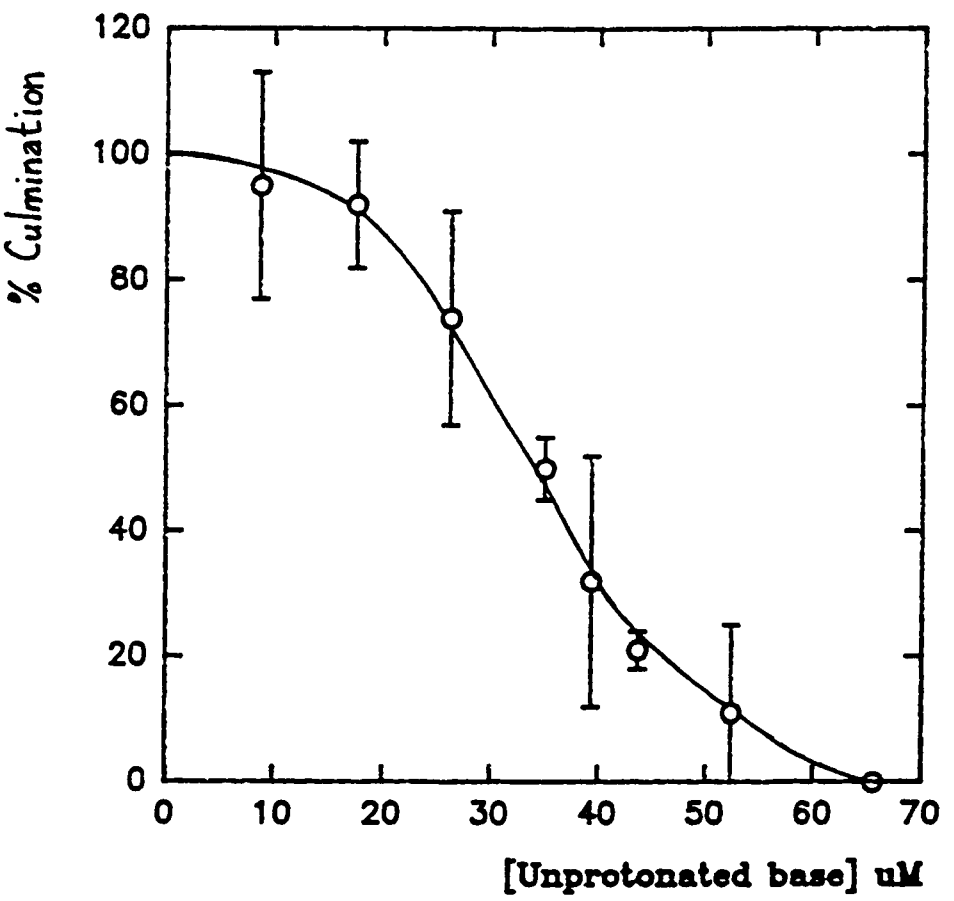


Figure 3.5: Inhibition of culmination on filters at pH 7.3 by propylamine (left hand sequence) and imidazole (right hand sequence). Again base concentrations are expressed as the unprotonated form. **Propylamine**: (A) LPS control, (B) 27µM, (C) 39µM. **Imidazole:** (A) LPS control, (B) 18.3mM, (C) 31mM.

(A)



(B)

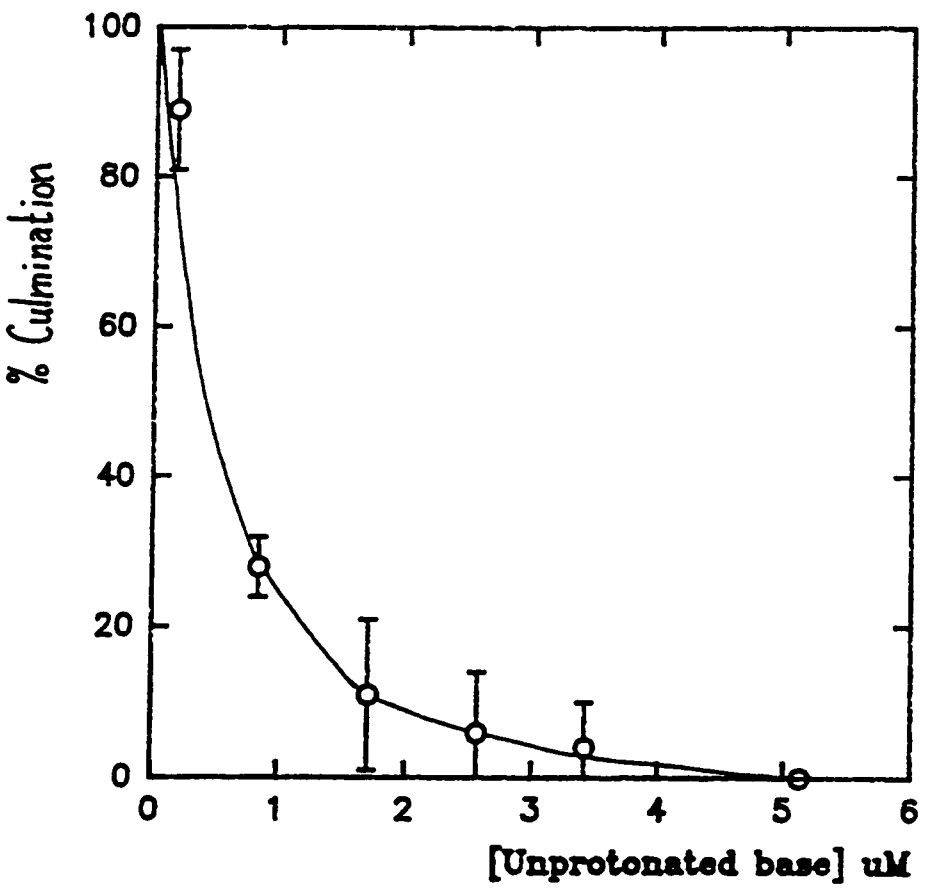


Figure 3.6: Quantitative measure of inhibition of culmination on filters at pH 7.3 by (A) methylamine and (B) chloroquine

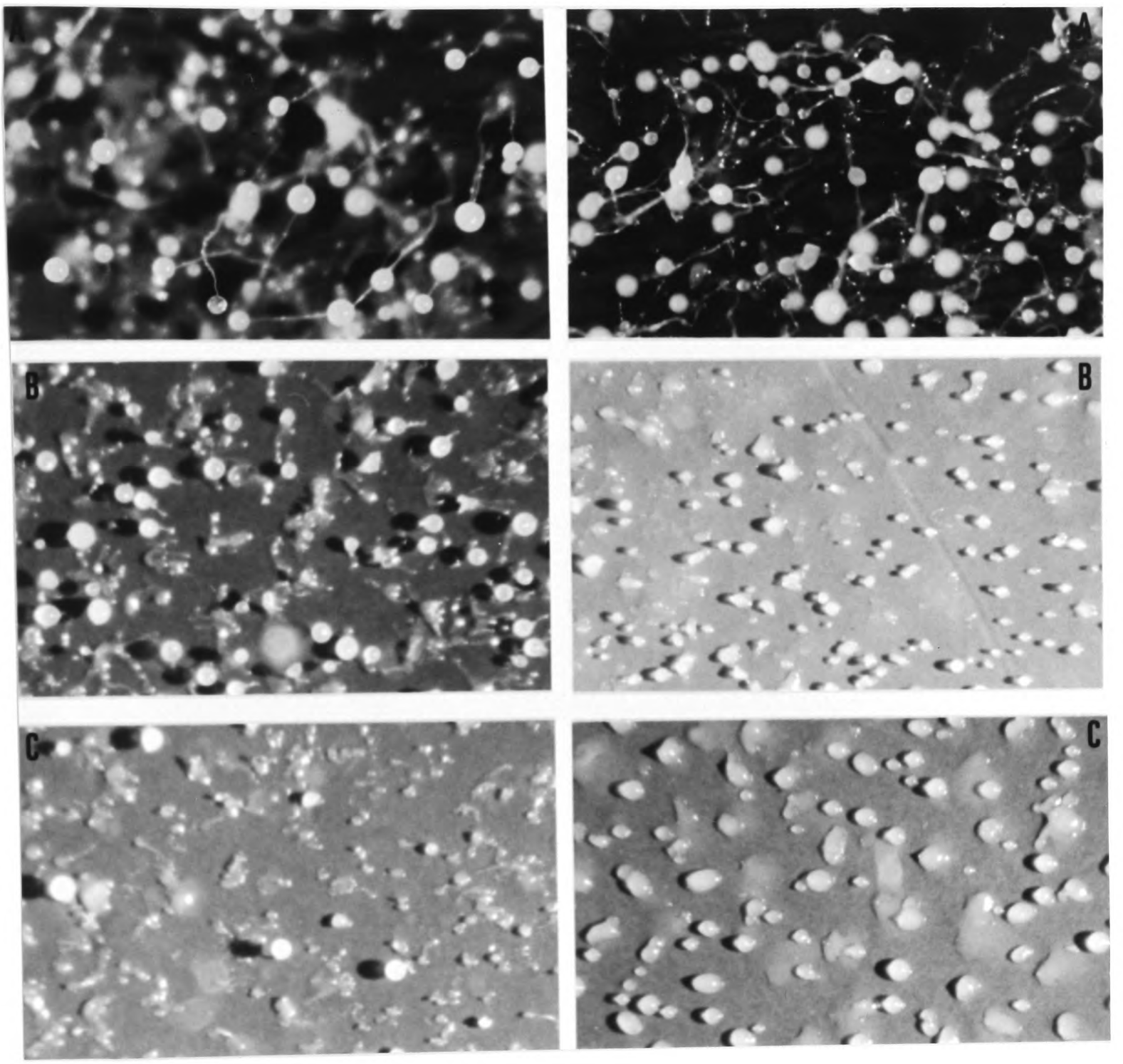


Figure 3.7: The effect of the weak base reservoir volume on the inhibition of culmination in NC4. The left hand sequence shows the extent of culmination on filters in contact with 2.25ml solution in a support pad. The right hand sequence shows the extent of culmination when filters are exposed to a large (30ml) volume of solution. For both (A) LPS control, (B) 550µM ammonia, (C) 1.4mM ammonia.

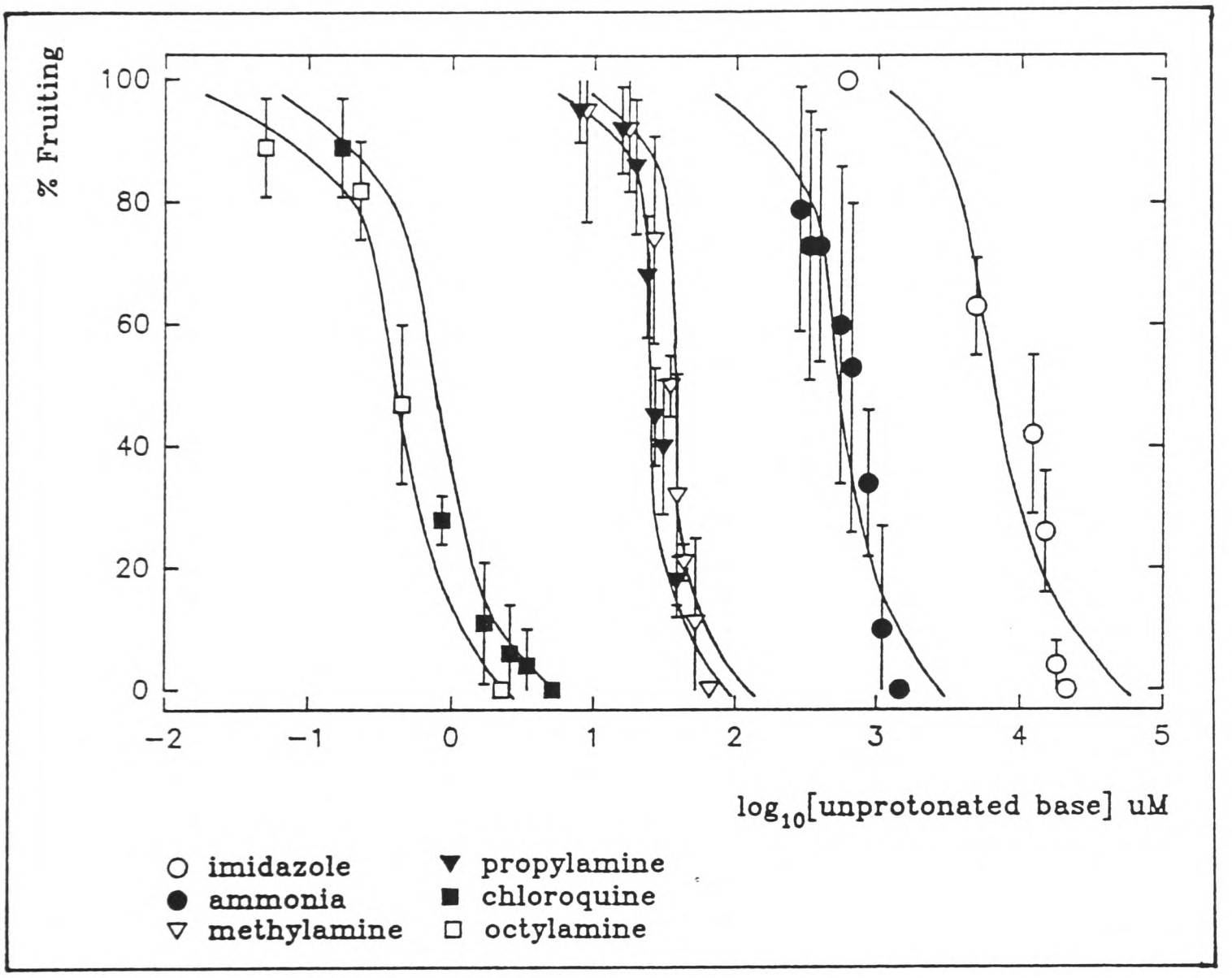


Figure 3.8: Comparison of the effects of the weak bases in inhibiting culmination - a $\log_{10}$dose-response curve for each base. Culmination is expressed as a percentage relative to the control.

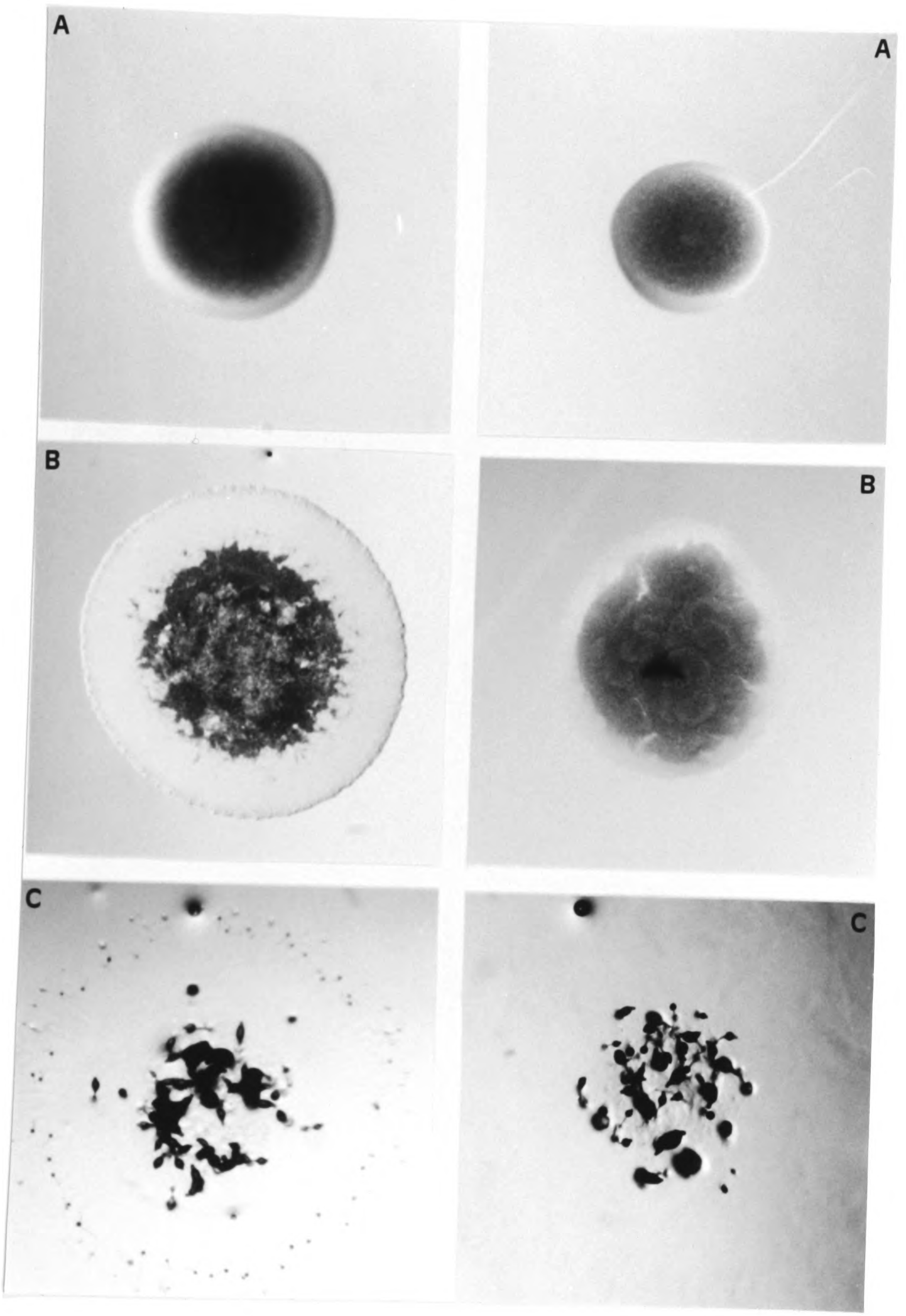


Figure 3.9: Chemotaxis on LPS-agar (pH 7.3) with cAMP (1mM, left hand sequence) or without cAMP (right hand sequence). (A) 0h, (B) 6h, (C) 24h. Appearance of an annulus indicates that a chemotactic response has occurred.

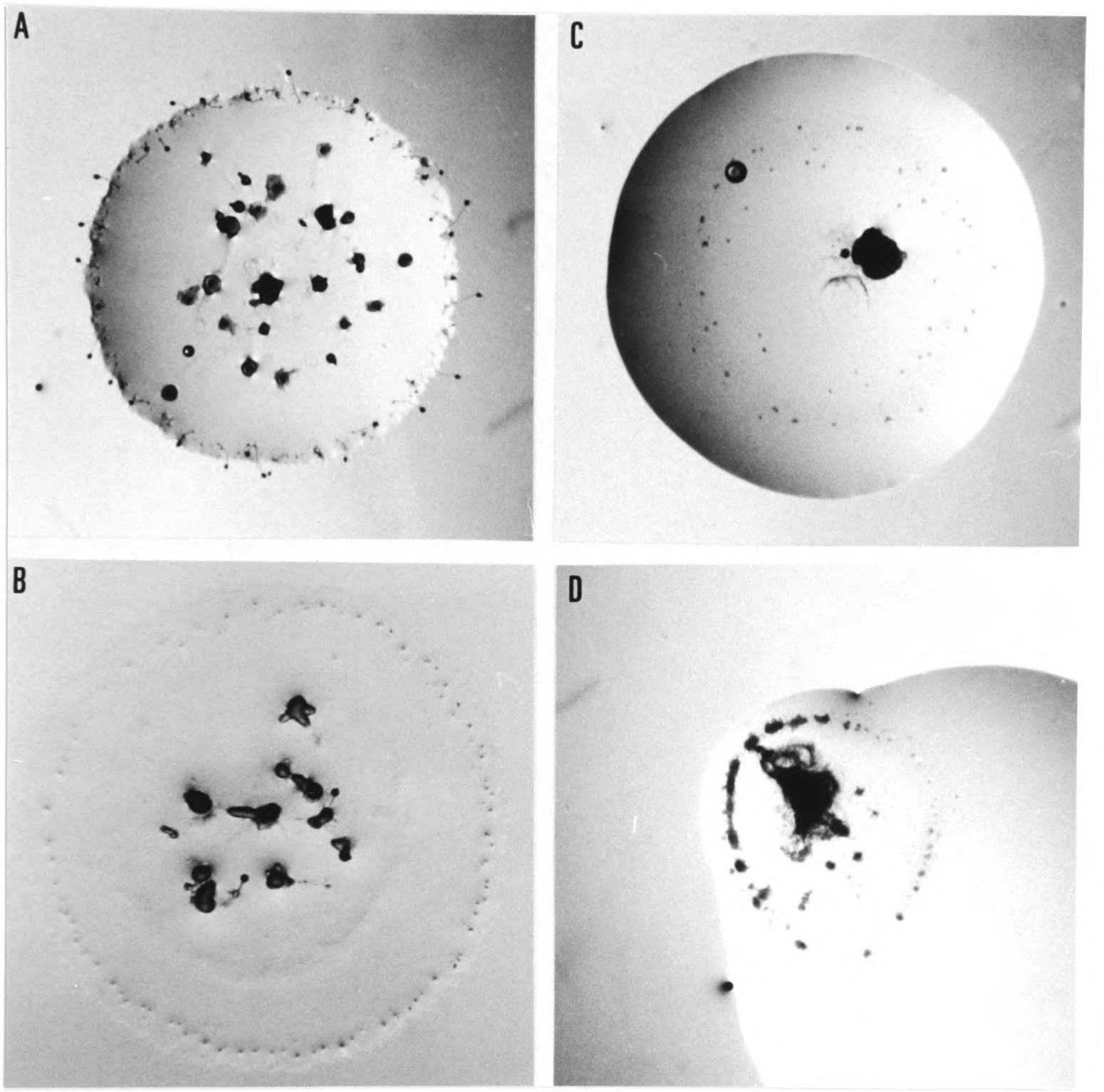


Figure 3.10: Chemotaxis in the presence of ammonia on LPS-agar (pH 7.3). (A) 11μM, (B) 110μM, (C) 220μM and (D) 550μM.

(a)

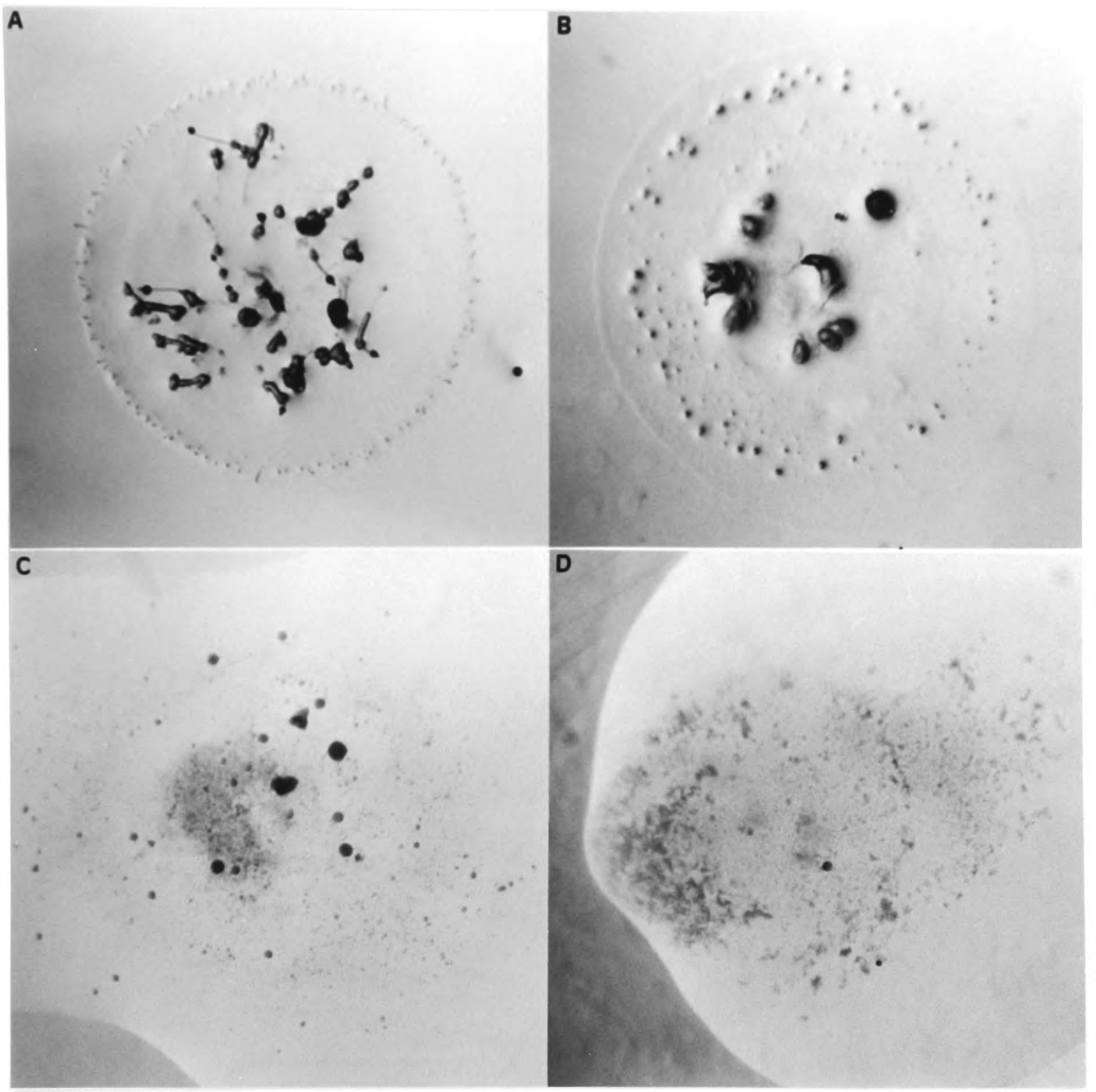


Figure 3.11 (a): Chemotaxis in the presence of imidazole (conditions as for figure 3.10). (A) 0.6mM, (B) 6.1mM, (C) 12.2mM and (D) 30.5mM.

(b)

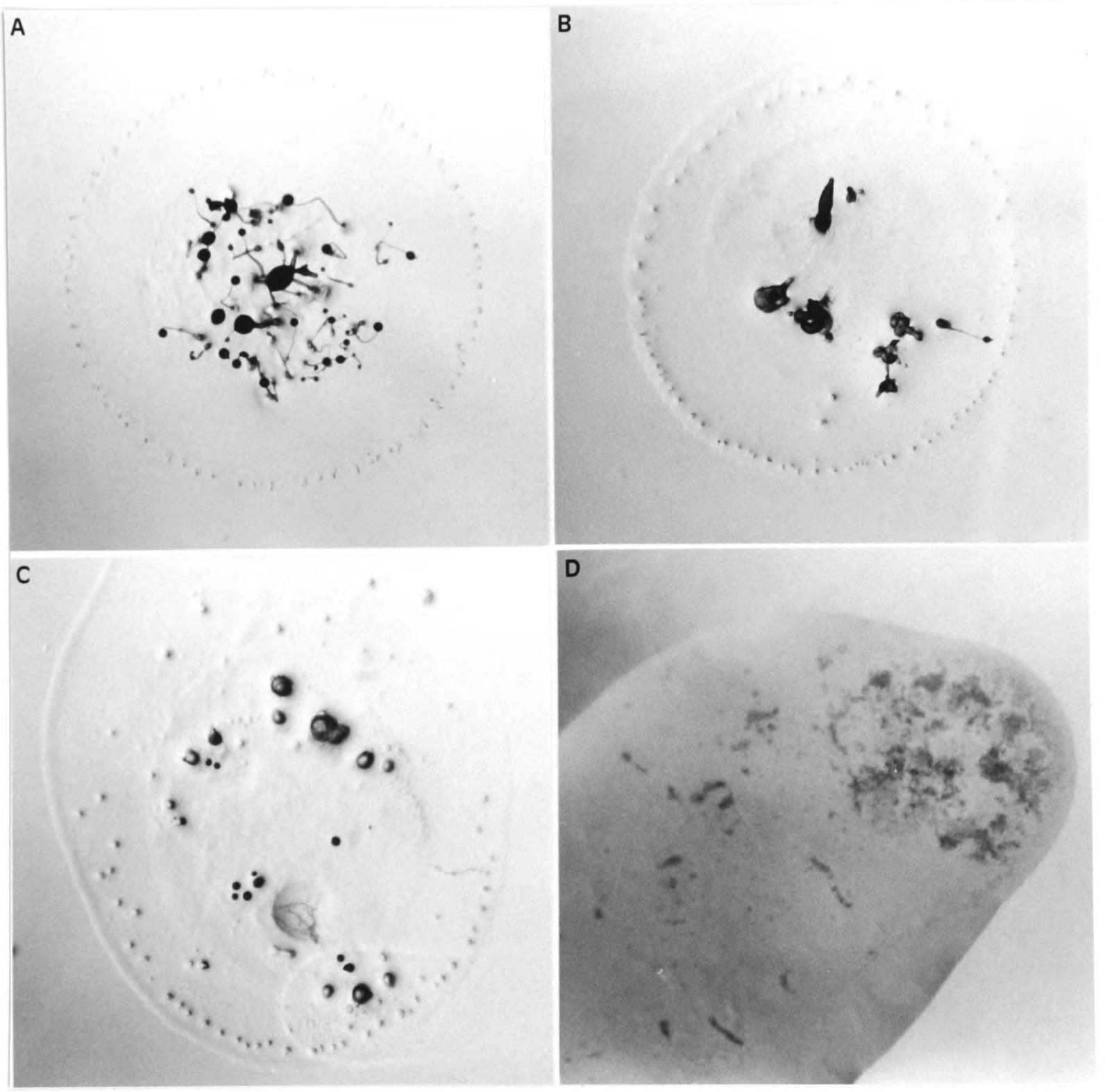


Figure 3.11 (b): Chemotaxis in the presence of propylamine. (A) 0.4μM, (B) 3.9μM, (C) 7.8μM and (D) 19.5μM.

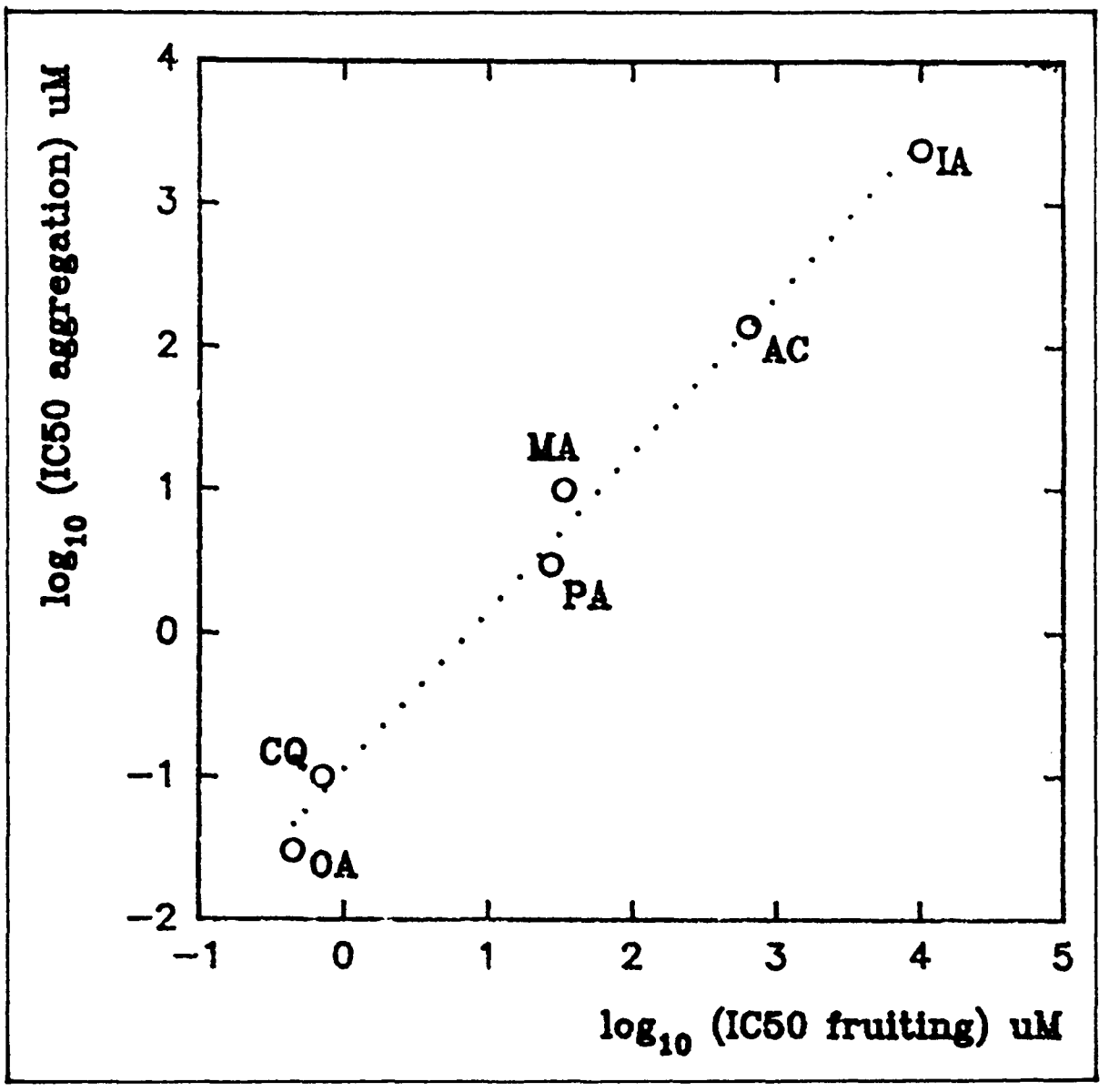


Figure 3.12: Correlation between the inhibitory effects of weak bases on aggregation and on culmination *in vivo*. The log of the IC_{50} of each base for aggregation is plotted against that for culmination.

Chapter 4

Chapter 4 *The Effects of Weak Bases on Vesicle Acidification in vitro*

4.0 Introduction

4.0.1 Aims of the experiments

In the previous chapter the inhibitory effects of the weak bases on the *in vivo* processes of aggregation and culmination were presented. Analysis of the results of those experiments suggested that the ammonia might be acting to neutralize an acidic vesicle, rather than raising cytoplasmic pH or directly inhibiting enzymes involved in aggregation or culmination. First, all the weak bases mimicked the action of ammonia and second, the more hydrophobic bases were the most effective inhibitors, suggesting that weak bases acted as proton shuttles across a vesicular membrane rather than raising cytosolic pH.

This chapter describes the effect of the bases on acidic vesicles isolated from whole cells. The *in vitro* system gives a direct test of the ability of the bases to dissipate a pH gradient in these vesicles and allows the inhibitory efficiencies of the bases to be studied without interference from any possible cytoplasmic effects such as active extrusion of a base from a cell or sequestration of a base in a cytoplasmic sink. In particular, the prediction that chloroquine is actively effluxed from the cell can be tested: if active efflux occurs, chloroquine should be far more effective in inhibiting acidification in the isolated vesicle than in the whole cell. Effectively, the isolated vesicle is used as a model system to study the passage of weak bases in their charged and uncharged forms across biological membranes in the presence of a pH gradient.

4.0.2 Acidic vesicles in Dictyostelium

Figure 4.1 presents a generalized diagram of an acidic vesicle. The membrane is rich in vacuolar H^+-ATPase (Padh *et al.*, 1989a; 1989b), contains a proton-translocating Ca^{2+}-ATPase (Rooney & Gross, 1992) and anion transporters. These vesicles show ATP-dependent calcium uptake (Rooney & Gross, 1992; Rooney *et al.*, 1994) and are thought to be fragments of the contractile vacuole complex (Heuser *et al.*, 1993), which has been shown to be associated with calmodulin (Zhu *et al.*, 1993) and may therefore act as a calcium storage site. The pH gradient between the cytosol and the intravesicular space provides a driving force for the transport of ions and molecules (Yamashiro & Maxfield, 1988). Maintenance of the correct vesicular pH is also essential for such processes as protein targetting and post-translational protein modification (described in detail in chapter 1).

4.1 Results

4.1.1 Assay of vesicular acidification by fluorescence spectroscopy

The basis of the assay is as follows. Excitation of monomeric Acridine Orange (AO, see **appendix V** for structure) occurs at 495nm and fluorescence emission at 530nm. Since the dye is a membrane-permeable tertiary amine, it accumulates in acidic vesicles. As its concentration increases, dimerization is induced, resulting in an absorbance decrease at 495nm (the dimer absorbs at 465-470nm) and fluorescence quenching at 530nm due to the decreasing monomer concentration. Spectral evidence (Palmgren, 1991) suggests that the absorbance decrease and quenching seen in these assays is due solely to dimerization (and subsequent oligomerization) of the dye, not to protonation of AO or to dye-membrane interactions. Since the extent of accumulation of the dye is determined by the level of vesicular acidification (Gluck *et al.*, 1982; Palmgren, 1991), the method gives a qualitative measure of the extent of

vesicular acidification. No quantitative measure of acidification can be obtained, since the spectral changes do not arise from the protonation of the AO molecule. A limitation of the assay is that vesicles with low acidification levels will appear to have lower acidification levels than is actually the case since they will concentrate AO, but at insufficient concentrations for dimerization, hence fluorescence intensity changes will not be observed despite the fact that the vesicles have concentrated some acridine orange. Despite this limitation, the assay provides a useful measure of the extent of acidification of the vesicle.

The endomembrane fraction of the cell was isolated by sucrose density gradient centrifugation (Rooney & Gross, 1992), pelleting at 39,000g in 10% sucrose. This fraction is relatively free of mitochondrial, lysosomal, plasma membrane and soluble markers (Padh *et al.*, 1989b). Mitochondrial contamination does not pose problems for interpretation of results as the internal mitochondrial pH is higher than the cytosolic pH (Addanki *et al.*, 1968), thus they do not concentrate weak bases. Therefore, mitochondrial ATPase inhibitors were omitted from the assay buffer.

Purified vacuoles containing vacuolar H^+-ATPase activity were shown to be capable of acidifying by their quenching of acridine orange fluorescence in the presence of ATP. Vesicle solutions containing between 30 and 120µg of protein were made up in assay buffer (AB) containing 2µM AO and the dye allowed to equilibrate across the membranes for a few seconds, resulting in a steady baseline reading on the spectrofluorometer. Acidification of the vesicles was then induced by addition of ATP to a final concentration of 2mM and the acidification rate measured as the rate of fluorescence quenching over 120s (see **figure 4.2** for representative spectra). The fluorescence intensity decayed as AO concentrated in the vesicles in response to the generation of a pH gradient and dimerized, leading to an overall decrease in the concentration of AO monomers, with a consequent decrease in the fluorescence intensity. In order

to determine the effects of weak bases, vesicles were preincubated in assay buffer containing weak bases at various concentrations for roughly one minute before the addition of ATP. The chloride salt of the base was used as this ion is already present in the assay buffer, so addition of ammonium chloride does not introduce any new anions which might affect vesicular function. Nitrate (Moriyama & Nelson, 1989) and sulphate (Wang & Gluck, 1990) for example, both impair V-type ATPase activity.

In the range of protein concentrations used, the extent of fluorescence quenching was shown to be roughly linear to protein concentration in any one experiment (**figure 4.3**). However, results are presented as percentage acidification relative to the control situation on that particular day, which eliminates any possible variability from day to day due to differing levels of contaminant protein (*eg.* residual mitochondria, plasma membrane) and affords easy comparison with the aggregation and culmination data from chapter 3.

4.1.2 The effects of weak bases on vesicular acidification in the wild-type strain NC4

All of the weak bases which were used in the *in vivo* developmental studies were tested for their effects on isolated acidic vesicles and each was found to inhibit the ATP-dependent acidification of vesicles in a dose-dependent manner. The full range of concentrations tested is shown for ammonium chloride, some intermediate concentrations are omitted with the other bases for clarity. As it is the unprotonated form of the weak base that is freely permeable across the vesicular membrane, results are based on this concentration rather on that of the total weak base. The proportion of unprotonated base existing at pH 7.3 in the buffer was calculated with the Henderson-Hasselbalch equation (see **appendix II** for calculations).

In **figure 4.4**, the effect of ammonia is shown in detail. In the control situation (lower line), addition of ATP leads to quenching of fluorescence from

a maximum (designated 100%, t=10 seconds) as vacuoles acidify in response to the activation of the vacuolar H^+-ATPase by ATP. Without addition of ATP, no significant fluorescence quenching is seen (not shown); so any quenching seen in its presence can be ascribed to acidification of the vesicle. Acridine orange then concentrates in the vesicles, giving an overall decrease in the fluorescence intensity. The rate of acidification of the vesicles is proportional to the rate of fluorescence quenching and follows a sigmoidal course. A short lag phase is observed (5-10 seconds) followed by acidification at a maximum rate until a plateau level is reached.

Each of the weak bases that was tested inhibited acidification. Inclusion of weak base in the assay buffer inhibits acidification according to the dose of weak base applied (**figure 4.4**, upper lines). In the case of ammonia, a significant effect is seen even with 0.6µM and total inhibition occurs at 44µM. Other weak bases have similar effects, but the concentrations required for inhibition of acidification vary greatly. Shown in **figure 4.5** are the effects of imidazole **(a)**, methylamine **(c)**, propylamine **(d)**, octylamine **(e)**, chloroquine **(f)** and ammonia **(b)** for comparison. Each of the bases inhibits acidification, but with differing efficiencies in the order (least efficient first): imidazole < ammonia < methylamine < propylamine < octylamine < chloroquine. With the exception of chloroquine, the efficiencies parallel those found *in vivo* for inhibition of culmination and aggregation. Possible reasons for the increased potency of chloroquine *in vitro* are discussed later (**section 4.2.3**).

4.1.3 Similar results are seen for inhibition of vesicular acidification in the axenic strain Ax2

The axenic strain Ax2 was also tested to ensure that the effects observed with NC4 were not strain-specific. Axenic strains are able to grow in a buffered solution supplemented with yeast extract and peptone, as they have an increased rate of fluid-phase pinocytosis, whereas bacterially grown cells rely primarily on phagocytosis for their food supply (Kayman & Clarke, 1983).

Since the axenic strain Ax2 was used for generating the vacuolar acidification mutants discussed later in this study (chapters 6 and 7), it was necessary to ensure that Ax2 was similar in its acidification capacity to NC4 and that it responded similarly to weak bases.

In Ax2 and NC4, the extent of fluorescence quenching in the absence of weak bases was tested and correlated with the sample protein concentration. In the control situation, Ax2 gave an average decrease in fluorescence intensity of 0.738 ± 0.203 /µg protein (n=14) compared with 0.433 ± 0.144 /µg protein (n=21) in NC4, demonstrating that Ax2 has naturally higher rates of acidification than NC4. This could indicate that the vacuolar H^+-ATPases are more active in the axenic strain than in NC4. An alternative explanation for the difference in acidification rates could be that a greater percentage of the endosomal volume is acidosome in Ax2 than in NC4. Therefore, per unit of endosomal protein, there would be fewer acidic vesicles in NC4 than in Ax2. This result shows that Ax2 is a suitable strain to use for comparison with acidification-defective strains, since its acidification capacity is at least equal to that of NC4. Differences between these two strains and the acidification-defective strains (chapter 6) should be clearly visible. Later results on acidification-defective strains will be compared to Ax2, as the mutants are in an Ax2 genetic background, therefore showing equivalent IC_{50} values for Ax2 and NC4 for *in vitro* acidification allows comparison of the acidification-defective strains with the NC4 results from chapter 3.

As with NC4, the bases tested inhibited acidification in a dose-dependent manner. In **figure 4.6**, the effects of ammonia **(a)**, propylamine **(b)**, octylamine **(c)** and chloroquine **(d)** are shown and are closely comparable to the results obtained for NC4 (see **figure 4.5**). Acidification in the presence of bases is presented as a percentage of the control value, as before. IC_{50} values for the inhibition of acidification are derived from **figure 4.6** and are compared with IC_{50} values for NC4:

	IC_{50} vesicular acidification (μM) NC4	IC_{50} vesicular acidification (μM) Ax2
ammonia	7.5	7.8
propylamine	0.2	0.5
octylamine	0.1	0.2
chloroquine	0.004	0.005

Table 4a: Correlation between IC_{50} values for inhibition of vesicle acidification in NC4 and Ax2. The concentrations are those of the unprotonated base.

This demonstrates that the response of these two strains to weak bases is similar. Slightly higher concentrations are required for inhibition in Ax2, which may result from the fact that the natural acidification capacity of this strain is higher than that of NC4.

4.2 Discussion

4.2.1 Effect of the bases on vesicular acidification

The results above show that the IC_{50} values of the bases for inhibition of *in vitro* acidification differ by orders of magnitude (**table 4a**). Imidazole and ammonia were found to be the least efficient inhibitors (IC_{50}s of 420μM and 7.5μM respectively) and chloroquine the most efficient (IC_{50} = 0.004μM). In chapter 1 (section **1.4**), it was shown that the effective passage of a base across a membrane is dependent upon its lipid solubility (hydrophobicity) and its conformation. **Table 4b** (below) shows that the IC_{50} values for acidification in NC4 correlate well with the calculated hydrophobicity of the bases, with the exception of imidazole. The same conclusions are drawn for the axenic strain

Ax2 since the IC_{50} values for both strains are similar (**table 4a**).

Weak base	IC_{50} acidification *in vitro* (μM)	Hydrophobicity log $P_{octanol}$
imidazole	420	0.13
ammonia	7.5	-1.37[*1]
methylamine	0.8	-0.57
propylamine	0.2	0.31
octylamine	0.1	2.90
chloroquine	0.004	4.29 ± 0.12[*2]

Table 4b: Correlation between the hydrophobicity of the bases and their ability to inhibit vesicular acidification *in vitro* in NC4. Hydrophobicity is expressed in terms of partitioning in octanol (log $P_{octanol}$). Higher values indicate greater hydrophobicity. All values are taken from the data of Leo et al. (1971) and represent observed log $P_{octanol}$ values with the exceptions of [*1] which is an extrapolation from log P_{CHCl3} and [*2] which derives from a calculation based on the method of Leo et al. (1971) for calculating the log $P_{octanol}$ of unknown compounds (see **Appendix III** for calculation).

Figure 4.7 shows that there is a correlation between the hydrophobicity of a base (measured by log$P_{octanol}$: imidazole omitted) and the ability to inhibit acidification *in vitro*. Since permeability coefficients correlate with oil-water partition coefficients (Overton, 1899), the finding that the ability of the bases to inhibit vesicular acidification correlates with their hydrophobicity (with the exception of imidazole, discussed below) suggests that inhibition of acidification due to protonophoric activity (**figure 1.4**), not proton titration.

4.2.2 Correlation with the effects on aggregation and culmination

It seems that the potency of a base in inhibiting vesicular acidification *in vitro* is primarily a function of its ability to act as a proton-shuttle. A close correlation can be drawn between the potency of inhibition of the bases on acidification *in vitro* and on aggregation and culmination *in vivo* (**figures 4.8** and **4.9**), with the exception of chloroquine (possible reasons for this are discussed below).

The correlations between the *in vivo* and *in vitro* data support the notion that the target of the weak bases *in vivo* is the acidic vesicle. Potency of inhibition shows a similar dependence on the ability of a base to act as a proton shuttle *in vivo* as *in vitro*. If the bases are mimicking ammonia by acting directly upon the enzymes of aggregation and culmination, then one would not expect efficiency to increase with hydrophobicity. Similarly, if the bases were acting to raise cytosolic pH, they should be equally efficient, since they would distribute equally across the plasma membrane as there is no pH gradient across it. All the data therefore are consistent with the notion that the bases act via an acidic vesicle in producing their *in vivo* effects.

4.2.3 Differences between the in vivo and in vitro systems and implications for chloroquine

Having found a relationship between the ability to act as a proton shuttle and inhibition of aggregation and culmination *in vivo* for the bases in the primary alkylamine series, the relative inefficiency of chloroquine *in vivo* was surprising (see chapter 3). Since it is so hydrophobic (**table 4b, section 4.2.1**) chloroquine was expected to act as a highly efficient proton shuttle as the N^+ of the hydrophobic arm is shielded from the hydrophilic surface of the membrane by the inductive effect of alkyl groups on the arm (see **appendix I** for structure).

The experiments conducted *in vitro* show that chloroquine is far more potent an inhibitor of vesicular acidification in this assay than *in vivo* and that it acts *in vitro* according to expectation based on its hydrophobicity. In fact, in the isolated vesicle its efficiency is about a hundredfold greater than in aggregation (IC_{50} for aggregation is 0.3μM and 0.004μM for acidification *in vitro*). This suggests that some mechanism operates *in vivo* to prevent the entry of chloroquine into the acidic vesicle. Various possibilities exist:
(i) entry into the cytosol could be inhibited,
(ii) a cytoplasmic sink could exist,
(iii) an active catabolic pathway might operate in the cytosol,
or (iv) chloroquine could be actively extruded from the cell.
No evidence exists to suggest that entry is impeded, that a cytoplasmic sink or a hyperactive catabolic pathway exists.

Efflux of chloroquine could be due to increased rates of exocytosis which has been proposed as a mechanism for the removal of certain cytotoxic drugs in HL60 cells (Marquardt & Center, 1991). An intriguing alternative is that a multi-drug resistance (MDR) pump may operate in the plasma membrane of *D.discoideum* (Tatischeff,I., personal communication) bearing similarities to the mammalian MDR pump involved in extrusion of anti-cancer drugs (Higgins & Gottesman, 1992) and the chloroquine-removing MDR pump of the malarial parasite *Plasmodium falciparum* (Foote *et al.*, 1989; Wellems *et al.*, 1991). If an MDR-type chloroquine efflux system were operative in *D.discoideum* then it is likely that this would maintain the active concentration of the base in the cytosol at a few orders of magnitude lower than that in the external medium. A similar situation is reported for *Plasmodium falciparum* (Krogstad *et al.*, 1987), where chloroquine-resistant parasites take in chloroquine at normal rates initially, but fail to accumulate the drug and efflux rates are much higher than those of the chloroquine-susceptible strains. If such an MDR pump were operating in *D.discoideum*, then it would explain the discrepancy between the *in vivo* and *in vitro* results.

4.2.4 Possible reasons for the relative inefficiency of imidazole in inhibiting vesicle acidification

There are a number of reasons which may explain why imidazole is an inefficient dissipator of the pH gradient despite the fact that it is more hydrophobic than methylamine (log $P_{octanol}$ = 0.13). First, it is possible that the ring conformation of imidazole sterically hinders its entry to the bilayer, particularly if it is protonated. The positive charge would be delocalized around the ring, resulting in the formation of a large hydration shell around the ion. Such a hydrated structure would require a great deal of activation energy to be inserted into the membrane in comparison with a hydrophobic side-chain. Chloroquine also contains a ring system, but the charge density on the chloroquine ring is reduced by an electron-withdrawing chlorine group and it possesses a long hydrophobic side chain which would aid its intercalation into the bilayer. A second reason for the inefficiency of imidazole in inhibiting vesicle acidification is its low pK_a. The ability to dissipate pH is partially dependent upon the ability of a base to accumulate in the acidic vesicle. All the other bases used have very high pK_a values, whereas that of imidazole is lower (**Appendix I**). Equation 2 in section **1.4** (reproduced below) shows that bases with lower pK_a values have a greater tendency to distribute equally across the membrane than bases with high pK_a values, which accumulate according to the proton gradient. Therefore, imidazole (pK_a = 7.1) will not accumulate in acidic compartments to the extent of the other bases (pK_a values ranging from 9.3 to 10.7).

4.3 Conclusion

The permeability coefficient (Bar-On & Degani, 1985) and hydrophobicity of unprotonated alkylamines decreases markedly as the number of CH_2 groups decreases. However, the variations in efficiency are unlikely to be due to differences in the ability of the unprotonated species to cross the membrane as this would only translate into a small change in the rate of entry to the vesicle

of less than one second and since most of the bases have very high pK_as, they would accumulate in the vesicle to similar extents and trap protons to similar extents.

It is to be expected though that the permeability of the protonated bases would increase as their hydrophobicity increased, as hydrophobic bases are better able to shield positive charge from the membrane. The longer the hydrophobic alkylamine chain, the more easily the base can intercalate into the lipid bilayer. Therefore, leakage of ammonium across the bilayer is probably negligible, whereas the octylamine and chloroquine ions would partition readily into the bilayer. The low accumulation of imidazole and relative impermeability of its ion may explain why it is the least potent dissipator of pH of all the bases tested.

The use of the acidic vesicle *in vitro* as a model system for probing the mechanism of action of weak bases demonstrates that the differential potencies of the bases is probably due to differences in their innate abilities to act as proton shuttles across the vesicular membrane. Correlation between *in vivo* and *in vitro* effects (see **figures 4.8 and 4.9**) shows further that the likeliest *in vivo* targets of these bases are the acidic vesicles, supporting the notion that inhibition of aggregation and culmination by ammonia is mediated by these acidic vesicles. However, in order to determine unequivocally that the bases neutralize vesicular compartments without effect on the cytoplasmic pH, it is necessary to determine vesicular and cytoplasmic pH changes *in vivo*. Such experiments are therefore described in Chapter 5.

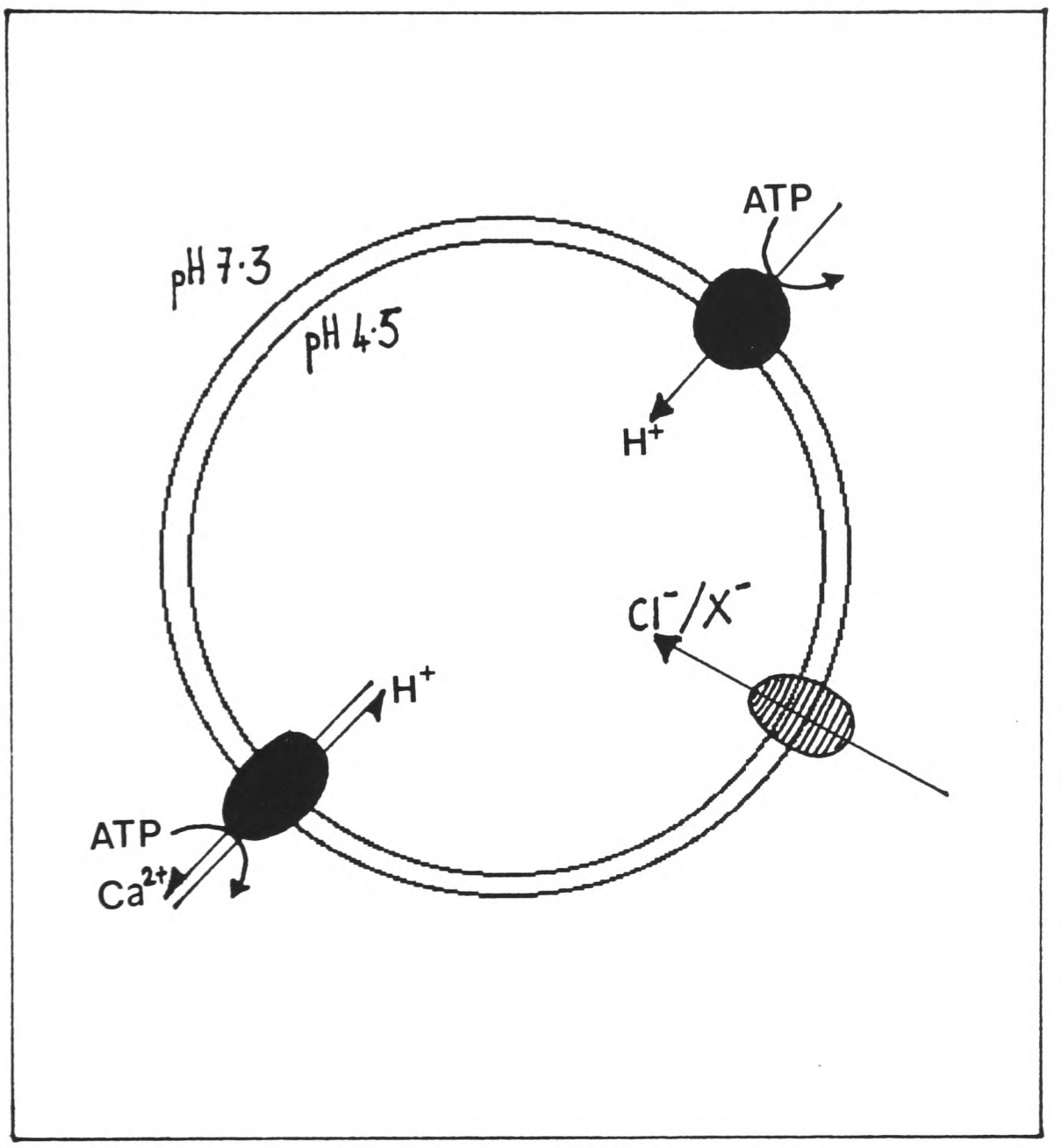


Figure 4.1: Diagram of an acidic vesicle (adapted from Rooney & Gross, 1992).

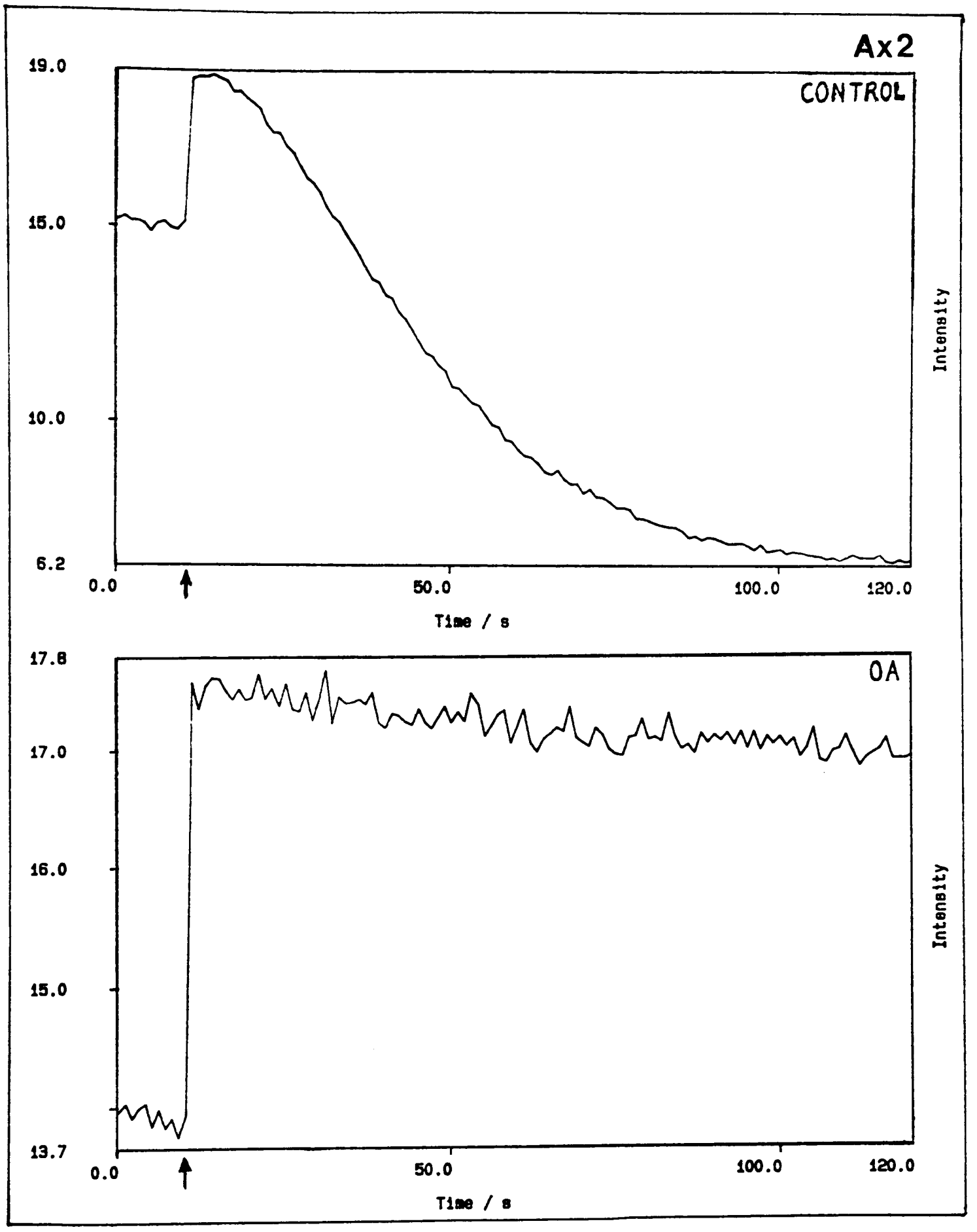


Figure 4.2: Rate of ATP-dependent acidification of an NC4-derived acidic vesicle fraction in the absence (A) and the presence (B) of weak base (octylamine is added at 1.8μM), measured by the acridine orange assay. The arrow represents the point at which ATP is added to the vesicle suspension; the fluorescence increase is due to the formation of ATP-AO complexes. The gradient of the decline thereafter is proportional to the rate of acidification.

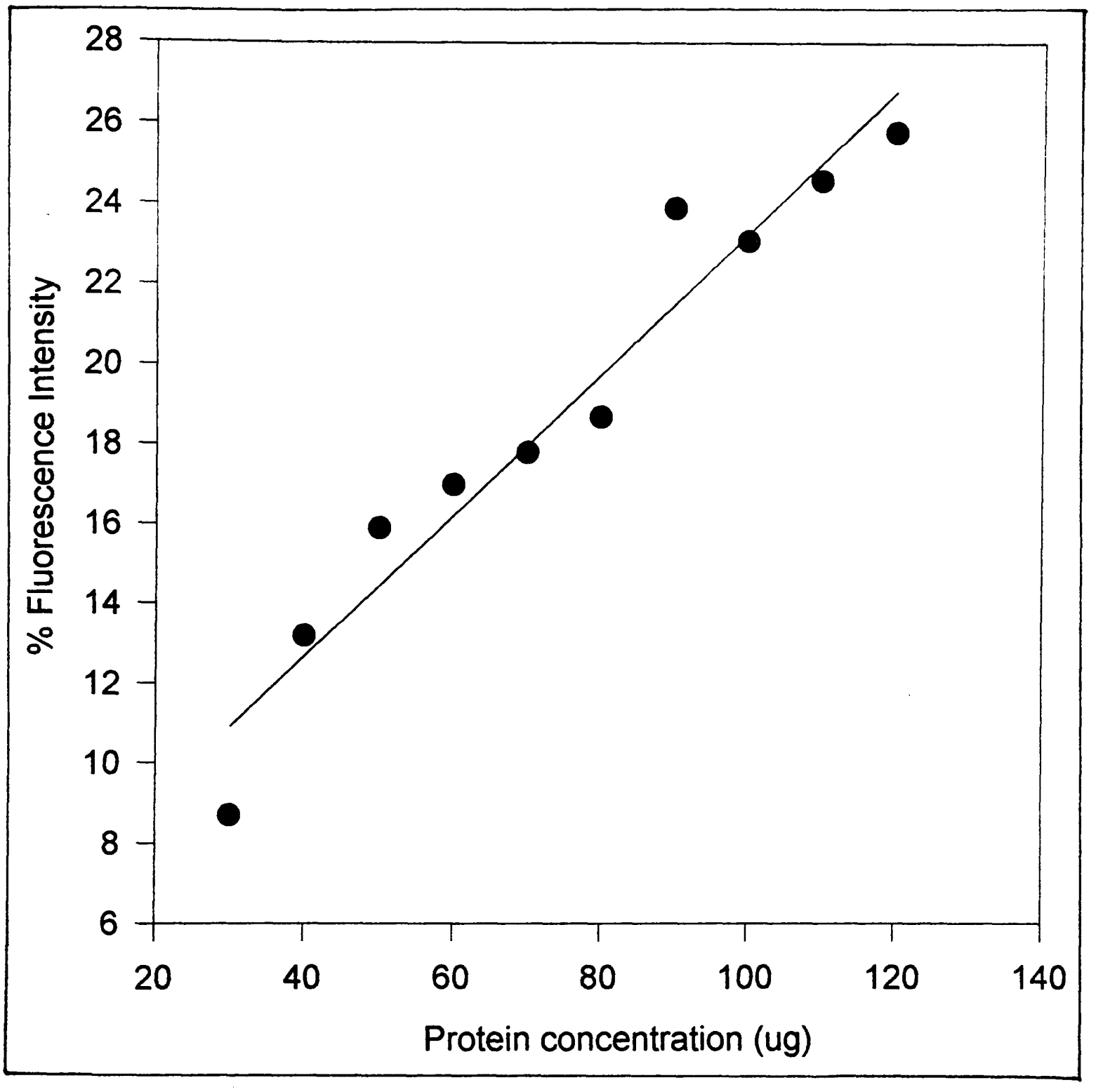


Figure 4.3: Linearity of the relative percentage change in fluorescence intensity with the NC4 vesicle protein concentration

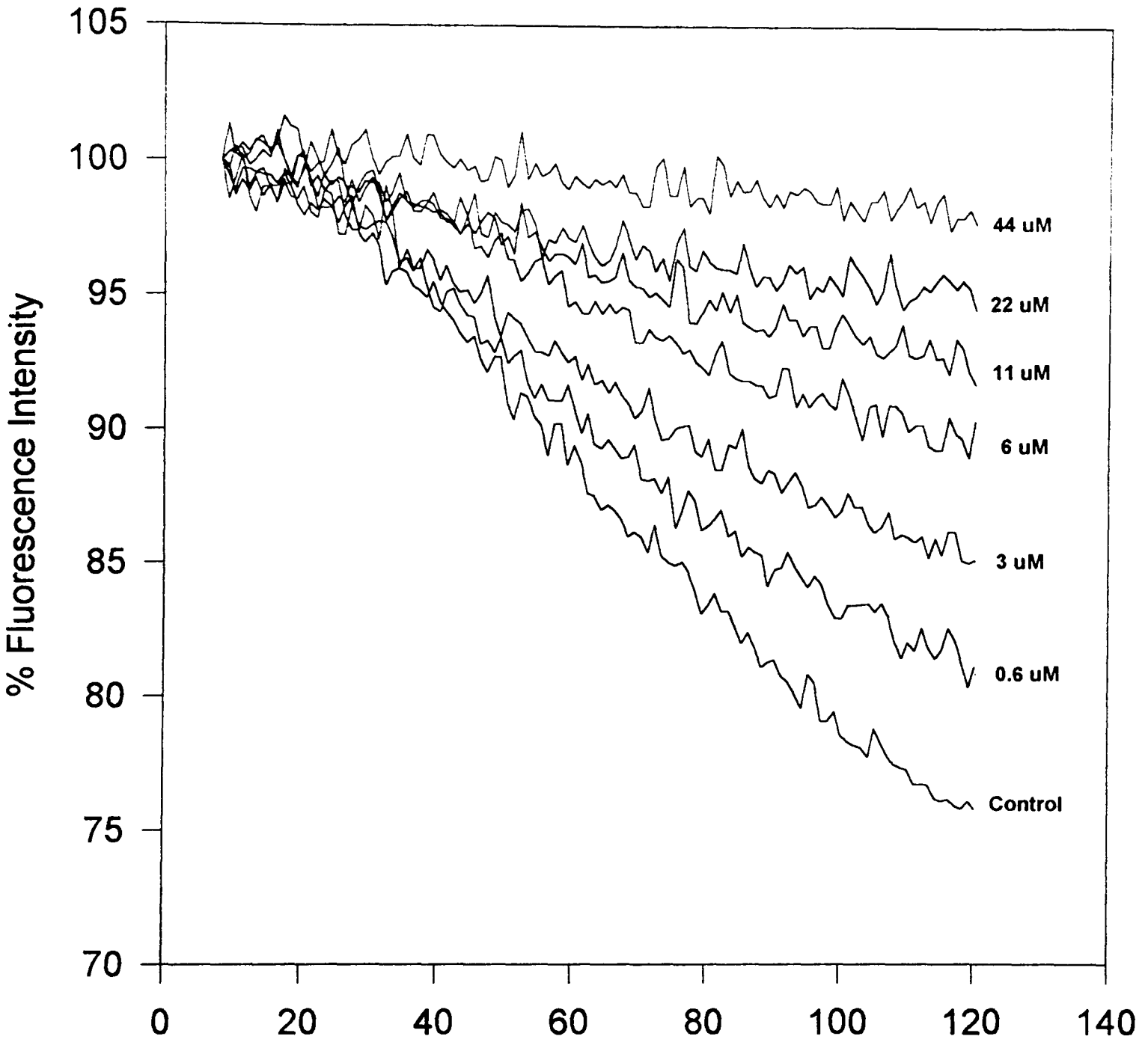
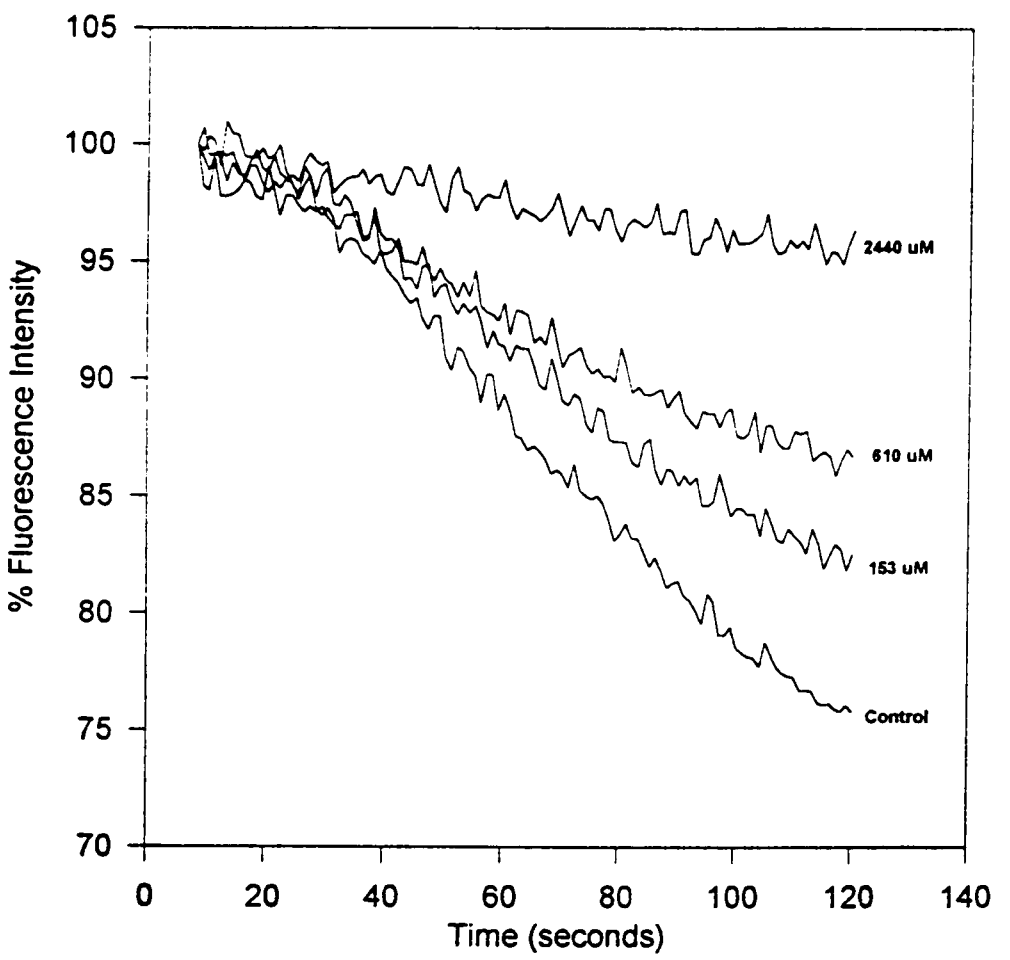


Figure 4.4: The effect of ammonia on NC4-derived vesicle acidification in detail (concentrations are those of the unprotonated base). The inhibition of acidification by ammonia is shown to be dose-dependent.

(a)



(b)

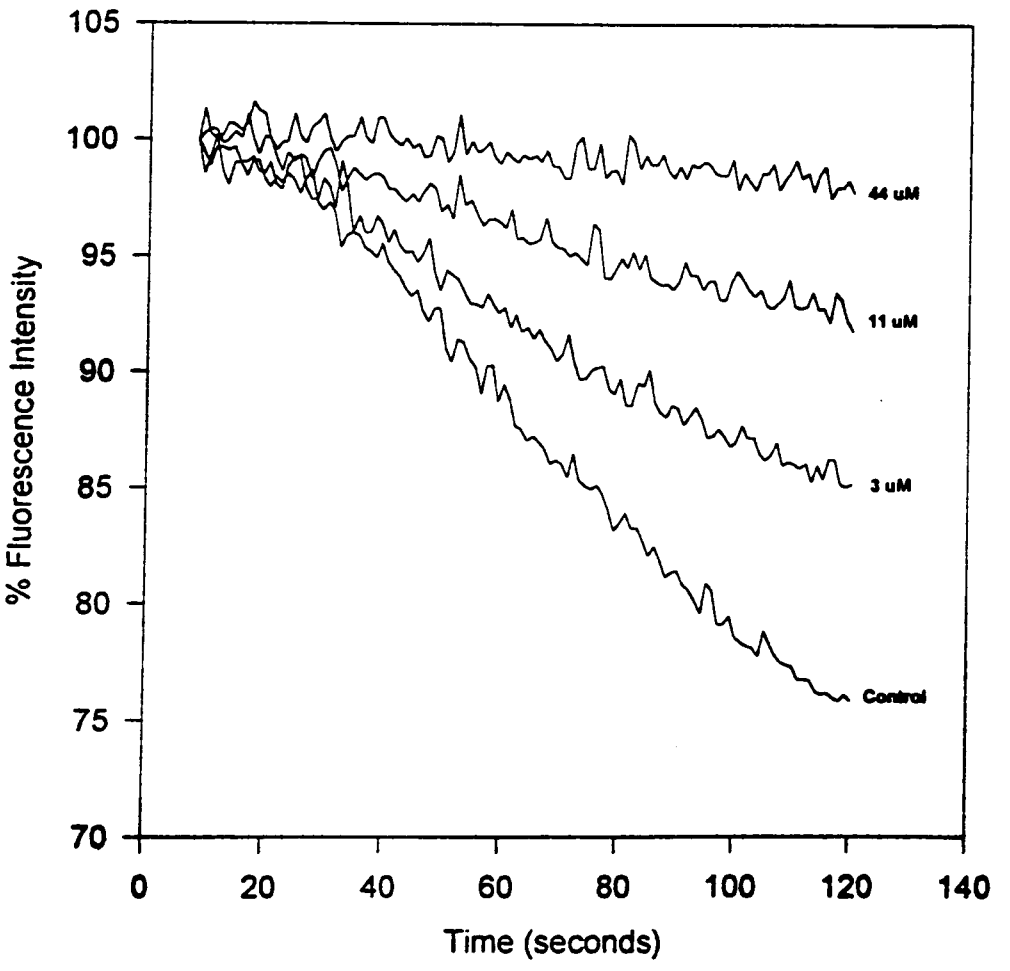
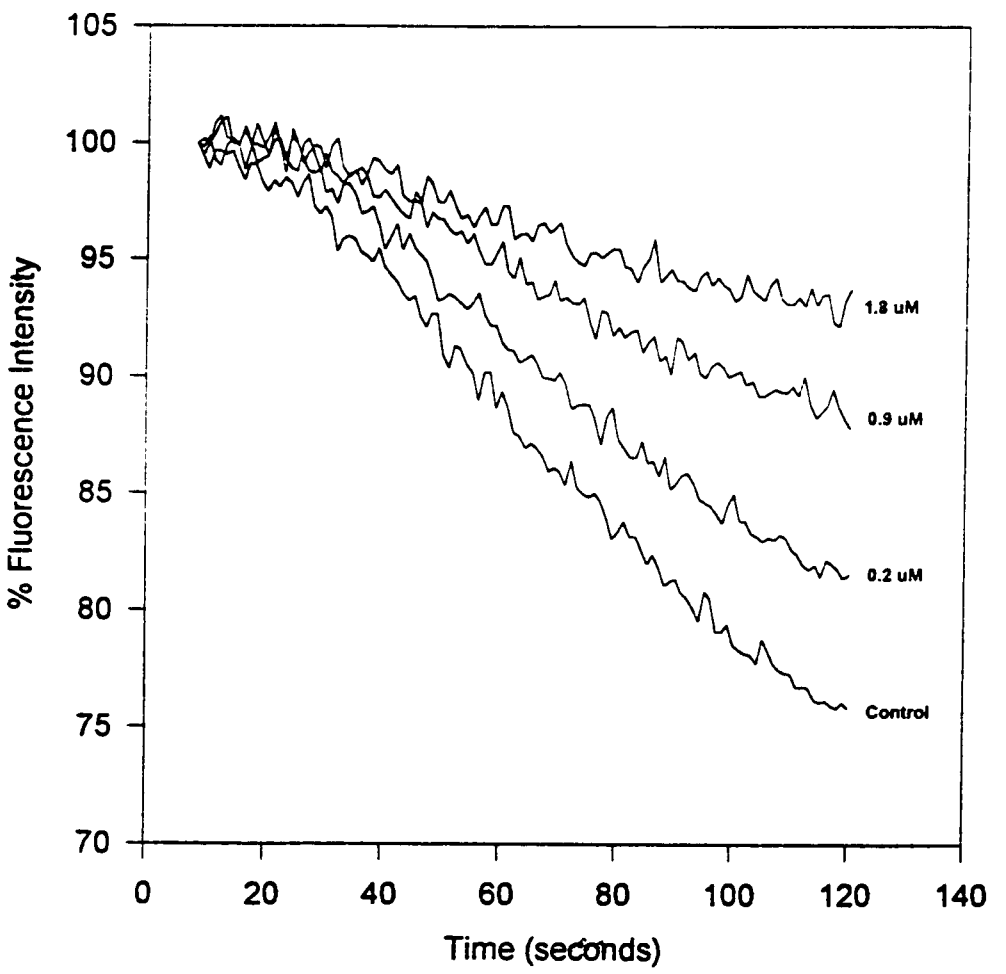


Figure 4.5: The effects of imidazole (a) and ammonia (b) on ATP-dependent NC4 vesicle acidification *in vitro*

(c)



(d)

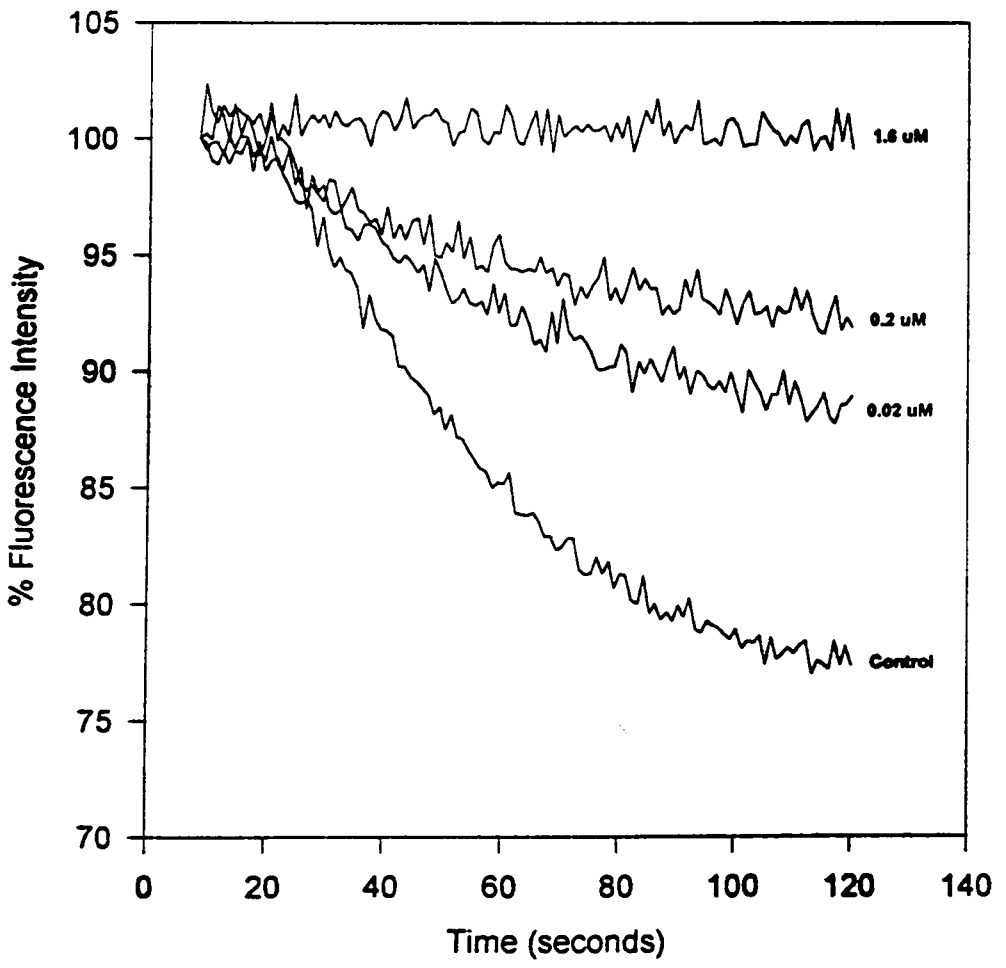
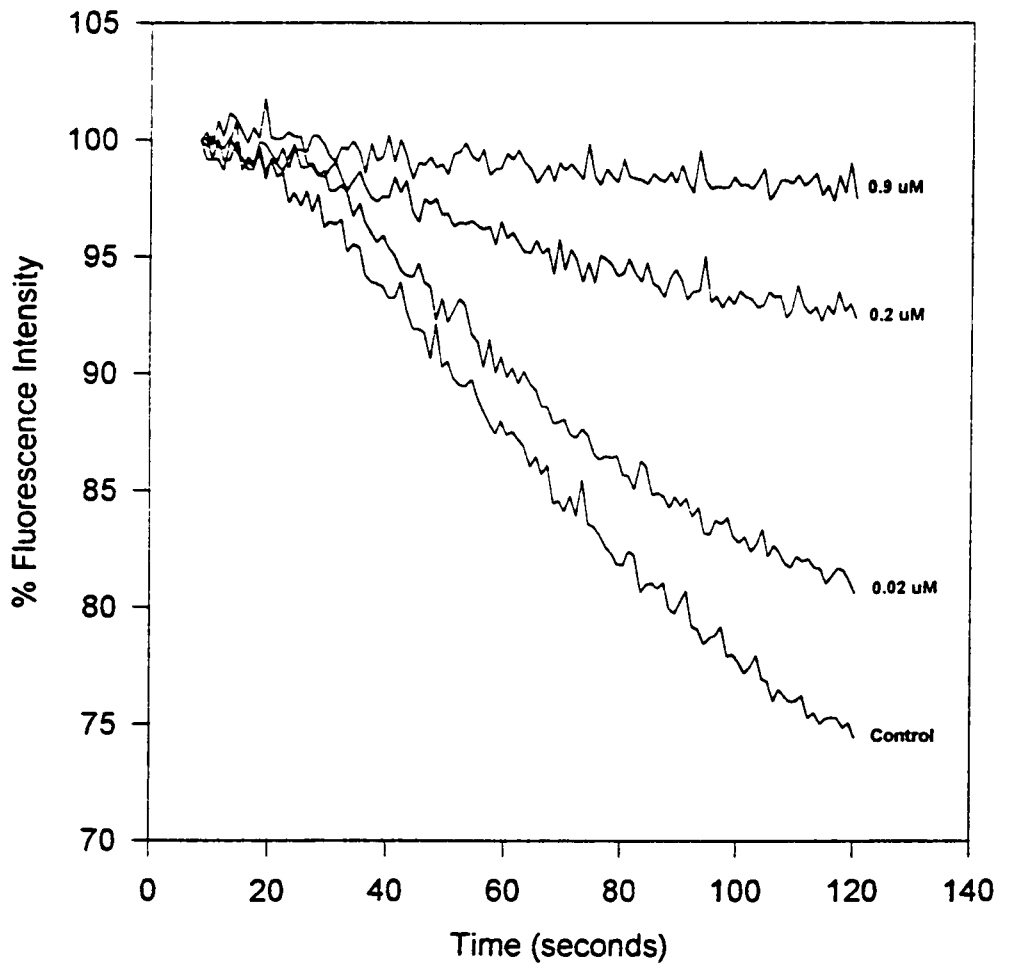


Figure 4.5 (continued): Effects of methylamine (c) and propylamine (d) on NC4 vesicle acidification *in vitro*.

(e)



(f)

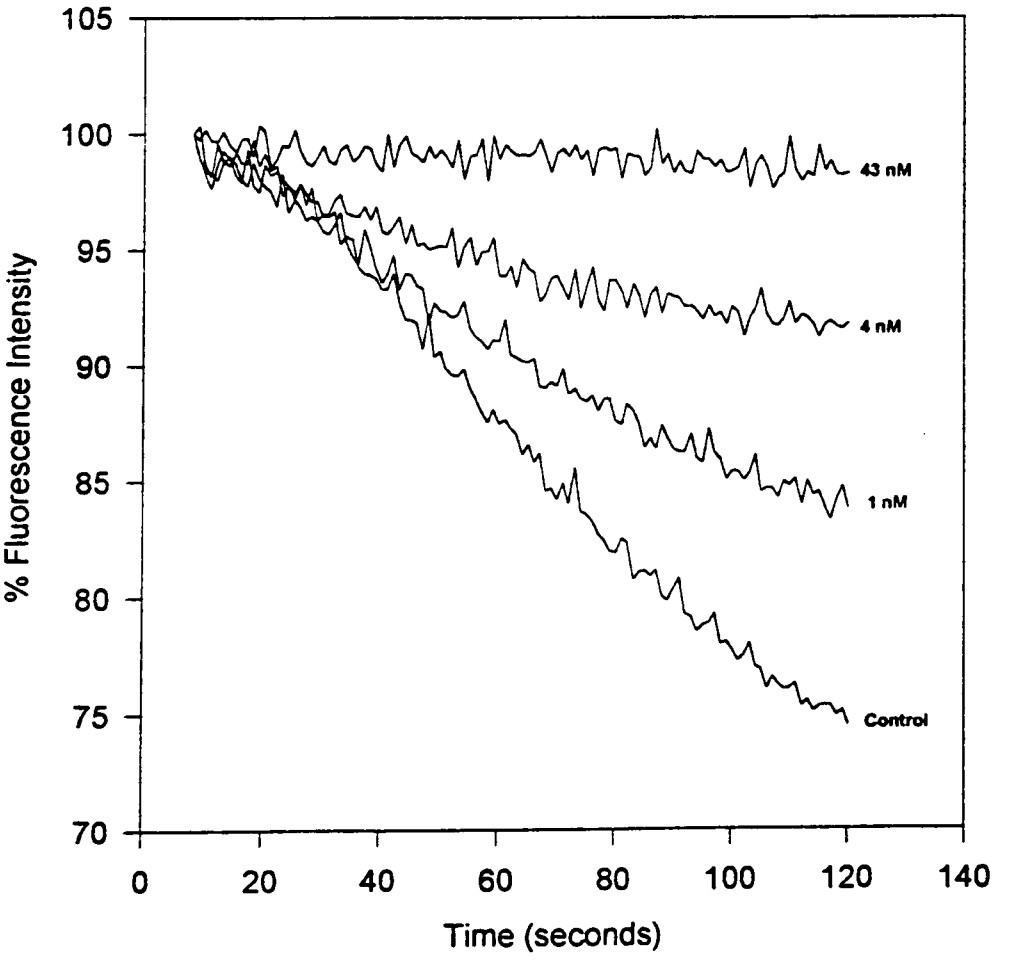


Figure 4.5 (continued): Effects of octylamine (e) and chloroquine (f) on NC4 vesicle acidification *in vitro*.

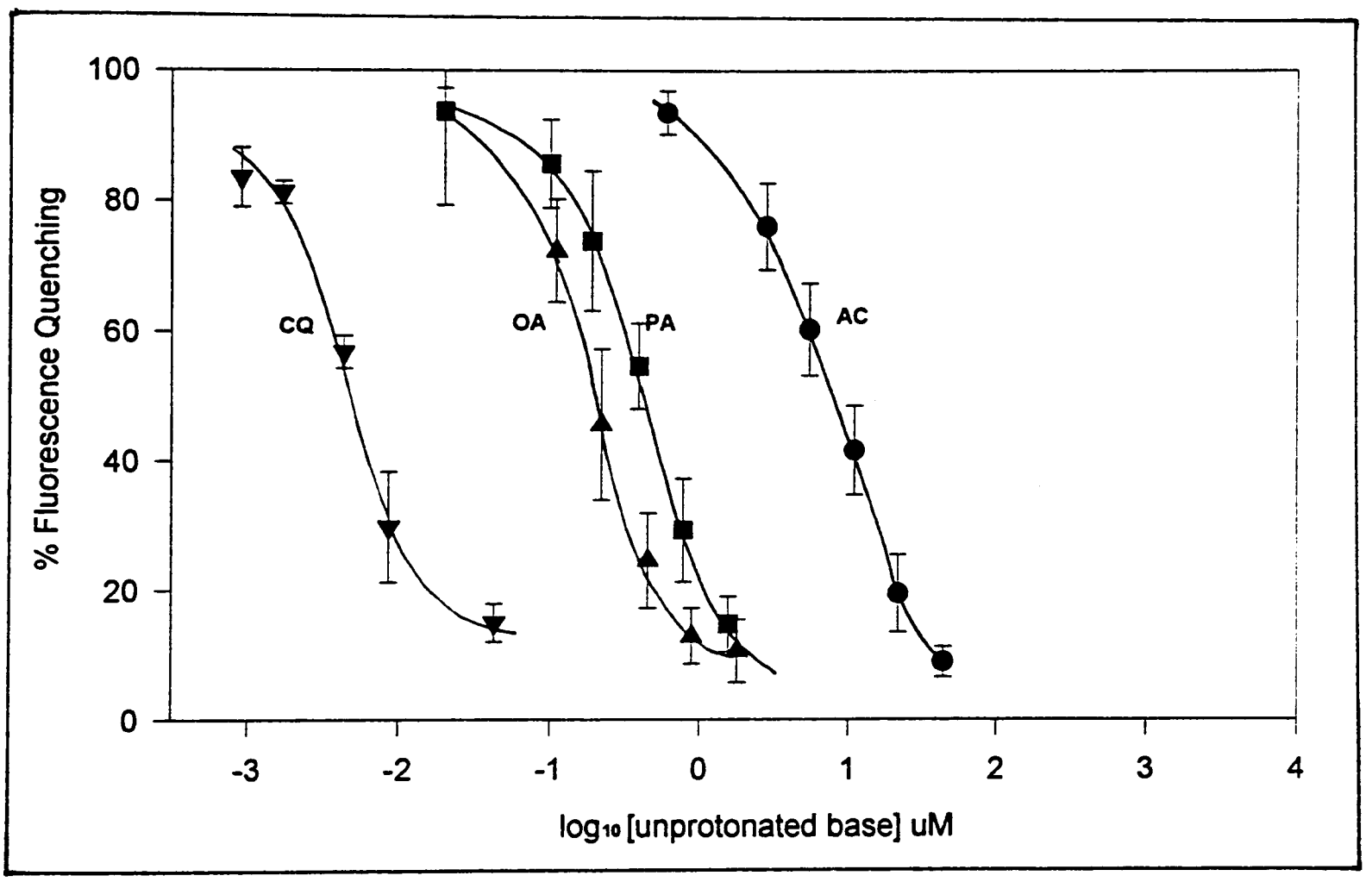


Figure 4.6: Comparison of the the effects of four bases (AC - ammonia, PA - propylamine, OA - octylamine and CQ - chloroquine) on vesicular acidification in the axenic strain Ax2.

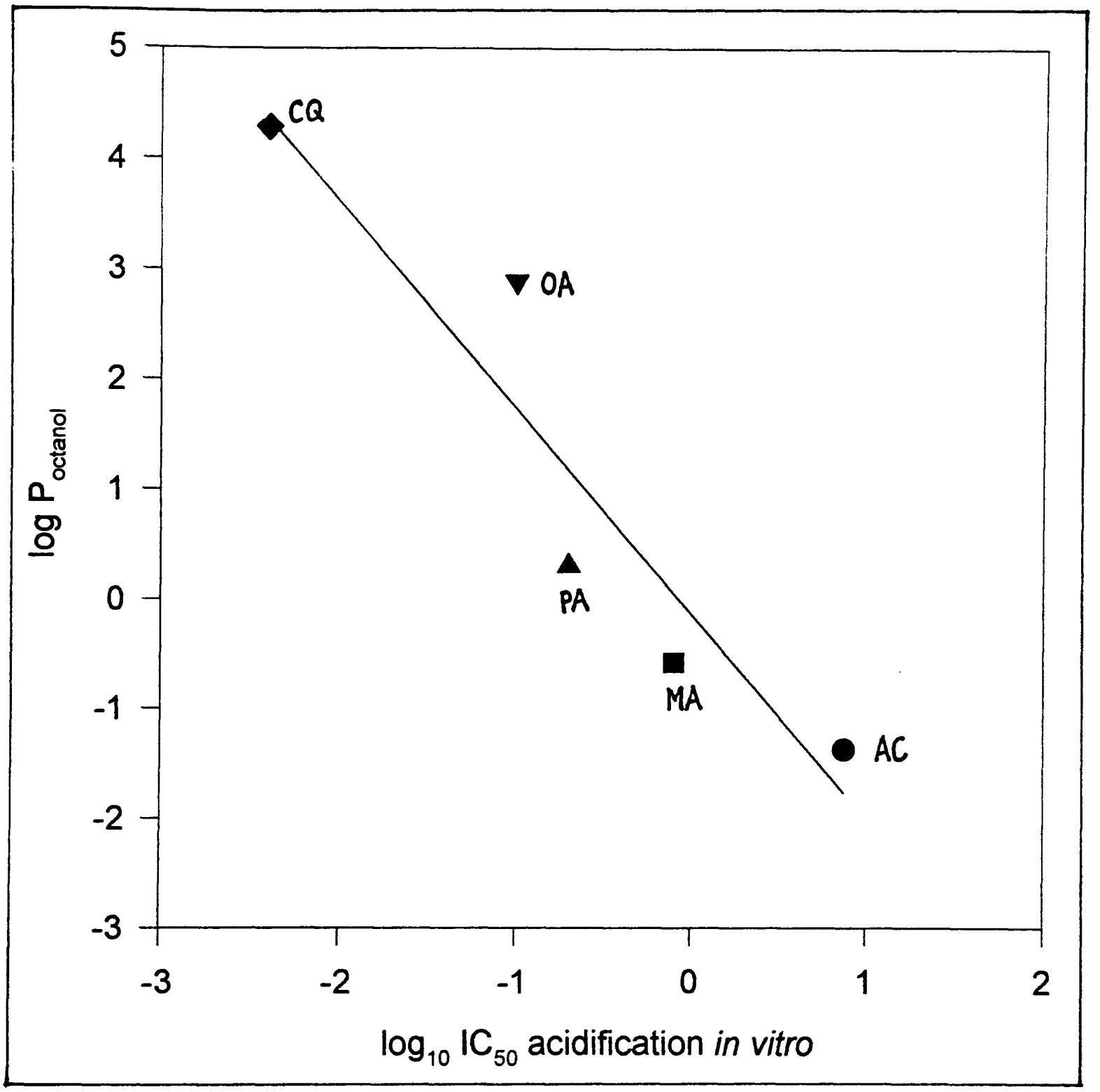


Figure 4.7: Correlation between the coefficients of the bases for partitioning between octanol and water ($logP_{octanol}$) and their ability to elicit *in vitro* vesicle acidification (Imidazole is omitted - see text p.77). AC - ammonia, MA - methylamine, PA - propylamine, OA - octylamine, CQ - chloroquine.

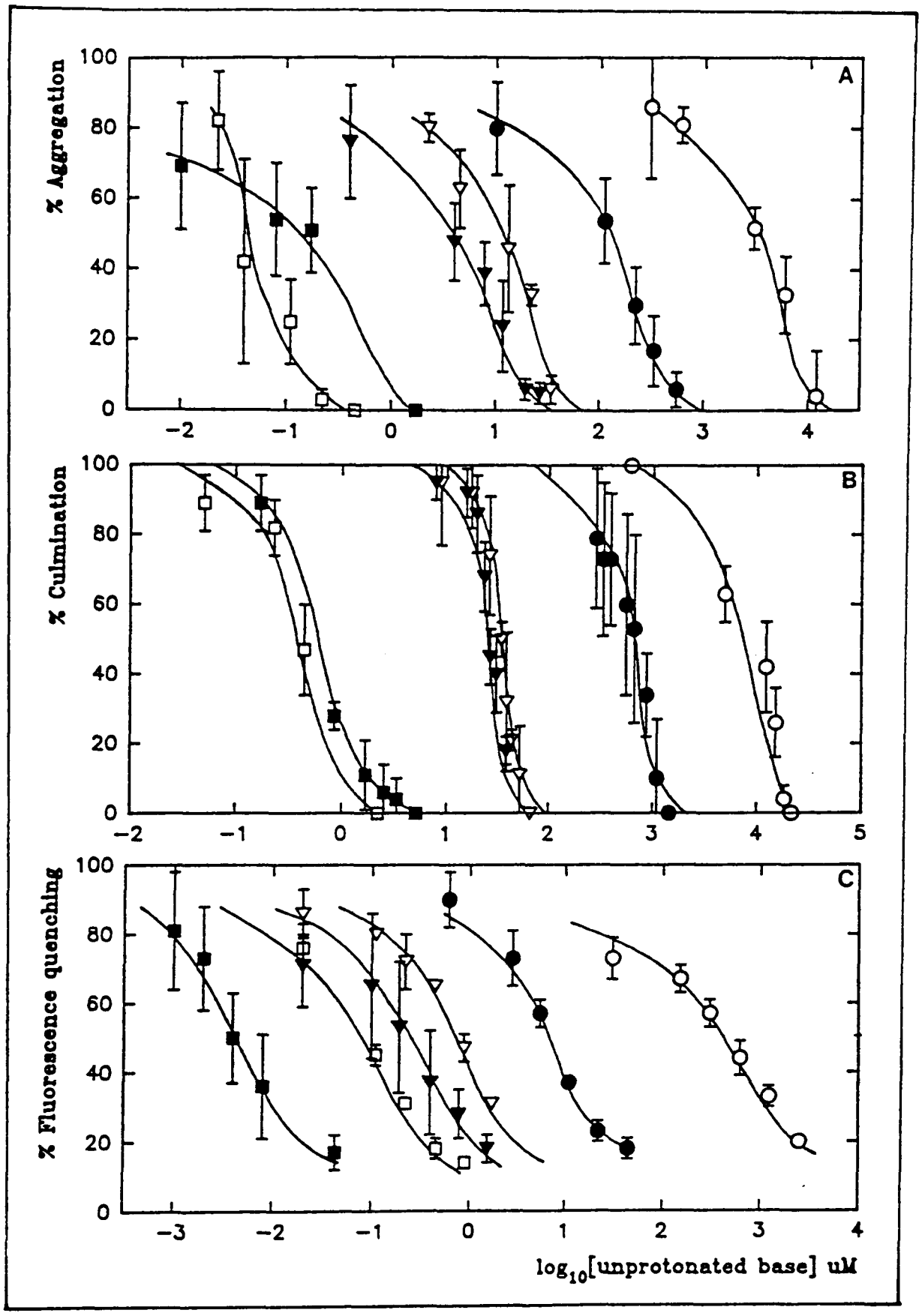
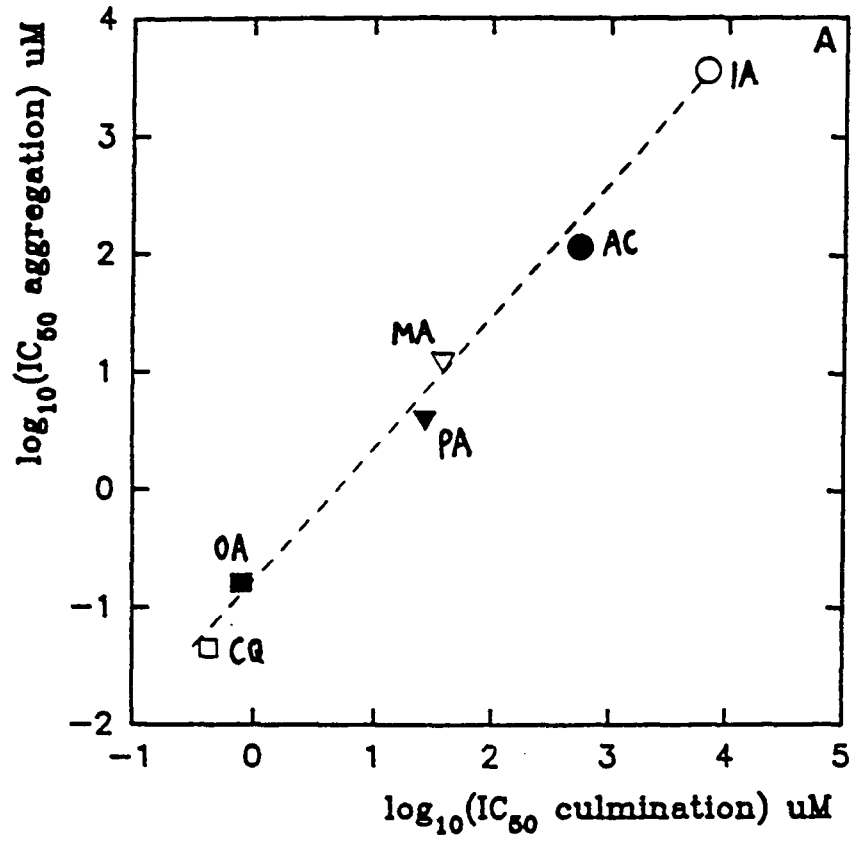


Figure 4.8: Comparison of the inhibitory capacities of the bases on (A) aggregation and (B) culmination of NC4 *in vivo* and upon (C) NC4 vesicle acidification *in vitro*.

(A)



(B)

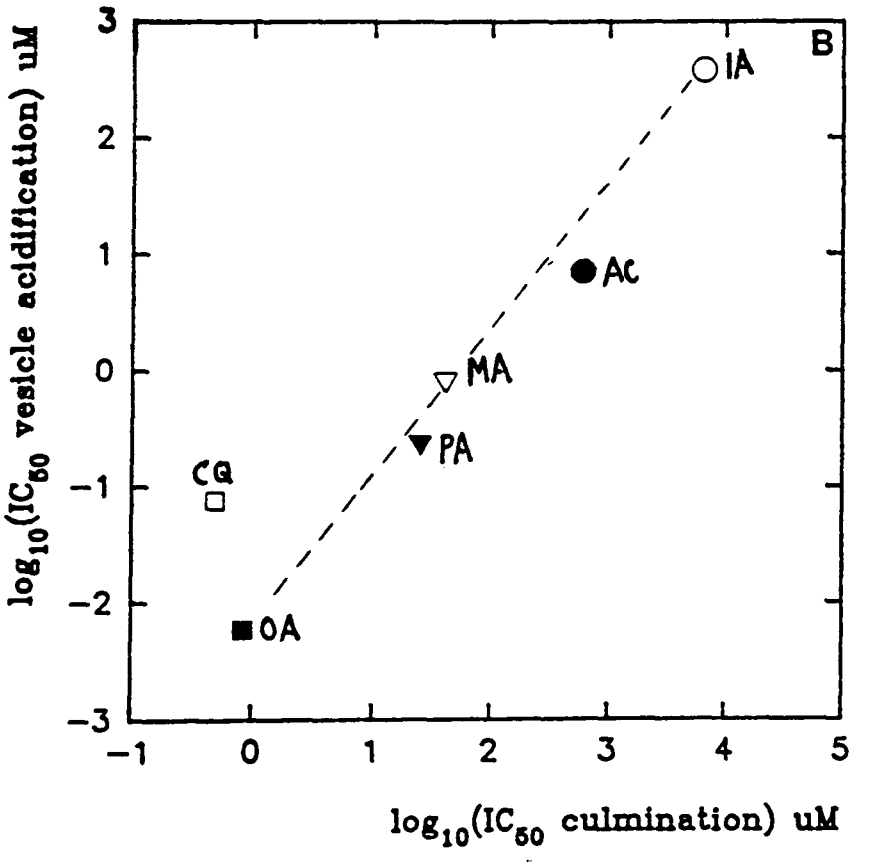


Figure 4.9: Correlation between (A) the IC_{50} values for aggregation and culmination *in vivo* (regression line calculated by least squares fit) and (B) the IC_{50} values for acidification *in vitro* and culmination *in vivo*. For (B), chloroquine is omitted from the regression calculation.

Chapter 5

Chapter 5 *The Effect of Weak Bases on Intracellular pH in vivo*

5.1 Introduction

In this chapter, ^{31}P-containing compounds are employed as intracellular pH indicators in living cells using ^{31}P-nuclear magnetic resonance: a technique which allows the pH of the endosomal system, the cytosol and the external space to be visualized simultaneously. In the experiments described below, weak bases are added to whole cells fed with such compounds, to determine whether the bases affect the pH of the cytosol or that of a vesicular compartment.

5.1.1 Use of NMR to measure pH in vivo

NMR relies on the fact that certain nuclei possess a magnetic moment or "spin", that is, that they have an odd number of protons. ^{31}P nuclei (spin = ½) in an applied magnetic field (B_z) can be aligned parallel (spin = +½) or antiparallel (spin = -½) to the field and then precess like small bar magnets around the NS axis of that field with a particular frequency (Larmor frequency). Since these ^{31}P nuclei can orient themselves with or against the direction of the field B_z, the population of nuclei is distributed between two "lower" (+½) and "upper" (-½) energy states. If electromagnetic radiation is then applied at the same frequency as the Larmor frequency for ^{31}P, the spins resonate and transitions can then occur between the lower and upper populations and *vice versa* (**figure 5.1**). However, the lower to upper transitions will predominate since there is naturally a slightly higher number of nuclei in the low energy state than in the high energy state, hence a small net absorption of energy from the applied radiation is observed. This enables an absorption spectrum to be produced.

A particular nucleus does not always resonate at the same frequency. The Larmor frequency of a ^{31}P nucleus is dependent upon its molecular environment, as the applied field can interact with bonding electrons adjacent to the nucleus to produce secondary fields which shield the nucleus from the applied field. The strength of the secondary field depends on the electron-withdrawing power of the groups bound to the ^{31}P nucleus. If the secondary field opposes the applied field (*ie.* if the nucleus is shielded), then the applied field must be increased slightly to make the ^{31}P nucleus resonate, on the other hand if the surrounding groups withdraw electrons from the bonding groups (*ie.* if the nucleus is unshielded), then the nucleus will resonate at a lower frequency than an isolated nucleus. The shielding power of a particular electron decreases as the electron-withdrawing power of the groups around it increases. These effects result in the displacement of the spectral absorption lines (chemical shift or "δppm") depending on the shielding power of the groups that surround the ^{31}P nucleus. This shielding property is particularly useful when looking at biological systems since identical nuclei in different environments will resonate at different frequencies of an applied magnetic field and will be distinguishable. For example, in *D.discoideum*, the ß-phosphate of ATP resonates at a chemical shift value (δppm) of -18.7 whereas the α-phosphate resonates at -10.6 ppm. (see **figure 5.2**).

D.discoideum contains an array of NMR-visible, phosphate-containing compounds, including phosphomonoesters, inorganic phosphate (P_i), IP_6 and nucleotides in addition to the phosphates of ATP mentioned above (Satre & Martin, 1985; Kay *et al.*, 1986; Martin *et al.*, 1987). Resonances arising from P_i can be used for intracellular pH determination since the chemical shift varies according to the surrounding pH. Altering the pH around a ^{31}P nucleus causes the shielding of that nucleus to change. So, intracellular compartments at different pH values can be distinguished (Satre *et al.*, 1986; Kay *et al.*, 1986), although the use of these peaks for pH determination is difficult, since *D.discoideum* contains a large amount of IP_6 which has a number of resonances

in the same area as P_i (Martin *et al.*, 1987). Another useful feature of these spectra is that they give relative measures of the cellular concentration of substances. The area under a resonance peak is directly proportional to the cellular concentration of that substance.

5.1.2 Use of probes to label the endocytic system

Several phosphonate compounds have been identified that are NMR-visible, have a wide variation of chemical shift with pH in the physiological range and are taken up into *D.discoideum* by endocytosis. Such compounds can enter the cell only by endocytosis and then leak slowly into the cytosol (Satre *et al.*, 1989; Pelorgeas *et al.*, 1992; Brénot *et al.*, 1992). Dichloromethane diphosphonate (Cl_2MDP) and 2-aminoethyl phosphonate (2-AEP) were used in this study. Both are cytotoxic at high concentration, but at the concentrations used here (5mM and 7.5mM respectively), cells routinely survive their presence for 6-8h without exhibiting cell stress.

2-AEP has a pK_a of 6.3 *in vivo* and its chemical shift varies from 16.5 to 19.1 within the pH range 4 to 9, meaning that the greatest variation in chemical shift and consequently the greatest resolution of peaks is around pH 6.3 (see **table 5a** and **fignre 5.3**; Brénot *et al.*, 1992). Whilst the pK_a of this probe makes it unsuitable for fine resolution of the resonances arising from the endosomal compartments (pH 4.3 - 6.0), it can be used very effectively for simultaneous visualization of the early endosomal compartment (pH 4.3) and the cytosol (pH 7.2 - 7.4).

Cl_2MDP on the other hand has a pK_a of 5.87 *in vivo* and its chemical shift varies within the limits 8.5 and 10.3 between pH 4 and 8 (Pelorgeas *et al.*, 1992). This makes it particularly suitable for close observation of pH changes in the endosomal compartments whose pH values range from 4.3 - 6.0 (see **table 5a** below).

	P_i[1]	Cl_2MDP[2]	2-AEP[3]
pK_a	6.8	5.9	6.3
δ_A(ppm)	0.15	8.46	19.1
δ_B(ppm)	2.70	10.28	16.5
limiting pH_A	3.4	3.6	3.9
limiting pH_B	9.2	8.1	8.7

Table 5a: Phosphate-containing compounds as ^{31}P-NMR pH probes. δ_A and δ_B are, respectively, the limiting acidic and basic chemical shifts; pH_A and pH_B are the pH values beyond which no further change in the δppm is seen. (Data obtained from [1] Martin *et al.*, 1987; [2] Pelorgeas *et al.*, 1992; [3] Brénot *et al.*, 1992).

In summary, the greatest resolution of chemical shift with pH occurs around the pK_a value. In consequence, compounds with a large variation in chemical shift with pK_a are most useful for determining the pH of intracellular compartments.

5.2 Results

5.2.1 Appearance of NMR spectra in the absence of probes

Figure 5.2 shows a typical spectrum obtained from *D.discoideum* amoebae in the absence of probe. It arises from a suspension of amoebae at roughly 4 x 10^8 cells/ml (in 20ml ie. 10^{10} cells) under continuous aeration in the NMR machine. Spectra are collected every 15 minutes, as this accumulation time allows peaks to be distinguished from the noise.

The compounds from which the various resonances derive are noted on **figure 5.2**. Cytosolic P_i resonates at 2.37ppm, corresponding to pH 7.47 (with a natural variation during the course of an experiment between 7.25 and 7.50) and provides a good internal marker for cytosolic pH. The external pH is about 6.5-6.7 from the resonance of the external P_i peak and it is worth noting that even when the amoebae are resuspended in highly buffered solutions at pH 7.3 they acidify their environment to pH 6.5-6.7 within 15min, therefore cell suspensions were made in buffer at pH 6.5 and external probe removed by washing cells if required. The pH of the various inorganic phosphate resonances can be calculated from their ppm values by the following equation

$$pH = pK_a + \log (\delta - \delta_A)/(\delta - \delta_B)$$

where δ is the observed chemical shift (in parts per million "ppm"), δ_A is the limiting acidic chemical shift for P_i, δ_B the corresponding basic limiting chemical shift (determined by Martin *et al.*, 1987). Conversion tables for ppm → pH are contained in **appendix IV**. Whilst these P_i resonances provide good internal markers for external and cytosolic pH, they are often obscured by adjacent resonances. Ideally, phosphonate probes which resonate far from other cellular resonances (see **figure 5.2**) are used for pH determination.

The NMR set-up allows one to see whether or not the cells are generally healthy throughout an experiment. At the far right hand side of the spectrum are peaks arising from ATP and other phosphonucleotides. If cell health declines during the experiment, then the ATP levels decrease with a concomitant rise in other markers of cell stress. For example, peaks arise in the phosphodiester region of the spectrum (0.00 - 2.00ppm, see **figure 5.2**) that are characteristic of nucleotides, indicating that nucleic acid is being broken down. Even spectra from initially healthy cells begin to display these hallmarks of cell stress after prolonged periods (>8h) in the NMR situation and is due to the cytotoxicity of the probes and incomplete sample aeration.

This system does not enable very rapid changes (*ie.* those that occur in less than 15 minutes) in cell resonances to be observed, but serves well for observing the long term effects of weak bases. To improve the time resolution, data could be collected after 5 minutes but the resolution of peaks above noise then becomes difficult. It is not possible to increase the cell concentration to allow faster data collection since cells at concentrations higher than 4×10^8 /ml show signs of stress due to impaired aeration.

5.2.2 Resonances arising from 2-AEP in the absence of bases

Figure 5.4 shows the kinetics of 2-AEP entry into *D.discoideum* amoebae. (Surrounding resonances are omitted since these do not change significantly during the course of the experiment). The left hand sequence shows how 2-AEP, added externally at a concentration of 7.5mM, enters amoebae. After 15 minutes, 2-AEP has entered the early endosomal compartment (**a**, pH 4.9) and a shoulder peak is just visible on the right hand side of the large external peak (**b**), as the probe begins to enter the cytosol (pH 7.31 ± 0.12). After 30 minutes, the peak arising from cytosolic 2-AEP resonance (**c**) increases dramatically in height as more probe is transported into the cytosol from the endosomes. The existence of some shoulder peaks (particularly at the 30 minute stage) indicates that there is heterogeneity in the endosomal population. Unfortunately, the resolution of the technique is not sufficient to distinguish clearly between these various resonances. By 45 minutes the level of probe in the cytosolic compartment exceeds that in the early endosomal compartment. After 1h in the NMR machine the level of probe in the endosomal compartment stabilizes and then begins to decrease slowly, therefore weak bases were added after a 45 minute loading period.

As outlined above, it is possible in this situation to see peaks that may arise from late endosomal compartments, but they are largely obscured by a large peak at pH 6.5 due to the high external concentration of 2-AEP. Displacement of this external 2-AEP peak to a higher pH was attempted, but cells

resuspended in pH environments above 6.5 rapidly re-acidify their environment to pH 6.5 in 15-20 minutes, before the first spectrum can be collected. It was not considered prudent to lower the external pH as this would obscure the early endosomal resonance. Therefore, after ensuring that the cells had been labelled with 2-AEP they were repeatedly washed before being returned to the NMR machine. The procedure did not affect cell viability, and was therefore used to highlight the late endosomal resonances. The right hand sequence of **figure 5.4** shows a typical spectrum obtained after washing. It is notable that the late endosomal resonance initially (15min spectrum) is virtually zero, which would imply that the late endosomal compartment is very small, very short-lived or that the probe passes quickly from these endosomes to the cytosol. After 30mins, the external 2-AEP resonance recovers (this also contains a component of the late endosomal resonance), with a corresponding decrease in the early endosomal resonance.

In summary, it is possible by this method to see the resonances arising from the early endosome and the cytosol, but the external and late endosomal resonances are impossible to distinguish. Washing enables shifts in the endosomal peaks to be seen more clearly, but probe tends to leak out of the cells quickly. Consequently, washed cells were usually used to look at compartment pH shifts in response to a single challenge of weak base whereas unwashed cells were used to delineate the dose-dependent effects of the bases on endosomal and cytosolic resonances.

5.2.3 Effect of the weak bases on 2-AEP resonances

Having established a time when the probe had reached all the relevant internal compartments, weak bases were added to the external medium at pH 6.5 to see their effect on the resonances.

(a) Effect of ammonia

Figure 5.5 shows the effect of ammonia (left hand sequence) on the endosomal and cytosolic resonances in washed cells. Ammonia induces a decline in the signal from the probe in the early endosomal compartment, which is greater than the decline normally seen in the absence of base (compare **figure 5.4** at 30 minutes after washing). No effect is seen on the cytosolic pH. A similar decay rate in the early endosomal compartment is seen when unwashed cells are used (**figure 5.6 a**). Within 15 minutes, the early endosomal resonance has almost disappeared and a new resonance (**figure 5.5 d**) is visible close to the external resonance, indicating that the pH of that compartment has shifted to around pH 6.0, an increase of more than one pH unit.

A small peak at pH 4.9 remains after addition of sub-maximal ammonia dosages. This effect was observed in all the experiments using this weak base, implying that instead of slightly raising the pH of all the vesicles of the early endosomal compartment, ammonia somehow "targets" a number of these endosomes and collapses their pH gradient, leaving some endosomes still at pH 4.9. This was clearly demonstrated in experiments where the dosage of ammonia was progressively increased (**figure 5.6 a** and **b**). As the ammonia concentration increases, a gradual decrease in the area of the early endosomal resonance is seen, until the resonance disappears at 990µM.

It might be expected that the pH gradient would collapse completely in the presence of base *ie.* to reach the pH of the cytosol (pH 7.3) but, the area under the cytosolic curve does not increase in the presence of the base, indicating that the early endosomal pH does not increase to pH 7.3. In the control situation (**figure 5.4**) the area of the cytosolic resonance increases slowly both before and after washing. Since the extra peak appears in the vicinity of the external resonance, the early endosomal pH seems to approach that of the external pH (pH 6.5). Possible reasons for this will be discussed later (**section 5.3**).

Cytosolic pH does not change in the presence of the base. No decline is seen in the peak area and neither does the peak shift. Additional testimony to its stability is given by the cytosolic P_i peak (not shown) whose δppm value is unchanged after base addition. This implies that that increasing the pH of endosomes by adding ammonia stops passage of the probe into the cytosol, since the cytosolic peak area does not increase after base is added.

(b) Effect of imidazole

Imidazole also targets the early endosomal compartment (**figure 5.5**, right hand sequence) without affecting cytoplasmic pH, but its effect on the early endosomal compartment is somewhat different from that of ammonia. Rather than seeing an immediate elimination of the early endosomal peak upon addition of base as occurred with ammonia (propylamine and chloroquine), the peak broadens and gradually shifts to the right towards the external probe peak, indicating that the pH of the compartment is increasing. Also, the height of the peak declines very slowly in comparison with the rapid decline seen in the presence of ammonia. In **figure 5.7** the dose-dependent nature of the early endosomal pH change in response to imidazole can be seen. Early endosomal pH rises by more than one pH unit from pH 4.74 in the control to pH 5.85 upon addition of 34mM imidazole. Whether any further increase in the pH of this compartment occurs cannot be determined accurately, since the early endosomal peak merges with other resonances at imidazole concentrations higher than 34mM (not shown). As there is a 15 minute interval between spectra, one cannot say whether an increase in a cytosolic or external peak area is due to a contribution from the early endosome whose pH has been increased or to natural efflux of the probe from the endosomal compartment into the cytosol and the external space.

(c) Effect of propylamine and chloroquine

Like ammonia, propylamine induces a rapid decline in the area of the early endosomal peak rather than a gradual shift of the pH towards higher values

(**figure 5.8**) and the effect occurs at lower free base concentrations than with ammonia (**table 5b, section 5.3.1**). At 19.5 μM unprotonated propylamine, the effect is not maximal and a small peak remains after addition of the base. So the action of propylamine mimics that of ammonia very closely in producing a rapid increase in the pH of part of the early endosomal population, with an apparently "resistant" population remaining. Again, the cytosolic pH (as measured from the cytosolic AEP peak and the cytosolic P_i peak) remains stable. Chloroquine produces similar effects (**figure 5.8**, right hand sequence), except that the maximal effect is achieved at yet lower unprotonated base concentrations than is the case with either ammonia or propylamine. Again, no change is seen in the cytosolic resonance position.

Summary of weak base effects on 2-AEP resonances

In summary, the pH of the cytosolic compartment remains stable in the presence of the weak base. Therefore any effect on this compartment would have to be transient and should not contribute significantly to long-term biological effects. In contrast, the early endosomal compartment is dramatically affected, showing a decline in peak area or a shift to higher pH values after the addition of weak base (**figures 5.5** and **5.8**). Ammonia, propylamine and chloroquine act similarly in producing a dose-dependent decline in the area of the endosomal resonance. In some cases, a new peak appears at higher pH values, otherwise any new resonance is obscured by the external resonance. Imidazole is the exception in that it induces a gradual shift in the early endosomal resonance towards a higher pH.

5.2.4 Resonances arising from Cl_2MDP in the absence of bases

Since the late endosomal compartment was not well resolved from the external resonance in the 2-AEP system, Cl_2MDP was used as an alternative probe. Whereas 2-AEP allows simultaneous visualization of changes in cytosolic and early endosomal pH, Cl_2MDP allows the interplay of the various vesicular compartments in response to weak base challenge to be observed in more

detail. In particular, the external and late endosomal resonances are clearly resolved, since the pK_a of Cl_2MDP is lower (pK_a = 5.9) than the pK_a of 2-AEP (**figure 5.3**). Hence the effects of weak bases on all of the vesicular compartments can be evaluated. The disadvantage is that the cytosolic resonance is indistinguishable from the external resonance. However, an estimation of the cytosolic pH may still be obtained from the cytosolic P_i resonance.

Figure 5.9 shows the resonances arising from Cl_2MDP taken up by pinocytosis. As with 2-AEP (**figure 5.4**), the surrounding resonances are omitted for clarity. Fifteen minutes after the addition of the probe to the external medium, Cl_2MDP is apparent in the early endosomal compartment (**a**, left hand sequence). At 30 minutes the amount of probe in this compartment has increased but transfer into the late endosomal compartment does not occur until about 45 minutes (**c**).

Upon washing the cells, the late endosomal resonance is evident to the left of that of the early endosomal compartment. This compartment is not visible at this stage in the equivalent 2-AEP experiments, which implies that Cl_2MDP enters the late endosomal compartment more efficiently than 2-AEP. If Cl_2MDP were less efficiently transported into the cytosol at the early endosomal stage than 2-AEP, this could also contribute to the increased late endosomal resonance. A peak remains at the the left hand side of the late endosomal resonance, which is skewed slightly to the left of the normal external peak position. This may be the cytosolic component of the Cl_2MDP resonance that is not resolved from the external peak before washing and a component could be residual external Cl_2MDP left after washing. However this is unlikely since the same residual peak was seen in nine independent experiments. Alternatively it could be that probe has effluxed from the cell within 15 minutes of washing.

5.2.5 Effect of weak bases on the Cl_2MDP-derived resonances

(a) Effect of imidazole

The effect of imidazole on the early endosomal Cl_2MDP resonance (**figure 5.10**, left hand sequence) closely resembles its effect on the equivalent 2-AEP resonance (**figure 5.5**, left hand sequence); vesicular pH shifts from pH 4.45 to a pH ≥ 6.20 (compartments at pH values above this cannot be resolved). After washing the cells, it can be seen that addition of imidazole does not increase the area under the late endosomal peak; rather, the left hand peak area increases. Since efflux of Cl_2MDP occurs constantly after washing (as shown in **figure 5.9**) this peak is a composite of the cytosolic and external resonances, which are indistinguishable since the pK_a of Cl_2MDP is so low. So, it is impossible to tell whether the pH of the early endosomal compartment increases to equate with that of the external compartment or with that of the cytosol.

The results of the washed spectra suggest that the early endosomal compartment does not merge with the late endosomal compartment since the peak area of the latter does not increase markedly with pH. This suggests that imidazole does not promote fusion of endosomal compartments.

(b) Effect of ammonia and propylamine

Ammonia and propylamine give very similar effects, in other words, a dramatic decline in the early endosomal peak height. In the case of ammonia (see **figure 5.10**, central sequence) the late endosomal peak also disappears but the appearance of a shoulder on the external/cytosolic peak could indicate that the early and late endosomal compartments are displaced to a higher pH (roughly 6.0-6.2). The effect of propylamine is slightly less dramatic, but this may simply be a function of the concentration of free base used. Upon addition of the base, the early endosomal peak declines in height, the late endosomal resonance broadens and the external/cytosolic resonance increases in area,

indicating that the pH of the early endosomal compartment has increased to pH equal to or greater than 6.0.

In sum, these results show that the most dramatic effect of the bases is upon the early endosomal resonance as was demonstrated with the 2-AEP data. But also, the late endosomal resonance is displaced to a higher pH in some of the experiments, and it is possible that this occurs with all of the bases once a threshold base concentration is reached. This proved difficult to demonstrate in these experiments as dose-dependent base effects on the late endosomal compartment could not be probed after washing the cells due to the rapid efflux of probe from the cells. Due to time limitations, further experiments with unwashed cells could not be performed.

5.2.6 Stability of the cytoplasmic pH in the presence of bases

Even at the highest base concentrations used, the cytoplasmic pH remained stable. **(table 5b)**

Base	Cytosolic pH
control	7.31 ± 0.12 (n=21)
imidazole (18mM)	7.28 ± 0.12 (n=12)
ammonia (550µM)	7.30 ± 0.09 (n=12)
propylamine (20µM)	7.26 ± 0.04 (n=10)

Table 5b: Stability of the cytosolic pH in the presence of weak bases. The cytosolic pH was also stable in the presence of chloroquine, but insufficient data are available for statistical treatment of the results.

5.3 Discussion

5.3.1 Effect of the bases on endosomal pH

Effect on the early endosome

The peaks arising from the endosomal compartments are strikingly affected by weak bases. **Figures 5.5, 5.6, 5.8** and **5.10** demonstrate that the effect of the bases (no matter whether 2-AEP or Cl_2MDP is used as a probe) is always upon the acidic vesicle rather than the cytosol or any other NMR-visible compartment. **Figure 5.11** illustrates the differences in the efficiencies of the bases in reducing the peak area or increasing the pH of the early endosomal compartment (where no error bars are shown, insufficient data was available for statistical determinations). The table below gives the IC_{50} values (derived from **figure 5.11**) of the bases for their effect on the early endosomal compartment.

Base	**IC_{50} for inhibition of vesicular acidification (*in vivo*)**
imidazole	9333 μM
ammonia	269 μM
propylamine	21 μM
chloroquine	3 μM

Table 5c: The effect of weak bases on *in vivo* acidification of the early endosomal compartment as measured by ^{31}P-NMR. The effect of imidazole is measured as an increase in pH with base concentration whereas the effects of the other bases reflect the decline in peak area as a result of base addition (see **figures 5.5 - 5.8, 5.10** and **5.11**).

As with *in vitro* acidification (chapter 4), the rank order of effectiveness of the bases (least efficient first) is imidazole < ammonia < propylamine < chloroquine. This order is in keeping with the expected order of efficiency based on lipid solubility and other structural parameters, lending further weight to the theory that the weak bases' efficiency in inhibiting vesicular acidification is a function of their ability to act as proton shuttles.

Imidazole (the least efficient weak base as discussed in chapter 4), produces a gradual dose-dependent increase in the early endosomal pH (**figure 5.7**). This base enters the acidic early endosomes and accumulates within them, resulting in a slow rise in their pH, which is visible as a shift in the early endosomal resonance towards the external resonance. In the presence of the other bases, if any pH shift occurs, it is too rapid to be observed within the spectrum accumulation time and the increase in the early endosomal pH can be visualized only as a rapid decline in the peak area. Unexpectedly, it was still possible to observe dose-dependent effects of ammonia, propylamine and chloroquine. The lowest dosages used elicited a small decline in the peak area whilst higher dosages obliterated the early endosomal resonance completely.

This implies that the bases ammonia, propylamine and chloroquine do not affect all components of the early endosomal population equally. Rather than raising the pH of the entire vesicle population slightly, low base concentrations seem to reduce the number of highly acidic vesicles. This is most likely to be due to the high cell concentration in the NMR situation (>10^8 cells/ml) which could cause cell clumping and thus restrict access of the weak bases to a proportion of the cells. Their vesicles would then appear to be unaffected by base. Increased base dosage would affect a larger percentage of the vesicles as it would penetrate the cell clump further. In the case of imidazole, any residual unaffected vesicle population is probably hidden under the peak, since it shifts only slightly with each aliquot of imidazole. An alternative explanation for this phenomenon is that the peak arising from the early

endosomal resonance represents a heterogeneous vesicle population and that a sub-population of the vesicles are more resistant to alkalinization than others. This is unlikely as one would have to explain why imidazole does not differentiate between various members of this putatively heterogeneous population. As an inefficient protonophore, imidazole should induce greater swelling of the early endosomal compartments than the other bases, since efflux of the base as the protonated species cannot occur. This in turn could prevent the fusion of the early endosomal compartment with other compartments that might be induced by the other bases. A precedent for the promotion of vesicular fusion by weak bases with other vesicular compartments has been established in macrophages (Young *et al.*, 1990). However, in *D.discoideum* ammonia, propylamine and chloroquine act identically whereas Young et al. (1990) report that ammonia induces tubular lysosomal disassembly and chloroquine acts to induce spherical lysosomal assembly into tubular lysosomes. Fusion with other vesicles at higher pH values might explain the sudden disappearance of sections of the vesicular population.

It is difficult to determine the maximal pH reached by the early endosomal compartments upon weak base treatment, even in the case of imidazole. The early endosomal peak shifts to higher pH values but also declines in area, so it is impossible to say with certainty whether or not an increase in the area of another peak is due to a new contribution from the early endosomal compartment or simply due to natural efflux of the base from the vesicular compartments. Even in control experiments the area of the cytosolic peak increases in height both before and after washing.

Effect of weak bases on the late endosome

There is little change in the pH of the late endosomal compartment upon addition of low base concentrations. Presumably, all the available base is first targetted to the most acidic early endosomal compartment. Subsequent changes in the late endosomal compartments are then difficult to see for a

number of reasons. First, the late endosomal resonances are partly obscured by the external probe peak, even after washing the cells the external resonance recovers relatively quickly and second, the movement of the early endosomal peaks to higher pH values complicates interpretation of the late endosomal resonance, since this then contains a component of the early endosomal resonance (**figure 5.5** and **figure 5.10**). In **figure 5.10**, addition of ammonia after washing increases the pH of the late endosomal resonance whilst a component of the early endosomal compartment remains. This is probably due to the fact that access of the base to all vesicles is restricted due to cell clumping. In order to delineate the effects of the bases on the various endosomal compartments more clearly, a probe with a greater variation of chemical shift around a pK_a value of about 5.0 would be needed to obtain greater resolution of the peaks in this area. Such a probe would enable the heterogeneity of the endosomal population to be studied with more precision.

Reversibility of the weak base effects

That the cellular effects of the bases is reversible was shown by the experiments in which cells which had been treated with bases were washed and then re-examined. In all cases the early endosomal resonance reappeared at the same pH as that of the control situation and the cells showed none of the signs of cell stress or reduced viability beyond that normally observed in the NMR situation, supporting the idea that the effects of the weak bases on aggregation and culmination are unlikely to be due to reduced cell viability.

5.3.2 Cytoplasmic pH remains stable in the presence of bases

In no case did addition of base increase the cytosolic pH (**table 5b**). Neither was a decline in the cytosolic peak area seen that was greater than that obtained in the control situation, which supports the notion that the bases do not affect the cytosol and that pH_{cyt} remains stable. In most cases, the cytosolic peak area increased slightly upon addition of weak bases, indicating that the probe passes from the endosomal compartments to the cytosol or that

the endosomal peak pH has increased so much that it then resonates in the same position as the cytosolic pH.

This technique would not reveal any transient base effects on cytoplasmic or vesicular pH, as the spectra must be collected over 15 minutes in order to obtain a high signal:noise ratio. According to the theory discussed in the introduction, weak bases would be expected to raise the cytosolic pH initially due to the influx of membrane-permeable unprotonated base down a concentration gradient. However, since spectra collected after 15 minutes show no increase in cytosolic pH, this implies that the buffering capacity of the cytosol is high. This is in contrast to results obtained by Boron & De Weer (1976) with giant squid axons, where the addition of NH_4Cl externally induced a rapid increase in pH_i (measured with a glass pH electrode) followed by a fall over 30 minutes to the resting level. Since these workers used concentrations of free base that were double the highest base concentration used here (0.25mM NH_3 compared to a maximum of 0.14mM NH_3 in these NMR experiments), the long-lasting increase in pH_i may be due simply to the inability of the squid axon cytosol to buffer such high unprotonated base concentrations. Alternatively, the buffering capacity of the squid axon may naturally be lower than that of *D.discoideum*; or, insertion of a glass electrode may lead to disturbance of the cytosol and reduced buffering capacity.

There is some evidence that transient alkalinization has physiological significance in *D.discoideum*, for example, Aerts et al. (1985) have demonstrated that the pH_i undergoes transient cyclic alkalinizations during the cell cycle, varying between pH 7.2 and 7.4 over 4-5 hours and that the maximal DNA synthesis and protein production occurred when the pH peaked. They found also that increased rates of protein and DNA synthesis could be induced by artificially raising pH_i with ammonia. In contrast, another cellular process that is stimulated when pH_i is high (glycolysis) failed to be stimulated by artificially increasing pH_i with ammonia (Aerts *et al.*, 1986).

5.3.3 Comparison with aggregation, culmination and in vitro acidification

There is a good correlation between the IC_{50} values obtained for the inhibition of vesicular acidification *in vivo*, measured by ^{31}P-NMR and those for inhibition of aggregation and culmination *in vivo* (**table 5d** and **figure 5.12**).

Base	IC_{50} *in vivo* (NMR)	IC_{50} *in vitro* (vesicles)	IC_{50} $Culm^n$	IC_{50} Agg^n
IA	7413	420	10300	3300
AC	282	7.5	680	130
PA	24	0.2	27	3
CQ	3	0.004	0.6	0.3

Table 5d: A comparison of the IC_{50} values of weak bases for inhibition of aggregation, culmination and vesicle acidification *in vivo* and for vesicle acidification *in vitro*. $Culm^n$ = culmination and Agg^n = aggregation.IC_{50}s are expressed in µM concentrations.

The IC_{50} values from the NMR experiments lie between those obtained for aggregation and culmination with the exception of chloroquine, which is slightly higher (the *in vivo* acidification result for chloroquine cannot be treated with complete confidence since insufficient experiments were conducted for statistical analyses). The NMR IC_{50} values for *in vivo* acidification were expected to be slightly higher than those obtained for aggregation. Although in both cases the bases are being added to single cells, the cell density in the aggregation experiments is far lower (5×10^6 cells/cm^2) than that in the NMR experiments (4×10^8 cells/ml) and a large reservoir of fluid surrounds the cells in the aggregation experiment. In consequence there is more base available

per cell in the filter situation and less of a barrier to diffusion than in the NMR situation. In addition, it is possible that the continuous aeration required for maintaining the cells in the NMR set-up results in the removal of volatile bases.

Conversely, in the NMR set-up there is less of a barrier to base diffusion than in the first finger during the culmination experiment. The slime sheath around the first finger normally operates as a barrier to ammonia diffusion *in vivo*. Thus, it also presents a barrier to base diffusion from the exterior to the centre of the aggregate, so the IC_{50} values of the bases for culmination are expected to be higher than the IC_{50}s for vesicle acidification *in vivo*. *In vitro* acidification is inhibited by far lower concentrations of base *in vivo* acidification, since there is virtually no barrier to base diffusion in the *in vitro* situation.

The IC_{50} for chloroquine for vesicle acidification *in vivo* is of a similar order of magnitude to that required for aggregation and culmination *in vivo*, lending support to the hypothesis that chloroquine is prevented from exerting full activity *in vivo*, possibly via a multidrug resistance mechanism. A consideration of the regression coefficients for the least squares fit regression lines of **figure 5.12** underlines the difference in the action of chloroquine *in vitro* and *in vivo*. In **A**, inclusion of chloroquine gives a regression coefficient (r^2) of 0.9873 (not shown), its omission from the regression calculation improves the fit of the line (r^2 = 0.9959). The converse is true if the two *in vivo* situations are compared (**figure 5.12, B**). Inclusion of chloroquine improves the fit of the regression line (r^2 = 0.9810 without chloroquine and 0.9903 in its presence). This suggests that the action of chloroquine *in vitro* is significantly different to its action *in vivo*.

5.3.4 Conclusion and summary

The results discussed above confirm the conclusion of chapters 3 and 4, that the intracellular target of weak base action is the acidic vesicle population. The peaks arising from the early endosomal vesicle population are dramatically affected by weak base addition. This results either in a gradual shift of the pH to a higher value in the case of imidazole, reflecting the relative inefficiency of this weak base's action, or in a rapid decline in the level of the early endosomal resonance in the case of the other, more efficient bases. In contrast, the cytosolic pH remains stable at 7.2-7.4 even at the highest base concentrations. Neither is a decline in the area of the cytosolic probe peak seen in response to base challenge. Indeed, within the time resolution of the NMR experiment, no effect whatsoever is seen on the cytosolic pH.

These data render it unlikely that the effects of weak bases on aggregation and culmination are due to transient alkalinization of the cytoplasm. The long-term effect of the bases is on the early endosomal compartments and the effects on aggregation and culmination require long exposure to weak bases. If inhibition of *in vivo* processes by bases was due to transient alkalinization, one would expect brief exposure to a base to elicit an inhibitory effect. This is not the case, since aggregates treated with weak bases will resume a normal developmental cycle if weak bases are removed, even after several hours exposure to weak bases. Hence the continued presence of the base is essential for inhibition. These NMR experiments support the notion that the intracellular target of the bases is the acidic vesicle. Genetic evidence in support of this vesicular model for weak base action is presented in chapters 6 and 7.

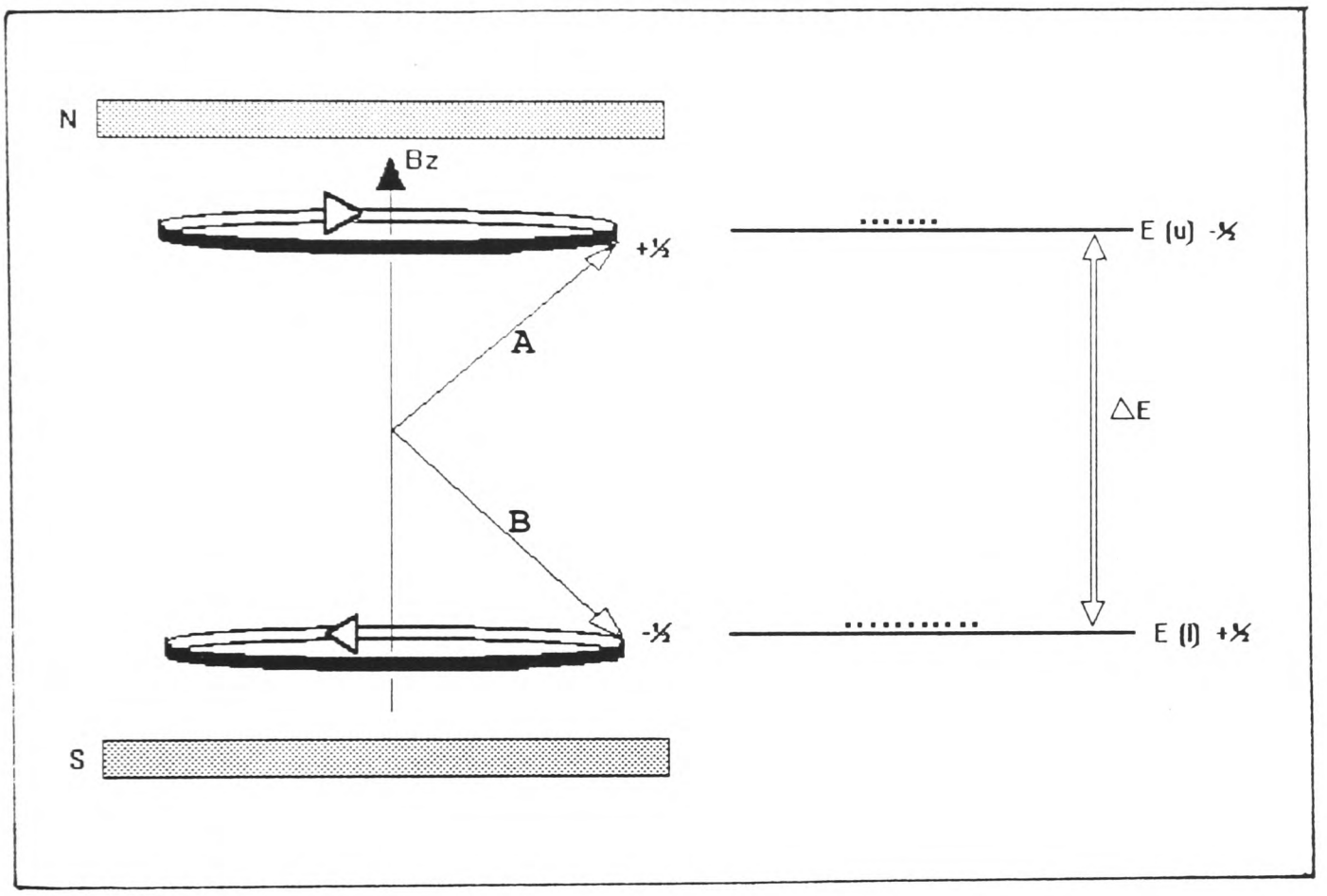


Figure 5.1 : Larmor frequency diagram. Arrows A and B represent nuclei in spin orientations +½ and -½ respectively. The energy separation between the +½ states and the -½ states is shown on the right hand side. Δ E is influenced by the molecular environment of the nuclei.

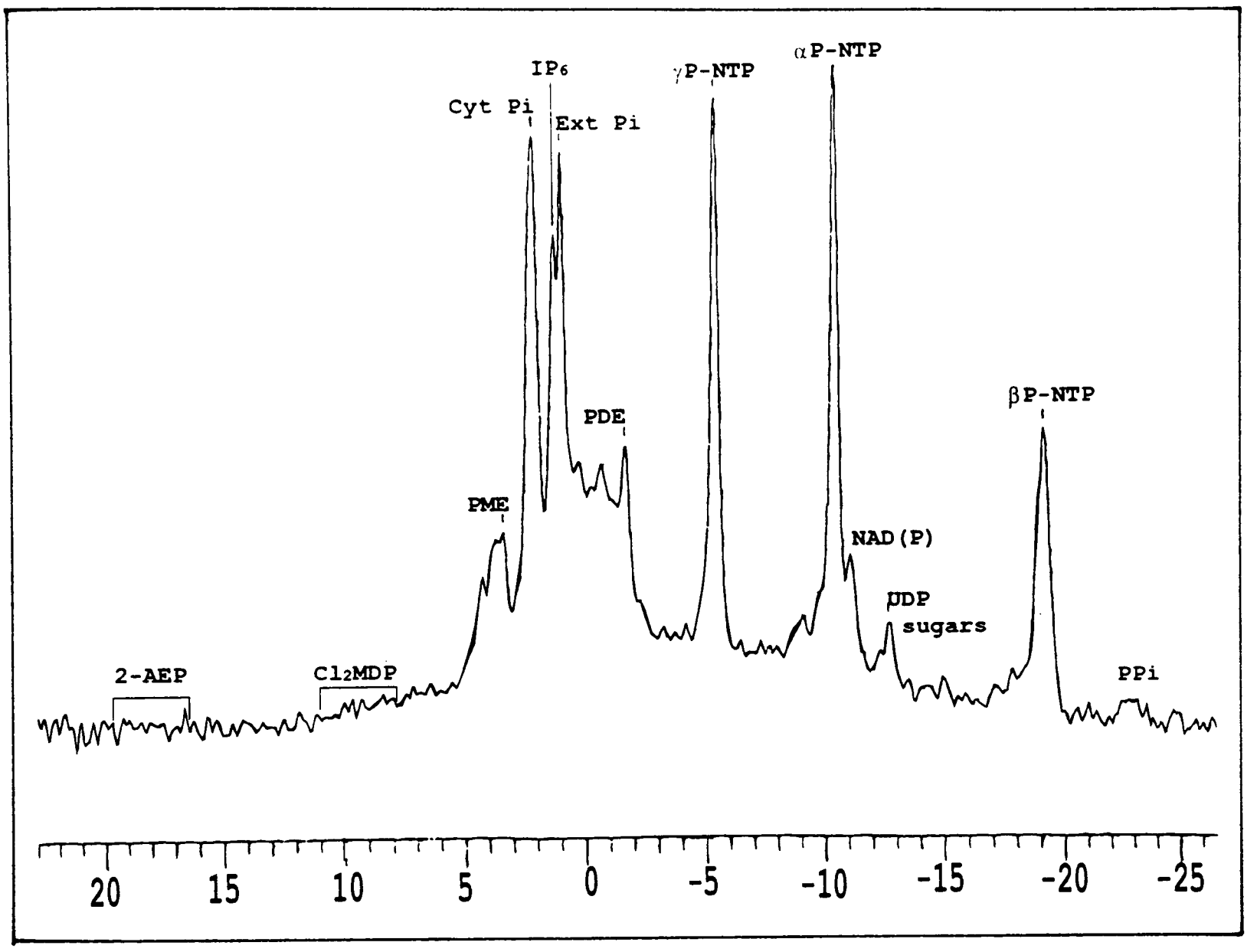


Figure 5.2: Typical spectrum of Ax2 amoebae in the absence of probes. 2-AEP and Cl_2MDP represent regions of the spectrum where probe resonances arise. PME - phosphomonoesters, PDE - phosphodiesters, PP_i - pyrophosphate.

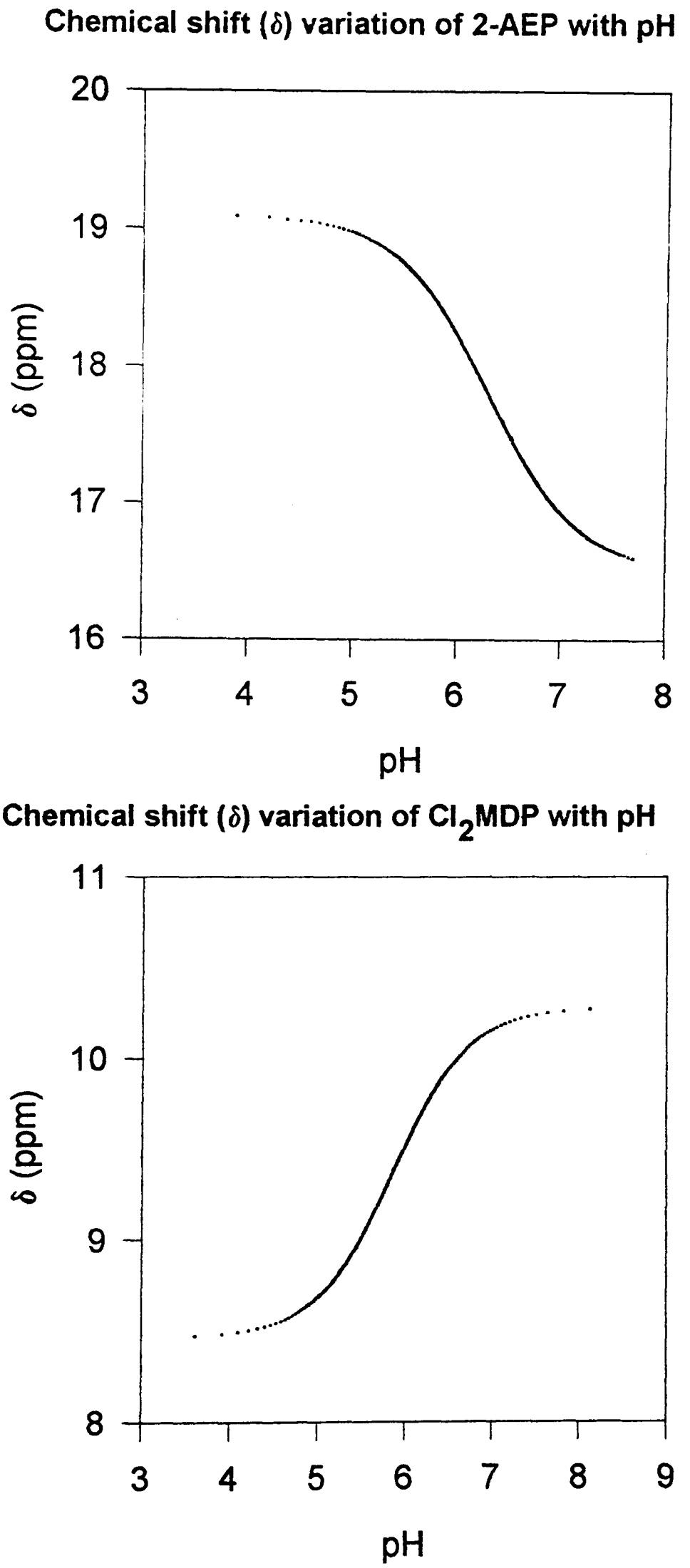


Figure 5.3: Chemical shift variation of the endocytic probes Cl_2MDP (upper) and 2-AEP (lower) with pH.

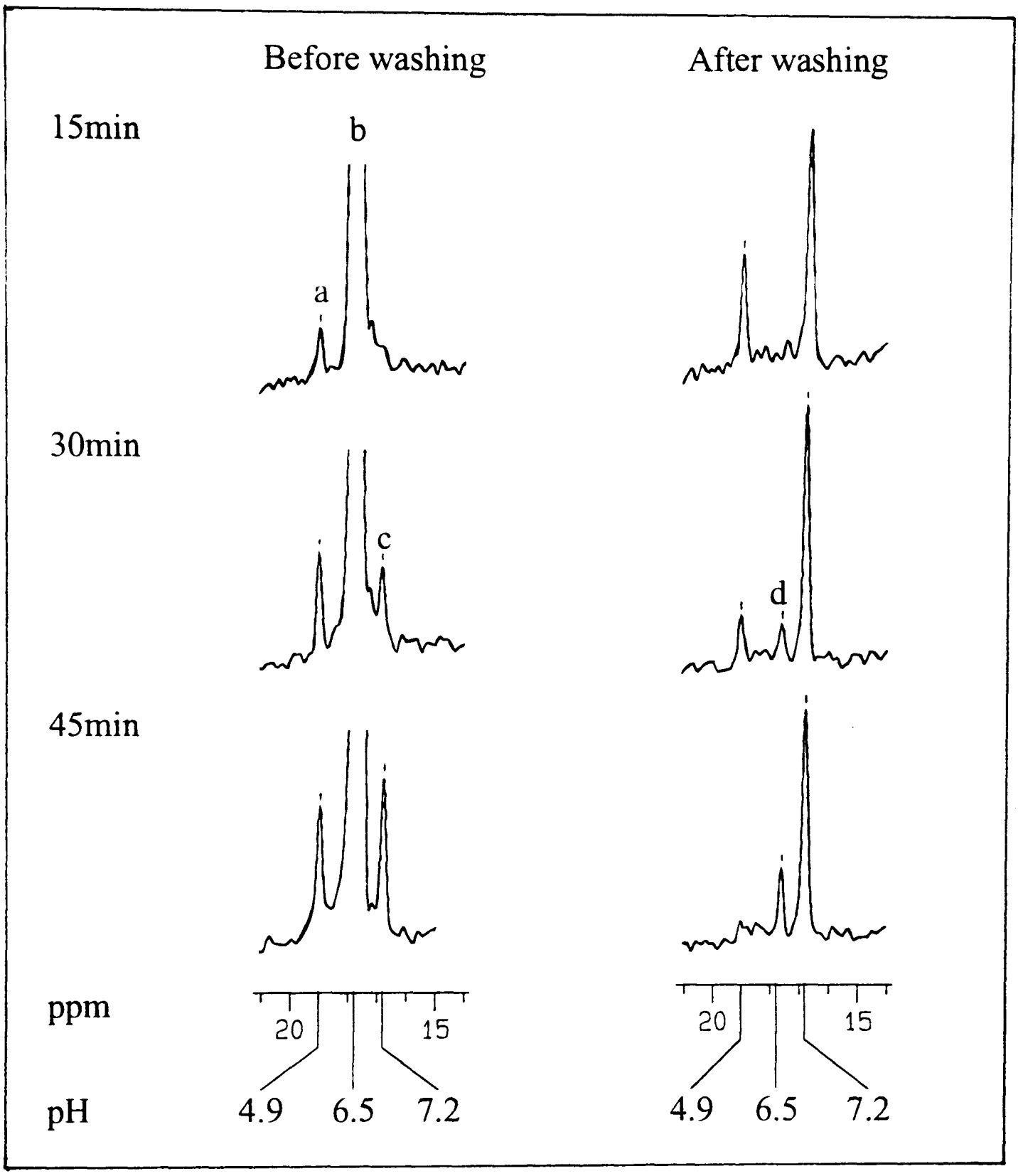


Figure 5.4: Kinetics of 2-AEP entry into amoebae.

a = early endosomal compartment (pH 4.9), **b** = external compartment (pH 6.5), **c** = cytosolic compartment (pH 7.2) and **d** = late endosomal and external compartments (pH 6.5)

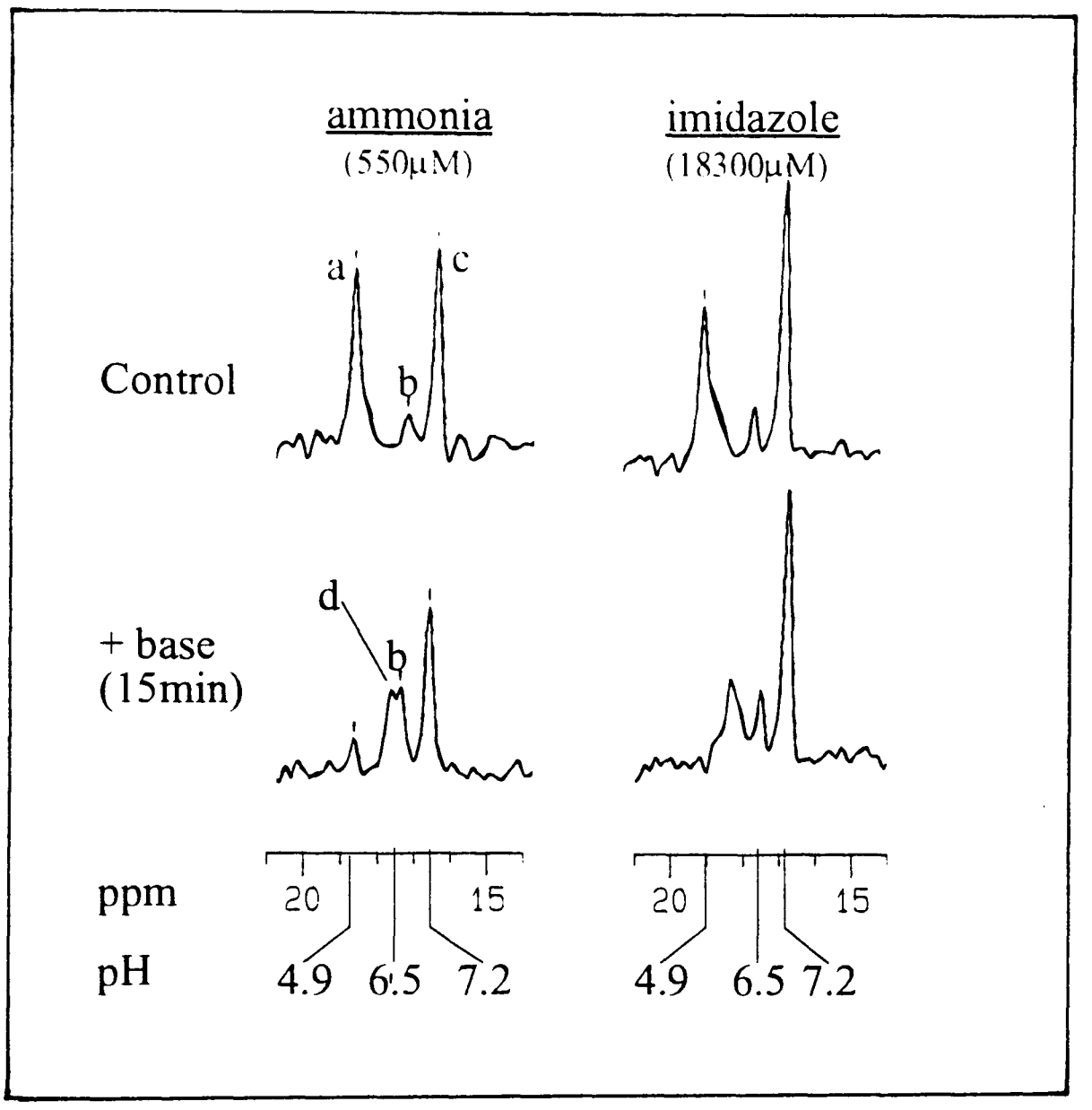


Figure 5.5: Effect of ammonia (550µM) and imidazole (18.3mM) on 2-AEP-derived resonances. **a** = early endosomal compartment (pH 4.9), **b** = external compartment (pH 6.5), **c** = cytosolic compartment (pH 7.2) and **d** = endosomal compartment (pH 6.0). Cells are shown post-wash.

(a)

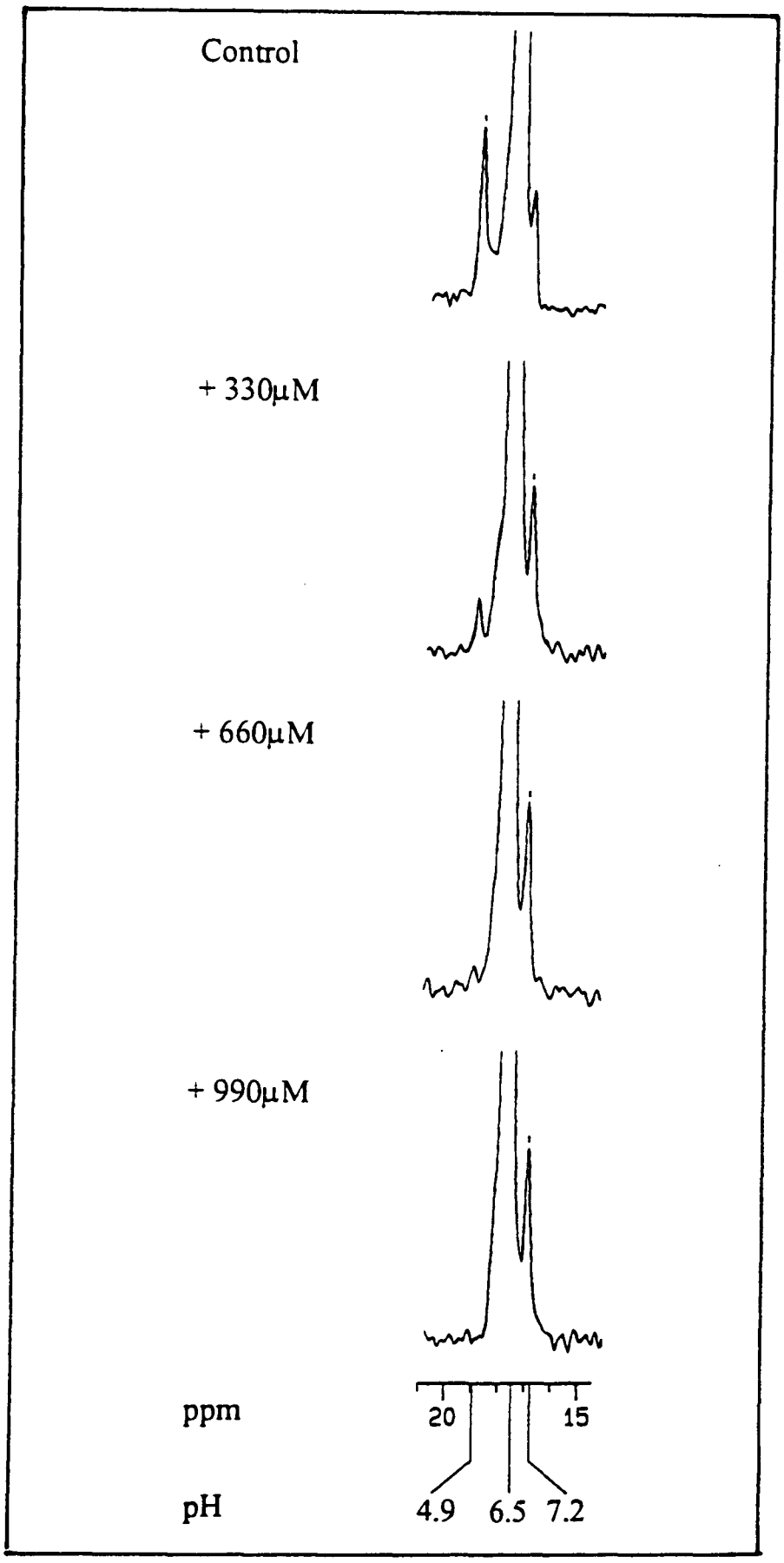


Figure 5.6 (a): Dose-dependent effect of ammonia on 2-AEP derived resonances (unwashed cells).

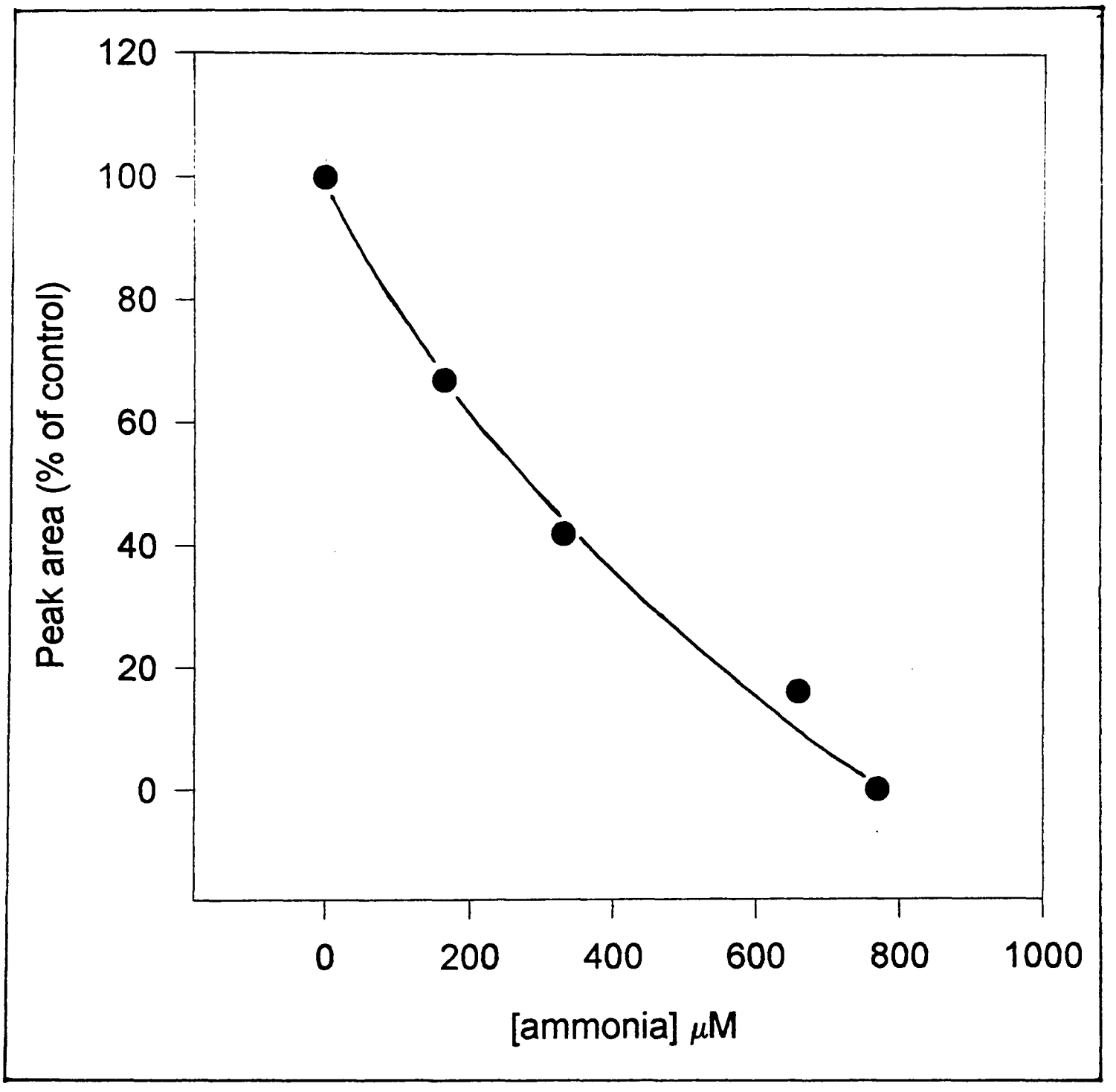


Figure 5.6 (b): Effect of ammonia on early endosomal peak area (a measure of the concentration of probe present in a compartment at a particular pH).

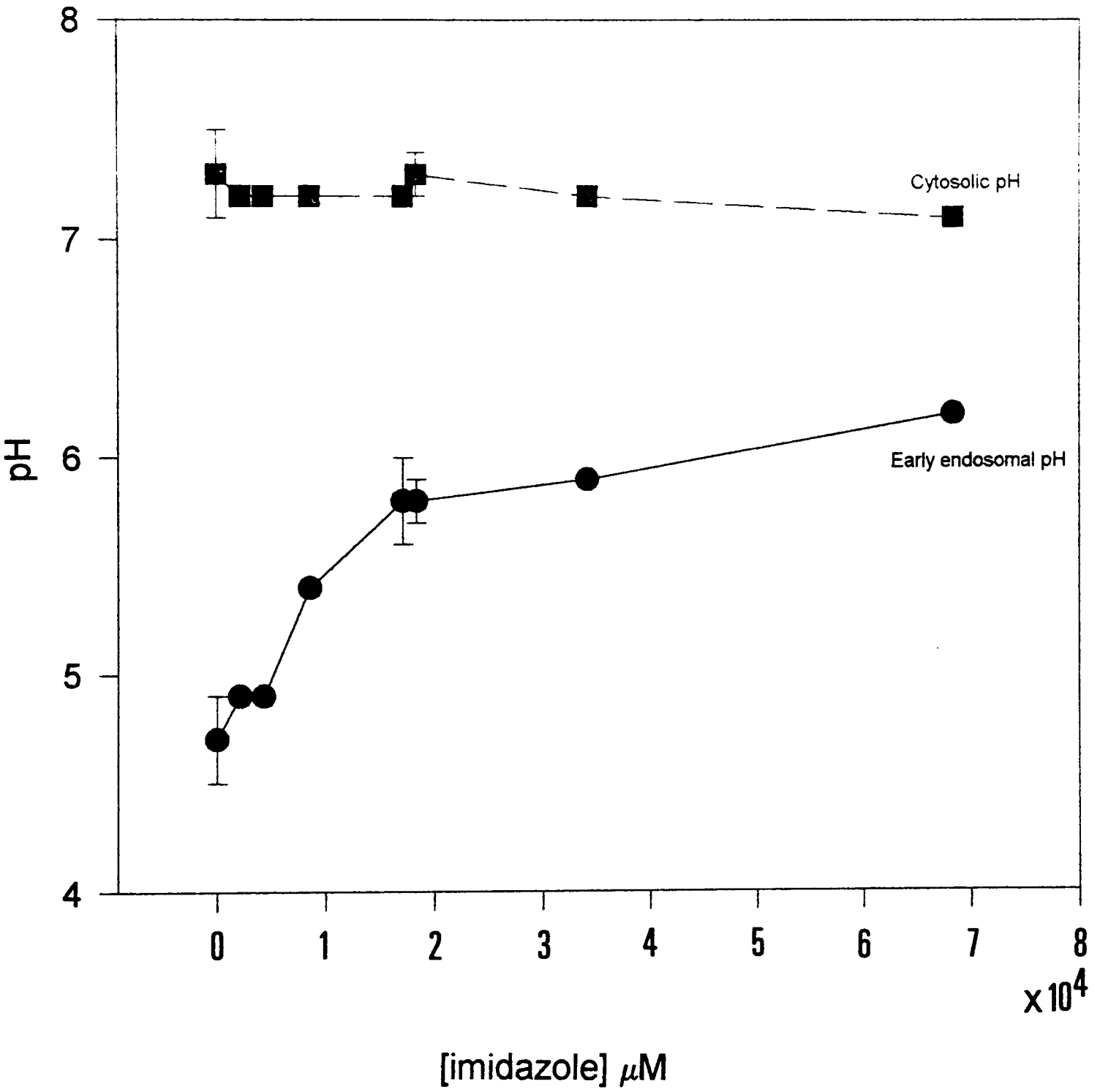


Figure 5.7: Effect of imidazole on the pH of the early endosome and the cytosol (calculated by conversion of ppm values for 2-AEP resonances to pH).

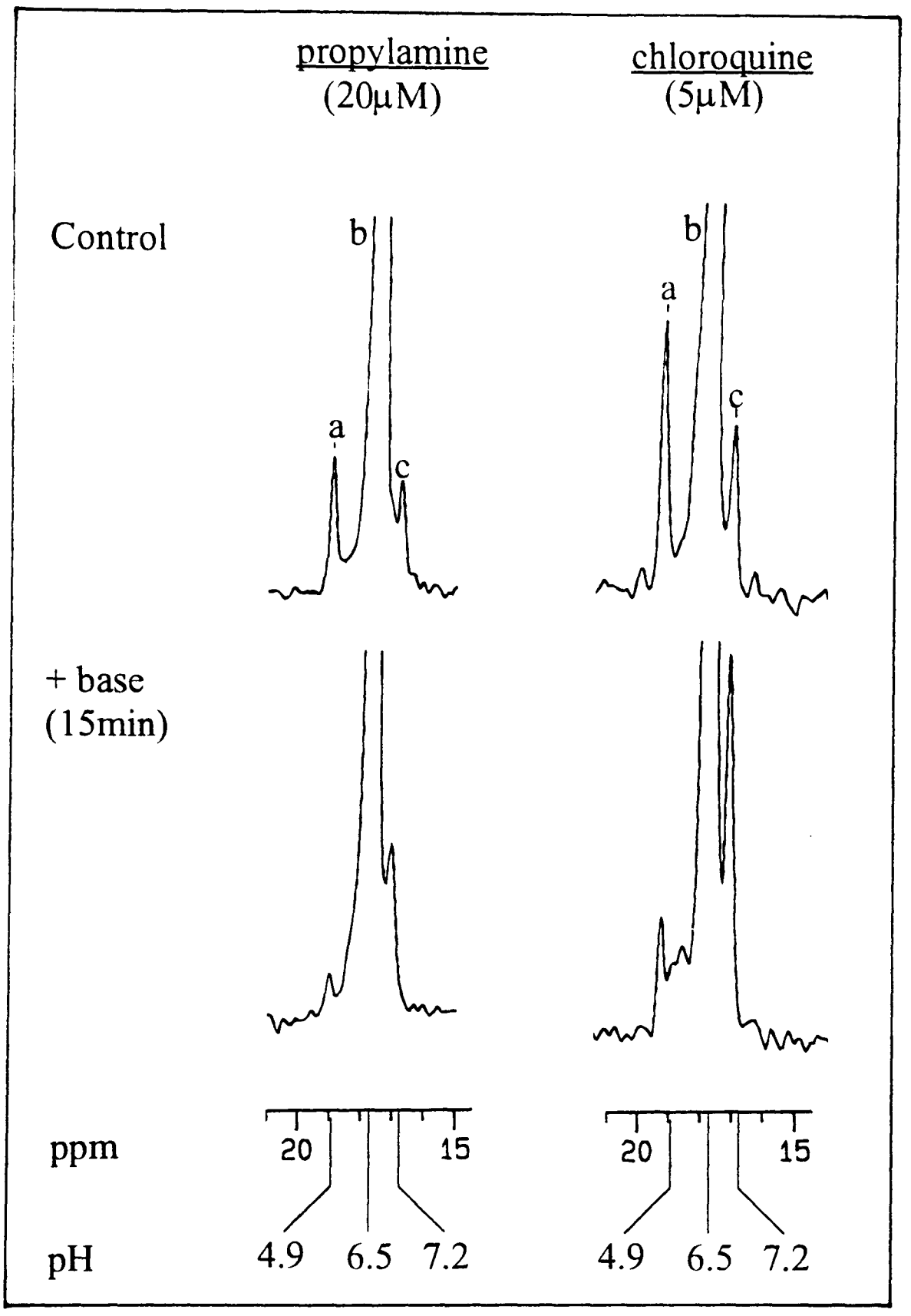


Figure 5.8: Effect of propylamine (20μM) and chloroquine (5μM) on the endosomal and cytosolic resonances. **a** = early endosomal compartment (pH 4.9), **b** = external compartment (pH 6.5), **c** = cytosolic compartment (pH 7.2). Unwashed cells are used.

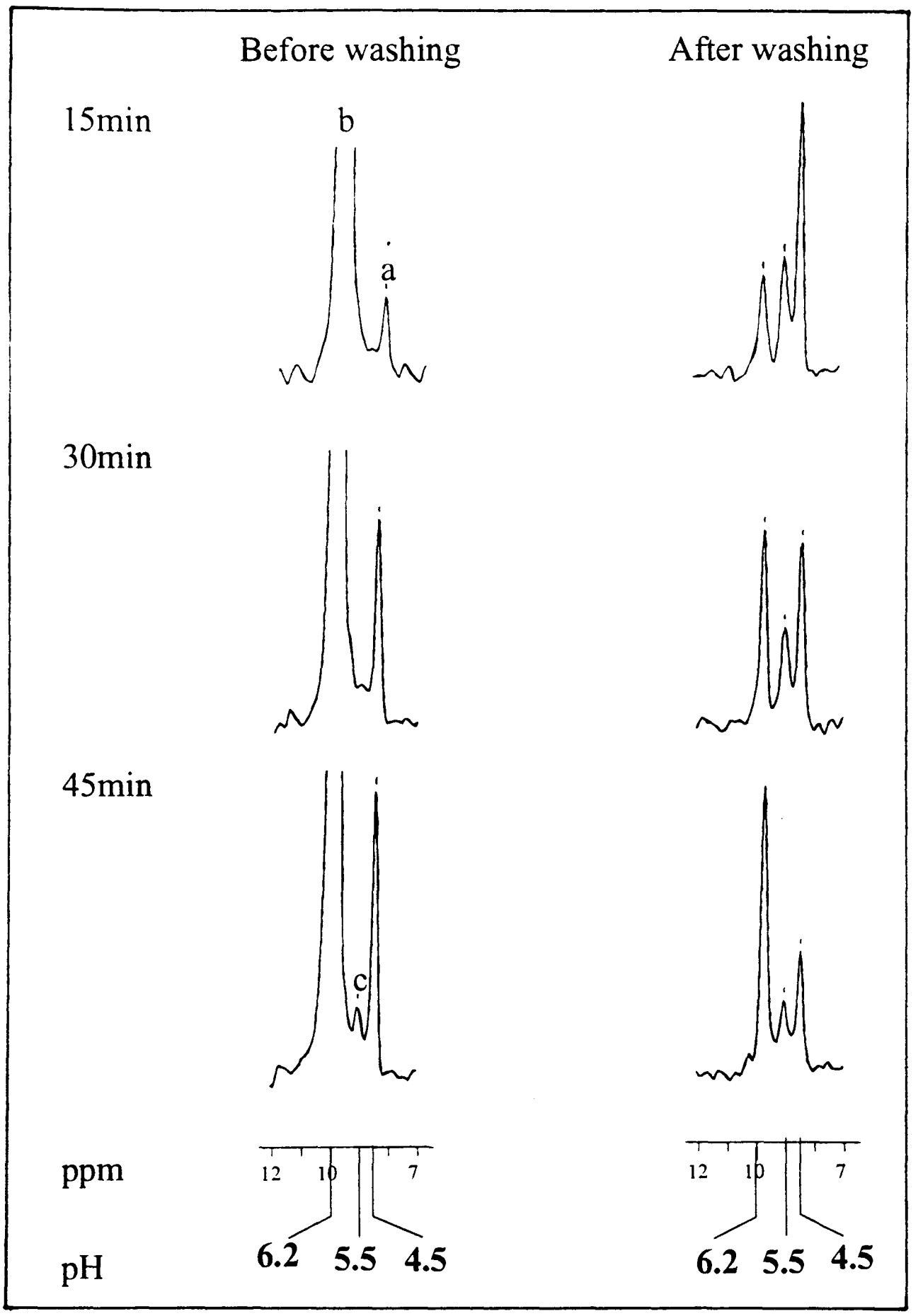


Figure 5.9: Kinetics of Cl_2MDP entry into amoebae.

a = early endosomal compartment (pH 4.5), **b** = external and cytosolic compartments (pH 6.2-7.3), **c** = late endosomal compartment (pH 5.5). Both washed cell resonances are shown to highlight the late endosomal compartment.

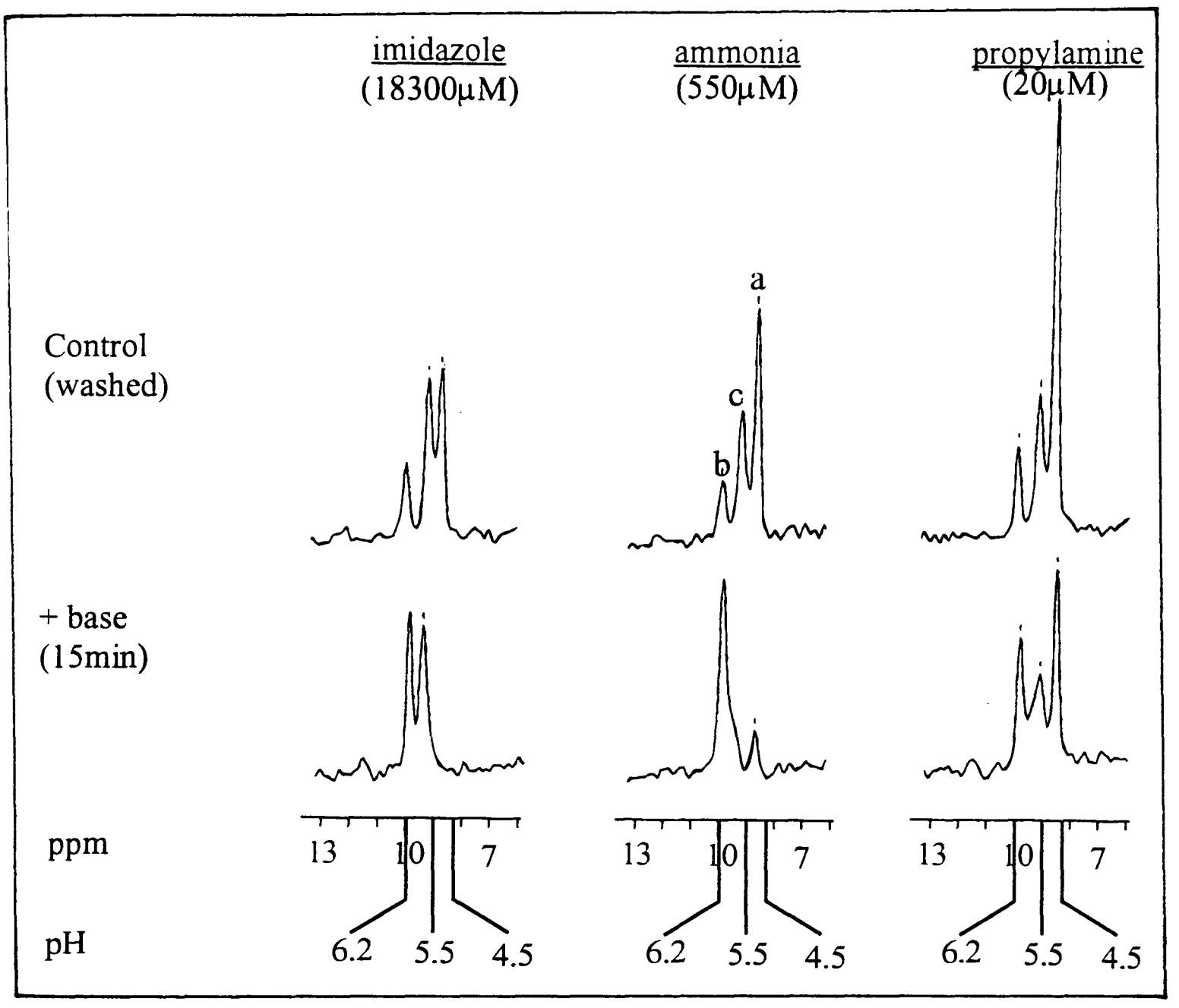


Figure 5.10: Effect of weak bases on Cl_2MDP-derived resonances. **a** = early endosomal compartment (pH 4.5), **b** = external and cytosolic compartments (pH 6.2-7.2), **c** = late endosomal compartment (pH 5.5).

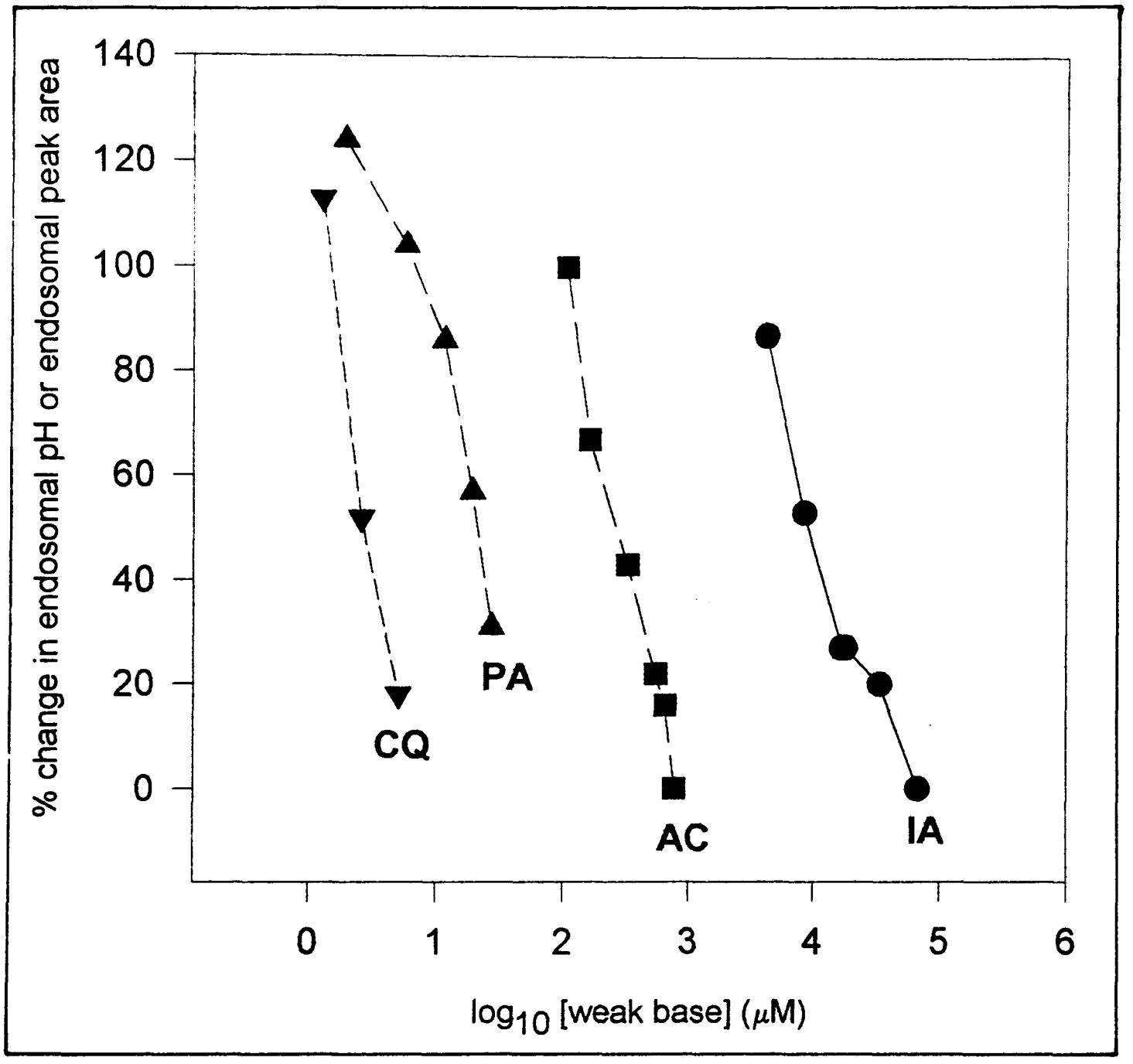


Figure 5.11: Comparison of the relative potencies of the weak bases in inhibiting early endosomal acidification *in vivo*. AC - ammonia, IA - imidazole, PA - propylamine, CQ - chloroquine. The effect of imidazole is quantified as the % shift in pH of the compartment relative to the control, whereas the effects of ammonia, propylamine and chloroquine derive from calculation of the dose-dependent changes in the endosomal peak area.

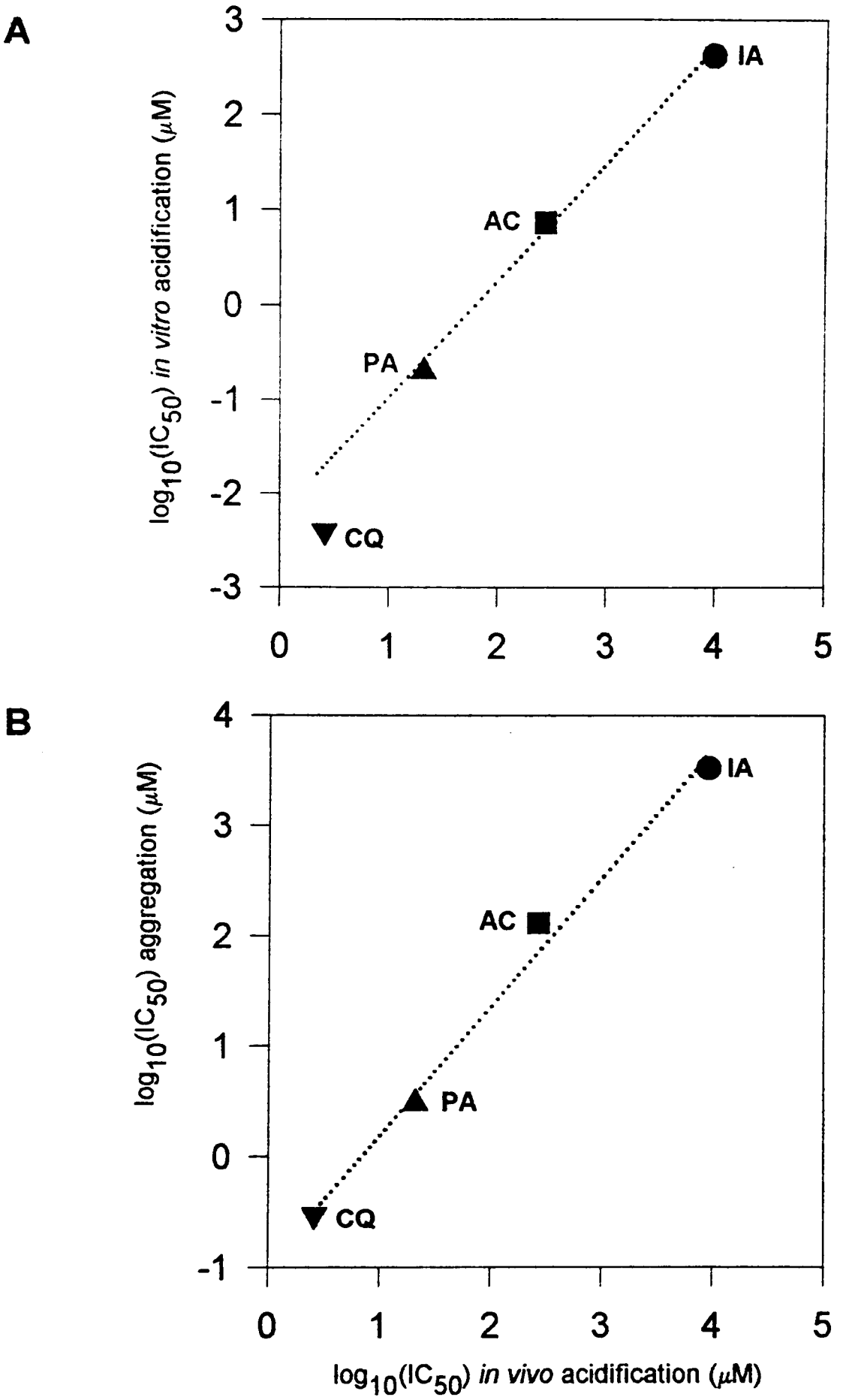


Figure 5.12: (A) Correlation of the *in vivo* and *in vitro* inhibitory potencies of the weak bases for vesicle acidification. Chloroquine is omitted from the regression calculation (see text, p.101). (B) Correlation of weak bases potencies for *in vivo* inhibition of aggregation and the *in vivo* inhibition of endosomal acidification (regression lines calculated by least squares fit).

Chapter 6

Chapter 6 *Acidification-defective (Hgr) Mutants and their Response to Weak Bases*

6.1 Introduction

A prediction of the work considered in the previous chapters is that *D.discoideum* strains that are specifically defective in vesicular acidification should resemble weak base-treated wild-type strains in their morphology and developmental behaviour and that they should be hypersensitive to inhibition of development by weak bases.

The Hgr mutants were made from the parent strain Ax2 by chemical mutagenesis using N-methyl-N'-nitro-N-nitrosoguanidine (Bof *et al.*, 1992). Endocytosis-deficient mutants were selected by incubating nitrosoguanidine-treated Ax2 cells with the metabolic poison methylene diphosphonate (MDP) at 5mM. This substance is normally taken up into cells by pinocytosis and transported into the cytoplasm where it is converted into cell-cytotoxic products; namely, a methylene analogue of ATP and methylene tetraphosphate (Klein *et al.*, 1988). Cells deficient in endocytosis survive a tenfold greater MDP challenge than Ax2 since they do not accumulate it to the same extent as the wild-type axenic strain.

Endocytosis defects in some of these isolates could be due to reduced vesicular acidification. The average endosomal pH of the isolates Hgr5 and Hgr8 are 6.08 ± 0.24 and 6.10 ± 0.17 respectively, compared to 5.73 ± 0.19 for the wild-type Ax2 (Bof *et al.*, 1992). Fluorescence probe measurements show that whereas Ax2 rapidly acidifies its early endosomes to a minimum pH of 4.6, the pH_{min} of Hgr8 is only 6.0 (Aubry *et al.*, 1993). Hgr5 shows a similar deficiency: the very acidic pH 4.3 compartment of Ax2 observed by ^{31}P-NMR with an endocytic probe is absent in Hgr5 (Bof *et al.*, 1992). Both Hgr5 and Hgr8 show a decrease in vacuolar H^+-ATPase activity (Bof *et al.*, 1992)

In this chapter four strains are studied: Hgr1, 4, 5 and 8. Neither Hgr 1 nor Hgr 4 have been tested for their vacuolar H^+-ATPase activity, so the genetic lesions responsible for their phenotype may affect any one of a number of areas: ATPase activity, membrane proton permeability, the endosomal ion channels essential for generation and maintenance of a pH gradient or the association of endocytic vesicles with acidosomes (Padh *et al.*, 1991) although Hgr5 and Hgr8 certainly have reduced vacuolar H^+-ATPase activity.

6.2 Results

6.2.1 Growth characteristics of Hgr strains

The growth rates of these mutant strains differ greatly from that of Ax2. **Figure 6.1** shows the growth rates of the various strains in medium at pH 6.0. At pH 6.5, the pH normally used for growing Ax2 axenically, it was found that strain Hgr 5 did not grow at all, but that the growth rates of the other strains did not differ significantly (data not shown), therefore all strains were grown at pH 6.0. Reduction of the medium pH to 5.0 did not improve the growth rate of Hgr5. It was expected that lowering the pH would produce a significant increase in the growth rate of the strains, as is the case with acidification-defective yeast strains (Umemoto *et al.*, 1991), but no such effect was seen with these strains. It is possible that *D.discoideum* are more resistant than yeast to "artificial" vacuolar acidification by lowering the external pH. It is also possible that these strains harbour additional mutations that affect the growth rate. Corroborative evidence for this latter theory is presented later in **section 6.2.2** and **6.2.3**, where, briefly, the experiments show that the degree of developmental defect does not correlate with the observed acidification/growth rate deficiency. The following table (**6a**) gives the doubling times of the various Hgr strains:

Strain	Doubling time (h)	Cells/ml at plateau
Ax2	8	1.8×10^7
Hgr 1	18	1.5×10^7
Hgr 4	12	1.2×10^7
Hgr 5	29	4.0×10^6
Hgr 8	18	8.0×10^6

Table 6a: Doubling times of Hgr strains in axenic medium at pH 6.0. The doubling times are calculated from growth rate graphs which are the result of at least 4 independent growth rate determinations. Errors are in the region of ± 2h per strain. the cell concentration level at plateau is a rough estimation.

For Hgr5 and Hgr8, the doubling times are longer than those reported in Bof *et al.*'s 1992 study (13.3 h and 12.2 h respectively). This is most likely to be due to differences in growth conditions; for example, liquid media are variable since peptone batches are not identical, the shaking speed of the cells could be different, or the MDP concentrations used to maintain the cell stocks might differ.

In addition to having growth defects in axenic media, the strains are reported to be phagocytosis-deficient (M.Satre, personal communication) with the possible exception of Hgr 4 (M.Maniak, unpublished results), an observation which is supported by the fact that the strains do not grow well on bacterial lawns. Clearance of a lawn is retarded to the greatest degree in Hgr5 and 8, less so in Hgr1 and 4, which is consistent with the growth rates of the strains in axenic medium. In the case of Hgr5, differentiation does not occur at all

when grown on bacterial lawns and the other strains show severely stunted morphologies (with the exception of Hgr4, which forms small fruiting bodies).

6.2.2 Developmental characteristics of Hgr strains

Under conditions where the wild type axenic strain develops and culminates normally, for example at neutral pH, the development of the Hgr mutants is severely restricted. **Figure 6.2** compares the timing of the developmental cycles of Ax2 and Hgr5 at pH 7.3 on millipore filters. After 14h, Ax2 forms tipped aggregates, whereas the only indication that aggregation is commencing in Hgr5 is a faint rippling or "patchiness". These patches become more defined by 20h, forming a large aggregation field which splits up into a number of tipped aggregates rather like a bunch of grapes, which might indicate that there is a cAMP signalling defect in these mutants (see later discussion, **section 6.3**). By this time, Ax2 has reached the late culminant stage and forms fruiting bodies by 24h. Even at 36h, no comparable structures have formed in the case of Hgr5. Rather the aggregates are small and slug- or first finger-like, with occasional thickening at the apex of the first finger, indicating that some form of culmination may commence. Development is delayed to varying degrees in the other Hgr strains also. The table below summarizes the effects seen at pH 7.3.

Strain	14h	20h	36h
Ax2	tipped mounds	culminants	culminants
Hgr1	-	streaming	mounds/slugs
Hgr4	streaming	mounds	culminants
Hgr5	-	mounds	culminants
Hgr8	early mounds	slugs	culminants

Table 6b: delay in the developmental cycle (at pH 7.3) of the Hgr mutants in comparison to Ax2. "Culminants" refers to the final morphology. For Ax2 this refers to mature fruiting bodies, in the mutant strains, the final morphology is often indistinguishable from the first finger/slug/early culminant stage.

Therefore, defective vesicular acidification leads to retarded aggregation in the case of each of the mutants. It is worth noting that Hgr1 exhibits the greatest delay in aggregation, despite the fact that it has one of the better growth rates. Hgr 4 and 8 are delayed only by a few hours. Therefore, it does not appear that the degree of developmental delay correlates with the growth rate of the strain.

6.2.3 The effect of pH on the developmental morphologies

If the aberrant morphologies and delays in aggregation seen in the Hgr strains at pH 7.3 were due solely to defective acidification of acidic compartments, then the phenotype might be rescuable by development at low pH if the endocytic system can be artificially acidified by a low pH external medium.

Development of the Hgr strains was conducted over the pH range 5.0 to 8.0 and the development of the Hgr strains (but not Ax2) was found to be highly dependent on the pH environment. Higher pH values (pH 8.0) inhibited Hgr development completely, but at lower pH the phenotype of culminants became progressively less mutant. This was the case for all of the mutants although

the degree of "rescue" by low pH was not the same for all of the mutants.

Figure 6.3 illustrates the effect of altering the pH of the environment of the developing aggregates. At pH 5.0 and 7.0 there is little difference in the morphologies of the Ax2 culminants, neither was the timing of development significantly affected. At both pH values, mature stalk cells and mature, oval, refractive spores could be observed at high magnification (not shown). Culmination of Hgr1 barely occurred at pH 7.0, a few first fingers only were produced at 40h and development did not proceed further even after 72h. Lowering the pH to 5.0 improved culmination to the extent that a bulbous spore mass was formed at the apex of a thickened stalk. Under a fluorescence microscope, some small, rounded and poorly refractive spores were observed in aggregates developed at pH 5.0 whilst none were observed at pH 7.0. No mature stalk cells were seen in either case (not shown). In the case of Hgr4, culmination did occur at pH 7.0 (albeit delayed in comparison to Ax2), but the stalks produced were severely thickened and the spore heads glassy. At pH 5.0 however, culmination was almost normal, with the majority of culminants displaying large spore heads and narrow stalks. Upon examination of the aggregates at higher magnification, mature spores were absent at pH 7.0 and lowering the pH to 5.0 yielded a few, very rounded, spores. Similar phenomena were seen with Hgr5 and Hgr8. In both cases at pH 7.0, severely stunted culminants were produced, containing a few rounded, refractive spores. No mature stalk cells were seen in either case. At pH 5.0, recognisable stalks and spore heads were produced by both mutants, although closer examination of the spores revealed that they were for the most part rounded and poorly refractive. **Table 6c** summarizes the effect of lowering the pH on the production of mature stalk and spore cells

Strain	Spore cells	Stalk cells
Ax2 pH 5.0	+++	+++
pH 7.0	+++	+++
Hgr1 pH 5.0	+	-
pH 7.0	-	-
Hgr4 pH 5.0	+	+
pH 7.0	-	+
Hgr5 pH 5.0	++	+
pH 7.0	+	-
Hgr8 pH 5.0	++	++
pH 7.0	+	+

Table 6c: Formation of spore and stalk cells in Ax2 and the various Hgr mutants at different pH values. Spore and stalk estimations were made from aggregates after 40 h of development.

It is notable that the severity of the phenotype does not correlate exactly with the degree of growth defect. For example, Hgr1 has a higher growth rate than either Hgr5 or Hgr8, yet its phenotype at pH 7.0 is the most severe of all the mutants. Possible reasons for this are discussed in section **6.3**. Many of the morphologies exhibited by the Hgr mutants are reminiscent of weak base-treated wild-type cells. If culminants are produced by the Hgr strains, then they tend to be stunted, with large spore heads, as in ammonia-treated NC4 (see chapter 3, **figure 3.5**). In addition, at high pH values, the terminal morphology of the Hgr strains is often slug- or first finger-like, and comparable to the arrested structures formed by NC4 at the higher base concentrations used (see chapter 3, **figures 3.5** and **3.6**).

6.2.4 The effects of weak bases on the development of selected Hgr strains

The various mutants were allowed to develop in the presence of weak bases, to test them for hypersensitivity to these bases. Inhibition of aggregation was tested rather than inhibition of culmination, since the differences in the culminants produced by each strain made it difficult to describe and quantify culmination for all of the strains.

Inhibition of aggregation in Ax2 and Hgr5 in response to three bases: imidazole, ammonia and propylamine is shown in **figure 6.4**. Hgr5 is hypersensitive to inhibition of aggregation in the presence of each of the bases, aggregation being inhibited at concentrations where the parent strain, Ax2, fruits. Although aggregation does occur at the lowest base concentrations used, for example at 0.6mM imidazole or at 0.4µM propylamine (unprotonated concentrations), the morphologies of the culminants in such conditions are stunted with respect to the parent strain. It appears therefore that even the lowest base concentrations severely inhibit development.

Figure 6.5 shows the hypersensitivity of Hgr5 to imidazole, ammonia and propylamine graphically, indicating that the aggregation of Hgr5 is roughly 17 times more sensitive to inhibition by weak bases than that of Ax2. Hgr1, 4 and 8 were also shown to be hypersensitive to the effects of bases. **Figure 6.6** demonstrates their hypersensitivity with respect to the wild type and below, a comparative table gives the IC_{50} values for the inhibition of aggregation by imidazole.

Strain	IC_{50} for aggregation unprotonated [imidazole] (mM)
Ax2	13
Hgr1	9
Hgr4	10
Hgr5	0.7
Hgr8	4

Table 6d: Sensitivity of the Ax2 and the Hgr strains to the inhibition of aggregation by imidazole at pH 7.3. Base concentrations are expressed in terms of the unprotonated base.

6.3 Discussion

6.3.1 Similarity of acidification-defective strains to weak base-treated wild-type strains

In many ways the morphology and behaviour of the Hgr strains is similar to weak base-treated wild-type strains. Their culmination is poor, forming stunted fruiting bodies with large spore heads, if they culminate at all. Often the strains seem to arrest in the early stages of development: at high pH values especially, slug and first finger-like structures are frequently the terminal morphologies of aggregates. This is consistent with the notion that their developmental phenotypes are the result of defective vacuolar acidification and with the idea that weak bases exert their developmental effects by interfering with vesicle acidification. In some respects, the morphology of the Hgr mutants is similar to that of slugger mutants, which are commonly defined as those that spend an abnormally long period as migrating

slugs (Newell & Ross, 1982), since the Hgr strains remain as slug-like creatures at neutral pH. However, under no conditions could the Hgr mutants be induced to migrate across filters or water agar plates. Neither would the slugs formed orient towards a light source. Certain phototactically "blind" slugs exist (Bonner & Williams, 1994) and it is possible that the Hgr mutants could resemble these blind sluggers biochemically. Certain of the slugger strains are reported to be hypersensitive to the effects of ammonia (Schindler & Sussman, 1979; Newell & Ross, 1982; Gee *et al.*,1994) and ammonia itself prolongs the slugging period in wild-type strains. Since the Hgr strains are defective in vesicular acidification, they would be expected to be hypersensitive to weak bases and perhaps to be sluggers. However, the level of the acidification defect in these strains may preclude their movement, hence they remain as stationary slugs. Additional mutations could be responsible for the lack of migratory slugging, but it is unlikely that all of the Hgr strains should be affected by an identical double mutation. It is more likely that the lack of movement is a direct consequence of the defective acidification of the strains.

6.3.2 Correlation between growth rates and hypersensitivity to inhibition of aggregation

It was speculated that the differences in the growth rates of the mutants correlated with the degree of the acidification defect. However, the growth rate of Hgr5 is the lowest, despite the fact that Hgr8 is reported to have a greater defect in endosomal acidification (Bof *et al.*, 1992). The exact nature of the defects in the strains Hgr1 and Hgr4 has not been elucidated.

Comparison of the growth rate and the sensitivity of aggregation to weak base inhibition shows that the defect in the growth rate correlates roughly with sensitivity to inhibition by weak bases (**table 6e**, below).

Strain	IC_{50} aggregation (imidazole)	Doubling times (h)
Ax2	13	8
Hgr1	9	18
Hgr4	10	12
Hgr5	0.7	29
Hgr8	4	18

Table 6e: Comparison of the growth rates of Ax2 and the Hgr strains with their sensitivity to inhibition of aggregation by weak bases.

Assuming that the degree of hypersensitivity to weak base is related solely to an acidification defect, this suggests that their ability to grow in axenic medium is related solely to their endocytic acidification capacity. However, in terms of the developmental phenotype, it is more difficult to make links between the growth rate and the degree of defect. Despite the fact that it has one of the higher growth rates of the strains and lesser sensitivity to weak base inhibition of aggregation, Hgr1 displays one of the most severe developmental phenotypes. Also, its development is not improved greatly by lowering the pH of the developmental buffer. An explanation could be that Hgr1 may harbour an additional mutation affecting its development. Alternatively, modifying mutations that increase the growth rate may be selected for. It is notable that slugger mutants also show a poor correlation between their degree of acidification defect and their growth rate (Gee, 1993; Gee *et al*.,1994).

6.3.3 Other defects induced by defective endosomal acidification

In the parent strain Ax2, aggregation at any pH (5.0 - 8.0) leads usually to the formation of individual, separate mounds. In contrast, all of the Hgr strains display "patchy" aggregation, where mounds are bunched together in clumps (**figure 6.2** gives Hgr5 and Ax2 as examples). The occurrence of this phenotype could suggest that cAMP signalling is defective in the Hgr strains. Synergy experiments with the wild-type could be used to determine whether any such defect was due to cAMP signalling or to a defective cAMP response. Preliminary experiments using a mixture of labelled Hgr5 and Ax2 show that Hgr5 do not participate in the formation of the aggregates (data not shown), suggesting that Hgr5 is defective in its cAMP response.

Testing of the culminants for the presence of mature spore and stalk cells indicates that cell differentiation may be perturbed in the Hgr strains. In each case, the spores produced by the mutants are rounded and poorly refractive rather than displaying the characteristic oval shape and high refractivity of the parental strain. Lowering the pH increases the production of spore cells slightly and greatly improves stalk cell formation. This is consistent with a model in which a lower vesicular pH is necessary for stalk formation than for spore formation, although it appears from these experiments that vesicular acidity is required in some measure for spore formation also. It is possible that lowering the vesicular acidity leads to promotion of the prespore pathway at the expense of the prestalk pathway (Gross *et al.*, 1988), which is supported by these experiments as spore formation seems to be less strongly inhibited than stalk formation in these acidification-defective mutants (with the exception of Hgr4, see **table 6c**). It is possible that the expression or intracellular targetting of stalk cell-surface proteins are particularly sensitive to the endosomal pH.

6.4 Conclusion

In summary, the Hgr mutants display the following properties: they are defective in vacuolar acidification, in growth and in development. They aggregate slowly, show some signs of cAMP signalling defects and cannot culminate at high pH values. Their morphologies at high pH are in many respects similar to those displayed by the wild-type or parent strains in the presence of high weak base concentrations, providing support for the theory that the *in vivo* effects of ammonia are mediated by neutralization of an acidic vesicle. However, with these mutants, it is difficult to tell to what extent the observed phenotypes are due to an acidification defect, since secondary mutations affecting development cannot be excluded. Therefore, in the following chapter, mutants will be presented which are specifically defective in their vacuolar ATPases, to see whether or not they share similar properties with the Hgr strains and with weak base-treated wild-type cells.

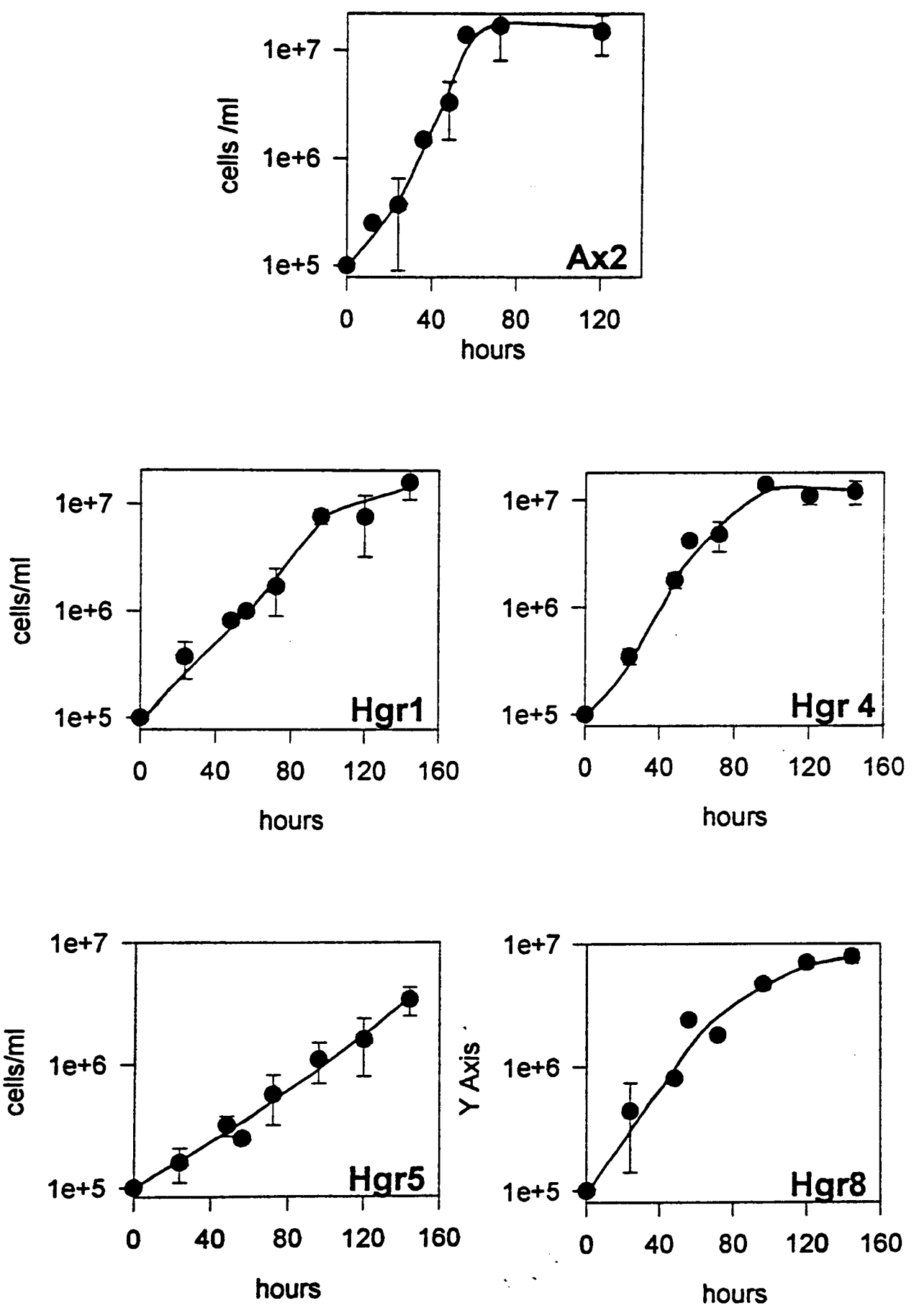


Figure 6.1: Growth rates of the Hgr strains (with Ax2 for comparison) in axenic medium at pH 6.0. Where error bars are omitted, they lie within the data points.

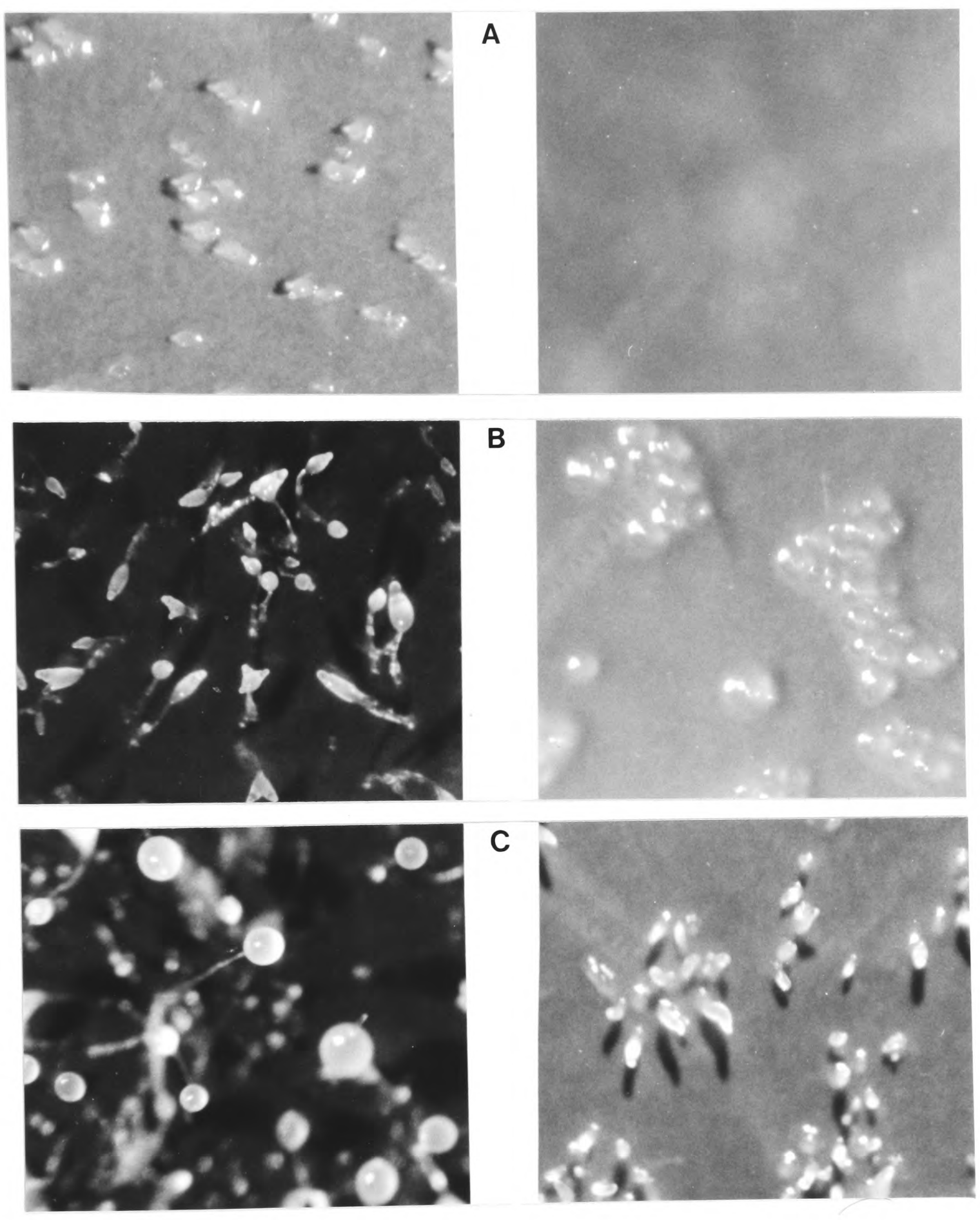


Figure 6.2: Comparison of the developmental timing of Ax2 and Hgr5 strains on filters at pH 7.3. Initial cell density was 5 x 10^6cells/cm^2. Timing: (A) 14h, (B) 20h, (C) 36h.

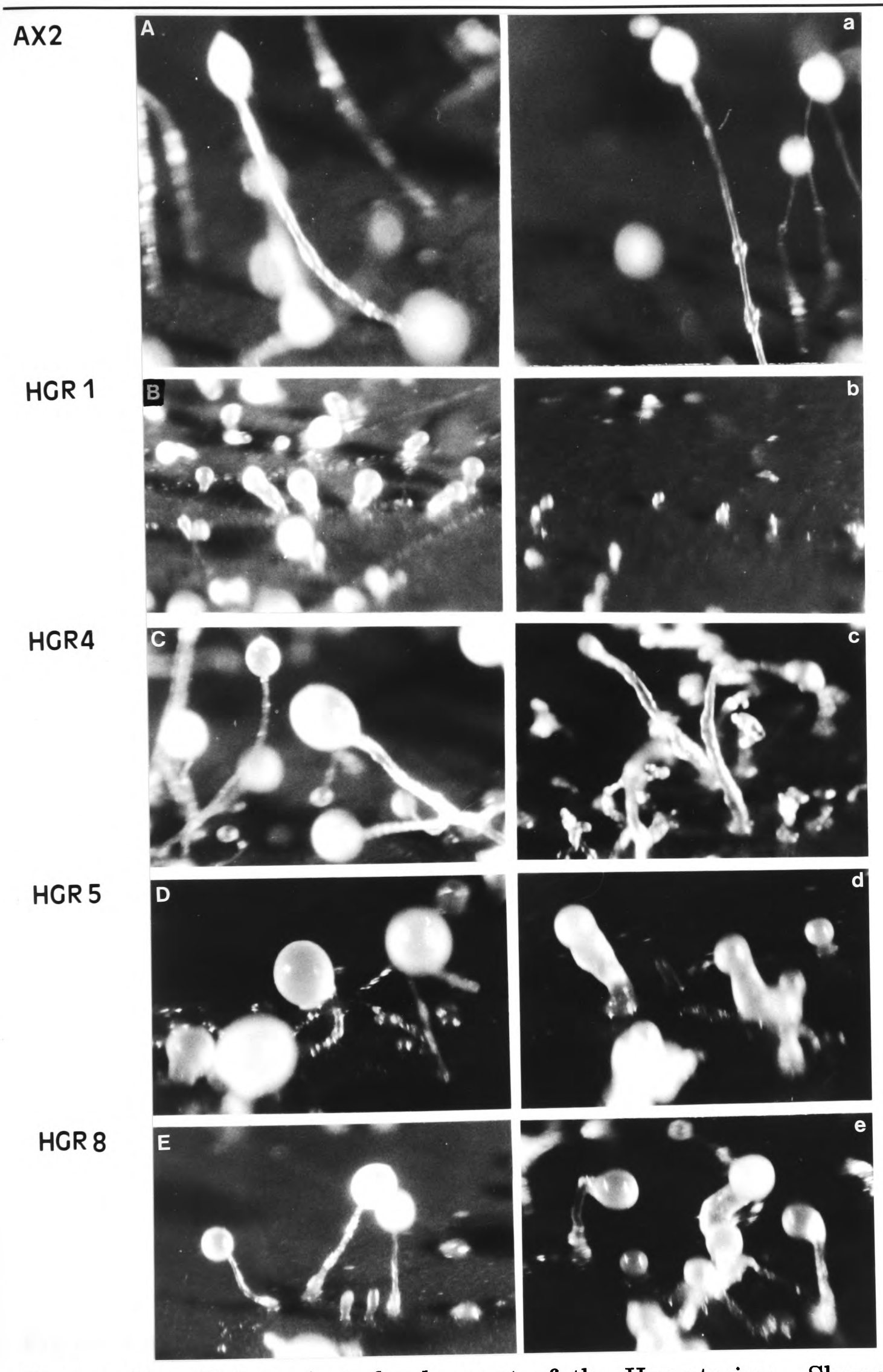


Figure 6.3: pH-dependent development of the Hgr strains. Shown are morphologies at pH 5.0 (**A** - **E**) and 7.0 (**a** - **e**) after 72h development.

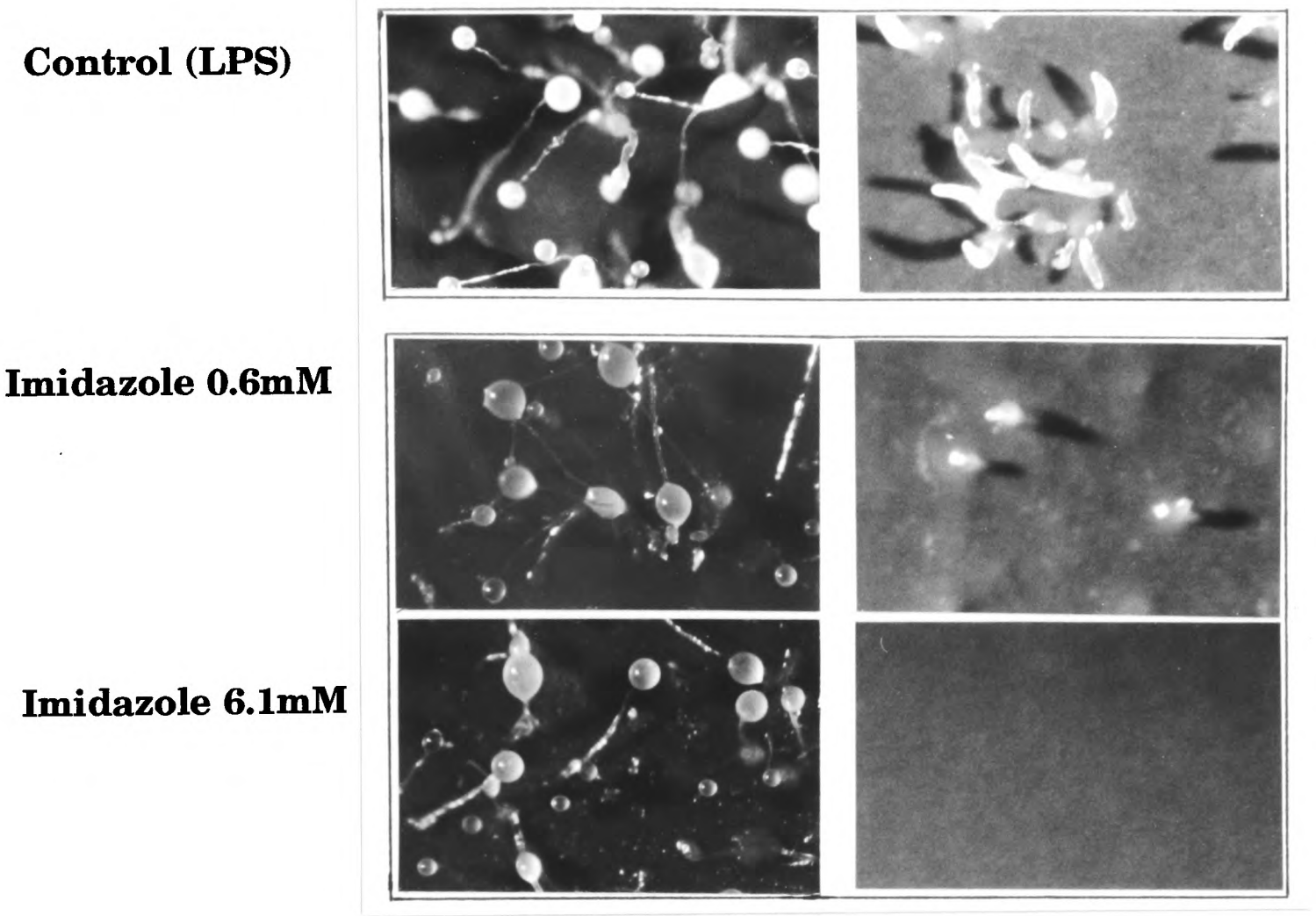


Figure 6.4: Hypersensitivity of Hgr5 to inhibition of aggregation by weak bases. Development was conducted on filters at pH 7.3 and the morphologies photographed at 48h (continued over page).

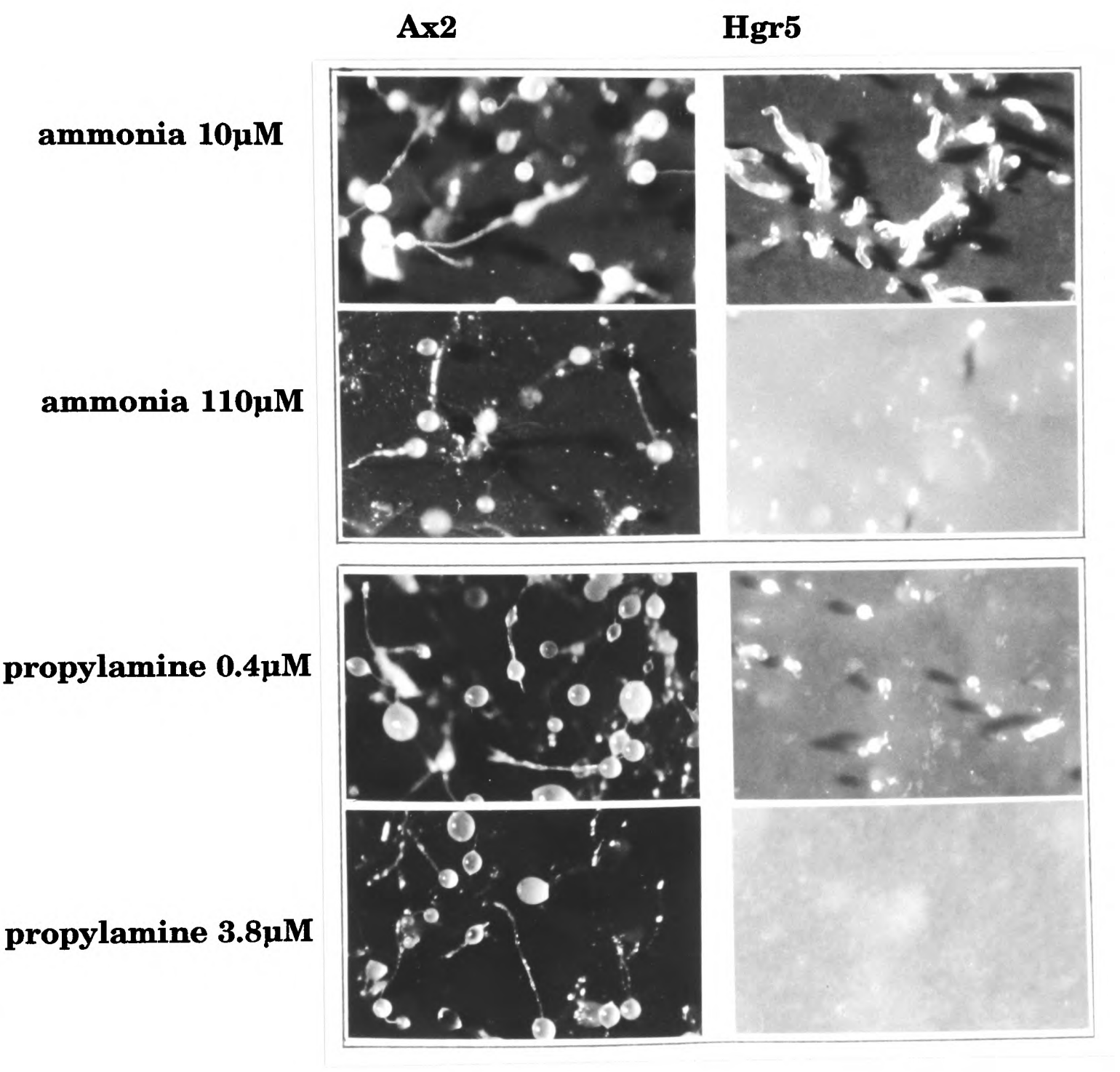


Figure 6.4 (continued): Hypersensitivity of Hgr5 to inhibition of aggregation by weak bases. Development was conducted on filters at pH 7.3 and the morphologies photographed at 48h.

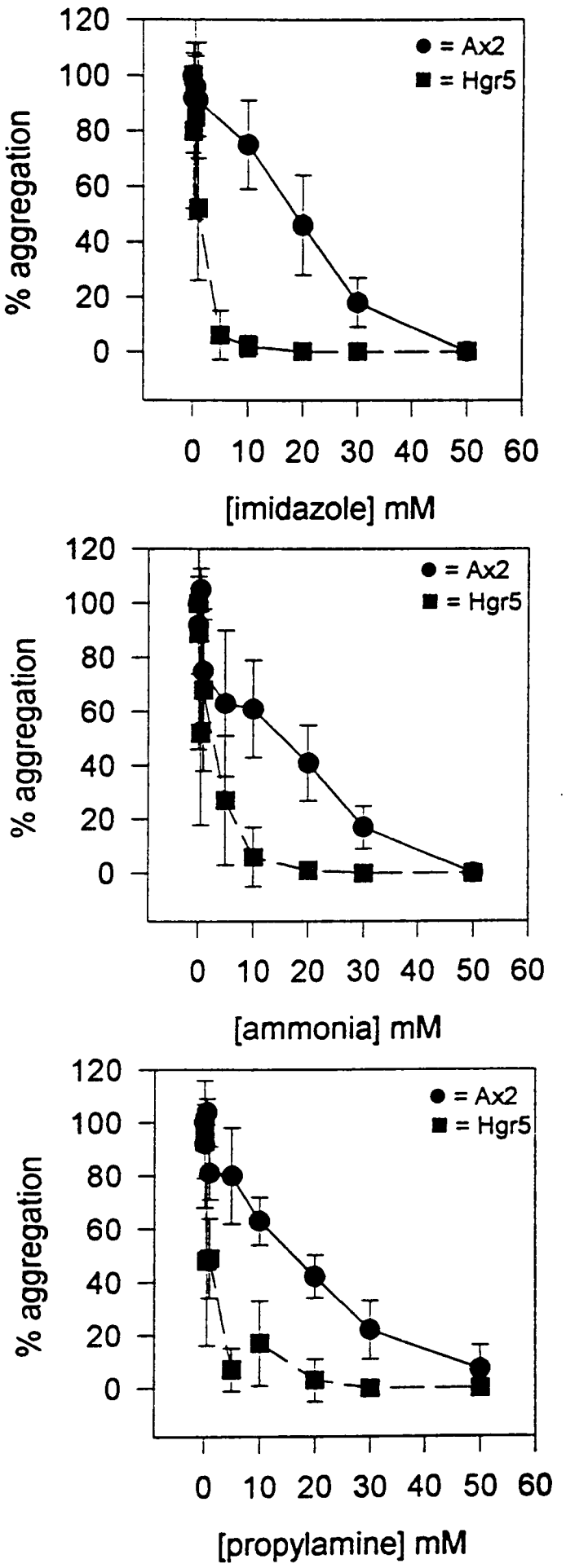
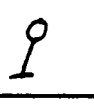
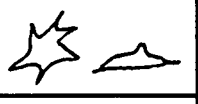
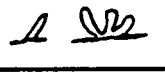
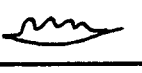
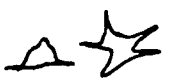
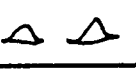
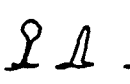
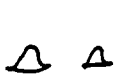
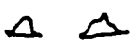


Figure 6.5: Quantitation of the hypersensitivity of Hgr5 to imidazole, ammonia and propylamine. Development was conducted at pH 7.3 in LPS or weak base solutions on filters.

	Ax2	Hgr1	Hgr4	Hgr5	Hgr8
Control					
IA 0.6mM					
IA 6.1mM				-	-
IA 15.3mM		-	-	-	-
IA 30.5mM	-	-	-	-	-

IA = imidazole (unprotonated base concentrations)

Figure 6.6: Developmental morphologies of the Ax2 and Hgr strains at 30h, showing the hypersensitivity of the Hgr strains to imidazole.

Chapter 7

Chapter 7 *Acidification-defective Strains Generated by Antisense Inhibition of the Vacuolar H⁺-ATPase B subunit*

7.1 Introduction

In chapter 6, it was shown that strains which are deficient in endocytosis and endosomal acidification display aberrant development. Their culmination is defective and their aggregation hypersensitive to inhibition by weak bases. In this chapter, antisense vacuolar H^+-ATPase constructs are described and their development compared to that of the Hgr strains and to weak base-treated wild-type. Since these mutants are created specifically by interfering with vacuolar H^+-ATPase expression, their phenotype can be ascribed specifically to this defect and not to any secondary mutation, as is possible in the case of the Hgr mutants. The vacuolar H^+-ATPase mutants described below were created by antisense inhibition of one of the H^+-ATPase subunits, as deletion/mutation of an H^+-ATPase gene was considered to be potentially lethal. A number of vacuolar H^+-ATPase mutants created by gene disruption have been reported in yeast (Anraku *et al.*, 1992) and their growth is severely inhibited. Similarly, the growth of the Hgr mutants was poor and development was seriously affected (chapter 6). Antisense inhibition was used to allow regulation of the level of vacuolar H^+-ATPase B subunit expression from a plasmid, providing the possibility of generating a range of phenotypes.

The structure of the vacuolar H^+-ATPase is described in chapter 1 (**figure 1.6**). In these experiments, the B subunit was the target for antisense inhibition, by expression of a partial cDNA of the B subunit of the vacuolar H^+-ATPase (kindly provided by Dr R. Dottin). It has been shown in yeast that inhibiting the expression of this subunit prevents the functioning of the ATPase (Ohya *et al.*, 1991; Yamashiro *et al.*, 1990), so it was considered to be a good target for antisense inhibition.

7.2 Results

7.2.1 Cloning the antisense fragment into the pVeII plasmid

A cDNA fragment ("dvac") of the B subunit of the vacuolar H^+-ATPase of *D.discoideum* was obtained from Dr R.Dottin (Hunter College, New York), consisting of 830 bp at the 3' end of the gene. The full-length cDNA has not been isolated, but is estimated to be roughly 1.5kb on the basis of comparison with that of *Arabidopsis thaliana*, with an estimated molecular weight of 57 kDa (R.Dottin, personal communication). The sequence of bases 1-450 at the 5' end of dvac and 1-243 at the 3' end was provided by Dr R. Dottin, whilst the remainder of the cDNA was sequenced by me by constructing primers based on the data provided. Its sequence is shown in **figure 7.1**, and shows roughly 75% homology at the nucleotide level to the B subunits of the vacuolar H^+-ATPases of *A.thaliana* and *Neurospora crassa*. In addition, the amino acid sequence is >90% homologous and >85% identical to the equivalent *N.crassa* sequence (R.Dottin, personal communication).

The dvac fragment had been inserted in the PstI site of the multiple cloning site of plasmid PTZ 18U (**figure 7.2a**). Sequencing around the insertion sites was carried out to confirm the identity and integrity of the sequence. At this stage, the cDNA was also used as a probe in a Southern blot of the genomic DNA of Ax2. **Figure 7.3a** shows that it hybridizes to a number of restriction fragments of roughly 7.1 and 10 kb, indicating that a genomic copy exists in this strain, and that the genomic fragment is probably bounded by the restriction sites PstI, EcoRI, XbaI and HindIII (**figure 7.3b**).

Since no suitable restriction sites were available for direct cloning of dvac in the antisense direction from PTZ 18U into the *discoidin I* promoter-containing vector pVeII, it was first cloned into the multiple cloning site of pBluescript (**figure 7.2b**). An asymmetrically-located BglII site was used to determine the orientation of the dvac in pBluescript by cutting with BglII/EcoRI. A

KpnI/BamHI fragment was then excised and placed in the antisense direction under the discoidin I promoter (**figure 7.2c**) in the plasmid pVeII (**figure 7.2d**), creating the plasmid "pdv". This plasmid was chosen for antisense expression as its discoidin I promoter is only induced at low levels in axenically growing cells, ensuring minimal expression of the potentially lethal antisense fragment during the growth phase. This promoter has been used frequently in *D.discoideum* to direct antisense expression (Crowley *et al.*, 1985; Liu *et al.*, 1992), having the advantage that expression is low during the growth phase and can in principle be regulated by folate (Blusch *et al.*, 1992), although added folate is quickly broken down by axenically growing cells (Berstein & Van Driel, 1980; Berstein *et al.*, 1981) and so must be frequently replenished in the medium.

A further plasmid was also constructed "pdv-gal"(**figure 7.2e**), bearing a fragment containing the *lacZ* reporter gene of pAct15-gal (**figure 7.2f**) which was inserted into the PvuII site of pdv by blunt end ligation. This plasmid was created to facilitate the isolation of transformants. Each of the plasmids pVeII, pdv and pdv-gal retains a neomycin (G418) resistance gene for the selection of transformants in axenic medium.

7.2.2 Developmental phenotype of the antisense strains

Plasmids pdv and pdv-gal were transformed into *D.discoideum* by calcium phosphate precipitation, with pVeII as a control transformant. Initially, transformants were selected by growing up individual transformant colonies in axenic culture at low (20µg/ml) concentrations of the selection agent G418. Colonies arising from single cells were then isolated by plating aliquots of cells in association with *K.aerogenes* on nutrient agar plates. The developmental morphologies of each set of transformants were then scored.

(a) pVeII transformants

The colonies showed normal developmental morphologies (**figure 7.4a**), with large well-proportioned fruiting bodies appearing within 24 hours of aggregate formation. Further transformation experiments yielded similar results, with an occasional mutant colony arising, presumably due to integration of the plasmid into a developmentally-important gene.

(b) pdv transformants

A number of developmentally-impaired colonies were observed which were arrested in the slug stage of development, even after 4 days (**figure 7.4b**). Variable degrees of slug migration occurred and a few culminants eventually formed on the agar plate, although such culminants tended to be short and squat (some non-aggregating colonies were also seen). Slugger-type colonies were subcultured once onto a bacterial lawn to confirm their developmental morphology and then amoebae were returned to axenic culture. It was not considered to be prudent to maintain transformant stocks on agar, as G418-resistant bacteria were unavailable at this stage, making it impossible to continue selection for the pdv plasmid. The pdv transformants isolated in this way grew extremely slowly on SM-agar in association with bacteria and if plated at very high density, were unable to aggregate. Observation of cells under the light microscope revealed highly variable cell sizes. Upon transfer to axenic medium, the growth rate was often slow (**section 7.2.2**).

(c) pdv-gal transformants

Since pdv transformants often proved to be difficult to grow, it was speculated that their plasmid copy number was high and that transformants bearing lower copy number produced borderline morphologies that were not detected in the selection process. To facilitate isolation of lower copy number transformants, the pdv-gal plasmid was used to transform Ax2. Colonies were generated on agar plates as before. However, nitrocellulose filters were then placed over the colonies to create a "negative" of the colony pattern which could be stained with

X-galactose (X-gal) to identify pdv-gal transformants (**figure 7.5**). On SM-agar plates, X-gal-positive colonies tended to slug for prolonged periods (**figure 7.4c**), although some normal culminants were observed within an aggregate field, indicating that there was heterogeneity in the level of antisense expression or that local conditions allowed the culmination of some aggregates. In general, the more deeply-stained aggregates (*eg.* pdv-gal 2, **figure 7.5**) displayed more severe abnormalities than the lightly stained aggregates (*eg.* pdv-gal 1 & 5), but still grew reasonably well (see next section). Therefore, pdv-gal2 was selected for further study.

7.2.3 Growth characteristics of the strains in axenic culture

Initially the strains were grown in 20µg/ml G418, in medium buffered at pH 6.0. In these conditions, the control strain pVeII grew well, at a rate only slightly lower than that of the parent strain Ax2 (**figure 7.6**). The growth rate of pdv was low at this pH, displaying a doubling time of 25-27 hours, with little growth beyond 1-2 x 10^6 cells/ml (**figure 7.6**). Increasing the G418 concentration to 40µg/ml completely prevented growth. At higher pH values, growth was completely inhibited and the majority of cells died after 24h in shaking culture (not shown). Addition of folate gave no improvement in growth.

The poor growth rate of this strain is surprising, since the discoidin promoter should be minimally expressed during growth. It is possible that this strain contains a high plasmid copy number and that even the low level of promoter activity during growth is sufficient to inhibit much of the vacuolar H^+-ATPase activity. The hypothesis that this transformant has a high copy number is supported by the fact that the developmental phenotype is severe and that raising the G418 concentration is lethal for growth. An alternative is that the phenotype observed is not due to antisense inhibition of vacuolar H^+-ATPase B subunit expression, rather that the genomic copy of the B subunit gene has been interrupted by homologous recombination with the dvac partial cDNA: a

possibility that could be tested by Southern blotting. The fact that the growth rate is improved upon lowering the pH is consistent with a vacuolar H^+-ATPase defect, as it has been reported that the growth rate of vacuolar H^+-ATPase-defective yeast cells is highly sensitive to pH (Ohya *et al.*, 1991; Anraku *et al.*, 1992). In addition, the growth rate of Hgr mutants is inhibited at pH values greater than 7 (chapter 6).

The growth rate of pdv-gal2 was intermediate between that of pVeII and pdv (**figure 7.6**). At 20µg/ml G418, no growth occurred above pH 6.5, but reducing the pH below the standard pH of 6.0 gave no improvement in the growth rate (not shown). Presumably, there is a limit to the extent to which the endosomal system can be artificially acidified. Increasing the G418 concentration did not affect the growth rate at pH 6.0 (not shown), but the developmental phenotype became more severe, with cells barely aggregating at 140µg/ml G418 (**figure 7.8**).

7.2.4 Western analysis of vacuolar H^+-ATPase expression

That the observed phenotypes of the pdv and pdv-gal strains could be ascribed to a reduction in vacuolar H^+-ATPase B subunit expression was demonstrated by Western immunoblotting of the B subunit in these and the control pVeII strain. For this purpose, a polyclonal antiserum against the B subunit of the vacuolar H^+-ATPase in *D.discoideum* was obtained from Prof.T.Steck (University of Chicago). This antibody has been shown to specifically label only the B subunit (57 kDa) in whole cell lysates and in microsomal fractions (T.Steck, personal communication).

B subunit expression in whole cell lysates of the pveII, pdv and pdv-gal2 strains is shown in **figure 7.7**. Equivalent total cellular protein concentrations were loaded in each lane. At 20µg/ml G418, a significant reduction (29.3% ± 6.9) was seen in the level of B subunit expression in pdv cells in comparison to pVeII (0% ± 9.6, **figure 7.7a**). A dose-dependent effect of G418 upon B subunit

expression could not be demonstrated as higher G418 concentrations proved lethal to the cells. In the case of pdv-gal, no reduction in B subunit expression could be seen when the cells were grown at 20µg/ml G418, therefore the G418 concentration for cell growth was slowly raised. **Figure 7.7b** shows the effect of growth in 140µg/ml and 200µg/ml G418 on B subunit expression. Here, a dose-dependent effect of G418 is clear. At 200µg/ml of the selective agent, the reduction in expression is marked (86.5% ± 2.1) and correlates with a severe phenotype in which the cells barely aggregate on SM-agar; whilst at 140µg/ml the percentage reduction in B subunit expression is 30% ± 2.1 and some aggregation and first finger formation occurs (**figure 7.8**).

7.2.5 Development at various pH values

In addition to displaying a growth sensitivity to pH, the development of the antisense cells was also shown to be pH-sensitive. **Figure 7.9** illustrates the effect of developing antisense and pVeII cells on filters in LPS at pH 5.0, 6.0 and 7.0. The pVeII cells culminate at all of the pH values tested, whereas development of the mutants is blocked completely at pH 7.0. At lower pH values, both pdv (20µg/ml G418) and pdv-gal (140µg/ml G418) are able to aggregate, but their culmination is impaired.

7.2.6 Sensitivity of aggregation to weak bases

As is the case with the Hgr strains (chapter 6), the antisense strains are hypersensitive to inhibition of aggregation by weak base. Aggregation of pVeII, pdv-gal and pdv in response to imidazole was compared (**figure 7.10**). Each of the antisense strains is hypersensitive to the effect of imidazole, with no significant difference between the strains.

7.2.7 Slugging in the antisense strains

Placing cells on water-agar with a unidirectional light source provides the most favourable conditions for slug migration. Under these conditions, it was found that whilst pdv and pdv-gal stayed as stationary slugs for the whole course of

the experiments (2-3 days) and pVeII slugs culminated in 30h, the greatest extent of slug migration occurred with the control strain pVeII. Slugs of pdv and pdv-gal were impaired in migration and were deficient in phototaxis (**figure 7.11**).

7.2.8 Measurement of intracellular pH in the antisense strains by NMR

As in chapter 5, both the pVeII strains and the antisense strains were labelled with the endosomal probe Cl_2MDP for observation of the pH of the endosomal system. This probe is taken up by endocytosis into the endosomal system and is a sensitive indicator of vesicular pH. In pVeII, the probe enters the cell as in the parent strain Ax2 (**figure 7.12a**: compare chapter 5, **figure 5.9**), giving a peak at pH 4.5 which corresponds to the early endosomal compartment.

In contrast, in the mutant strain pdv-gal (40µg/ml G418), the peak at pH 4.5 is very small and broad, due to the presence of a number of overlapping peaks at pH 4.5 - 5.5 (**figure 7.12b**). This spectrum shows that in these cells, the vesicle population on average has an increased pH. Also, very little probe enters the cells, indicating that they are endocytosis-deficient. This is consistent with a reduction in endosomal acidification, since Hgr5 cells (which have increased endosomal pH), do not take up phosphonate probes. Therefore, in pdv-gal cells endocytosis (and probably endosomal acidification) is perturbed even at 40µg/ml. Endosomal acidification in cells grown at higher G418 concentrations was not measured as it proved impossible to grow sufficient numbers of such cells for the NMR experiment. A similar problem was encountered with the pdv cells.

7.3 Discussion

Antisense inhibition of the B subunit of vacuolar H^+-ATPase was used as a tool to produce constructs that were specifically defective in endosomal acidification. It was hoped that use of the discoidin promoter to direct expression of the antisense cDNA would allow growth to proceed unhindered until the late log phase and that expression of the vacuolar H^+-ATPase B subunit would be affected only during development. This would have allowed study of the effect of lowered endosomal pH on development whilst enabling cells to be grown easily, since the Hgr mutants had proven to be difficult to culture. However, the results above demonstrate that the antisense cells are also defective in growth, to differing degrees, indicating that even the minimal level of expression that occurs with the discoidin promoter during axenic growth (Blusch *et al.*, 1992) is sufficient to produce a phenotype. Little noticeable improvement in the growth rate was observed upon addition of folate (not shown), the most likely explanation being that folate is rapidly broken down in the medium as *D.discoideum* cells secrete folate deaminase (Bernstein & Van Driel, 1980; Bernstein *et al.*, 1981) which is reported to metabolise 30% of extracellular folate in about 3 minutes (De Wit *et al.*, 1986). The promoter is reported to be less active during the growth phase when cells are grown in association with bacteria, but G418-resistant bacteria were not available for use.

The pdv strain reached a plateau at very low density, probably as a result of a high copy number of the antisense plasmid, since the Western blots show a 30% reduction in the level of B subunit expression even at 20µg/ml G418. At this level of G418 selection, no reduction could be seen B subunit expression levels in the pdv-gal cells. The growth defect in the pdv-gal strain was less severe, even at the highest G418 concentration tested (**figure 7.6**). It is conceivable that regulation of the discoidin promoter could be different in these cells, perhaps as a result of the size of the pdv-gal plasmid. Alternatively, the differences in their growth rates could simply be due to variation in the

plasmid copy nubers. A semi-quantitative measure of the copy number in each strain could be obtained by Southern blots of this strain, which would also help to confirm that the defects in these strains are due to antisense inhibition rather than to mutations resulting from insertional events. However it should be emphasized that the step-wise reduction in B subunit expression seen on the Western blots in the case of pdv-gal (**figure 7.7**) upon raising the G418 concentration strongly supports the notion that the defects of this strain are due to inhibition by antisense.

It seemed *a priori* likely that the reduction in the level of B subunit expression seen in growth phase cells would not be maintained in later development since the discoidin promoter is inactive after aggregation and this might have allowed recovery of vacuolar H^+-ATPase B subunit expression. The developmental defects observed in the antisense constructs indicate that this was not the case. Northern blots would be required to determine mRNA levels in developing cells and immunoblotting of such cells could determine whether protein levels remained low. The half-life of the antisense message and the extent of vacuolar H^+-ATPase turnover are unknown. In bacteria, mRNA stability is known to be influenced by the length of the message, with faster decay if terminal stem-loop structures are absent (Belasco & Higgins, 1988) but the nature of mRNA regulation in eukaryotes is unclear. Since little cell division occurs after the initiation of development, the antisense message is probably not "diluted out" by cell division. It is highly unlikely that the developmental effects seen in these experiments are due to a non-specific event resulting from cell transformation (for example, random mutation in the genomic DNA or cell stress due to enforced plasmid expression) since the phenotypes of a number of pdv and pdv-gal transformants were similar. The phenotypes cannot be ascribed either to a G418 effect, as the control pVeII transformants show no growth or developmental defects even at 200µg/ml G418.

The NMR experiments demonstrate that inhibiting the vacuolar H^+-ATPase perturbs endosomal acidification and mimicks the endocytosis-deficient phenotype of the Hgr mutants. However, in this situation the antisense cells also show signs of stress, possibly as a result of incubation at high cell concentrations (above 10^8 cells/ml) a condition in which the discoidin promoter is maximally expressed.

The developmental defects displayed by the antisense strains are consistent with a defect in vacuolar acidification. Similar pH-sensitive growth defects are seen in yeast cells carrying mutations in endosomal acidification (Nelson & Nelson, 1990; Umemoto *et al.*, 1991). The development of the *D.discoideum* antisense constructs is pH-sensitive and they are hypersensitive to the inhibition of aggregation by weak bases, as were the Hgr strains studied in chapter 6. The phenotypes at the lower G418 concentrations used, resembled the slugger mutants (Gee *et al.*, 1994; Newell & Ross, 1982) in that they exhibited prolonged slugging phases with arrest in the slug phase, or abnormal culmination. Since slugging is promoted by ammonia (Schindler & Sussman, 1977; Inouye, 1988; Kosugi & Inouye, 1989) it is likely that the arrest of the antisense mutants in the slug phase is due to their hypersensitivity to endogenously-produced ammonia. Possible ways in which changes in the pH of acidic vesicles could affect the enzymes involved in the control of aggregation and culmination will be discussed in chapter 8.

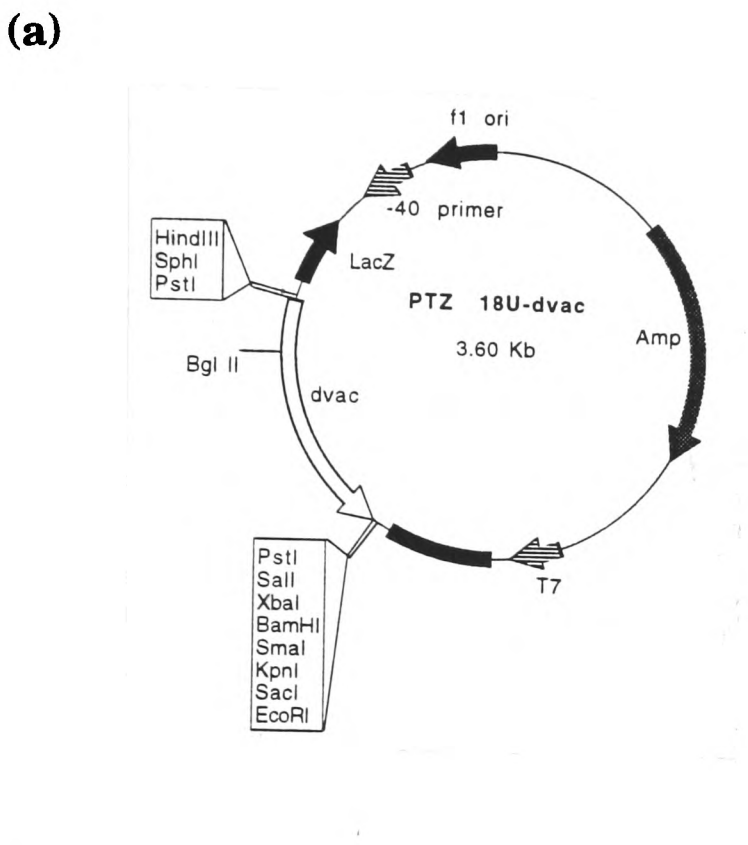
7.4 Conclusion

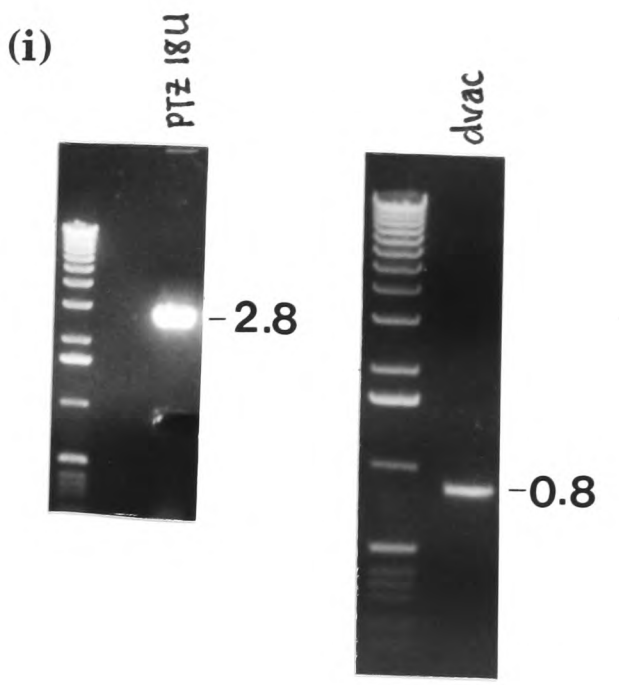
This study demonstrates that aberrant development can be induced simply by inhibition of vacuolar H^+-ATPase activity. The resultant cells are phenotypically similar to slugger mutants (Newell & Ross, 1982; Gee *et al.*, 1994) and to the Hgr mutants. Since the antisense, Hgr and some of the slugger mutants are hypersensitive to the effects of ammonia on aggregation, this supports the theory that the effects of ammonia at this stage are mediated

through neutralization of an acidic compartment. Since culmination is also affected in antisense cells and culmination can be inhibited by ammonia, the inhibition of culmination by ammonia is almost certainly mediated in the same way.

1 **TGTTAATATG GAAACTGCAT CATTTTTCAA ACGTGATTTC**
41 **GAAGAATCAG GTTCTATGGA TAGAACTGCT CTCTTCCTTA**
81 **ATTTAGCAGA TCATCCAACC ATCGAACGTA TTATTACTCC**
121 **ACGTCTTGCA TTGACCACCG CCGAATATCT TGCATATCAA**
161 **TGTGAAAAAC ACGTTTTAGT TCTTTTAACC GATATGTCTT**
201 **CATATGCTGA TGCTCTTCGT GAGGTATCTG CTGCTCGTGA**
241 **AGAAGTACCA GGTCGTCGTC GTTATCCAGG TTATATGTAT**
281 **ACAGATCTTT CAACCATTTA CGAACGTGCT GGTCGTATTC**
321 **AAGGTCGTAA TGGTTCTATC ACTCAAATTC CAATTTTGAC**
361 **TATGCCAAAT GATGATATTA CCCATCCAAT TCCAGATTTA**
401 **ACTGGTTACA TTACTGAGTC AAATTTTACT TGGATCGTCA**
441 **AATCAATAAC AAGCAGATCT ACCCACCAAT CAATGTATTA**
481 **CCATCACTTT CTCGTCTTAT GAAATCCGCC ATTGGTGACA**
521 **ACATGACCCG TGGCGATCAC TCTGAAGTCT CAAATCAAAT**
561 **GTATGCCACC TATGCCATCG GGAAAGATGC CACTGTCATG**
601 **AAAGCTGTCG TTGGTGAGGA AGCACTTTCT TCTGAAGATA**
641 **AACTCTACTT AGAATTTTTA GAACGTTTCG AATCATGCTT**
681 **TGTCGGTCAA AACCATTATG AAAATCGTGA TATCTTTAAT**
721 **TCATTGGATC TTGGTTGGTC TTTATTAAGA ACTTTCCCAA**
761 **GCAATCTCCT CAAACGTATC ACTGAAAAAA CTATTAAACA**
801 **ATACTATTCA GCTTCATCAA AGGGTACT**

Figure 7.1: Sequence of the 3' cDNA fragment of the B subunit of the vacuolar H^+-ATPase gene (cDNA provided by Dr R. Dottin, 75% sequenced).





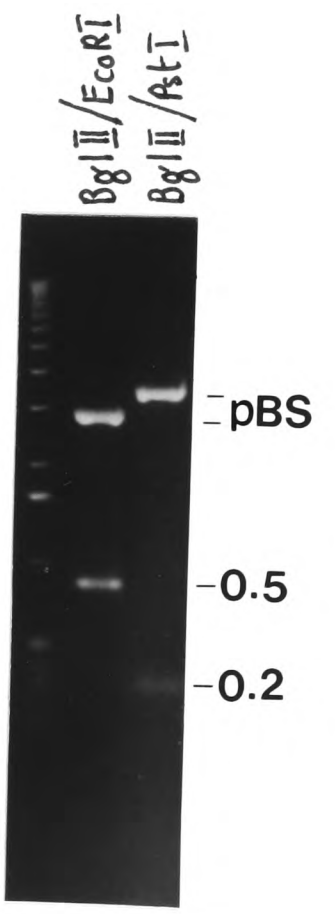
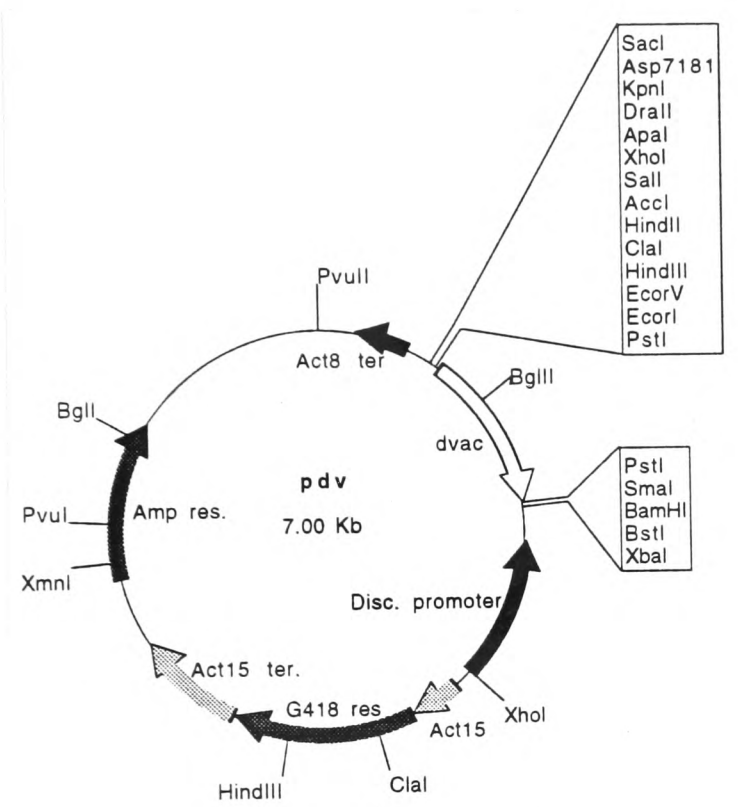
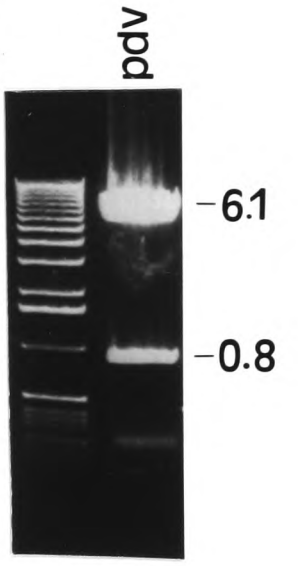


Figure 7.2: **(a)** plasmid PTZ-18U containing the dvac cDNA fragment in a multiple cloning site. **(b)** plasmid Bluescript SK$^-$ with the dvac fragment cloned into the MCS. **(i)** gel showing plasmid PTZ 18U (roughly 2.8kb) with the excised dvac fragment alongside (roughly 0.8kb). **(ii)** insertion of dvac into pBluescript: cuts with BglII/PstI (0.2kb fragment generated) and BglII/EcoRI (0.5kb fragment) show that the dvac is in the antisense orientation.

(c)



(iii)



(d)

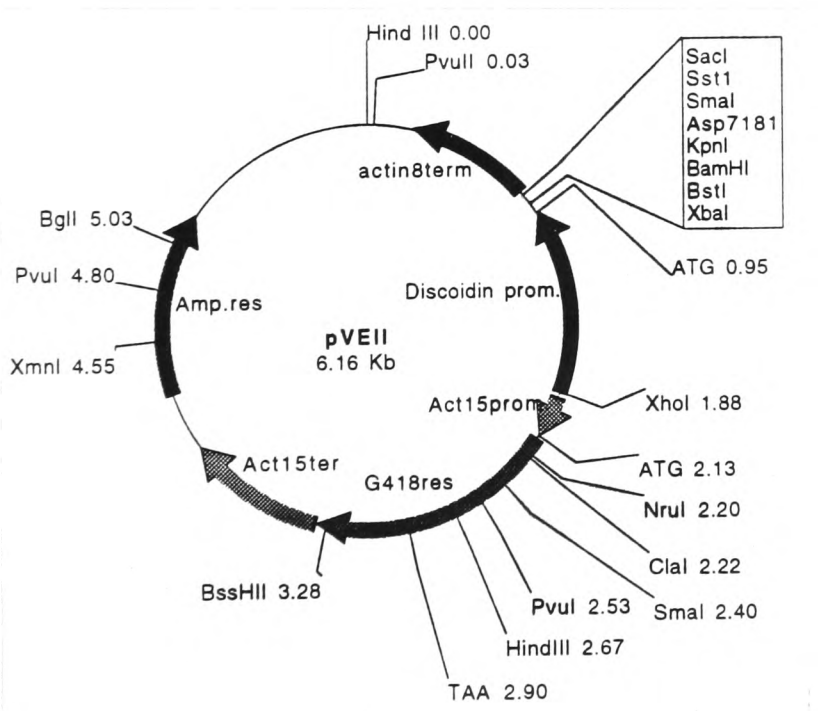
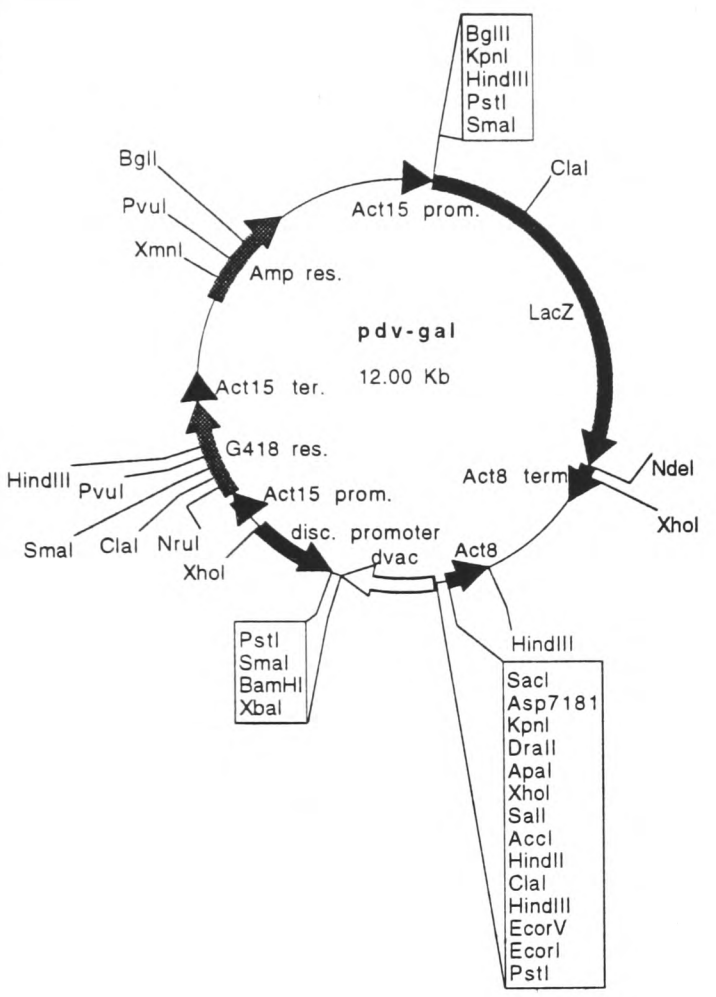
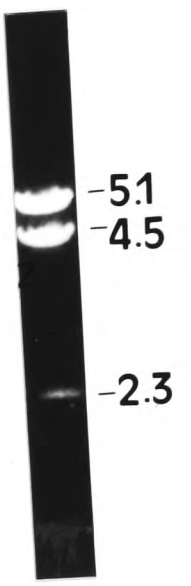


Figure 7.2 (continued): **(c)** plasmid pdv, which when cut with KpnI/BamHI **(iii)** generates the dvac fragment (0.8kb) and a fragment of roughly 7kb corresponding to the pVeII plasmid **(d)**.

(e)



(iv)



(f)

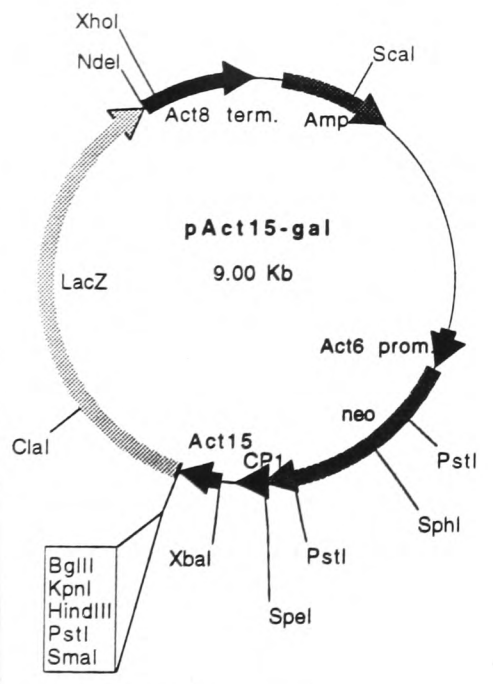
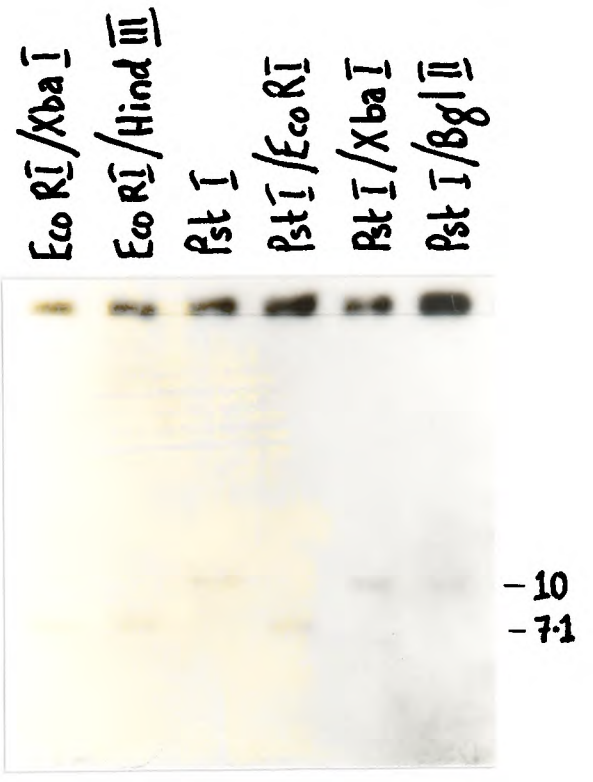


Figure 7.2 (continued): **(e)** plasmid pdv-gal, created by inserting the XbaI/ScaI fragment (*lacZ*) from pAct15-gal **(f)** into pdv **(c)**. Cutting pdv-gal with ClaI generates three fragments (5.1, 4.5 and 2.3 kb) confirming its identity **(iv)**.

(a)



(b)

Restriction fragment	Approximate fragment length
EcoRI/XbaI	7.1 kb
EcoRI/HindIII	7.2 kb
PstI	10.0 kb
PstI/EcoRI	7.1 kb
PstI/XbaI	10.0 kb
PstI/BglII	10.0 kb

Figure 7.3: **(a)** Southern blot using the dvac cDNA as a probe picks up a number of fragments of 7.1/10kb, the lengths of which are noted in **(b)**

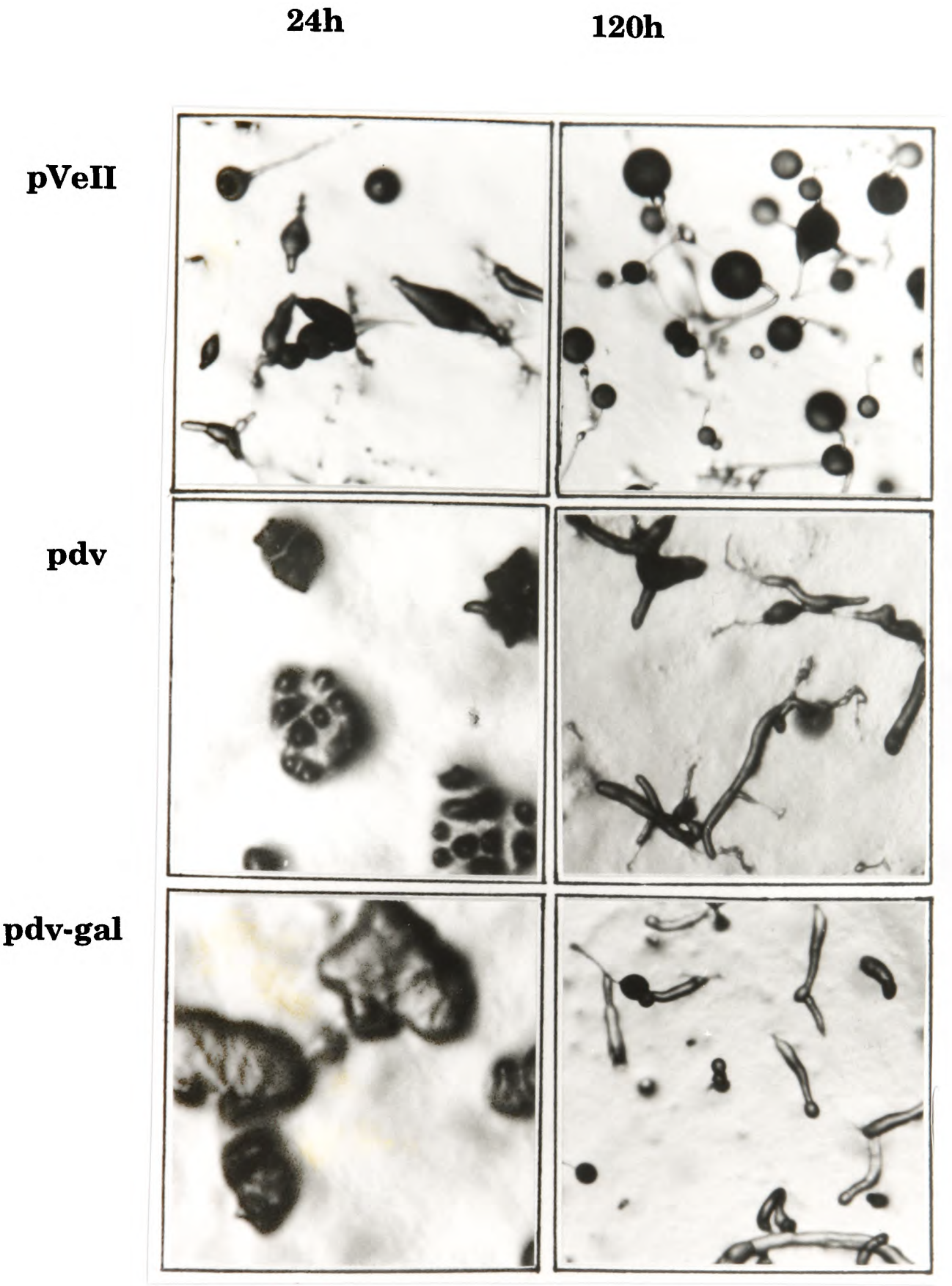


Figure 7.4: **(a)** pVeII-transformed (control) cells, **(b)** pdv-transformed cells and **(c)** pdv-gal -transformed cells. All grown at 20µg/ml G418 in axenic mediuma and then grown in association with bacteria on SM-agar plates (pH 7.0).

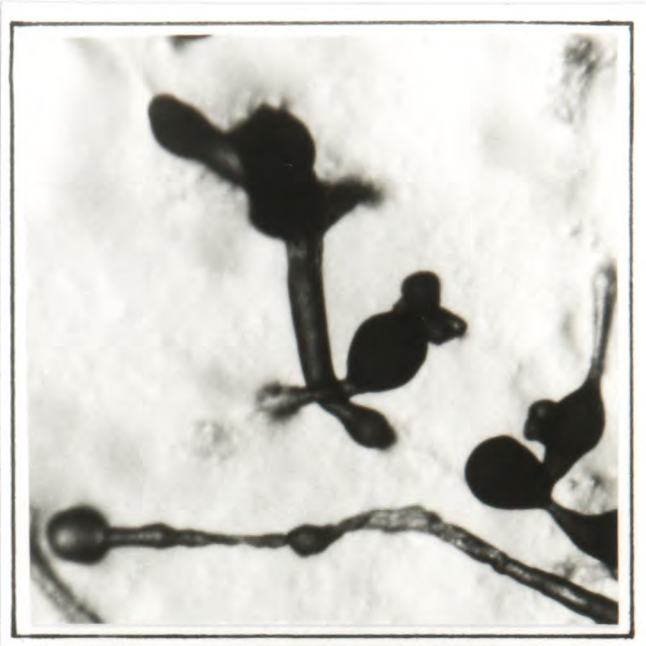
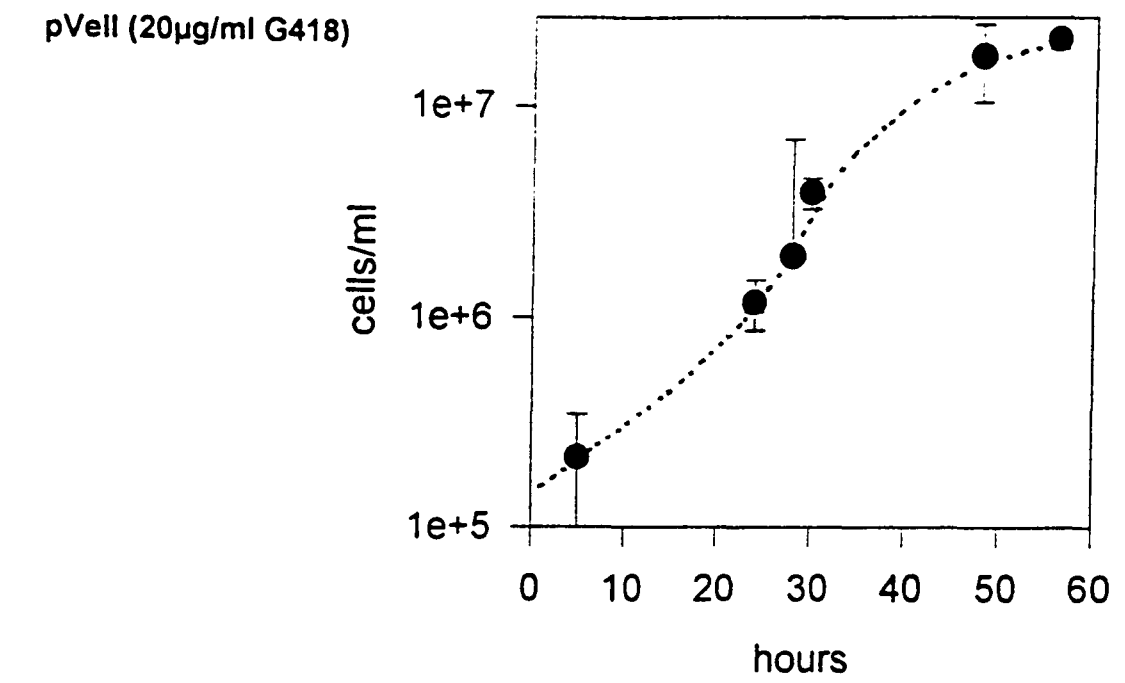
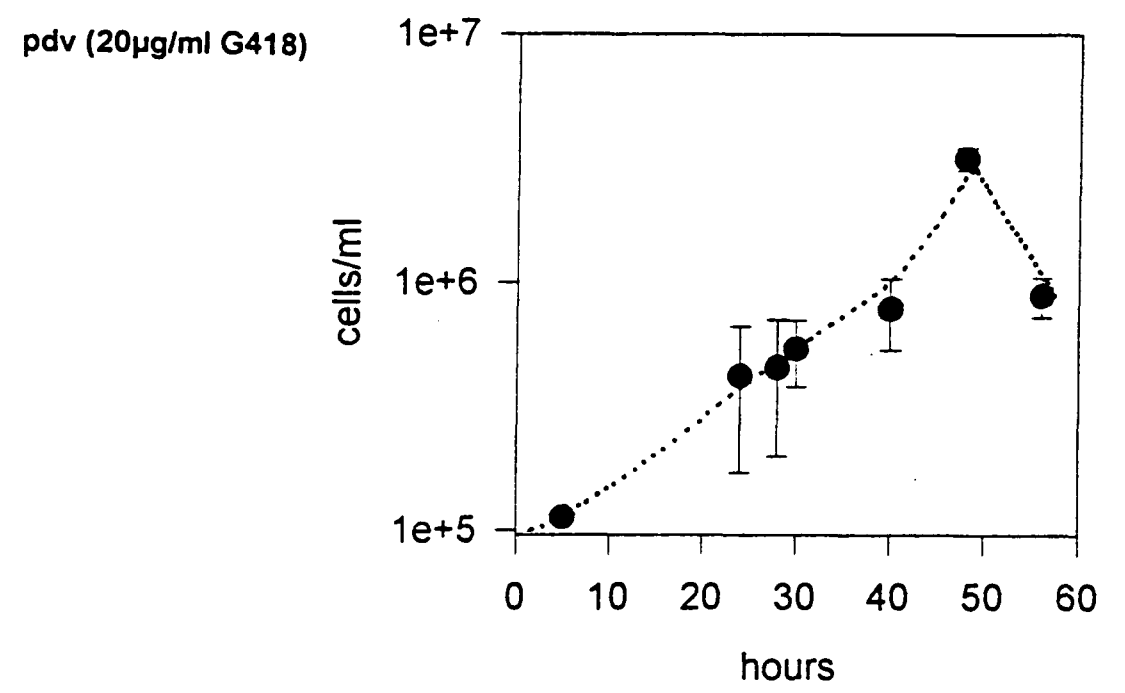
	X-gal staining	developmental morphology
pdv-gal 2		
pdv-gal 5		

Figure 7.5: Correlation of the severity of developmental defect with the level of antisense plasmid. X-gal staining levels give a relative measure of plasmid levels in each of the strains pdv-gal 2 and pdv-gal 5





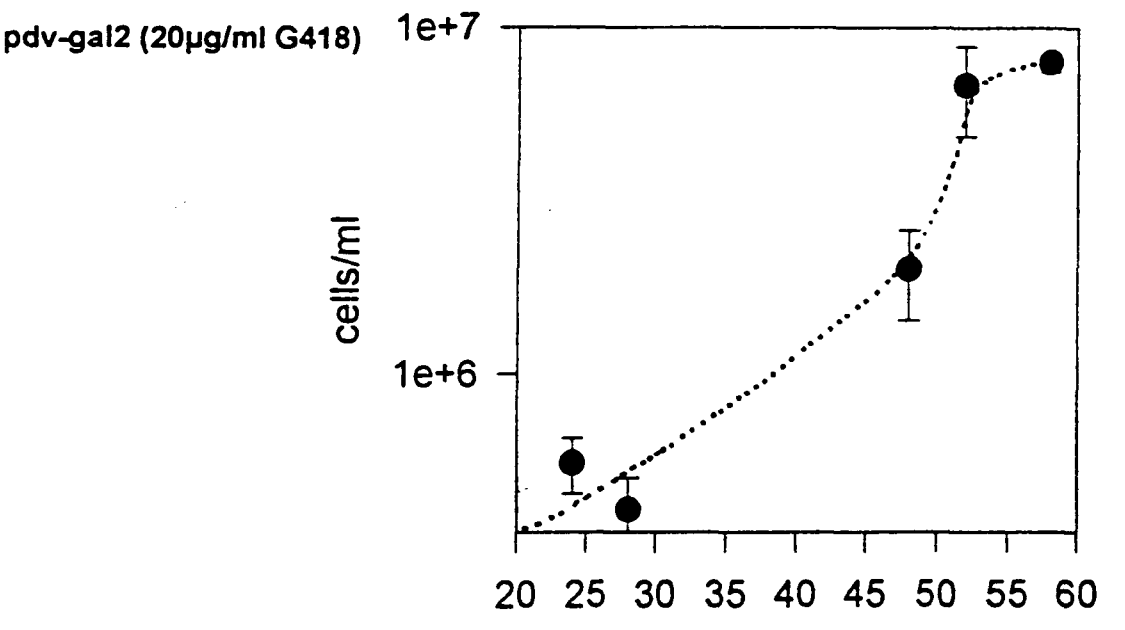
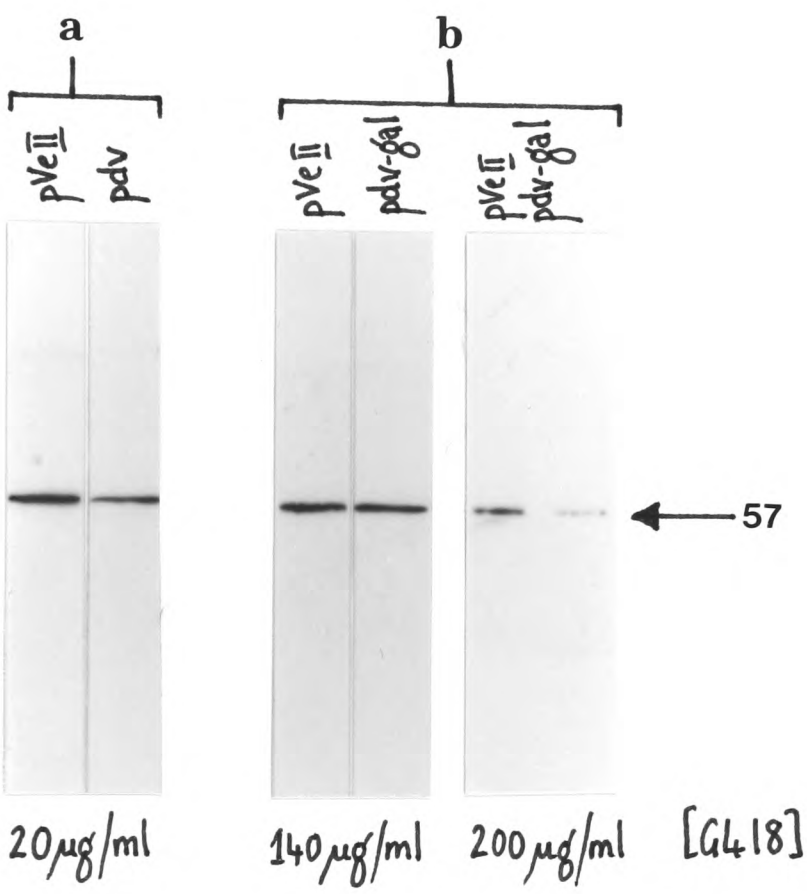


Figure 7.6: Growth rates of the antisense strains and the control transformant pVeII in axenic medium at pH 6.0. All growth media contained 20µg/ml G418.



Transformant	[G418] µg/ml	% reduction in B subunit expression
pdv	20	29.3 ± 6.9
pdv-gal2	140	30.0 ± 2.1
pdv-gal2	200	86.5 ± 2.1

Figure 7.7: Immunoblotting of 57kDa B subunit in the antisense strains pdv and pdv-gal2. Pdv-gal2 shows a significant decrease in B subunit expression upon increasing selection for the plasmid (probed with antibody provided by Prof.T.Steck). The control transformant shows a 9.6% variation by image densitometry of the Westerns, therefore all the above reductions are significant.

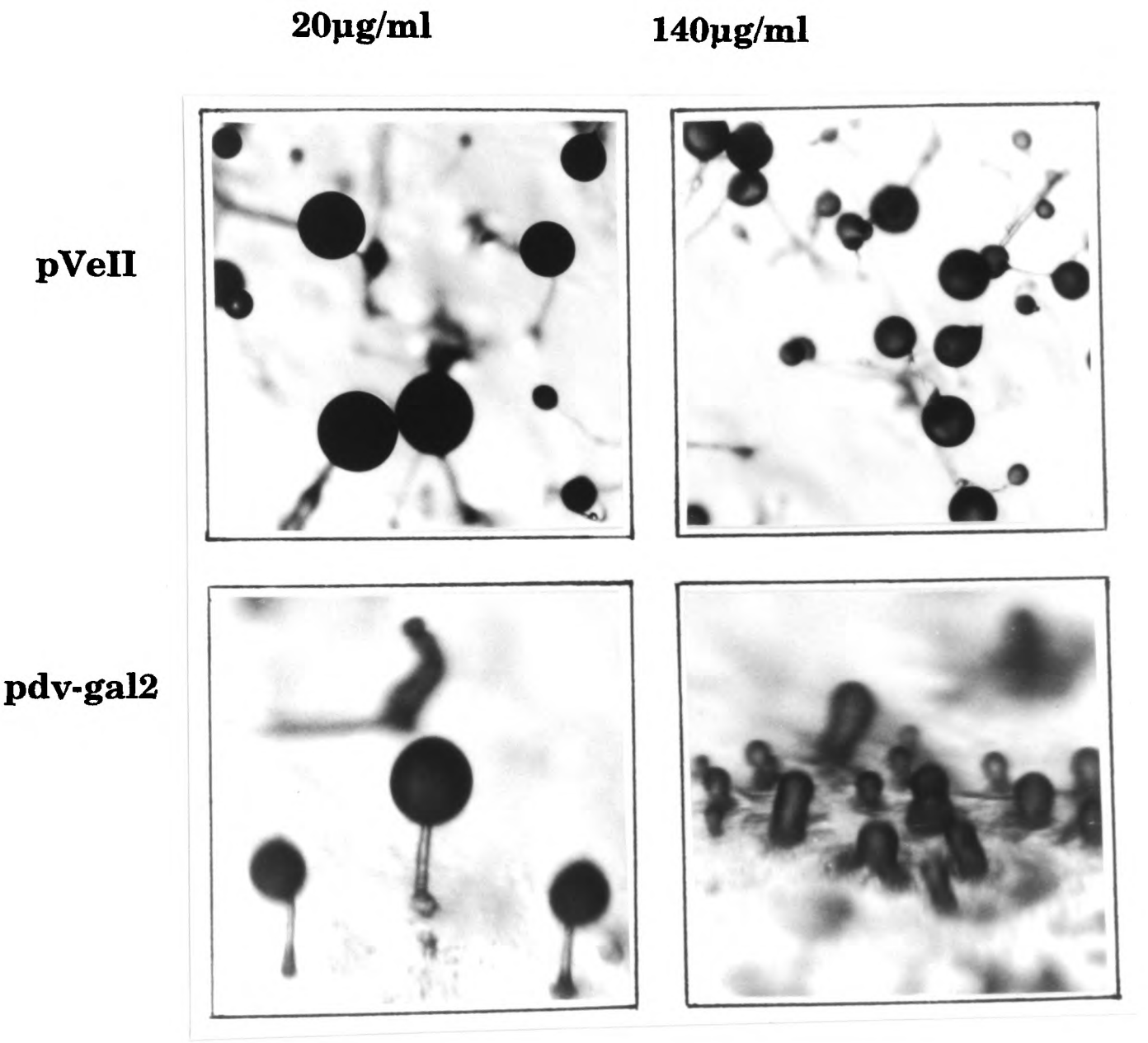


Figure 7.8: Developmental morphology of pVeII (control) and pdv-gal2 at low (20µg/ml) and high (140µg/ml) G418 concentrations. Development is conducted on SM agar.

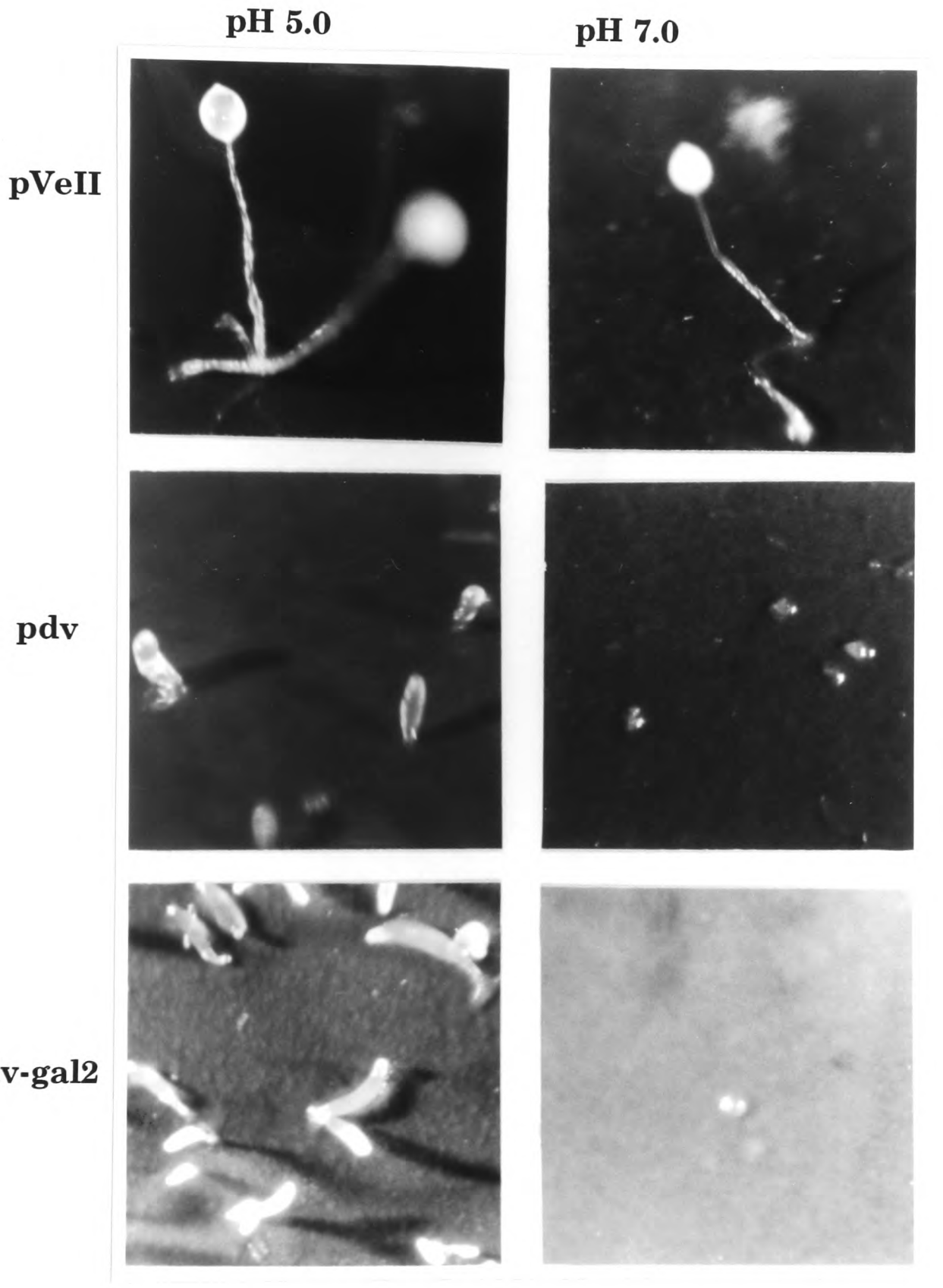
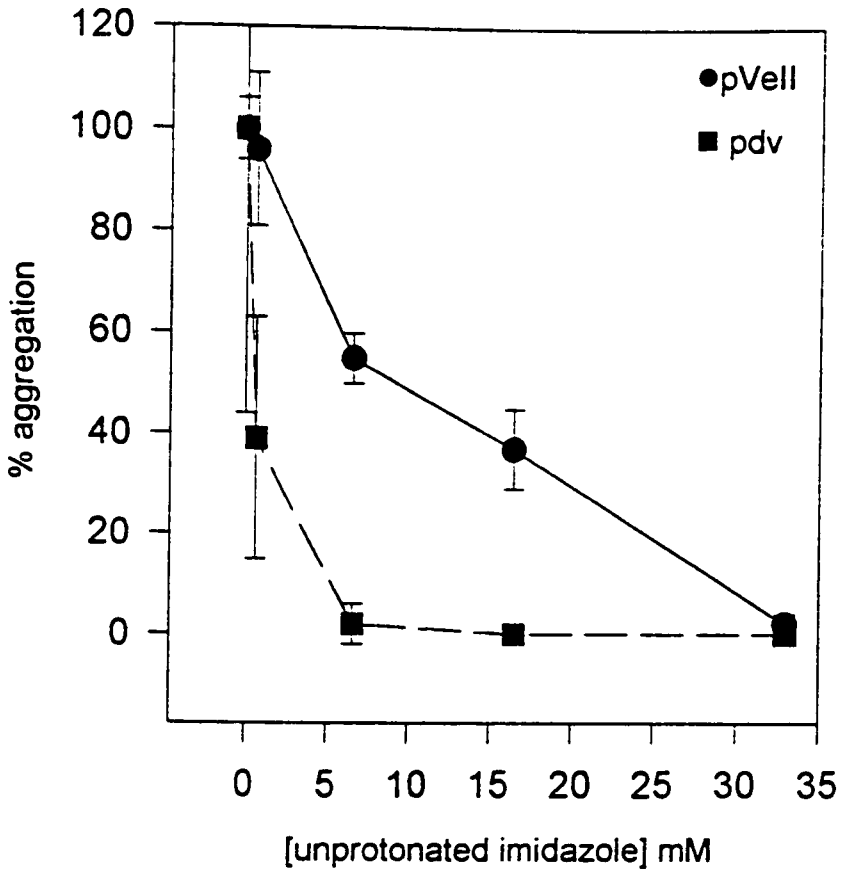


Figure 7.9: pH dependence of development in the antisense strains. pVeII and pdv-gal2 are grown at 140µg/ml G418 and pdv at 20µg/ml G418. Development is conducted on filters with LPS.

(A)



(B)

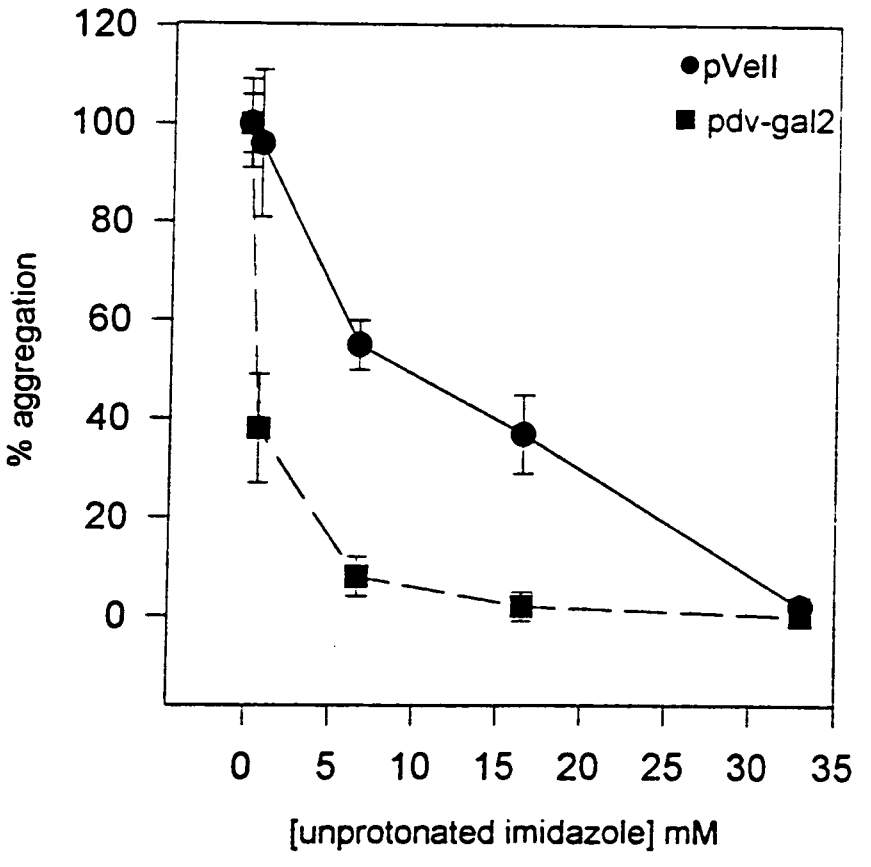


Figure 7.10: Hypersensitivity of the antisense strains to inhibition of aggregation by imidazole. **(A)** pVeII and pdv grown at 20µg/ml G418 **(B)** pVeII and pdv-gal2 grown at 140µg/ml G418. Cells were plated on filters at 5 x 10^6cells/cm^2 and developed at pH 7.0 with imidazole.

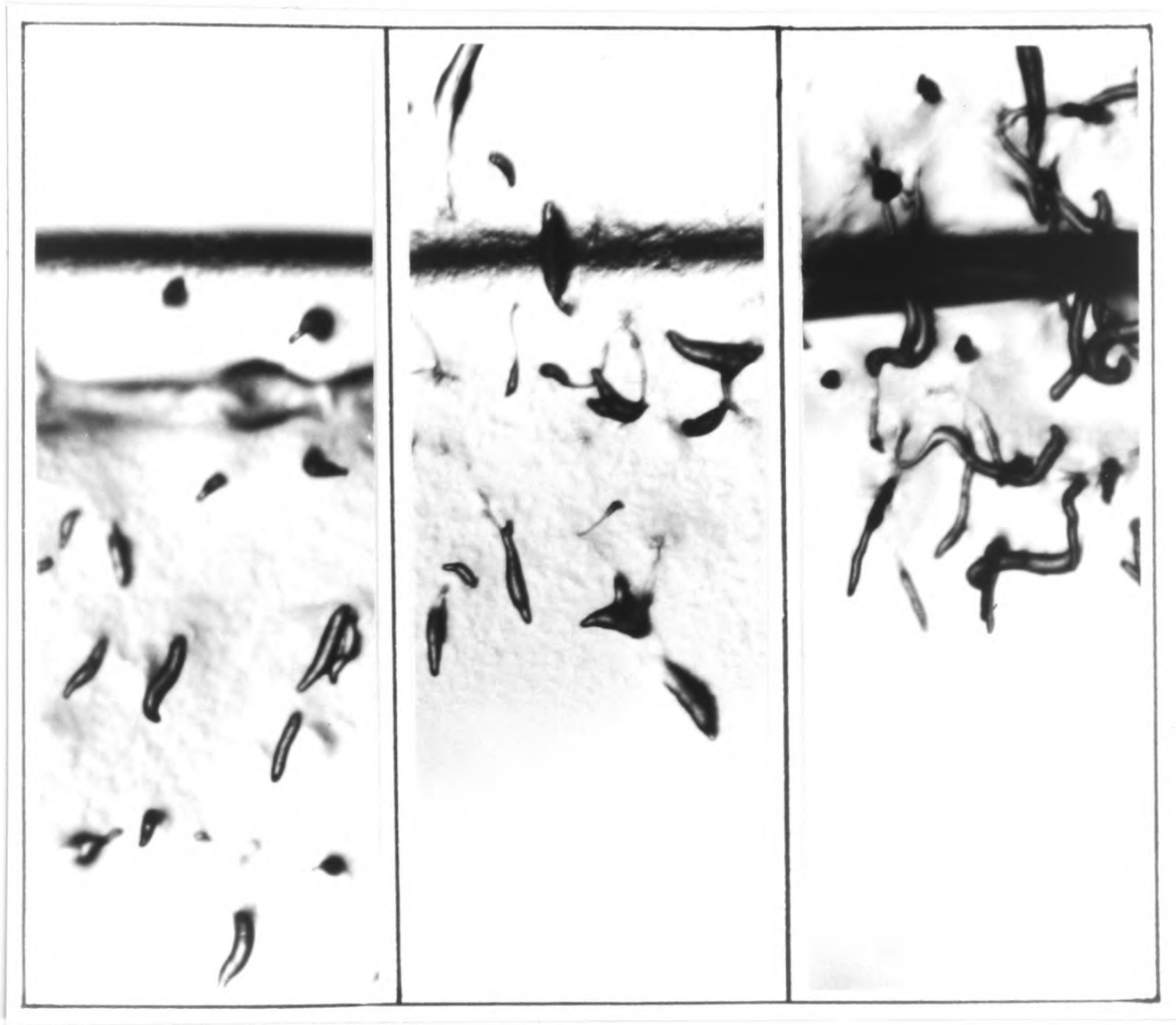


Figure 7.11: Slugging behaviour in the antisense strains. Cells were placed in a thick (10^8 cells/ml) band on water agar and left in a humid chamber with a unidirectional light source (marked). Photographs are taken at 36h.

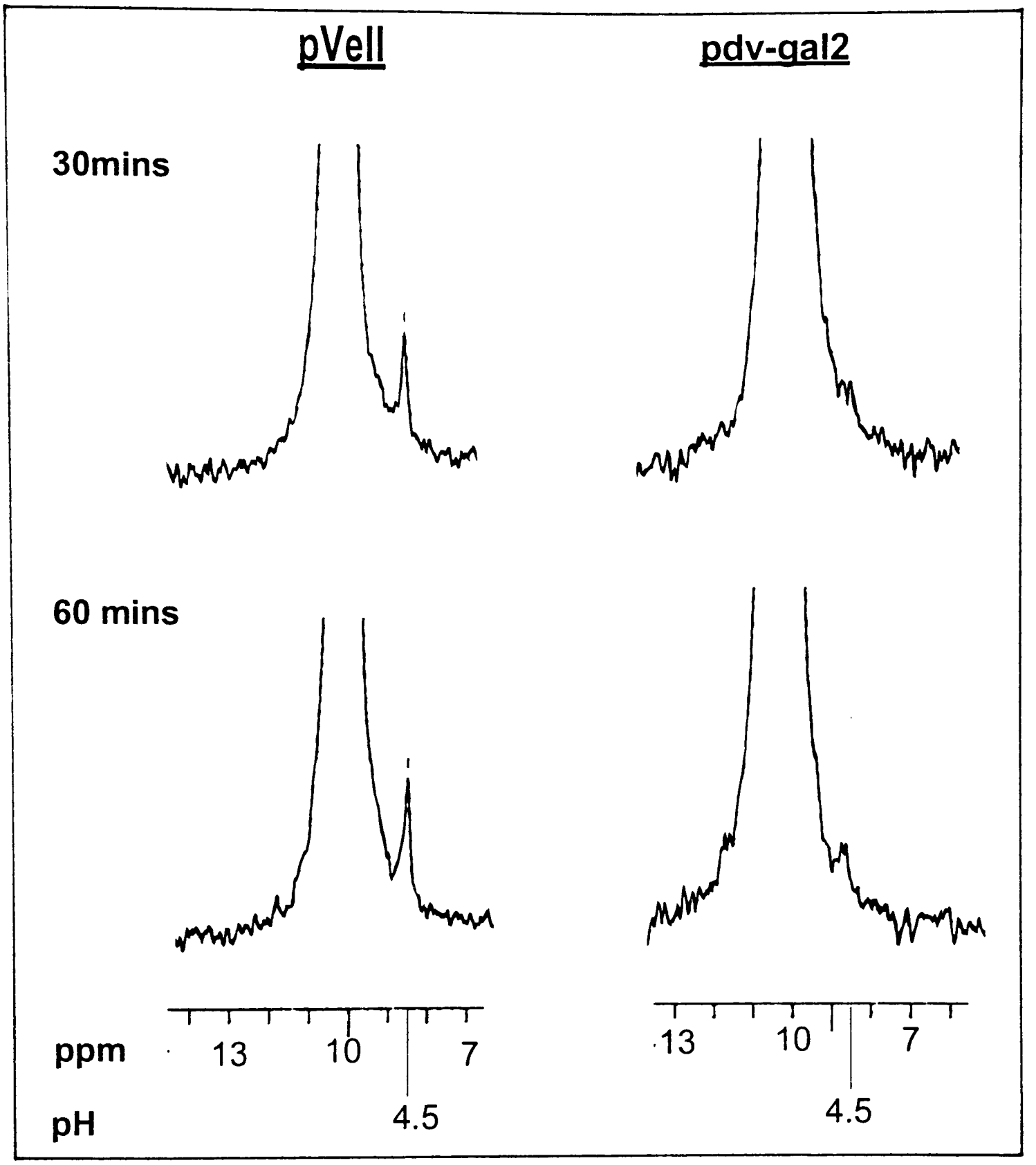


Figure 7.12: Uptake of the endosomal probe Cl_2MDP into pVeII cells **(a)** and pdv-gal2 cells **(b)** (both grown at 40µg/ml G418). The compartment at pH 4.5 is the highly acidic early endosomal compartment.

Chapter 8

Chapter 8 *Conclusion*

The aim of this thesis was to investigate the inhibitory effect of ammonia on development in *D.discoideum*, concentrating on the possible role of intracellular acidic compartments in mediating inhibition. A combination of cell biological, physical and genetic techniques were used to approach this question.

8.1 Summary

8.1.1 Effects of weak bases on aggregation and culmination

Chapter 3 shows that at least two processes in development (aggregation and culmination) are inhibited by all the weak bases tested, demonstrating that the effect of ammonia *in vivo* is due to its weak base activity as it can be mimicked by a range of chemically dissimilar weak bases. This extends previous work indicating that it is the unprotonated moiety (NH_3) of ammonia that is the active species in inhibition of aggregation and culmination. Lowering the pH of externally-added ammonium salts (hence decreasing the NH_3:NH_4^+), reduced the efficiency of inhibition by the base (Schindler & Sussman, 1977; Sternfeld & David, 1979; Gross *et al.*, 1983; Neave *et al.*, 1983; Riley & Barclay, 1990), showing clearly that the unprotonated form of the weak base is the active agent. These workers speculated that ammonia must either exert its effect intracellularly or that some extracellular receptor or enzyme is specifically inhibited by the unprotonated form. No evidence has been presented to show that the unprotonated form is a direct inhibitor of any intracellular or extracellular enzyme; neither are the inhibitory effects ascribable to an inhibition of chemotaxis. The remaining option was that ammonia might act as a weak base to raise cytoplasmic pH (Gross *et al.*, 1983) or the pH of acidic compartments (Gross *et al.*, 1988). Equal concentrations of the unprotonated form of weak bases (having similar pK_a values) would have the same effect on the cytoplasmic pH, since they are all highly membrane-permeable. However, their effect on acidic compartments was expected to vary according to their

protonophoric ability (Poole & Ohkuma, 1981; Krogstad *et al.*, 1985; Nissani & Ginsburg, 1989). It was found that the most effective bases in inhibiting aggregation and culmination were those that were the most hydrophobic and therefore the better protonophores (chapter 3), indicating that the primary target in inhibition of development was an intracellular acidic compartment.

8.1.2 Intracellular pH in response to weak base challenge

Direct testing of the protonophoric capacity of weak bases was achieved by measuring inhibition of acidification by these bases in isolated acidic vesicles. Again, inhibition of vacuolar H^+-ATPase-generated vesicular acidification correlated strongly with the calculated protonophoric activity of the bases. Protonophoric activity was shown to be dependent upon the hydrophobicity, conformation and size of the base.

Further to this, non-invasive *in vivo* determinations of intracompartmental pH were made in whole cells in the presence of weak bases by ^{31}P-NMR. Concentrations of bases that were effective in inhibiting aggregation and culmination raised the pH of intracellular acidic compartments without raising cytosolic pH within the time resolution of the NMR technique. Even if the bases did raise cytosolic pH transiently upon addition to the extracellular medium, this would not be sufficient to explain their developmental effects, since these are elicited over a period of hours and require continuous exposure of the aggregates to the base. In addition, these experiments showed that prolonged exposure to bases does not affect the general health of cells.

8.1.3 Genetic confirmation of the role of vesicles in development

Finally, vacuolar acidification-defective cell strains (Hgr and antisense constructs) were examined, as they were expected to resemble weak base-treated wild type strains morphologically. Both the chemically-mutagenized Hgr strains and the antisense vacuolar H^+-ATPase strains resembled weak base-treated wild type cells in that they were arrested in the slug stage of

development or made stunted culminants with large irregular spore heads. Moreover, the acidification-defective strains were hypersensitive to inhibition of aggregation by weak bases. Therefore, raising the pH of intracellular acidic compartments is sufficient to reproduce the developmental effects of excess weak base. Taken together, these results show that raising the pH of an acidic compartment is the primary effect of weak bases and the effects of endogenously-produced ammonia on aggregation and culmination are likely to be mediated via this compartment.

8.2 Implications for the signal transduction pathway of ammonia in vivo

8.2.1 Properties of intracellular acidic vesicles

Acidic intracellular compartments in both plants and animals are involved in a variety of regulatory processes. Vesicles serve as storage sites for amino acids, ions (*eg.* Ca^{2+}, Na^{+}, K^{+} and phosphate) and carbohydrates. An additional rôle is that of protein sorting (Yamashiro & Maxfield, 1988; Klionsky *et al.*, 1992; Stevens, 1992). Inhibition of vesicular acidification by weak bases could therefore affect many aspects of cell behaviour.

It has been reported that ammonia and chloroquine interfere with lysosomal enzyme processing (Cardelli *et al.*, 1989). The expression of cell surface markers and secreted proteins could also be affected since these are processed through acidic compartments for targetting to the cell surface. For example in yeast, disruption of vacuolar acidification leads to missorting of carboxypeptidase Y (Klionsky *et al.*, 1992). If temporally-regulated expression of cell surface markers is required for completion of the developmental sequence in *D.discoideum* then weak bases might interfere with development via this mechanism.

An alternative is that ammonia could modulate intracellular signal transduction by affecting vesicular ion concentrations. The eukaryotic vacuolar H^+-ATPase is electrogenic and the membrane potential generated is dissipated by the counterflow of cations such as Na^+, K^+ and Ca^{2+} and possibly by the co-transport of Cl^-. Zhu & Clarke (1992) report that the contractile vacuole of *D.discoideum* is associated with the calcium-binding protein calmodulin. Staining cells with a Ca^{2+}-sensitive fluorescent marker shows that Ca^{2+} is sequestered in hydrophobic sites such as membranes (Saran *et al.*, 1992). Milne & Coukell (1989) report that a calcium transport system is associated with an intracellular vesicle, constituting a very large percentage of the calcium store in *D.discoideum* (roughly 97-98%) whereas the IP_3-sensitive store contains only about 2-3% of the total sequestered calcium. Endosomal compartments can also concentrate $^{45}Ca^{2+}$ in response to the generation of a transmembrane pH gradient (Rooney & Gross, 1992). The cytosolic Ca^{2+} concentration is reported to be roughly 0.05-1 µM (Rasi-Caldogno *et al.*, 1982; Rooney *et al.*, 1994) and is regulated by accumulation and extrusion in acidic vesicles. In yeast cells it is reported that inhibition of vacuolar H^+-ATPase activity raises the cytosolic Ca^{2+} concentration from 0.15µM to roughly 0.9µM (Ohya *et al.*, 1991), potentially disrupting the regulation of calcium-sensitive cytosolic enzymes.

In *D.discoideum* there is a wealth of evidence that calcium fluxes play a part in developmental regulation. Saito (1979) noted that reduction of the external calcium concentration leads to a decrease in the time required to form fruiting bodies and Van Haastert (1985) reports that external Ca^{2+} can partially inhibit internal cAMP production. Key regulators of development also elicit changes in intracellular calcium concentrations. For example, an increase in cytosolic Ca^{2+} is seen in response to cAMP binding (Abe *et al.*,1988). Recent data from Saran *et al.* (1994) using cells transformed with apoaequorin, a calcium indicator, has confirmed this and indicates that cAMP signalling leads to a rapid release of Ca^{2+} from intracellular stores. This result is supported by

the work of Europe-Finner & Newell (1986), who demonstrate that inositol 1,4,5-triphosphate (IP_3), one of the signals generated by cAMP stimulation, induces calcium release from a non-mitochondrial pool and that cAMP binding leads to an internal cGMP pulse, which is blocked by TMB-8, a Ca^{2+} antagonist (Europe-Finner & Newell, 1984). In the longer term, an influx of calcium from the medium is induced (Bumann *et al.*, 1984; Wick *et al.*, 1978). Changes in cytosolic calcium have been proposed to play a part in regulating differentiation as well as aggregation and culmination.

8.2.2 Possible effects of ammonia and changes in the vesicular pH (pH_v) on components of the cAMP signal transduction pathway

Initially, a hypothesis in which NH_3 exerts its many developmental effects by interfering with cAMP production was proposed by Schindler & Sussman (1978). Since the relay system is essential for aggregation and a burst of $cAMP_i$ synthesis essential for culmination, ammonia might affect aggregation and culmination by interfering indirectly, via pH_v, with the production of cAMP by adenylate cyclase or could affect components of the pathway downstream of cyclic AMP.

There is little evidence to suggest that pH_v might affect cAMP signalling via calcium. Brenner & Thoms (1984) reported that treatment of cells with the calcium ionophore A23187 inhibited the cAMP relay system, but Schaap *et al.* (1994) have shown that neither the aggregation nor the germination adenylate cyclase is affected by cytosolic calcium at physiological levels. However these experiments were conducted in cell lysates and therefore do not exclude an indirect effect of calcium on adenylate cyclase requiring a spatially organized signal transduction pathway. For example, Kincaid *et al.* (1991) suggest that cAMP-regulated pathways may be modulated by Ca^{2+} via a CaM-dependent protein phosphatase and Winckler *et al.* (1991) report the existence of Ca^{2+}/CaM-regulated enzymes in *D.discoideum* at the aggregative stage. In mammalian systems, agonist-stimulated adenylate cyclase activity is inhibited

by increased cytosolic calcium (DeBernardi *et al.*, 1991), although a delay is seen between the calcium rise and adenylate cyclase inhibition, suggesting that the effect on AC activity is indirect.

Until recently, the available evidence suggested that the developmental effects of ammonia involved a modification of cAMP production, though not necessarily via Ca^{2+} regulation. Hopper *et al.* (1993) suggested that cAMP-dependent protein kinase A (cAMP-dependent PKA) might be regulated by ammonia. These workers produced cells in which the regulatory subunit of PKA (R) is no longer able to bind cAMP (R_M). Under the control of a prespore promoter (pspA), expression of the R_M subunit prevents activation of sporulation-specific genes and the development of such cells is hypersensitive to the effects of ammonia. It was proposed that ammonia inhibited cAMP production and thus prevented PKA-dependent culmination. Williams *et al.* (1984) showed that NH_3 inhibited $cAMP_i$ accumulation and Schindler & Sussman (1979) have shown that AC activation is hypersensitive to inhibition by ammonia in the slugger mutant KY3.

In contrast, the work of Riley & Barclay (1990) indicates that NH_3 raises $cAMP_i$ levels. In the face of such conflicting results, Schaap *et al.* (1994) have conducted an extensive survey of the effect of NH_3 (and its fellow weak base methylamine) on the activity of the two adenylate cyclases that have so far been identified in *D.discoideum* (Pitt *et al.*, 1992) and found that the aggregation adenylate cyclase (ACA), which constitutes the major adenylate cyclase activity of *D.discoideum*, was inhibited only transiently by ammonia (K_i = 4mM unprotonated base) and methylamine (K_i = 38mM) if these bases were added concurrently with the cAMP stimulus. However, if added pre-stimulus, then their effect on ACA activity was stimulatory up to 19mM and then inhibitory at higher concentrations; an inhibition that could be mimicked by NaCl and hence was due to an osmotic effect. In disaggregated cells from slugs, they found that ammonia retarded the natural increase in $cAMP_i$ just

before culmination twofold, but the cells finally achieved a normal $cAMP_i$ level regardless of the presence of ammonia. This could indicate that cAMP is not an upstream regulator of PKA-dependent gene expression or would indicate that ammonia does not act as an upstream regulator of cAMP-dependent PKA. In agreement with the former conclusion, Pitt *et al.* (1993) found that if 2-deoxy-cAMP (which activates cell surface receptors but not PKA) was added to *aca*$^-$ cels, then both fruiting and prestalk/prespore expression occurred, indicating that ACA is not essential for PKA activation and that an alternative activation pathway may exist. It is possible that the stimulatory effects of ammonia and methylamine on ACA observed by Schaap *et al.* (1994) may be due to the high weak base concentrations used. It is possible that the cytosol cannot buffer such high concentrations of weak base, so the cytosolic pH would increase and stimulate ACA since its optimum pH is 8.6. In other words, the stimulatory effect of ammonia on ACA observed here may well be due to direct activation of these enzymes by raising pH_{cyt}. *In vivo*, the cytosolic pH is 7.2-7.4, and concentrations of bases which have developmental effects do not change pH_{cyt} (see chapter 5), so ammonia in this case might be acting via an indirect signal transduction pathway rather than directly raising pH_{cyt}.

There are many alternative ways in which pH_v could influence PKA-dependent aggregation, culmination and gene expression rather than through cAMP:
(a) cAMP and pH_v might both be regulators of a factor influencing PKA activity
(b) pH_v could influence a separate signal tranduction pathway leading to PKA regulation from that controlled by cAMP
(c) pH_v might be inhibiting an adenylate cyclase other than ACA or ACG
(d) pH_v could regulate elements of the aggregative and culminative signal transduction pathways other than PKA.

A summary of the possible interactions of ammonia and pH_v with developmental signal transduction pathways is presented in **figure 8.1**.

8.2.3 Implications for the control of differentiation

Ammonia has also been implicated in the control of cell differentiation in *D.discoideum*. Numerous studies report that ammonia stimulates the spore pathway and suppresses stalk cell differentiation (Bradbury & Gross, 1989; Wang & Schaap, 1989; Kwong & Weeks, 1990; Riley & Barclay, 1990; So & Weeks, 1992). The effects of ammonia on differentiation might be transduced by cAMP and PKA. Cyclic AMP is essential for the induction of post-aggregative gene expression (reviewed in Gerisch, 1987) as is PKA, since expression of dominant-negative regulatory subunits under a prespore promoter prevents prespore cell formation (Hopper *et al.*, 1993). However, it is doubtful that cAMP-dependent gene expression acts solely through PKA, since *adenylate cyclase*$^-$ cells can synthesize developmental gene products (Pitt *et al.*, 1993). Therefore, cAMP-dependent and PKA-dependent pathways may regulate gene expression independently or their signal transduction pathways might be convergent. It is possible that ammonia and pH_v could interact with either pathway.

There is evidence also that variation in cytosolic calcium levels may have a role in prespore and prestalk differentiation, generation or maintenance of the prestalk/prespore pattern. Sequestered calcium levels in prestalk cells are higher than in prespore cells (Saran *et al.*, 1992; Tirlapur *et al.*, 1991). In addition, the use of calcium channel blockers (which inhibit mobilization of calcium from intracellular stores), or agents that interfere with Ca^{2+}-calmodulin interactions (such as W-7) have shown that cAMP-mediated prespore accumulation is dependent upon the presence of adequate cytosolic Ca^{2+} levels (Schaap *et al.*, 1986; Blumberg *et al.*, 1989).

8.3 Conclusion and future directions

This work demonstrates that ammonia exerts its inhibitory effect on development by raising the pH of an intracellular acidic vesicle. Further studies are needed to link ammonia with a signal transduction pathway mediated by an acidic vesicle. Particularly as the vesicle is a sequestration site for calcium, the possible role of calcium in affecting the enzymes (*eg.* PKA) involved in aggregation, culmination and differentiation, deserves investigation. This could be approached in the first instance by further study of the vacuolar ATPase mutants, to determine whether PKA and adenylate cyclase are correctly activated. Moreover, the effects of vesicular pH upon differentiation could be investigated by determining whether correct temporal expression of prespore and prestalk gene products is activated in these mutants. Synergistic development of the ß-gal-labelled antisense strain with Ax2 would determine whether the mutant preferentially differentiated along a prespore pathway, as is implied by the fact that weak base-treated wild type strains and the acidification-defective strains have enlarged spore heads and stunted stalks.

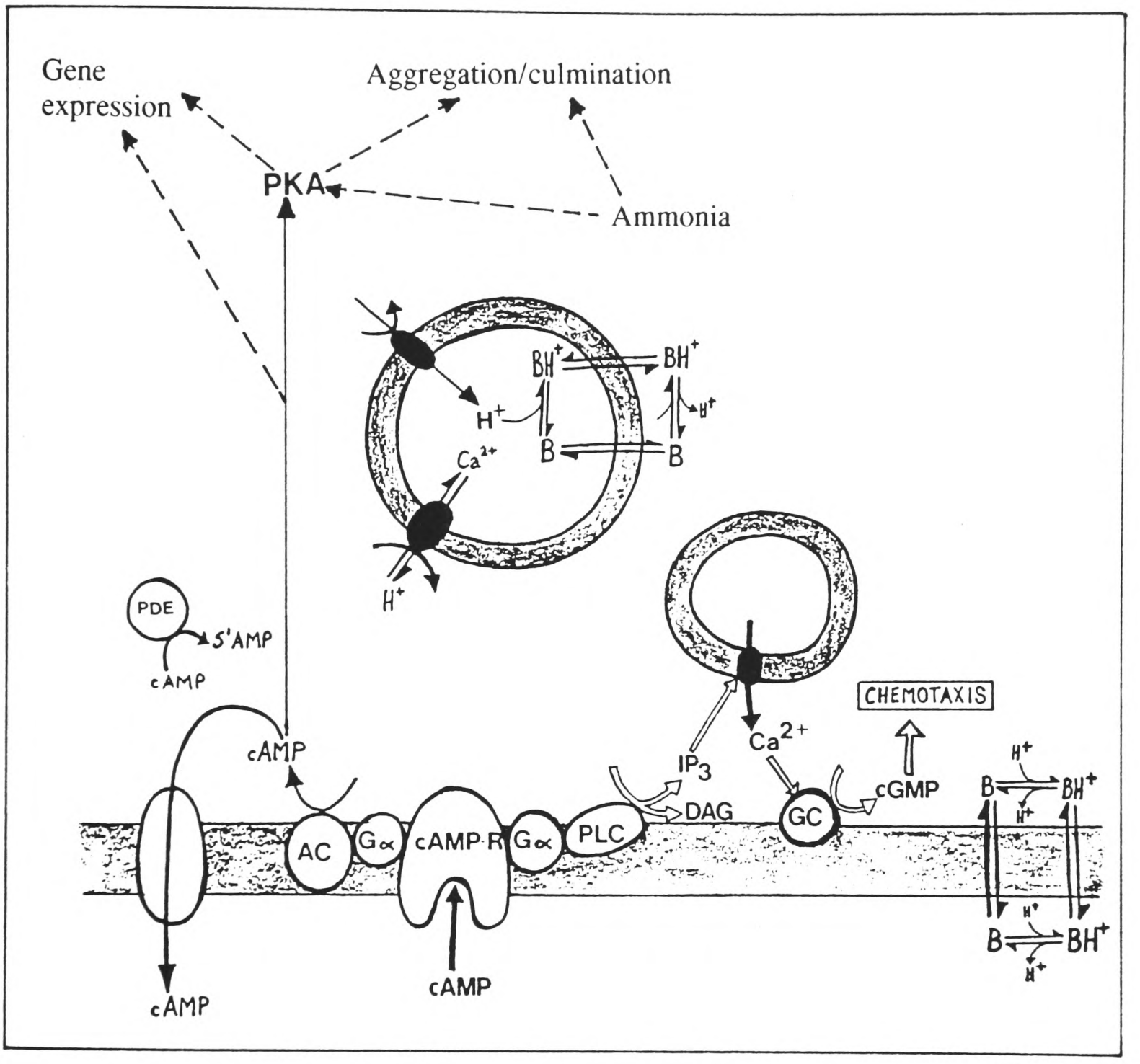
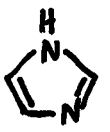
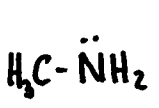
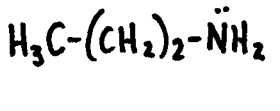
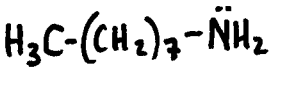
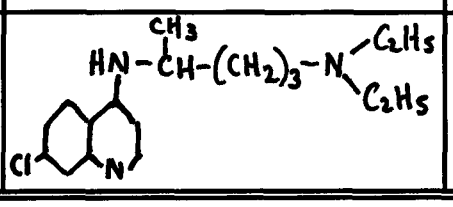


Figure 8.1: Possible interactions of ammonia and pH_v in influencing developmental signal transduction.

Appendices

Appendix I

Structure, molecular weight, hydrophobicity and pK_a of the bases used in this study

Base	Structure	$logP_{oct}$	M_R	pK_a
imidazole (IA)		0.13	68	7.1
ammonia (AC)		-1.37	18	9.3
methylamine (MA)		-0.57	32	10.7
propylamine (PA)		0.31	60	10.7
octylamine (OA)		2.90	130	10.7
chloroquine (CQ)		4.29 ± 0.12	515	8.1/10.2

$logP_{oct}$ refers to the ratio of partitioning of the compound in between octanol and water and is a measure of hydrophobicity.

Appendix II Conversion of total base concentrations to unprotonated base concentrations using the Henderson-Hasselbalch equation

The ratio of unprotonated to protonated base at any pH can be calculated using the following formulation

$$pH = pK_a - \log_{10} \frac{[B]}{[BH^+]}$$

where B is the unprotonated form and BH^+ the protonated form. Therefore,

$$\frac{[B]}{[BH^+]} = 10^{(pKa - pH)}$$

and

$$\frac{[B]}{[B + BH^+]} = \frac{10^{(pKa - pH)}}{1 + 10^{(pKa - pH)}}$$

For chloroquine, the proportion of unprotonated base relative to the monoprotonated and diprotonated forms is calculated. Conversion factors used to calculate the unprotonated base concentrations are shown below.

$[B + B(H^+)_n] \rightarrow [B]$	**Conversion factors**
ammonia	x 0.011
methylamine	x 4.37×10^{-4}
propylamine	x 3.89×10^{-4}
octylamine	x 4.47×10^{-4}
chloroquine	x 1.71×10^{-4}
imidazole	x 0.61

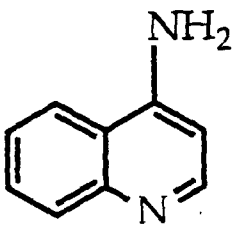
Appendix III

Since no direct measurement of the $logP_{octanol}$ value of chloroquine has been made, it was calculated using the method of Leo *et al.* (1971). A closely related compound with a known $logP_{octanol}$ is taken and a series of synthetic steps undertaken to generate chloroquine. Each step has been assigned a $logP_{octanol}$ value and an associated standard deviation (Leo *et al.*, 1971), which are added to the $logP_{octanol}$ value of the starting compound. A number of alternative syntheses were considered and that with the lowest standard deviation taken to be the most likely $logP_{octanol}$ value for chloroquine. The chosen starting compound is 4-NH_2-quinoline ($logP_{octanol}$ = 1.16)

1.16

+ 0.39 ± 0.04 (+ Cl)

1.55 ± 0.04



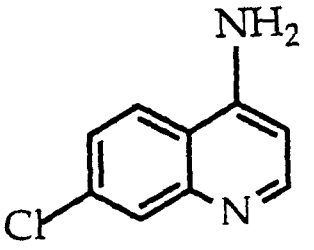
—Cl

1.55 ± 0.04

+ 0.50 ± 0.02 ($+ CH_3$)

+ 0.50 ± 0.02

+ 0.50 ± 0.02



+ 3 (CH_3)

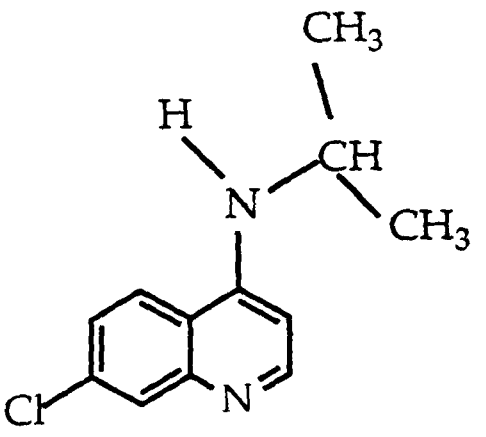
- 0.20 ± 0.02 (+ branch)

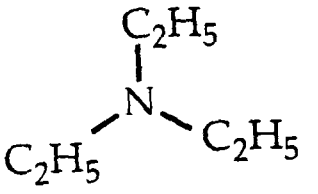
2.85 ± 0.12

2.85 ± 0.12

+ 1.44 ± 0.00 (+ triethylamine)

4.29 ± 0.12





Appendix IV

Conversion tables (ppm → pH) for 2-AEP, P_i and Cl_2MDP *in vivo*. The pH values for each probe are calculated from the chemical shift values using the following equation (Martin *et al.*, 1987):

$$pH = pK_a + \log (\delta - \delta_A)/(\delta - \delta_B)$$

where δ is the observed chemical shift in parts per million (ppm), δ_A is the limiting acidic chemical shift value for that particular compound, δ_B is the corresponding limiting basic chemical shift and δ is the observed chemical shift. Experimentally determined values for each probe are given in chapter 5, **table 5a** (Martin *et al.*, 1987; Brénot *et al.*, 1992; Pelorgeas *et al.*, 1992). Conversion tables are given overleaf.

(A) dichloromethylene diphosphonate

Cl_2MDP (ppm)	pH (in Mg^{2+})	pH (Mg^{2+}-free)
8.40	---	4.47
8.45	---	4.56
8.50	4.22	4.65
8.55	4.59	4.73
8.60	4.79	4.81
8.65	4.94	4.88
8.70	5.05	4.95
8.75	5.15	5.03
8.80	5.23	5.10
8.85	5.31	5.17
8.90	5.37	5.25
8.95	5.44	5.33
9.00	5.50	5.42
9.05	5.55	5.51
9.10	5.60	5.62
9.15	5.66	5.75
9.20	5.71	5.91
9.25	5.75	6.14
9.30	5.80	6.58
9.35	5.85	---
9.40	5.90	---
9.45	5.95	---
9.50	5.99	---
9.60	6.04	---
9.70	6.09	---

Mg^{2+} pH values were normally used for calculations.

(B) 2-Aminoethyl phosphonate

2-AEP (ppm)	pH
16.60	7.70
16.70	7.38
16.80	7.18
16.90	7.04
17.00	6.92
17.10	6.82
17.20	6.73
17.30	6.65
17.40	6.58
17.50	6.50
17.60	6.43
17.70	6.37
17.80	6.30
17.90	6.23
18.00	6.17
18.10	6.10
18.20	6.02
18.30	5.95
18.40	5.87
18.50	5.78
18.60	5.68
18.70	5.56
18.80	5.42
18.90	5.22
19.00	4.90
19.10	---

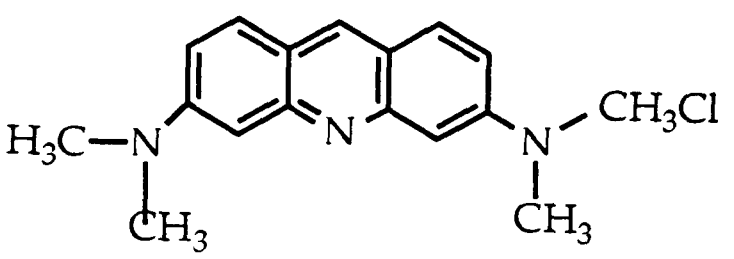
(C) Inorganic phosphate

P_i (ppm)	pH
0.20	5.12
0.30	5.62
0.40	5.86
0.50	6.02
0.60	6.15
0.70	6.26
0.80	6.35
0.90	6.44
1.00	6.52
1.10	6.59
1.20	6.67
1.30	6.73
1.40	6.80
1.50	6.87
1.60	6.94
1.70	7.01
1.80	7.08
1.90	7.16
2.00	7.24
2.10	7.33
2.20	7.43
2.30	7.55
2.40	7.70
2.50	7.89
2.60	8.21
2.70	---

Appendix V

Chemical structures

Acridine Orange



References

References

Abe,T., Maeda,Y. & Iijima,T. (1988). Transient increase of the intracellular Ca^{2+} concentration during chemotactic signal transduction in *Dictyostelium discoideum* cells. "Differentiation" 39, 90-96

Abe,K. & Yanagisawa,K. (1983). A new class of rapidly developing mutants in *D.discoideum*: implications for cyclic AMP metabolism and cell differentiation. "Dev. Biol." 95, 200-210

Aerts,R.J., Durston,A.J. & Moolenaar,W.H. (1986). Cytosplasmic pH and glycolysis in the *Dictyostelium discoideum* cell cycle. "FEBS Lett." 196, 167-170

Anraku,Y., Hirata,R., Wada,Y. & Ohya,Y. (1992). Molecular genetics of the yeast vacuolar H^+-ATPase. "J.Exp.Biol." 172, 67-81

Aubry,L., Klein,G., Martiel,J.L. & Satre,M. (1993). Kinetics of endosomal pH evolution in *Dictyostelium discoideum* amoebae studied by fluorescence spectroscopy. "J.Cell Sci." 105, 861-866

Bar-On,Z. & Degani,H. (1985). Permeability of alkylamines across phosphatidylcholine vesicles as studied by ^{1}H-NMR. "Biochim.Biophys.Acta" 813, 207-212

Belasco,J.G. & Higgins,C.F. (1988). Mechanisms of mRNA decay in bacteria: a perspective. "Gene" 72, 15-23

Berks,M. & Kay,R.R. (1990). Combinatorial control of cell differentiation by cAMP and DIF-1 during development of *Dictyostelium discoideum*. "Development" 110, 977-984

Bernstein,R.L. & Van Driel,R. (1980). Control of folate deaminase activity of *Dictyostelium discoideum* by cyclic AMP. "FEBS Lett." 119, 249-253

Bernstein,R.L., Tabler,M., Vestweber,D. & Van Driel,R. (1981). Extracellular folate deaminase of *Dictyostelium discoideum*. "Biochim.Biophys.Acta" 677, 295-302

Blomberg,P, Wagner,E.G.H. & Nordström,K. (1990) Control of replication of the plasmid R1: the duplex between antisense RNA, CopA and its target CopT is processed specificaly in vivo and in vitro by RNaseII. "EMBO J." 9, 2331-2340

Blusch,J., Morandini,P. & Nellen,W. (1992). Transcriptional regulation by folate: inducible gene expression in *Dictyostelium* transformants during growth and early development. "Nuc.Ac.Res." 20, 6235-6238

Blumberg,D.D., Comer,J.F. & Walton,E.M. (1989). Ca^{2+} antagonists distinguish different requirements for cAMP-mediated gene expression in the cellular slime mould *Dictyostelium discoideum*. "Differentiation" 41, 14-21

Bof,M., Brenot,F., Gonzalez,C., Klein,G., Martin,J-B. & Satre,M. (1992). *Dictyostelium discoideum* mutants resistant to the toxic action of methylene diphosphonate are defective in endocytosis. "J.Cell Sci." 101, 139-144

Bonner,J.T. (1947) Evidence for the formation of cell aggregates by chemotaxis in the development of the slime mold *Dictyostelium discoideum*. "J.Exptl.Zool." 106, 1-26

Bonner,J.T., Kelso,A.P. & Gillmor,R.G. (1966). A new approach to the problem of aggregation in the cellular slime moulds. "Biol.Bulletin" 130, 28-42

Bonner,J.T. (1970). Induction of stalk cell differentiation by cyclic AMP in the cellular slime mould *Dictyostelium discoideum*. "Proc.Natl.Acad.Sci." 65, 110-113

Bonner,J.T., Hay,A., John,D.G. & Suthers,H.B. (1985). pH affects fruiting and slug orientation in *Dictyostelium discoideum*. "J.Embryol.Exp.Morph." 87, 207-213

Bonner,J.T., Har,D. & Suthers,H.B. (1989). Ammonia and thermotaxis: further evidence for a central role of ammonia in the directed cell mass movements of *Dictyostelium discoideum*. "Proc.Natl.Acad.Sci.USA" 86, 2733-2736

Bonner,J.T. & Williams,J.G. (1994). PstA-R_M slugs are defective in phototaxis. *in press*

Boron,W. & deWeer,P. (1976). Intracellular pH transients in squid giant axons caused by CO_2, NH_3 and metabolic inhibitors. "J.Gen.Physiol." 87, 91-119

Bowman,E.J., Siebers,A. & Altendorf,K.H. (1988). Bafilomycin A_1: a class of inhibitors of membrane ATPases from microorganisms, animal cells and plants. " Proc.Natl.Acad.USA" 85, 7972-7976

Boyajian,C.L., Garritsen,A. & Cooper,D.M.F. (1991). Bradykinin stimulates Ca^{2+} mobilization in NCB-20 cells leading to direct inhibition of adenylylcyclase. "J.Biol.Chem." 266, 4995-5003

Bradbury,J.M. & Gross,J.D. (1989). The effect of ammonia on cell-type-specific enzyme accumulation in *D.discoideum*. "Cell Diff. and Dev." 27, 121-128

Brenner,M. & Thoms,S.D. (1984). Caffeine blocks activation of cyclic AMP synthesis in *Dictyostelium discoideum*. "Dev.Biol." 101, 136-146 - calcium ionophore A23187 inhibits cAMP relay

Brénot,F., Aubry,L., Martin,J.B., Satre,M. & Klein,G. (1992). Kinetics of endosomal acidification in *Dictyostelium discoideum* amoebae: ^{31}P-NMR evidence for a very acidic early endosomal compartment. "Biochimie" 74, 883

Brookman,J.J., Town,C.D., Jermyn,K.A. & Kay,R.R. (1982). Developmental regulation of a stalk cell differentiation-inducing factor in *Dictyostelium discoideum*. "Dev.Biol." 91, 191-196

Brookman,J.J., Jermyn,K.A. & Kay,R.R. (1987). Nature and distribution of the morphogen DIF in the *Dictyostelium* slug. "Development" 100, 119-124

Bumann,J., Wurster,B. & Malchow,D. (1984). Attractant-induced changes and oscillations of the extracellular Ca^{2+} concentration in suspensions of differentiating *Dictyostleium* cells. "J.Cell.Biol." 98, 173-178

Cardelli,J.A., Richardson,J. & Miears,D. (1989). Role of intracellular acidic compartments in the biosynthesis of *Dictyostelium* lysosomal enzymes. "J.Biol.Chem." 264, 3454 - 3463

Crofts,A.R. (1967). Amine uncoupling of energy transfer in chloroplasts. "J.Biol.Chem." 242, 3352-3359

Crowley, Nellen,W., Gomer & Firtel,R.A. (1985). Phenocopy of Discoidin-I$^-$ mutants by antisense transformation in *Dictyostelium discoideum*. "Cell" 43, 633-641

Cubitt,A.B., Carrel,F., Dharmawardhane,S., Gaskins,C., Hadwiger,J., Howard,P., Mann,S.K.O., Okaishi,K., Zhou,K. & Firtel,R.A. (1992). Molecular genetic analysis of signal transduction pathways controlling multicellular development in *D.discoideum*. "Cold Spring Harbor Symp.Quant.Biol." 57,177-192

Darcy,P.K. & Fisher,P.R. (1990). Pharmacological evidence for a role for cAMP signalling in *Dictyostelium discoideum* slug behaviour. "J.Cell Sci." 96, 661-667

De Bernardi,M.A., Seki,T. & Brooker,G. (1991). Inhibition of cAMP accumulation by intracellular calcium mobilization in C6-2B cells stably transfected with substance K receptor cDNA "Proc.Natl.Acad.Sci.USA" 88, 9257-9261

De Chastellier,P., Ryter, A. & Thilo, L. (1983). Membrane shuttle between

plasma membrane, phagosomes and pinosomes in *Dictyostelium discoideum*. "Eur.J.Cell.Biol." 30, 233-243

De Duve,C., De Barsy,T., Poole,B., Trouet,A., Tulkens,P. & Van Hoof,F. (1974). Lysosomotropic agents. "Biochem.Pharmacol." 23, 2495-2531

De Gunzberg,J. & Veron,M. (1982). A cAMP-dependent protein kinase is present in differentiating *Dictyostelium discoideum* cells. "EMBO J."1, 1063-1068

Devine,K.M. & Loomis,W.F. (1985). Molecular characterization of anterior-like cells in *Dictyostelium discoideum*. "Dev.Biol." 107, 364-372

Devreotes,P.N. (1982). Chemotaxis. In "The Development of *Dictyostelium discoideum*. (ed. Loomis,W.) pp.117-168

De Wit,R., Bulgakov,R., Rinke de Wit,T.F. & Konijn,T. (1986). Developmental regulation of the pathways of folate-receptor-mediated stimulation of cAMP and cGMP synthesis in *Dictyostelium discoideum*. "Differentiation" 32, 192-199

Diamond,J.M. & Katz,Y. (1974). Interpretation of non-electrolyte partition coefficients between dimyristoyl lecithin and water. "J.Memb.Biol." 17, 121-154

Driever,W. & Nüsslein-Volhard,C. (1988). A gradient of *bicoid* protein in *Drosophila* embryos. "Cell" 54, 83-93

Dunn,K.W. & Maxfield,F.R. (1992). Delivery of ligands from sorting endosomed to late endosomes occurs by maturation of sorting endosomes. "J.Cell.Biol." 117, 301-310

Early,A.E. & Williams,J.G. (1988). A *Dictyostelium* prespore-specific gene is transcriptionally repressed by DIF *in vitro*. "Development" 103, 519-524

Early,A.E., McRobbie,S.J., Duffy,K.T., Jermyn,K.A., Tilly,R., Ceccarelli,A. & Williams,J.G. (1988). Structural and functional characterization of genes encoding *Dictyostelium* prestalk and prespore cell-specific proteins. "Dev.Genet." 9, 383-402

Early,A.E., Gaskell,M.J., Traynor,D. & Williams,J.G. (1993). Two distinct populations of prestalk cells within the tip of the migratory *Dictyostelium* slug with differing fates at culmination. "Development" 118, 353-362

Esch,R.K. & Firtel,R.A. (1991). cAMP and cell sorting control the spatial expression of a developmentally essential cell-type-specific ras gene in *Dictyostelium*. "Genes & Devel." 5, 9-21

Europe-Finner,G.N., McClue,S.J. & Newell,P.C. (1984). Inhibition of aggregation in *Dictyostelium* by EGTA-induced depletion of calcium. "FEMS Microbiol. Lett." 21, 21-25

Europe-Finner,G.N. & Newell,P.C. (1986). Inositol 1,4,5-triphosphate induces calcium release from a non-mitochondrial pool in amoebae of *Dictyostelium*. "Biochim.Biophys.Acta." 887, 335-340

Europe-Finner,G.N. & Newell,P.C. (1987). GTP analogues stimulate inositol triphosphate formation transiently in *Dictyostelium*. "J.Cell.Science"87,221-229

Europe-Finner,G.N., Gammon,B. & Newell,P.C. (1991). Accumulation of 3H-inositol into inositol polyphosphates during the development of *Dictyostelium*. "J.Cell.Sci." 87, 513-518

Feit,I.N. (1988). Ammonia can stimulate or inhibit aggregate density in *Dictyostelium mucoroides*: a quantitative test of the hypothesis that ammonia is the aggregation-suppressing gas "Dev.Genet." 9, 639-652

Feit,I.N., Bonner,J.T. & Suthers,H.B. (1990). Regulation of the anterior-like cell state by ammonia in *Dictyostelium discoideum*. "Dev.Genet." 11, 442-446

Ferrari,G.M. & Gross,J.D., unpublished data

Firtel,R.A. & Chapman,A.L. (1990). A role for cAMP-dependent protein kinase A in early *Dictyostelium* development. "Genes Dev." 4, 18-28

Firtel,R.A., Van Haastert,P.J.M., Kimmel,R.A. & Devreotes,P.N. (1989). G protein linked signal transduction pathways in development: *D.discoideum* as an experimental system. "Cell" 58, 235-239

Firtel, R.A. (1991). Signal transduction pathways controlling multicellular development in *Dictyostelium*. "Trends Genet." 7, 381-388

Flaadt,H., Jaworski,E., Schlatterer,C. & Malchow,D. (1993). Cyclic AMP- and Ins(1,4,5)P_3-induced Ca^{2+} fluxes in permeabilised cells of *Dictyostelium discoideum*: cGMP regulates Ca^{2+} entry across the plasma membrane. "J.Cell Sci." 105, 225-261

Fok, A.K., Clarke,M., Ma,L & Allen,R.D. (1993). Vacuolar H^+_ATPase of *Dictyostelium discoideum*. "J.Cell.Sci." 111, 58-72

Foote,S.J., Thompson,J.K., Cowman,A.F. & Kemp,D.J. (1989). Amplication of the multidrug resistance gene in some chloroquine resistant isolates of *P.falciparum*. "Cell" 57, 921-930

Frigerio,G., Burri,M., Baumgartner,S. & Noll,M. (1986). Structure of the segmentation gene *paired* and the *Drosophila* PRD gene set as part of a gene network. "Cell" 47, 735-766

Gaskell,M.J., Jermyn,K.A., Watts,D.J., Treffy,T. & Williams,J.G. (1992). Immunolocalisation and separation of multiple prestalk cell types in *Dictyostelium*. "Differentiation" 51, 171-176

Gee,K. (1993) The role of ammonia in *Dictyostelium* development. "D.Phil. thesis, University of Oxford"

Gee,K., Russell,F. & Gross,J.D. (1994). Ammonia hypersensitivity of slugger mutants of *D.discoideum*. "J.Cell Sci." 107, 701-708

Gerdes,K., Neilsen,A., Thorstead,P. & Wagner,H. (1992). Mechanism of gene activation. "J.Mol.Biol." 226, 637-649

Gerisch,G. (1987). Cyclic AMP and other signals controlling cell development and differentiation in *D.discoideum*. "Ann.Rev.Biochem." 56, 853-879

Giglione,C. & Gross,J.D. (1994). Unpublished observations.

Ginsburg,G.T., Louis,J.M. & Kimmel,A.R. (1994). cAR4 regulates cell patterning during late *Dictyostelium* development. "International *Dictyostelium* conference" San Diego, August 1994, p.6.1

Gluck,S. (1993). Vacuolar H^+-ATPases: H^+ pumps in eukaryotic cell function. "Int.Rev.Cytol." 37C, 105-137

Green,P.J., Pines,O. & Inouye,M. (1986). The role of antisense RNA in gene regulation. "Ann.Rev.Biochem." 55, 569-597

Gregg,J.H., Hackney,A.L. & Krivanek,J.O. (1954). Nitrogen metabolism of the slime mould *Dictyostelium discoideum* during growth and morphogenesis. "Biol.Bull." 107, 226-235

Griffiths,G. & Gruenberg,J. (1991). The arguments for pre-existing early and late endosomes. "Trends.Cell.Biol." 1, 5-8

Gross,J.D., Bradbury,J., Kay,R.R. & Peacey,M.J. (1983). Intracellular pH and the control of differentiation in *D.discoideum*. "Nature" 303, 244-245

Gross,J.D., Peacey,M.J. & Pogge von Strandmann,R. (1988). Plasma membrane proton pump inhibition and stalk cell differentiation in *Dictyostelium discoideum*. "Differentiation" 38, 91-98

Haberstroh,L. & Firtel,R.A. (1990). A spatial gradient of expression of a

cAMP-regulated prespore cell-type-specific gene in *Dictyostelium*. "Genes Dev." 4, 596-512

Harwood,A.J., Hopper,N.A., Simon,M-N., Bouzid,S., Veron,M. & Williams,J.G. (1992). Multiple roles for cAMP-dependent protein kinase during *Dictyostelium* development "Devel. Biol."149, 90-99

Harvey,W.R. (1992). Physiology of V-ATPases. "J.Exp.Biol." 172, 1-172

Heuser,J., Zhu,Q. & Clarke,M. (1993). Proton pumps populate the contractile vacuoles of *Dictyostelium* amoebae. "J.Cell.Biol." 121, 1311-1327

Higgins,C.F. & Gottesman,M.M. (1992). Is the multidrug transporter a flippase? "TIBS" 17, 18-21

Hollemans,M., Oude-Elferink,R., deGroot,P., Strijland,A. & Tager,J.M. (1981). Accumulation of weak bases in relation to intralysosomal pH in cultured human skin fibroblasts. "Biochim.Biophys.Act." 643, 140-151

Hopper,N.A., Harwood,A.J., Bouzid,S., Véron,M. & Williams,J.G. (1993). Activation of the prespore and spore cell pathway of *Dictyostelium* differentiation by cAMP-dependent protein kinase and evidence for its upstream regulation by ammonia "EMBO J." 12, 2459-2466

Inouye,K. (1988). Induction by acid load of the maturation of prestalk cells in *Dictyostelium discoideum*. "Development" 104, 669-681

Inouye, K. (1989). Regulation of cytoplasmic pH in the differentiating cell types of the cellular slime mould *Dictyostelium discoideum*. "Biochim.Biophys.Acta." 1012, 64-68

Inouye,K. (1990). Control mechanism of stalk formation in the cellular slime mould *Dictyostelium discoideum*. "Forma"5, 119-134

Janssens,P.M.W., De Jong,C.C.C., Vink,A.A. & Van Haastert,P.J.M. (1989). Regulatory properties of magnesium-dependent guanylate cyclase in *Dictyostelium discoideum* membranes. "J.Biol.Chem." 264, 4329-4335

Jermyn,K.A. & Williams,J.G. (1991). An analysis of culmination in *Dictyostelium* using prestalk and stalk-specific cell autonomous markers. "Development" 111, 779-787

Kay,R.R. (1979). Gene expression in *D.discoideum*: mutually antagonistic roles of cyclic-AMP and ammonia. "J. Embryol.Exp.Morph." 52, 171-182

Kay,R.R. & Jermyn,K.A. (1983). A possible morphogen controlling differentiation in *Dictyostelium*. "Nature" 303, 242-244

Kay,R.R., Gadian,D.G. & Williams,S.R. (1986). Intracellular pH in *Dictyostelium*:a ^{31}P nuclear magnetic resonance study of its regulation and possible role in controlling cell differentiation. "J.Cell Sci." 83, 165-179

Kay,R.R., Berks,M., Traynor,D., Taylor,G., Masento,M. & Morris,H. (1988). Signals controlling cell differentiation in *Dictyostelium*. "Dev.Genet."9, 579-587

Kay, R.R. (1989). Evidence that intracellular cAMP triggers spore maturation in *D.discoideum*. "Development" 105, 753-759

Kimmel,A.C. & Firtel,R.A. (1991). cAMP signal transduction pathways regulating development of *Dictyostelium discoideum*. "Curr.Op.Genet.Devel." 1, 383-390

Kincaid et al. (1991). Cloning and developmental expression of a calmodulin-dependent protein phosphatase catalytic subunit in *Dictyostelium discoideum*. "International *Dictyostelium* conference" Vancouver

Klein,P., Vaughan,R., Borleis,J. & Devreotes,P.N. (1987). The surface cyclic AMP receptor in *D.discoideum*. "J.Biol.Chem." 262, 358-364

Klein,P., Sun,T.J., Saxe,C.L., Kimmel,A.R. Johnson,R.L. & Devreotes,P.N. (1988). A chemoattractant receptor controls development in *D.discoideum*. "Science" 241, 1467-1472

Klionsky,D., Nelson,N. & Nelson,H. (1992). Compartment acidification is required for efficient sorting of proteins to the vacuole in *S.cerevisiae*. "J.Biol.Chem." 267, 3416

Konijn,T., Van De Meene,J., Bonner,J.T. & Barkley,D. (1967). The acrasin activity of adenosine 3',5' cyclic phosphate. "Proc. Natl.Acad.Sci. USA" 58, 1152-1154

Kopachik,W., Oohata,A., Dhokia,B., Brookman,J.J. & Kay,R.R. (1983). *Dictyostelium* lacking DIF, a putative morphogen. "Cell" 33, 397-403

Kosugi,I. & Inouye,K. (1989). Negative chemotaxis to ammonia and other weak bases by migrating slugs of the cellular slime moulds. "J.Gen.Microbiol." 135, 1589-1598

Krogstad,D.J., Schlesinger,P.H. & Gluzman,I.Y. (1985). Antimalarials increase vesicle pH in *Plasmodium falciparum* "J.Cell Biol." 101, 2302-2309

Kwong,L. & Weeks,G. (1989). Studies on the accumulation of the differentiation-inducing factor (DIF) in high-cell-density monolayers of

Dictyostelium discoideum. "Dev.Biol." 132, 554-588

Kwong,L. & Weeks,G. (1990). The effect of presumptive morphogens on prestalk and prespore gene expression in monolayers of *D.discoideum*. "Differentiation" 44, 88-94

Kwong,L., Xie,Y., Daniel,J., Robbins,S.M. & Weeks,G. (1990). A *Dictyostelium* morphogen that is essential for stalk cell formation is generated by a sub-population of prestalk cells. "Development" 110, 303-310

Leo,A., Hansch,C. & Elkins,D. (1971). Partition coefficients and their uses. "Chem.Rev." 71, 525-616

Liu, Williams & Clarke (1992). Inducible expression of CaM antisense RNA in *Dictyostelium discoideum* inhibits the completion of cytokinesis. "Mol.Biol.Cell" 3, 1403-

Lonski,J. (1976) The effect of ammonia on fruiting body size and microcyst formation in the cellular slime moulds. "Dev.Biol" 51, 158-165

Loomis,W. (1971) Sensitivity of *D.discoideum* to nucleic acid analogues "Exptl.Cell.Res." 64, 484-486

Loomis,W.F. (1972) Role of the cell surface sheath in the control of morphogenesis in aggregation of *Dictyostelium discoideum*. "Nature New Biol." 240, 6-9

Maeda,Y. & Gerisch,G. (1977). Vesicle formation in *Dictyostelium discoideum* cells during oscillation of cAMP synthesis and release. "Exp.Cell Res." 110, 119-126

McPherson & Singleton (1992). V4, a gene required for the transition from growth to development in *Dictyostelium discoideum*. "Dev.Biol." 150, 231-242

MacWilliams,H.K. (1982). Transplantation experiments and pattern mutants in cellular slime mould slugs. "Developmental order: Its origin and regulation" Liss Inc. pp 463-483

Mann,S.K.O & Firtel,R.A. (1991). A developementally regulated, putative serine/threonine protein kinase is essential for development in *Dictyostelium*. "Mech.Devel." 35, 89-101

Marquardt,D. & Center,M.S. (1991). Drug transport mechanism in HL60 cells isolated for resistance to adriamycin. "Cancer Res." 52, 3157-3163

Martin,J-B., Foray,M.F., Klein,G. & Satre,M. (1987). Identification of

inositol hexaphosphate in ^{31}P NMR spectra of *Dictyostelium discoideum* amoebae: relevance to intracellular pH determination. "Biochim.Biophys Acta" 931, 16-25

Masento,M.S., Morris,H.R., Tayl or,G.W., Johnson,S.J., Skapsi,A.C. & Kay,R.R. (1988). Differentiation-inducing factor from the slime mould *Dictyostelium discoideum* and its analogues: synthesis, structure and biological activity. "Biochem.J." 256, 23-28

McConaghy,J.R., Saxe,C.L., Williams,G.B. & Sussman,M. (1984). Reversible inhibition of aggregation-related cohesivity in *Dictyostelium discoideum* by diffusible metabolites. "Dev.Biol." 105, 389-395

Mee,J.D., Tortolo,D.M. & Coukell,M.B. (1986). Chemotaxis-associated properties of separated prestalk and prespore cells of *Dictyostelium discoideum*. "Biochem.Cell.Biol." 64, 722-732

Mellman,I., Fuchs,R. & Helenius,A. (1986). Acidification of the endocytic and exocytic pathways. "Ann.Rev.Biochem." 55, 663-700

Merkle,R.K., Cooper,K.K. & Rutherford,C.L. (1984). Localization and levels of cyclic AMP during development of *Dictyostelium discoideum*. "Cell Differ." 14, 257-266

Milne,J.L. & Coukell,M.B. (1989). Identification of a high-affinity Ca^{2+} pump associated with endocytic vesicles in *Dictyostelium discoideum*. "Exp.Cell.Res."185, 21-32

Milne,J.L. & Devreotes,P.N. (1993). The surface cyclic AMP receptors, cAR1, cAR2 and cAR3, promote Ca^{2+} influx in *D.discoideum* by a G_O2-independent mechanism. "Mol.Biol.Cell" 4, 283-292

Moriyama,Y. & Nelson,N. (1988). The vacuolar H^+-ATPase: a proton pump controlled by a slip. "Prog.Clin.Biol.Res." 273, 387-394

Morris,H.R., Masento,M.S., Taylor,G.W. Jermyn,K.A. & Kay,R.R. (1988). Structure and elucidation of two differentiation inducing factors (DIF-2 and DIF-3) from the cellular slime mould *Dictyostelium discoideum*. "Biochem.J." 249, 903-906

Mitchell,P. (1966). Uncoupling by amines across biological membranes. "Biol.Rev." 41, 445-502

Naylor,O., Insall,R. & Kay,R.R. (1992). Differentiation-inducing factor dechlorinase,a novel cytosolic dechlorinating enzyme from *Dictyostelium discoideum*. "Eur.J.Biochem." 208, 531-536

Neave,N., Sobolewski,A. & Weeks,G. (1983). The effect of ammonia on stalk cell differentiation in submerged monolayers of *D.discoideum*. "Cell Diff." 13, 301-307

Nellen,W. & Lichtenstein,C. (1993). What makes an mRNA anti-sense-itive? "TIBS" 18, 419-423

Nelson,N. (1992). Organellar proton-ATPases. "Curr.Op.Cell.Biol." 4, 654-660

Nelson,H. & Nelson,N. (1990). Disruption of genes encoding subunits of yeast vacuolar H^+-ATPase causes conditional lethality. "Proc.Natl.Acad.Sci." 87, 3503-3507

Newell,P.C., Telser,A. & Sussman,M. (1969). Alternative developmental pathways determined by environmental conditions in the cellular slime mould *Dictyostelium discoideum*. "J.Bacteriol." 100, 763-768

Newell,P.C. & Ross,F.M. (1982). Genetic analysis of the slug stage of *Dictyostelium discoideum*. "J.Gen.Microbiol." 128, 1639-1652

Newell,P.C. & Liu,G. (1992). Streamer F mutants and chemotaxis of *Dictyostelium*. "Bioessays" 14, 473-479

Nissani,E. & Ginsburg,H. (1989). Protonophoric effects of antimalarial drugs and alkylamines in *Escherichia coli* membranes. "Biochim.Biophys.Acta" 978, 293-298

Nolta,K.V., Padh,H. & Steck,T.L. (1991). Acidosomes from *Dictyostelium* - initial biochemical characterization. "J.Cell.Biol." 266, 18313 - 18323

Nolta,K.V., Padh,H. & Steck,T.L. (1993) An immunocytochemical analysis of the vacuolar proton pump in *Dictyostelium discoideum*. "J.Cell Sci." 110, 5-15

Ohsumi,Y. & Anraku,Y. (1983). Calcium transport driven by a proton motive force in vacuolar membrane vesicles of *Saccharomyces cerevisiae*. "J.Biol.Chem." 258, 5614-5617

Ohya,Y., Umemoto,N., Tanida,I., Ohta,A., Iida,H. & Anraku,Y. (1991). Calcium-sensitive *cls* mutants of *Saccharomyces cerevisiae* showing a Pet^- phenotype are ascribable to defects of vacuolar membrane H^+-ATPase activity. "J.Biol.Chem." 266, 13971-13977

Overton,E. (1899). Uber die algemeinen osmotischen eigenschaften der Zeller. "Vjschr.Naturforsch.Ges.Zurich" 44, 88

Oyama,M. & Blumberg,D.D. (1986). Cyclic AMP and NH_3/NH_4^+ both

regulate cell-type-specific mRNA accumulation in the cellular slime mould *Dictyostelium discoideum*. "Dev.Biol." 117, 557-566

Padh,H., Lavasa,M. & Steck,T.L. (1989a). Prelysosomal acidic vacuoles in *Dictyostelium discoideum*. "J.Cell Biol." 108, 865-874

Padh,H., Lavasa,M. & Steck,T.L. (1989b). Characterization of vacuolar proton ATPase in *Dictyostelium discoideum*. "Biochim.Biophys.Acta" 982, 271-278

Padh,H., Lavasa,M. & Steck,T.L. (1991). Endosomes are acidified by association with discrete proton-pumping vacuoles in *Dictyostelium*. "J.Biol.Chem." 266, 5514-5520

Palmgren,M.G. (1991). Acridine orange as a probe for measuring pH gradients across membranes: mechanisms and limitations. "Analyt.Bioch." 192, 316-321

Pelorgeas,S., Martin,J-B. & Satre,M. (1992) Cytotoxicity of dichloromethylene diphosphonate and of 1-hydroxyethane-1,1-diphosphonate in amoebae of the cellular slime mould *Dictyostelium discoideum*. "Biochem.Pharmacol." 44, 2157-2163

Peterson,G.L. (1977). A simplification of the protein assay method of Lowry *et al.* which is more generally applicable. "Anal.Biochem."83, 346-356

Pitt,G.S., Milona,N., Borleis,J., Lin,K.C. Reed,R.R. & Devreotes,P.N. (1992). Structurally distinct and stage-specific adenylyl cyclase genes play different roles in *Dictyostelium* development. "Cell" 69, 305-315

Pitt,G.S, Brandt,R., Lin,K.C., Devreotes,P.N. & Schaap,P. (1993). Extracellular cAMP is sufficient to restore developmental gene expression and morphogenesis in *Dictyostelium* cells lacking adenylate cyclase. "Genes & Dev."7,2172

Poole,B. & Ohkuma,S. (1981). Effect of weak bases on the intralysosomal pH in mouse peritoneal macrophages. "J.Cell Biol." 90, 665-669

Pupillo,M., Insall,R., Pitt,G.S & Devreotes,P.N. (1992). Multiple cyclic AMP receptors are linked to adenylyl cyclase in *D.discoideum*. "Mol.Biol.Cell" 3, 1229-1234

Rand,K.D. (1985). Ph.D. thesis. University of Pittsburgh, Pennsylvania

Raper,K.B. (1940). Pseudoplasmodium formation and organization in *Dictyostelium discoideum*. "J.Elisha Mitchell Sci.Soc." 56, 241-282

Raper,K.B. (1984). "The Dictyostelids", Princeton University Press.

Riley,B.B. & Barclay,S.L. (1990). Ammonia promotes accumulation of intracellular cAMP in differentiating amoebae of *D.discoideum*. "Development" 109, 715-722

Rooney,E.K. & Gross,J.D. (1992). ATP-driven Ca^{2+}/H^{+} antiport in acid vesicles from *Dictyostelium*. "Proc.Natl.Acad.Sci.USA" 89, 8025-8029

Rooney,E.K., Gross,J.D. & Satre,M. (1994). "Cell calcium" *in press*

Roos,A. & Boron,W.F. (1981). Intracellular pH. "Physiol.Rev." 61, 296-434

Rottenberg,H., Grunwald,T. & Avron,M. (1972). Determination of the pH gradient in chloroplasts. 1.Distribution of [^{14}C] methylamine. "Eur.J.Biochem." 25, 54-63

Saito,M. (1979). Effect of extracellular Ca^{2+} on the morphogenesis of *Dictyostelium discoideum*. "Exp.Cell.Res."123, 79-86

Sambrook,J., Fritsch,E.F. & Maniatis,T. (1989). "Molecular Cloning. A laboratory manual" Cold Spring Harbor Laboratory Press, New York, USA.

Saran,S., Nakao,H., Tasaka,M., Iida,H., Tsuji,F.L. Nanjundah,V. & Takeuchi,I. (1994). Intracellular free calcium level and its response to cAMP stimulation in developing *Dictyostelium* cells transformed with jellyfish apoaequorin cDNA. "FEBS Lett." 317, 43-47

Satre,M. & Martin,J-B. (1985). ^{31}P NMR analysis of intracellular pH in *Dictyostelium*. "Biochem.Biophys.Res.Comm." 132, 140-146

Satre,M., Martin,J-B. & Klein,G. (1989). Methyl phosphonate as a ^{31}P-NMR probe for intracellular pH measurements in *Dictyostelium* amoebae. "Biochimie" 71, 941-948

Saxe,C.L., Johnson,R.L., Devreotes,P.N. & Kimmel,A.R. (1992). Expression of a cAMP receptor gene of *D.discoideum* and evidence for a multigene family. "Genes & Dev." 5, 1-8

Saxe,C.L.III., Yu,Y., Bear,J., Berry,S. & Bauman,A. (1994). Analysis of cAR2 and cAR3 cAMP receptor expression in *Dictyostelium*. "International *Dictyostelium* conference", August 1994, p.10.3

Schaap,P. Konijn,T.M. & van Haastert,P.J.M. (1984). cAMP pulses coordinate morphogenetic movement during fruiting body formation of *Dictyostelium minuteum*. "PNAS USA" 81, 2122

Schaap,P. & Van Driel,R. (1985). Induction of post-aggregative gene expression in *Dictyostelium discoideum* by cAMP. "Exp.Cell.Res."159, 388-398

Schaap,P., Van Lookeren Campagne,M.M., Van Driel,R., Spek,W., Van Haastert,P.J.M. & Pinas,J. (1986). Postaggregative differentiation induction by cyclic AMP in *Dictyostelium*: intracellular transduction pathway and requirement for additional stimuli. "Dev.Biol." 118, 52-63

Schaap,P., Brandt,W. & Van Es,S. (1994). "personal communication"

Scherczinger, Yates & Knecht (1992). Variables affecting antisense RNA inhibition of gene expression. "Annals N.Y. Acad.Sci." p.45

Schindler,J. & Sussman,M. (1977). Ammonia determines the choice of morphogenetic pathways in *Dictyostelium discoideum*. "J.Mol.Biol." 116, 161-169

Schindler,J. & Sussman,M. (1979). Inhibition by ammonia of intracellular cAMP accumulation in *Dictyostelium discoideum*: its significance for regulation of morphogenesis. "Dev.Genet." 1, 13-20

Siegert,F. & Weijer,C. (1989). Digital image processing of optical density wave propagation in *Dictyostelium discoideum* and analysis of the effects of caffeine and ammonia. "J.Cell Science" 93, 325-335

Siegert,F. & Weijer,C.J. (1992). Three-dimensional scroll waves organize *D.discoideum* slugs. "Proc.Natl.Acad.Sci. USA" 80, 6596-6600

Simon,M-N., Driscoll,D., Mutzel,R., Part,D. Williams,J.G. & Veron,M. (1989). Overproduction of the regulatory subunit of the cAMP-dependent protein kinase blocks the differentiation of *Dictyostelium discoideum*. "EMBO J." 8, 2039-2043

Siu,C-H. (1990). Cell-cell adhesion molecules in *Dictyostelium*. "Bioessays" 12, 357-362

Small,N.V., Europe-Finner,G.N. & Newell,P.C. (1986). Calcium induces cGMP formation in *Dictyostelium*. "FEBS Lett." 203, 11-14

So,J-S. & Weeks,G. (1992). The effects of presumptive morphogens on prestalk and prespore cell gene expression in monolayers of *D.discoideum*. "Differentiation" 51, 73-78

Sternfeld,J. & David,C.N. (1979). Ammonia plus another factor are necessary for differentiation in submerged clumps of *D.discoideum*. "J.Cell Sci." 8, 181-191

Sternfeld,J. & David,C.D. (1982). Fate and regulation of anterior-like cells in *Dictyostelium* cells. "Dev.Biol." 93, 111-118

Stevens,T.H. (1992). Structure and function of the fungal V-ATPase. "J.Exp.Biol." 172, 47-55

Sun,T.J. & Devreotes,P.N. (1991). Gene targetting of the aggregation stage cAMP receptor cAR1 in *Dictyostelium*. "Genes Devel." 5, 572-582

Sussman,M. (1966) Protein synthesis and the temporal control of genetic transcription during slime mould development. "Proc.Natl.Acad.Sci." 55, 813-818

Sussman,M. (1987). Cultivation and synchronous morphogenesis of *Dictyostelium* under controlled experimental conditions. "Methods Cell Biol." 28, 9-30

Tasaka,M. & Takeuchi,I. (1981). Role of cell sorting in pattern formation in *D.discoideum*. "Differentiation"18, 191-196

Theibert,A. & Devreotes,P.N. (1986). Surface receptor-mediated activation of adenylate cyclase in *D.discoideum*. "J.Biol.Chem." 261, 15121-15125

Tirlapur,U.K., Gross,J.D. & Nanjundah,V. (1991). Spatial variation of sequestered calcium in the multicellular stage of *Dictyostelium discoideum* as assayed by chlortetracycline fluorescence. "Differentiation" 48, 137-146

Tomchik,K.J. & Devreotes,P.N. (1981). cAMP waves in *Dictyostelium discoideum*: a demonstration by isotope dilution fluorography. "Science",121, 443

Town,C.D., Gross,J.D. & Kay,R.R. (1976). Cell differentiation without morphogenesis in *Dictyostelium discoideum*. "Nature" 262, 717-719

Town,C.D. & Gross,J.D. (1978). THe role of cyclic nucleotides and cell agglomeration in postaggregative enzyme synthesis in *D.discoideum*. "Dev.Biol." 63, 412-420

Town,C.D., Dominov,J.A., Karpinski,B.A. & Jentoft,J.E. (1987). Relationships betwen extracellular pH, intracellular pH and gene expression in *Dictyostelium discoideum*. "Dev.Biol." 122, 354-362

Traynor,D., Kessin,R.H. & Williams,J.G. (1992). Chemotactic sorting to cAMP in the multicellular stages of *D.discoideum* development. "Proc.Natl.Acad.Sci. USA" 89, 8303-8307

Umemoto,N., Ohya,Y. & Anraku,Y. (1991). *VMA11*, a novel gene that encodes a putative proteolipid is indispensable for expression of yeast vacuolar membrane H^+-ATPase activity. "J.Biol.Chem." 266, 24526-24532

Van Duijn,B. & Inouye,K. (1991). Regulation of movement speed by

intracellular pH during *Dictyostelium discoideum* chemotaxis. "Proc.Natl.Acad.Sci.USA" 88, 4951-4955

Van Haastert,P.J.M. & Kein,E. (1983). Binding of cAMP derivatives to *Dictyostelium discoideum* cells. "J.Biol.Chem."258, 9636-9642

Van Haastert,P.J.M. (1985). cAMP activates adenylate and guanylate cyclases of *Dictyostelium discoideum* cells by binding to different classes of cell surface receptors. A study with extracellular calcium. "Biochim.Biophys.Acta." 846, 324-333

Van Haastert (1987). Down-regulation of cell surface cAMP receptors . "J.Cell. Biol."105,2301-2306

Van Haastert,P.J.M. (1991). transmembrane signal transduction pathways in *Dictyostelium*. "Adv.Second.Mess.Res." (ed.Greengard & Robinson), Raven Press, N.Y

Vaughan, R. & Devreotes,P.N. (1988). Ligand-induced phosphorylation of the cAMP receptor from *D.discoideum*. "J.Biol.Chem." 263, 14538-14543

Wang,M., Van Driel,R. & Schaap,P. (1988). Cyclic AMP-phosphodiesterase induces dedifferentiation of prespore cells in *D.discoideum* slugs: evidence that cyclic AMP is the morphogenic signal for prespore differentiation. "Development" 103, 611-618

Wang,M. & Schaap,P. (1989). Ammonia depletion and DIF trigger premature stalk cell differentiation in intact *D.discoideum* slugs. "Development" 105, 569-574

Wang,M., Roelfsema,J.H., Williams,J.G. & Schaap,P. (1990). Cytoplasmic acidification facilitates but does not mediate DIF-iinduced prestalk gene expression in *Dictyostelium discoideum*. "Dev.Biol."140, 182-188

Weeks,G. & Gross,J.D. (1991). Potential morphogens involved in pattern formation during *Dictyostelium* differentiation. "Biochem.Cell.Biol." 69, 608-617

Weijer,C.J., Duschl,G. & David,C.N. (1984). A revision of the *D.discoideum* cell cycle. "J.Cell Sci." 70, 111-131

Wick,U., Malchow,D. & Gerisch,G. (1978). Cyclic-AMP stimulated calcium influx into aggregating cells of *Dictyostelium discoideum*. "Cell Biol.Intl.Repts" 2, 71-79

Williams,G.B., Elder,E.M. & Sussman,M. (1984). Modulation of the cAMP relay in *D.discoideum* by ammonia and other metabolites: possible

morphogenetic consequences. "Dev.Biol." 105, 377-388

Williams,J.G., Ceccarelli,A., McRobbie,S.J., Mahbubani,H., Kay,R.R., Early,A.E., Berks,M. & Kay,R.R. (1987). Direct induction of *Dictyostelium* prestalk gene expression by DIF provides evidence that DIF is a morphogen. "Cell" 49, 185-182

Williams,J.G., Duffy,D.P., Lane,D.P., McRobbie,S.J., Harwood,A.J., Traynor,D., Kay,R.R. & Jermyn,K.A. (1989). Origins of the prestalk-prespore pattern in *D.discoideum*. "Cell"59, 1157-1163

Winckler,T., Dammann,H. & Mutzel,R. (1991). Ca/calmodulin binding proteins in *Dictyostelium discoideum* "Res.Microbiol." 142, 509-520

Yamada,Y. & Okamoto,K. (1992). Cell type-specific responsiveness to cAMP in cell differentiation of *D.discoideum*. "Dev.Biol." 149, 235-237

Yamamoto,A. & Takeuchi,I. (1983). Vital staining of autophagic vacuoles in differentiating cells of *Dictyostelium discoideum*. "Differentiation" 24, 83-87

Yamashiro,D.J. & Maxfield,F.R. (1988). Acidification of morphologically distinct endosomes in mutant and wild-type Chinese hamster ovary cells. "J.Cell Biol." 105, 2723-2733

Yamashiro,C.T., Kane,P.M., Wolczyk,D.F., Preston,R.A. & Stevens,T.H. (1990). Role of vacuolar acidification in protein sorting and zymogen activation: a genetic analysis of the yeast vacuolar proton-translocating ATPase. "Mol.Cell.Biol." 10, 3737-3749

Zhu,Q. & Clarke,M. (1992). Association of CaM and an unconventional myosin with the contractile vacuole complex of *Dictyostelium discoideum*. "J.Cell.Biol." 2, 347-358

Zhu,Q., Liu,T. & Clarke,M. (1993). Calmodulin and the contractile vacuole complex in mitotic cells. " J.Cell.Sci." 110, 130-144

* Additional references are listed on p.163

Publications

Publications

Davies,L., Satre,M., Martin,J-B & Gross,J.D. (1993) The target of ammonia action in *Dictyostelium*. "Cell"75, 321-327

Addanki,S., Cahill,F.D. & Sotos,J.F. (1968). Determination of intramitochondrial pH and intramitochondrial-extramitochondrial pH gradient of isolated heart mitochondria by the use of 5,5-dimethyl-2,4-oxazolidinedione."J.Biol.Chem." 243, 2337

Gluck,S., Cannon,C. & Al-Awqati,Q. (1982). Exocytosis regulates urinary infection in turtle bladder by rapid insertion of H^+ pumps into the luminal membrane. "Proc.Natl.Acad.Sci." 79, 4327-4321

Gogarten,J.P., Kibak,H., Dittrich,P., Taiz,L., Bowman,E.J., Bowman,B.J., Manolson,M.F., Poole,R.J., Date,T., Oshima,T., Konishi,J., Denda,K. & Yoshida,M. (1989). Evolution of the vacuolar H^+ ATPase: Implications for the origin of eukaryotes. "Proc.Natl.Acad.Sci." 86, 6661-6665

Good,N.E. (1960). Activation of the Hill reaction by amines. "Biochim.Biophys.Acta." 40, 502

Hirata,R., Ohsumi,Y., Nakano,A., Kawasaki,H., Suzuki,K. & Anraku,Y. (1990). Molecular structure of a gene *vmaI*, encoding the catalytic subunit of a H^+-translocating ATPase from vacuolar membranes of Saccharomyces cerevisiae. "J.Biol.Chem." 265, 6726-6733

Ish-Horowicz,D. & Burke,J.F. (1981). Rapid and efficient cosmid cloning. "Nuc.Ac.Res." 9, 2989-2998

Johnson,R.L., Saxe,C.L., Gollop,R., Kimmel,A.R. & Devreotes,P.N. (1993). Identification and targetted gene disruption of cAR3. "Gene.Devel." 7, 273

Kayman,S.C. & Clarke,M. (1983). Relationship between axenic growth of *Dictyostelium discoideum* strains and their track morphology on substrates coated with gold particles. "J.Cell.Biol." 97, 1001-1010

Krogstad,D.J. & Schlesinger,P.H. (1987). Acid-vesicle function, intracellular pathogens and the action of chloroquine against *Plasmodium falciparum*. "New.Eng.J.Med." 317, 542-547

Lieb,W.R. & Stein,W.D. (1969). Biological membranes behave as non-porous polymeric sheets with respect to the diffusion of non-electrolytes. "Nature" 224, 240-243

Nelson,N. & Taiz,L. (1989). The evolution of H^+-ATPases. "Trends Biochem.Sci." 14, 113-116

Ohkuma,S. & Poole,B. (1981). Cytoplasmic vacuolation of mouse peritoneal macrophages and the uptake into lysosomes of weakly basic substances. "J.Cell.Biol." 90, 656-664

St.Johnston,D. & Nusslein-Volhard,C. (1992). The origin of pattern and polarity in the *Drosophila* embryo. "Cell" 68, 201-209

Schindler,M., Sussman,M. & Kim,H. (1978). Sluggers, a new class of morphogenetic mutants of *D.discoideum*. "Exp.Cell.Res." 116, 217-227

Schuldiner,S., Rottenberg,H. & Avron,M. (1972). Determination of δpH in chloroplasts. "Eur.J.Biochem." 25, 64-70

Thilo,L. & Vogel,G. (1980). Kinetics of membrane internalization and recycling during pinocytosis in *Dictyostelium discoideum.* "Proc.Natl.Acad.Sci." 77, 1015-1019

Thomas,R.C. (1974). Intracellular pH of snail neurones measured with a new pH-sensitive glass microelectrode. "J.Physiol.London." 238, 159-180

Walter,A. & Gutknecht,J. (1986). Permeability of small non-electrolytes through lipid bilayer membranes. "J.Membr.Biol." 90, 207-217

Wang,Z.Q. & Gluck,S. (1990). Isolation and properties of bovine kidney brush border vacuolar H^+-ATPase. "J.Biol.Chem." 265, 21957-21965

Weaver,J.C., Powell,K.T., Mintzer,R.A., Sloan,S.R & Ling,H. (1984). The diffusive permeability of bilayer membranes: the contribution of transient aqueous pores. "Bioelectrochem.Bioenerg." 12, 405-412

Wellems,T.E., Walker-Jonah,A. & Panton,L.J. (1991). Genetic mapping of the chloroquine resistance locus on *P.falciparum* chromosome 7. "Proc.Natl.Acad. Sci." 88, 3382-3386

Young,M.R., Gordon,A.H. & D'Arcy-Hart,P. (1990). Tubular lysosomes and their drug reactivity in cultured resident macrophages and in cell-free medium. "Exp.Cell.Res." 190, 283-289